

AD _____

Award Number: W81XWH-09-1-0155

TITLE: Connexins in Prostate Cancer Initiation and Progression

PRINCIPAL INVESTIGATOR: Parmender P. Mehta, Ph.D.

CONTRACTING ORGANIZATION: University of Nebraska
Lincoln, NE 68588

REPORT DATE: November 2013

TYPE OF REPORT: Revised Final

PREPARED FOR: U.S. Army Medical Research and Materiel Command
Fort Detrick, Maryland 21702-5012

DISTRIBUTION STATEMENT: Approved for Public Release;
Distribution Unlimited

The views, opinions and/or findings contained in this report are those of the author(s) and should not be construed as an official Department of the Army position, policy or decision unless so designated by other documentation.

REPORT DOCUMENTATION PAGE

*Form Approved
OMB No. 0704-0188*

Public reporting burden for this collection of information is estimated to average 1 hour per response, including the time for reviewing instructions, searching existing data sources, gathering and maintaining the data needed, and completing and reviewing this collection of information. Send comments regarding this burden estimate or any other aspect of this collection of information, including suggestions for reducing this burden to Department of Defense, Washington Headquarters Services, Directorate for Information Operations and Reports (0704-0188), 1215 Jefferson Davis Highway, Suite 1204, Arlington, VA 22202-4302. Respondents should be aware that notwithstanding any other provision of law, no person shall be subject to any penalty for failing to comply with a collection of information if it does not display a currently valid OMB control number. PLEASE DO NOT RETURN YOUR FORM TO THE ABOVE ADDRESS.

1. REPORT DATE November 2013			2. REPORT TYPE Revised Final		3. DATES COVERED 1 September 2009 - 31 August 2013	
4. TITLE AND SUBTITLE Connexins in Prostate Cancer Initiation and Progression			5a. CONTRACT NUMBER			
			5b. GRANT NUMBER W81XWH-09-1-0155			
			5c. PROGRAM ELEMENT NUMBER			
6. AUTHOR(S) Parmender P. Mehta, Ph.D. Email: pmehta@unmc.edu			5d. PROJECT NUMBER			
			5e. TASK NUMBER			
			5f. WORK UNIT NUMBER			
7. PERFORMING ORGANIZATION NAME(S) AND ADDRESS(ES) University of Nebraska Lincoln, NE 68588			8. PERFORMING ORGANIZATION REPORT NUMBER			
9. SPONSORING / MONITORING AGENCY NAME(S) AND ADDRESS(ES) U.S. Army Medical Research and Materiel Command Fort Detrick, Maryland 21702-5012			10. SPONSOR/MONITOR'S ACRONYM(S)			
			11. SPONSOR/MONITOR'S REPORT NUMBER(S)			
12. DISTRIBUTION / AVAILABILITY STATEMENT Approved for Public Release; Distribution Unlimited						
13. SUPPLEMENTARY NOTES						
14. ABSTRACT Please see next pages.						
15. SUBJECT TERMS- none provided						
16. SECURITY CLASSIFICATION OF:			17. LIMITATION OF ABSTRACT UU	18. NUMBER OF PAGES 161	19a. NAME OF RESPONSIBLE PERSON USAMRMC	
a. REPORT U	b. ABSTRACT U	c. THIS PAGE U			19b. TELEPHONE NUMBER (include area code)	

Technical Abstract:

Parmender P. Mehta, Ph.D

Connexins in Prostate Cancer Initiation and Progression.

The role of cell-cell contact-dependent communication in the progression of prostate cancer from a slow-growing hormone (androgen)-dependent state to a highly malignant, hormone-independent state is not fully understood. Gap junctions, formed of proteins called connexins, provide a direct intercellular communication pathway for the passage of small growth regulatory signaling molecules between the cytoplasmic interiors of adjoining cells. Mutations in various connxin genes have been detected in a wide variety of diseases related to differentiation and proliferation. Connexins have been now documented to be legitimate tumor suppressors.

Our studies have shown that epithelial cells from prostate tumors show subtle alterations in the expression of connexins *in vivo* and *in vitro*. These alterations include intracellular accumulation of connexins in aggressive prostate tumors and their impaired trafficking and assembly into gap junctions. Re-expression of connexins in connexin-deficient, indolent prostate cancer cell line, LNCaP, retards growth *in vivo* and *in vitro* and induces differentiation.

Our long-term hypothesis has been that cell-cell communication through gap junctions constitutes a homeostatic mechanism for restraining the growth of incipient prostate cancer cells during prostate cancer progression. Our accomplished work further documents that:

1. The differentiated state of epithelial cells in normal prostate and in prostate tumors may depend on the assembly of connexins into gap junctions and that during the progression of prostate cancer, pathways governing the trafficking and assembly of connexins into gap junctions are impaired or altered.
2. Androgens selectively regulate the formation and degradation of gap junctions, which may be related to the maintenance of the differentiated state of luminal epithelial cells and their survival.
3. The expression of cadherin-subtype appears to determine the sub-cellular — junctional versus intracellular — fate of connexins.
4. Metastasis suppressing E-cadherin facilitates gap junction assembly whereas metastasis promoting N-cadherin disrupts assembly.

The proposed studies have two aims. The proposed experiments in aim 1 explore the molecular mechanisms by which formation of gap junctions retards cell growth *in vivo* and *in vitro*. The two questions addressed are: 1. Is the passage of small molecules through gap junctions required to retard tumor growth and invasion? 2. Does the formation of gap junctions retard tumor growth by inducing the assembly of other junctional and signaling complexes? Wild type connexins which form functional gap junctions and mutant connexins that form nonfunctional gap junctions will be used to address these questions. The proposed experiments in aim 2 will elucidate the molecular mechanisms by which E-cadherin and N-cadherin modulate gap junction assembly differentially. We have hypothesized that E-cadherin facilitates gap junction assembly by preventing endocytosis whereas N-cadherin disrupts assembly by inducing endocytosis. E- and N-cadherin will be over-expressed or knocked down in cells expressing these cadherins and gap junction assembly and disassembly will be determined using immunocytochemical and biochemical assays.

The proposed studies are innovative as they explore the molecular mechanisms by which connexins act as tumor suppressors by interrogating the existing paradigm that transmission of growth regulatory molecules through gap junctions may not be the sole mechanism. These studies will not only define further the role of connexins in the pathogenesis of prostate cancer but also serve as a guidepost in screening drugs that would facilitate the assembly of gap junctions.

Public Abstract

Parmender P. Mehta, Ph.D

Connexins in Prostate Cancer Initiation and Progression.

Prostate cancer is curable and is not life-threatening when detected at an early stage. In its late stages, when the cancer cells have disseminated to distant organs, this cancer becomes life-threatening as hormonal (androgen) ablation, surgical removal and radiation and chemotherapy are not curative. Because the factors that promote the progression of prostate cancer from its incipient form to a life-threatening form are not well understood, knowledge of the mechanisms involved in the transition of organ-confined prostate cancer to its metastatic form is critical not only in understanding its progression but also in designing alternative strategies for intervention. The incidence of prostate cancer escalates dramatically at ages when men confront other competing causes of mortality. Hence, there is need to develop cell culture models that would gauge changes in malignant prostate cancer cells as they disseminate from organ-confined environment to distant metastatic sites.

Most cells in tissues do not exist as single cells, but rather in groups of cells, because for the proper formation of tissues, various cells need to associate with one another and, at times, also need to dissociate from one another. This process of adhesion and dis-adhesion has to be precisely controlled because if this does not occur properly, the growth of a tissue becomes stunted, often leading to the development of cancer. Our research has identified 2 genes that might be important in regulating the invasive behavior of prostate cancer cells — that is, in controlling dissociation of prostate cancer cells from their neighbors. These genes code for proteins, called connexins, that assemble at cell-cell contact areas to form channels and cluster to form special structures called gap junctions.

Our research has shown that the channels embodied in gap junctions allow the exchange of small growth regulatory molecules among cells, which synchronize cellular behavior — a process which we call intercellular communication. Our studies have further shown that these proteins are gradually lost when prostate cancer progresses to a more advanced (life-threatening) stage and that reintroduction of these genes into prostate cancer cells corrects their cancerous behavior and influences the function of two other important proteins that have been shown to prevent the spread of cancer cells from prostate to distant organs (metastasis). Thus our studies have lead us to develop the notion that loss of one gene that controls the invasive behavior of malignant prostate epithelial cells might lead to the loss of function of other genes involved in controlling the similar behavior, and vice versa, although we do not understand the mechanistic basis of our findings.

The proposed studies are designed to understand the mechanistic basis of these novel findings. To do so we wish to define further the molecular mechanisms by which these genes(connexins) regulate the transition of prostate cancer from its indolent state to a more virulent state. The successful outcome of these studies will help us understand the mechanism by which prostate cancer cells become more agile and virulent. A good understanding of this process will allow us to design better drugs that will target and kill more motile and invasive cells that spread to various parts of the body and kill the cancer patients.

Innovation Statement

Prostate cancer has been estimated to be the second leading cause of death from cancer among men in the United States. Two hallmarks distinguish prostate cancer from other cancers: The first is the discrepancy between the high prevalence of latent cancer (histological changes recognizable as cancer) and the lower prevalence of clinical cancer (clinically recognizable disease). The second hallmark is its progression from a slow-growing, androgen-dependent state to a virulent, androgen-independent state. The development of metastatic lesions remains the predominant cause of death for most cancer patients. Thus, identification of molecular events that facilitate the clonal expansion and dissemination of organ-confined malignant prostate cancer cells to distant metastatic sites is crucial for designing strategies for intervention.

Gap junctions, formed of proteins called connexins, provide a direct intercellular communication pathway for the passage of small growth regulatory signaling molecules between the cytoplasmic interiors of adjoining cells. Connexins have been now documented to be legitimate tumor suppressors, but the molecular mechanisms by which they affect tumor growth are not understood. We have pioneered studies related to the role of connexins in the pathogenesis of prostate cancer. We have been using assembly of connexins into gap junctions as a surrogate markers for screening novel chemopreventive agents such as various non-toxic analogs of retinoids and vitamin D.

Decreased expression of cadherins and connexins has been reported separately to correlate with the degree of malignancy and tumor grade in many prostate tumors but many metastatic tumors continue to express both connexins and cadherins. Also, poor survival of the patients with normal E-cadherin expression has been linked to defective function of α -catenin. Despite these studies, the exact relationship between loss of cadherins and connexins in predicting the clinical outcome of prostate cancer is not clear. Our studies have pointed out that loss of one junctional component, for example cadherins, might pave a way for the loss of other junctional component and *vice versa*, and that there may be extensive cross-talk among various elements of separate junctional complexes in facilitating or disrupting each other's assembly.

Hence a rigorous investigation into the molecular mechanisms by which both cadherins and connexins act as tumor suppressors should define crucial checkpoints that are breached during invasion and metastasis. The proposed studies in aim 1 explore the molecular mechanisms by which Cxs act as tumor suppressors by interrogating the existing paradigm that transmission of growth regulatory molecules through gap junctions may not be the sole mechanism. Aim 2 explores yet another novel idea whether the assembly of connexins into gap junctions is the downstream target of signaling cascade triggered by the expression of N-cadherin which triggers tumor cell invasion *in vivo* and *in vitro*. These studies will not only define further the role of connexins in the pathogenesis of prostate cancer but also serve as a guidepost in screening drugs that would facilitate the assembly of gap junctions.

Impact Statement

Prostate cancer has been estimated to be the second leading cause of death from cancer among men in the United States. Two hallmarks distinguish prostate cancer from other cancers: The first is the discrepancy between the high prevalence of latent cancer (histological changes recognizable as cancer) and the lower prevalence of clinical cancer (clinically recognizable disease). The second hallmark is its progression from a slow-growing, androgen-dependent state to a virulent, androgen-independent state. The development of metastatic lesions remains the predominant cause of death for most cancer patients. Thus, identification of molecular events that facilitate the clonal expansion and dissemination of organ-confined malignant prostate cancer cells to distant metastatic sites is crucial for designing strategies for intervention.

The role of cell-cell contact-dependent communication in the progression of prostate cancer from a slow-growing hormone (androgen)-dependent state to a highly malignant, hormone-independent state is not fully understood. Gap junctions, formed of proteins called connexins, provide a direct intercellular communication pathway for the passage of small growth regulatory signaling molecules between the cytoplasmic interiors of adjoining cells. Connexins have been now documented to be legitimate tumor suppressors. Our studies have shown that the differentiated state of epithelial cells in normal prostate and in prostate tumors may depend on the assembly of connexins into gap junctions and that during the progression of prostate cancer, pathways governing the assembly of connexins into gap junctions are impaired or altered. Moreover, our studies have shown that androgens selectively regulate the formation and degradation of gap junctions, which are required to maintain the differentiated state of luminal epithelial cells and for their survival. Furthermore the expression of cadherin-subtype appears to determine the sub-cellular — junctional versus intracellular — fate of connexins with metastasis suppressing E-cadherin facilitating gap junction assembly whereas metastasis promoting N-cadherin disrupting it.

Decreased expression of cadherins and connexins has been reported separately to correlate with the degree of malignancy and tumor grade and decreased progression-free interval of prostate cancer as evidenced by several studies. Similarly, poor survival of the patients with normal E-cadherin expression has been linked to defective function of α -catenin. Despite these studies, the exact relationship between loss of cadherins and connexins in predicting the clinical outcome of prostate cancer is not clear.

Our studies point out that loss of one junctional component might pave a way for the loss of other junctional component and *vice versa*, and that there may be extensive cross-talk among various elements of separate junctional complexes in facilitating or disrupting each other's assembly. Thus loss of connexin expression might trigger the loss of other junctional component, leading to the loss polarized state, loss of cell-cell adhesion and metastasis. In the light of our proposed studies, and because of the potential interactions among different junctional components, an investigation into their additive and/or synergistic effects on the assembly and disassembly of connexins into gap junctions may shed light on the mechanism by which loss of one junctional component initiates a signaling cascade to promote invasion and motility of prostate cancer cells. The proposed studies may lead to the design of drugs that can be used to delay the progression of prostate cancer based on the assembly of connexins into gap junctions as an intermediate biomarker to monitor progression.

Parmender P. Mehta, Ph.D.

Table of Contents

	Page
Introduction	4-5
Body	5-18
Key Research Accomplishments	18
Reportable Income	18-19
Conclusions	20
References	20-26

1. Introduction:

Prostate Growth and Neoplasia. The prostate is a classical exocrine gland composed predominantly of two types of cells: the epithelial cells, which line the ducts and acini, and the mesenchymal cells, which form the stroma [1]. The epithelial cells lining the ducts and acini are presumed to be the prime target cell type in prostate cancer (PC) [2-4]. The growth and differentiation of normal prostate epithelial cells are influenced by androgens and androgen-regulated reciprocal mesenchymal-epithelial interactions [5]. Androgens may govern prostate growth and differentiation directly by binding to the androgen receptor in epithelial cells to control their proliferation, differentiation and apoptosis, or indirectly, by acting on the stromal cells and inducing them to release growth factors [6-10]. Although PC can be viewed as a disorder involving alterations in the endocrine, paracrine, and autocrine modes of cellular communication, the important question remains about how these modes affect cell-cell contact-dependent communication during the morphogenesis and oncogenesis of the prostate [11;12].

Cell Junctions, gap junctions and Tissue Homeostasis. The polarized and the differentiated state of epithelial cells is maintained by cell-cell and cell-matrix adhesion molecules, which assemble into large complexes called cell junctions [13] (**Figure 1**). The progression of PC from androgen-dependent state to androgen independent invasive state is characterized by loss of polarization and differentiation triggered by disruption of cell junctions [12;15-17]. Our studies have shown that direct communication through GJs is important in controlling the progression of PC [18-23]. Gap junctions are conglomerations of cell-cell channels that are formed by a family of 21 distinct proteins, called connexin (Cx)s. The Cxs are designated according to molecular mass and GJ assembly is a multistep process (**Figure 2**). Communication through GJs is crucial for maintaining homeostasis [14;24]. Impaired, or loss of, Cx expression has been documented in the pathogenesis of various carcinomas [14;18;23;25]. Moreover, many studies have shown that over-expression of Cxs in tumor cells attenuates the malignant phenotype *in vivo* and *in vitro*, reverses the changes associated with epithelial to mesenchymal transformation (EMT), and induces differentiation [18;23;26].

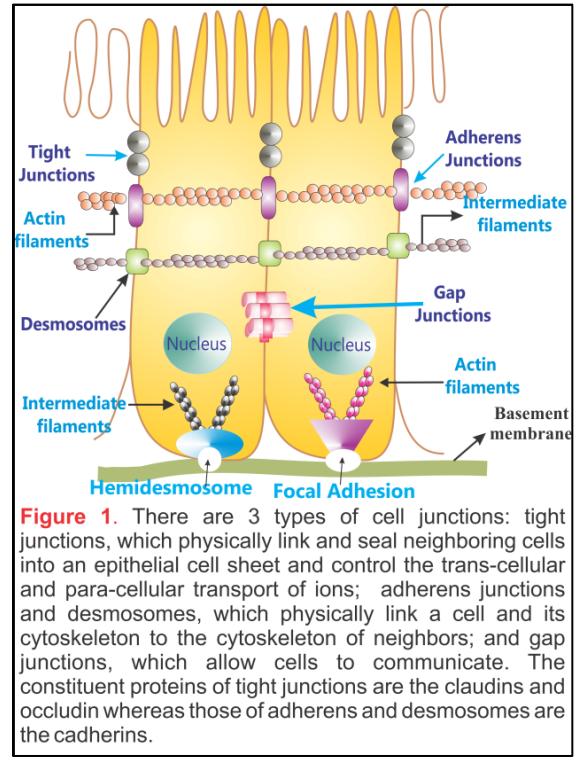


Figure 1. There are 3 types of cell junctions: tight junctions, which physically link and seal neighboring cells into an epithelial cell sheet and control the trans-cellular and para-cellular transport of ions; adherens junctions and desmosomes, which physically link a cell and its cytoskeleton to the cytoskeleton of neighbors; and gap junctions, which allow cells to communicate. The constituent proteins of tight junctions are the claudins and occludin whereas those of adherens and desmosomes are the cadherins.

Most cells in a polarized epithelium are also interconnected by gap junction (GJ)s, which permit the direct passage of small molecules, such as cAMP, Ca²⁺ and IP₃ between adjoining cells [14]. The progression of PC from androgen-dependent state to androgen independent invasive state is characterized by loss of polarization and differentiation triggered by disruption of cell junctions [12;15-17]. Our studies have shown that direct communication through GJs is important in controlling the progression of PC [18-23]. Gap junctions are conglomerations of cell-cell channels that are

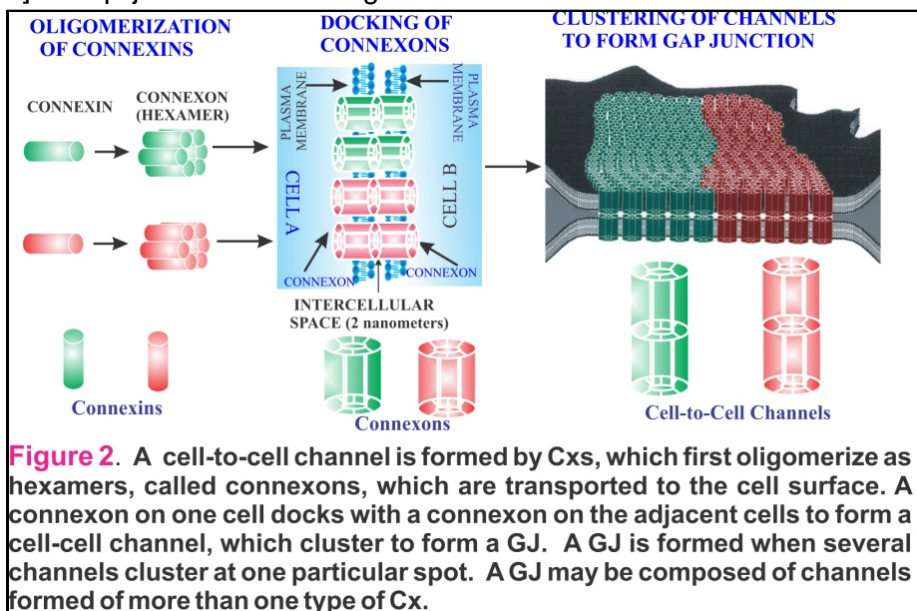


Figure 2. A cell-to-cell channel is formed by Cxs, which first oligomerize as hexamers, called connexons, which are transported to the cell surface. A connexon on one cell docks with a connexon on the adjacent cells to form a cell-cell channel, which cluster to form a GJ. A GJ is formed when several channels cluster at one particular spot. A GJ may be composed of channels formed of more than one type of Cx.

Parmender P. Mehta, Ph.D.

For example, Cx32 is expressed in the liver, lung, and exocrine glands, and knock out studies have shown that the incidence of carcinogen induced tumors in these mice is higher [27-29]. Finally, mutation in several Cx genes have been characterized in inherited diseases associated with aberrant proliferation and differentiation [14;30]. These studies support the notion that Cxs act as tumor suppressors. Despite this the molecular mechanisms by which GJs are assembled and disassembled during PC progression and how they regulate cell growth remain poorly understood.

2. Body

Gap junctional channels admit a wide range of cellular molecules. For example, the inorganic ions, virtually all metabolites, second messengers such as cAMP, Ca⁺² and IP₃, as well as vitamins [14]. Despite the fact that Cxs have been shown to act as tumor suppressors, it is as yet unknown how the exchange of these molecules is involved in retarding tumor growth [18;23;31]. Our studies with PC cell lines have shown that the introduction of Cx32 and Cx43 into Cx-null LNCaP cells retards cell growth *in vivo* and *in vitro* and induces differentiation. These effects were contingent upon the formation of GJs and restoration of junctional communication because no effect on cell growth was observed when the same Cxs were introduced into highly invasive cell line, PC-3, in which Cxs remained intracellular and failed to form GJs [20;32]. Recent studies have shown that over-expression of Cxs in Cx-deficient tumor cell lines retards tumor growth even when Cxs remain intracellular and fail to assemble into GJs. Also the effects on tumor growth and invasion seem to be Cx-specific, with some Cxs inhibiting growth while others producing no effect [26;33;34]. Intriguingly, expression of Cxs in LNCaP cells has recently been shown to increase their sensitivity to apoptotic stimuli triggered by TNF- α [35] and to growth inhibitory effects of retinoids [36]. Also, the channels composed of different Cxs not only form pores of different sizes but also act as molecular sieves by permitting the selective transfer some metabolites but not others [31;37]. For example, a Cx26 disease linked mutant selectively inhibits the transfer of only IP₃ [38]. Some disease-associated Cx mutants fail to traffic to the cell surface [14]. **Thus, the exchange of signals through GJs may not be the sole mechanism by which formation of GJs retards tumor growth and that GJ complexes may permit the assembly of other junctional complexes.** These findings raise two major questions with regard to the role of GJs in regulating cell growth *in vivo* and *in vitro*.

1. **Is the passage of small molecules through gap junctions required to retard tumor growth and invasion *in vivo* and *in vitro*?**
2. **Does the formation of gap junctions retard tumor growth by inducing the assembly of other junctional complexes at the site of cell-cell contact?**

The identification of scaffold proteins, such as ZO-1, that interact with Cxs on the cytoplasmic side raise the possibility that GJs may be transiently linked to the cytoskeletal elements as has been shown by our recent studies [30;39], and their formation might initiate or interrupt a signaling cascade through recruitment of other cell junction associated proteins. This notion is supported by recent studies which showed that formation of GJs induces tight junction formation [40;41]. The objective of our studies is to discern which of the above signaling mechanisms is ensued upon the formation of GJs. The specific aims proposed were:

Aim 1. **To investigate if formation of gap junctions retards prostate cancer cell growth *in vitro* and *in vivo* by permitting the transmission of growth regulatory molecules.**

Aim 2. **Elucidate the molecular mechanisms by which cadherins modulate gap junction assembly differentially.**

Parmender P. Mehta, Ph.D.

.Tasks

1. Generate stable polyclonal cultures of LNCaP cells, using recombinant retroviruses, that express various engineered connexin constructs anticipated to assemble into functional and nonfunctional gap junctions.(6-18 months)
2. Refine and further optimize biochemical assays for studying the assembly of connexins into gap junctions and those of cadherins into adherens junctions using Triton X-100 insolubility assay as well as ascertain that these assays are quantitative and reproducible (4-12).
3. Refine and optimize methods for studying the trafficking of connexins and their subsequent assembly into of gap junctions by quantitative immunocytochemical analyses using deconvolution microscopy and volume rendering. (4-8 months).
4. Perform functional assays, by micro-injecting gap junctional permeable fluorescent tracers, to confirm that mutant connexins are assemble into nonfunctional gap junctions as compared to those that express wild-type connexins. (8-18 months).
5. Determine if the expression of wild-type and engineered mutant connexins in LNCaP cells alters the detergent insolubility of E-cadherin and tight junction associated protein occludin. (12-18 months).
6. Determine if expression of wild-type and engineered mutant connexins affects the growth of polyclonal cultures of LNCaP cells *in vitro* using soft agar assay and by calculating the doubling times from the growth curves.
7. Determine the tumorigenesis of polyclonal cultures of LNCaP cells — that form functional and non-functional gap junctions — by transplanting them subcutaneously and orthotopically into athymic mice. For these studies 288 athymic nude mice will be used which are well-suited to undertake such type of experiments. (16-24 months)
8. Examine if wild-type and mutant connexins are assembled into gap junctions appropriately in tumors by immunocytochemical and western blot analysis of the total and detergent-soluble and -insoluble fractions.
9. Explore if trafficking and assembly of connexins into gap junctions are regulated differently by E-cadherin and N-cadherin in LNCaP cells. If yes, investigate the molecular basis of the difference by generating appropriate engineered cadherin and connexin constructs. (18-22 months)
10. Optimize, through transient transfection, the efficiency of knocking down components of clathrin or lipid raft/caveolae- mediated pathways in LNCaP cells using immunocytochemical and biochemical approaches.(20-24 months)
11. Optimize the concentrations of chloropromazine and filipin for inhibiting, respectively, clathrin and lipid raft/caveolae-mediated endocytosis, in LNCaP and PC-3 cells expressing connexin32 and

Parmender P. Mehta, Ph.D.

connexin43, using immunocytochemical and biochemical approaches.(20-24 months)

12. Develop as well as optimize methodology to knock down E-cadherin and N-cadherin in LNCaP and PC-3 cell lines using SiRNA and shRNAs.
13. Generate recombinant retroviruses harboring shRNAs targeting various components of clathrin and lipid raft mediated endocytic pathways using retroviral packaging cell lines such as Amphotropic and PTI67 (24-30 months).
14. Generate stable polyclonal cultures of LNCaP and PC-3 cells, using recombinant retroviruses, in which E-cadherin and N-cadherin has been knocked down or vice versa. (16-22 months)
15. Examine if knock down of E-cadherin or N-cadherin affects the trafficking of connexins and their subsequent assembly into gap junctions in E-cadherin expressing LNCaP cells and N-cadherin expressing PC-3 cells (20-32 months).
16. Characterize organelle-specific markers for localizing connexins to different sorting compartments and ascertain, or rule out, if knock down or over-expression of E-cadherin and N-cadherin alters the subcellular fate of connexin32 and connexin43, or their subsequent assembly into gap junctions, as assessed by quantitative immunocytochemical and biochemical analyses in LNCaP and PC-3 cells (16-32 months).
17. Summarize and interpret data (12-36 months).

TASKS

Task 1. **Generate stable polyclonal cultures of LNCaP cells, using recombinant retroviruses, that express various engineered connexin constructs anticipated to assemble into functional and nonfunctional gap junctions. (6-18 months).**

We retrovirally expressed wild type (WT) and mutant Cxs, shown in Figure 3, in LNCaP cells. We found that both wild type and mutant Cxs are expressed appropriately and are assembled into GJs (Figure 4). Note larger GJ size of the mutant Cx (Cx43Δ257) and the smaller size of Cx32Δ220 (Figure 4, arrows) compared to WT counterpart. Cxs are green whereas Epithelial cadherin (E-cad) and occludin in red.

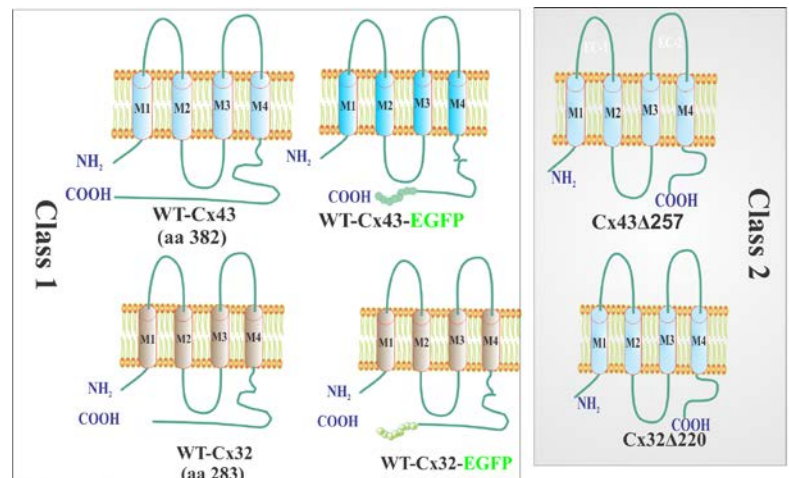


Figure 3. We constructed 2 types of wild-type and mutant Cxs and produced recombinant retroviruses. Class 1 Cxs are full length (WT-Cx32, WT-Cx32-EGFP; WT-Cx43, WT-Cx43-EGFP), and form **functional GJs**. Class 2 Cxs, shown in a grey box, form **non-functional GJs**, which are smaller (Cx32Δ220 in which cytoplasmic tail has been truncated at amino acid residue 220) or larger GJs (Cx43Δ257 in which cytoplasmic tail has been truncated at residue 257).

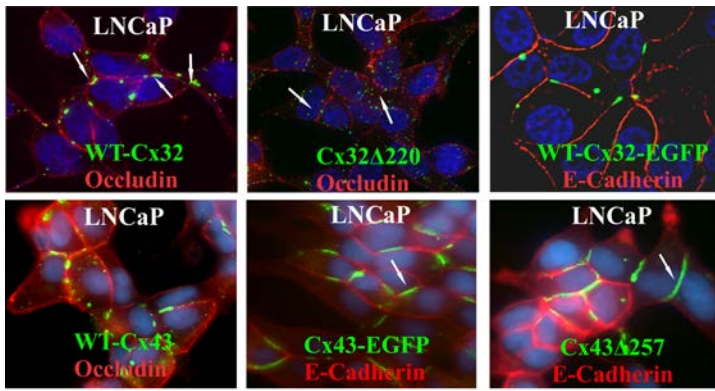


Figure 4. Mutants of both Cx32 and Cx43, which form smaller or larger GJs were constructed. LNCaP cells were infected with the retroviruses. GJs were examined immunocytochemically. Note compared to GJs (Green) formed by the wild-type Cxs, GJs formed by mutant Cxs (Cx43Δ257) are much larger and those formed by Cx32Δ220 are smaller than WT-Cx32 (arrows).

appended, see also **Figure 5**).

Task 2. Refine and further optimize biochemical assays for studying the assembly of connexins into gap junctions and those of cadherins into adherens junctions using Triton X-100 insolubility assay as well as ascertain that these assays are quantitative and reproducible (4-12).

To optimize biochemical assays for the assembly of Cxs into GJs and those of cadherins into cell junctions, we treated Cx32-expressing LNCaP cells with retinoids, 9-cis Retinoic acid (**9-CRA**) and all-trans-retinoid acid (**ATRA**), which have been shown to enhance the assembly of Cxs into GJs [36;42]. These studies showed that concomitant with an increase in the expression level of Cx32, treatment with 9-CRA and ATRA increased GJ assembly as assessed immunocytochemically (**Figure 6A**) and biochemically by Western blot analysis of total and Triton X (TX)-100-insoluble extracts [32;43;44] prepared at various times after treatment (**Figure 6B**).

Because E-cad has been shown to facilitate the assembly of Cxs into GJs [39;45], and Cx expression has been shown to facilitate the assembly of tight junctions [41], we also examined whether 9-CRA and ATRA increased the expression level of Cx32 and its assembly into GJs indirectly by facilitating the assembly of other cell junctions as assessed by the detergent-insolubility of their constituent and associated proteins. We found that

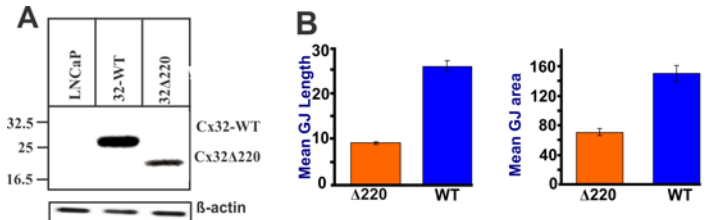


Figure 5. Western blot analysis showed that the Cx32-WT and Cx32Δ220 ran appropriately (A). We measured the size and area of 100-200 individual gap junctional puncta in LNCaP cells expressing Cx32-WT and Cx32Δ220 cells (B). The size of each fluorescent spot or a punctum at the interface was presumed to represent a single GJ plaque (39). We found that compared to Cx32-WT, Cx32Δ220 cells formed 2-3 fold smaller GJs both in regard to area and length (B). Functional assay showed that Cx32Δ220 did not form functional GJs (see Figure 9A).

Recombinant retroviruses harboring wild-type and mutant Cxs were produced and retroviral transduction and expression was achieved as described (reprints

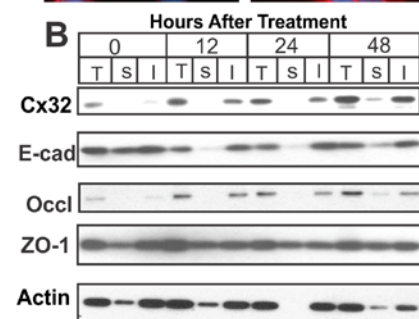
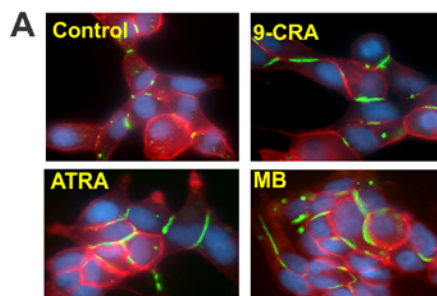


Figure 6. Assembly and detergent-solubility of Cx32 and cadherins into cell junctions. A. Cx32-expressing LNCaP cells were treated with 9-CRA and ATRA for various times. Cx32 assembly into Gjs (Green) was assessed immunocytochemically. E-cad is shown in red. Note that GJ formation was enhanced with 9-CRA and ATRA and MB (androgen) treatment. B. Assembly of Cx32 into Gjs, of tight junction associated protein, occludin and ZO-1, and of adherens junction protein, E-cad, was assessed by TX100-solubility assay. Note that both the total and the detergent-insoluble fraction of Cx32 increased significantly. Note also that the detergent-solubility of E-cad is not affected whereas that of tight junction associated protein, occludin, is marginally enhanced. In (A) the nuclei are blue.

both 9-CRA and ATRA had no significant effect on the expression level of adherens junction protein E-cad, however, the assembly of tight junction protein, occludin, but not its associated protein ZO-1, appeared to have been enhanced (**Figure 6B**). Thus our detergent-solubility assay is quantitatively reproducible, and reliably assesses the assembly of Cxs into GJs. In summary, we have refined assays to quantitatively assay the assembly of Cxs and cadherins biochemically.

Task 3. Refine and optimize methods for studying the trafficking of connexins and their subsequent assembly into of gap junctions by quantitative immunocytochemical analyses using deconvolution microscopy and volume rendering. (4-8 months).

Our previous studies have shown that Cxs are not assembled into GJs in invasive prostate tumors [20;46]. We have also found that when Cx32 and Cx43 are introduced into invasive PC3 cells, they fail to form GJs due to impaired trafficking [32]. We have refined methods to induce the assembly of Cxs into GJs. We have found that the trafficking of both Cx43 and Cx32 is induced when cells are grown on trans-well filters, which triggers partial cell polarization [39;45] (**Figure 7**). Moreover, the trafficking and assembly of Cx32 and Cx43 can be quantitatively studied by de-convolution microscopy (**Figure 8**). Thus, we have refined and optimized methods to study the trafficking of Cxs and their subsequent assembly into GJs.

Task 4. Perform functional assays, by micro-injecting gap junctional permeable fluorescent tracers, to confirm that mutant connexins are assembled into nonfunctional gap junctions as compared to those that express wild-type connexins. (8-18 months).

To determine whether GJs composed of Cx32 Δ 220 are non-functional, we microinjected GJ-permeable fluorescent tracers into cells (**Figure 9A**). We found that consistent with the immunocytochemical data (See **Figure 4**), GJs composed of mutant Cx32 Δ 220 were non-functional. For example,

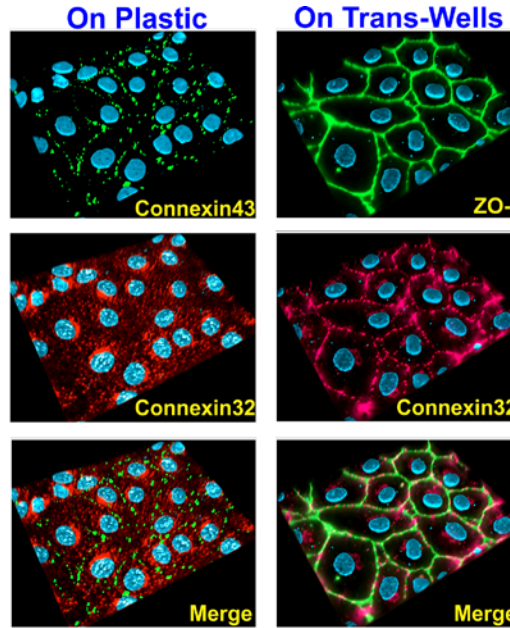


Figure 7. The assembly of Cx43 and Cx32 upon arrival at the cell surface is subject to regulatory mechanisms at the site of cell-cell contact that are Cx specific. When Cx32, which is expressed in polarized and differentiated cells, and Cx43, which is ubiquitously expressed, are introduced into human carcinoma cells, only Cx43 (green, top left) assembles into GJs whereas Cx32(red) does not (left column). Cx32 is assembled into GJs only when cells are grown on trans-well filters, which induces partial polarization (right column).

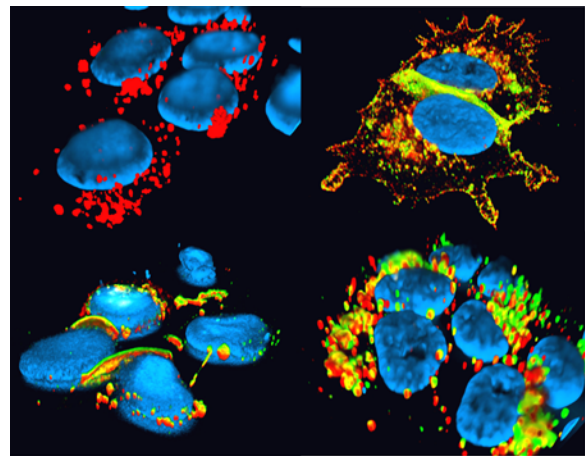


Figure 8. Deconvolution microscopy can be used to examine GJ assembly. The assembly of Cxs is impaired in tumor cells. The image shows that in tumor cells, Cx43 (red) fails to assemble into GJs as it is endocytosed prior to assembly, causing it to accumulate in the cytoplasmic vesicles (top, left). The assembly is restored upon expressing either a Myc-tagged sorting-motif mutant of Cx43 (green), which cannot be endocytosed (top right), or Myc-tagged mutant of Cx43, which cannot be phosphorylated on serine 279 (green, bottom left), resulting in the formation of large GJs. The assembly is not restored by expressing a Myc-tagged mutant of Cx43 in which serine 279 is replaced by the aspartate (green, bottom right). The images were deconvolved and 3-D rendered using Volocity. The nuclei are blue.

Parmender P. Mehta, Ph.D.

compared to cells expressing Cx32-WT, no transfer of Alexa 488 and Alexa 594 was observed in cells expressing Cx32 Δ 220 (**Figure 9A**). These data suggest that Cx32 Δ 220 is assembled into nonfunctional GJs in LNCaP cells.

Task 5. Determine if the expression of wild-type and engineered mutant connexins in LNCaP cells alters the detergent insolubility of E-cadherin and tight junction associated protein occludin. (12-18 months).

Expression of Cx32 has no effect on the detergent insolubility of cadherins and occludin. Our previous studies showed that Cx32 was degraded upon androgen depletion by endoplasmic reticulum associated degradation (**ERAD**), and that androgens, 9-CRA and ATRA enhanced GJ

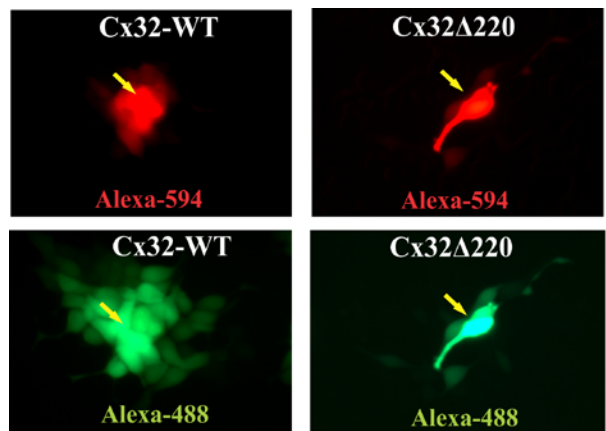


Figure 9A. Mutant Cx32 Δ 220 assembles into non-functional GJs. GJ permeable fluorescent tracers Alexa 488 (MW 570), Alexa 594 (MW 760) and Lucifer Yellow (MW 443, not shown), were injected into LNCaP cells expressing full length Cx32 (Cx32-WT) and Cx32 Δ 220. Note that both tracers go from microinjected cells to the neighboring cells in cells expressing Cx32-WT but not in cells expressing Cx32 Δ 220. Thus junctional transfer of GJ permeable fluorescent tracers, Alexa 488 and Alexa 594, is attenuated in cells expressing non-functional GJs. Microinjected cells are indicated by the arrows.

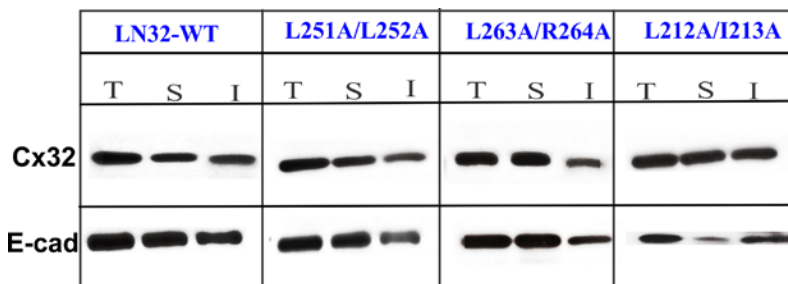


Figure 9B. Cx32 expression does not alter the detergent-solubility of E-cad in LNCaP cells. Detergent-solubility of Cx32-WT, Cx32L212A/I213A, Cx32L251A/L252A, and L263A/R264A in LNCaP cells was assayed using 1 % TX100 as indicated and cited in the text. Note that compared to Cx32-WT and mutants L251A/L252A and L263A/R264A, which form larger GJs and are more detergent-resistant, Cx32L212A/I213A fails to form GJs and is more soluble in TX100. Note that Cx32 expression has no discernible effect

Task 6. Determine if expression of wild-type and engineered mutant connexins affects the growth of polyclonal cultures of LNCaP cells in vitro using soft agar assay and by calculating the doubling times from the growth curves.

Task 7. Determine the tumorigenesis of polyclonal cultures of LNCaP cells — that form functional and non-functional gap junctions — by transplanting them subcutaneously and orthotopically into athymic mice. For these studies 288 athymic nude mice will be used which are well-suited to undertake such type of experiments. (16-24 months)

Task 8. Examine if wild-type and mutant connexins are assembled into gap junctions appropriately in tumors by immunocytochemical and western blot analysis of the total and detergent-soluble and -insoluble fractions.

Parmender P. Mehta, Ph.D.

Studies related to these tasks were not initiated.

Task 9. Explore if trafficking and assembly of connexins into gap junctions are regulated differently by E-cadherin and N-cadherin in LNCaP cells. If yes, investigate the molecular basis of the difference by generating appropriate engineered cadherin and connxin constructs. (18-22 months).

Expression of N-cadherin and R-cadherin disrupts gap junction assembly in Cx-expressing LNCaP cells.

The two hallmarks associated with the acquisition of the invasive state by tumor cells are: 1. Dysfunctional E-cad-mediated cell-cell adhesion. 2. Gain of mesenchymal cadherins such as neuronal cadherins (N-Cad), Cad-11 and R-cad. Cadherin switching has been commonly observed in tumor cells undergoing EMT [17;47]. Recent studies have highlighted the role of EMT in PC progression, and cadherin switching has been linked to metastasis and the emergence of androgen-independence and poor patient prognosis after androgen ablation [48-56]. Our studies with rat liver epithelial cells have shown that anti-invasive E-Cad facilitates, whereas pro-invasive N-Cad inhibits GJ assembly [45]. These findings prompted us to test if expression of N-Cad and R-Cad in E-Cad expressing LNCaP cells, which express retrovirally introduced Cx32 and Cx43, would disrupt GJ assembly. Our data showed that both cadherins promoted disassembly (**Figure 10**).

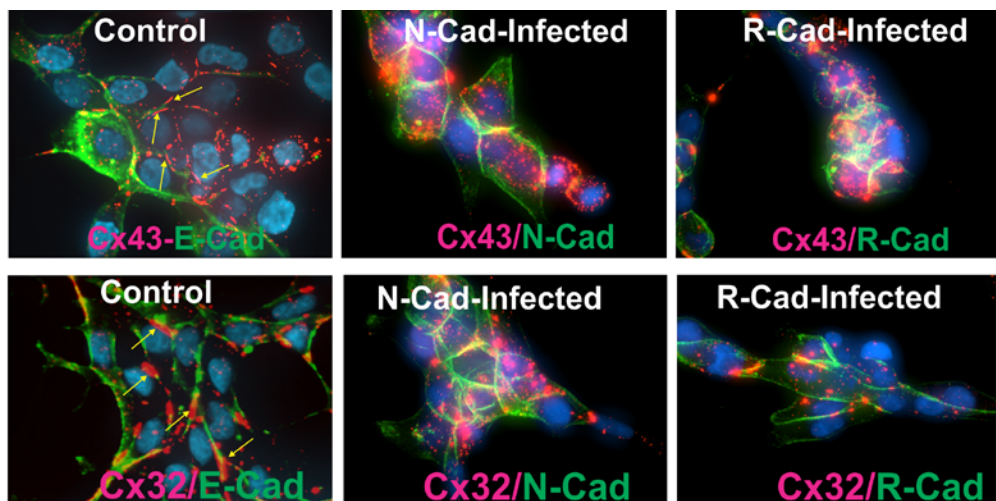


Figure 10. Cx43 and Cx32 expressing LNCaP clones, which express endogenous E-Cad, were infected with control or N-Cad or R-Cad harboring retroviruses and selected in puromycin. Pooled polyclonal cultures from approximately 2000 colonies were immunostained for Cx32 and Cx43 (red) and E-Cad, N-Cad and R-Cad (green). Note control LNCaP cells form large GJs (arrows) at areas of cell-cell contact. Note that GJs are disrupted or are smaller in cells infected with N-Cad or R-Cad and both Cx43 and Cx32 are seen as intracellular puncta. Note that E-Cad appears to be diffuse because it is on a different focal plane than Cx32 or Cx43.

Task 10. Optimize, through transient transfection, the efficiency of knocking down components of clathrin or lipid raft/caveolae- mediated pathways in LNCaP cells using immunocytochemical and biochemical approaches.(20-24 months).

Construction of Mutant Connexin43 and Connexin32. Connexins have been shown to be endocytosed by the clathrin-mediated pathway [57]. We engineered several mutants of both Cx43 and Cx32, which are not endocytosed efficiently, causing them to assemble into larger GJs. The carboxyl tail of Cx43 harbors an endocytic motif (**LSPMSPPGYKLV**) that targets it to internalization by clathrin mediated endocytosis [58] (Figure 11, left). We generated a Cx43 mutant, **Cx43Y286A/V289D**, in which tyrosine (Y) 286 and valine (V) 289 were substituted with alanine (A) and aspartate (D), respectively (Figure 11). Similarly, we have also found that the cytoplasmic tail of Cx32 harbors three dileucine [**DE]XXXL[LI]**-like motifs (for example, **QNEINKLL**), which control endocytosis of GJs (Figure 11, right). Hence, we also created the following mutants: 1. **L251A/L252A** in which both leucines (L) were replaced with alanines. 2. **L263A/R264A** in which leucine and arginine were replaced with alanine. 3. **L212A/I213A** in which leucine and isoleucine were replaced by alanine. These mutants were expected to be endocytosis-resistant and form large GJs.

Expression of Cx32 and Cx43 and their Mutants and Gap Junction Assembly. Human LNCaP cells are Cx-null [19]. We introduced WT-Cx32 and various mutants into early passage LNCaP cells using recombinant retroviruses as described in our earlier studies [59;60]. To examine if mutants were assembled into GJs, we immunostained infected cells with the antibodies against Cx32 and Cx43. Our results showed the following: 1. Cx43 mutant, Cx43Y286A/V289D, formed larger GJs. 2. Mutants L251A/L252A and L263A/R264A (not shown) — in which the dileucine-like motifs of Cx32 involved in the clathrin-mediated endocytosis have been mutated — formed larger GJs compared to those formed by WT-Cx32 (Figures 11 and 12, Cx32 and Cx43 in green). 3. Intriguingly, mutant L212A/I213A failed to assemble into GJs and remained scattered as discrete vesicular puncta throughout the cytoplasm (not shown).

The data shown in Figures 11 and 12 hinted that clathrin was involved in the endocytosis of Cx32. However, when we knocked down the AP2 subunit that is involved in clathrin-mediated endocytosis, we found that it had no effect on the

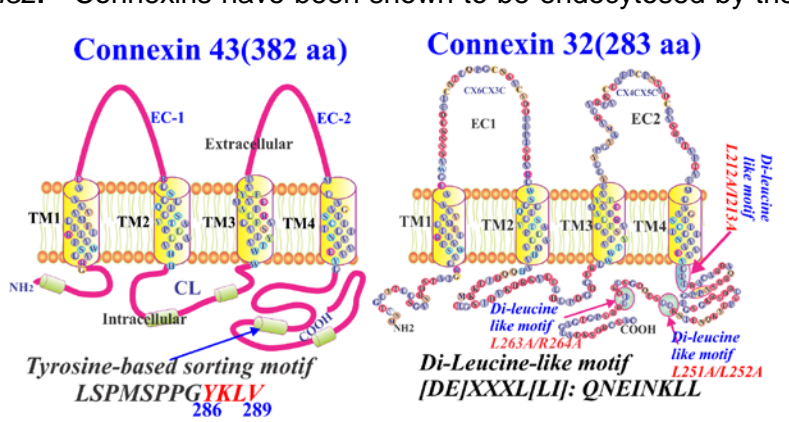


Figure 11. We generated an endocytosis-deficient Cx43 mutant, **Cx43Y286A/V289D**, in which tyrosine (Y) 286 and valine (V) 289 were substituted with alanine (A) and aspartate (D), respectively. We also generated dileucine-like motif deficient mutants of Cx32, **L251A/L252A** and **L263A/R264A**, in which leucines (L) and arginine(R) were replaced with alanines and **L212A/I213A**, in which leucine and isoleucine (I) were replaced by alanines.

These mutants were expected to be endocytosis-resistant and form large GJs.

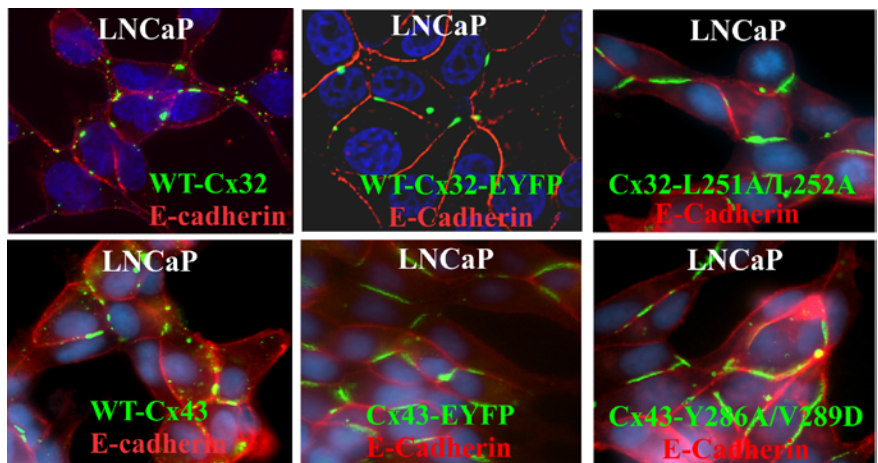


Figure 12. Wild-type and endocytosis-deficient mutants of Cx32 and Cx43 were introduced retrovirally in early passage LNCaP cells and formation of GJs was examined in pooled polyclonal cultures by immunocytochemical analysis. Note that compared to GJs formed by the wild-type Cxs, GJs formed by mutant Cxs (Cx43-Y286A/V289D, Cx32-L251A/L252A) are much larger. Note also that Cx43-EYFP also forms larger junctions as has been documented in earlier studies. This was used as a control. Cxs are green, E-Cadherin is red & nuclei are blue.

formation of GJs composed of Cx32-WT (**Figure 13**).

Task 11. Optimize the concentrations of chloropromazine and fillipin for inhibiting, respectively, clathrin and lipid raft/caveolae-mediated endocytosis, in LNCaP and PC-3 cells expressing connexin32 and connexin43, using immunocytochemical and biochemical approaches. (20-24 months).

Several studies have shown that Cxs and GJs are internalized by the clathrin-mediated pathway [61-64]. Also, previous studies had demonstrated either a direct or indirect interaction of Cx43 with caveolin 1 and caveolin 2 in NIH 3T3 cells and keratinocytes [65;66], suggesting a possible involvement of the non-clathrin-mediated pathway in the endocytosis of Cxs and GJs. Recently, GJs have also been found to be degraded by autophagy [67-70;70]. Because we observed no significant co-localization of Cx43 with clathrin, EEA1, and caveolin1 in static images (**See Figure 19 for images**) and because Cx43 trafficked normally to the cell surface yet failed to co-localize discernibly with endocytic markers in LNCaP cells, we used other approaches to examine which of the two pathways mediated endocytosis of Cx43.

We first used hypertonic sucrose to inhibit the clathrin-mediated pathway [71] and filipin to inhibit the non-clathrin-mediated pathway [72]. The specificity of inhibition of each pathway was assessed by measuring uptake of Alexa594-labeled transferrin or epidermal growth factor and Alexa594-labeled cholera toxin, which are predominantly endocytosed by the clathrin-mediated and the non-clathrin-mediated pathway, respectively [73] for 10-30 minutes. As assessed by immunocytochemical analysis, these

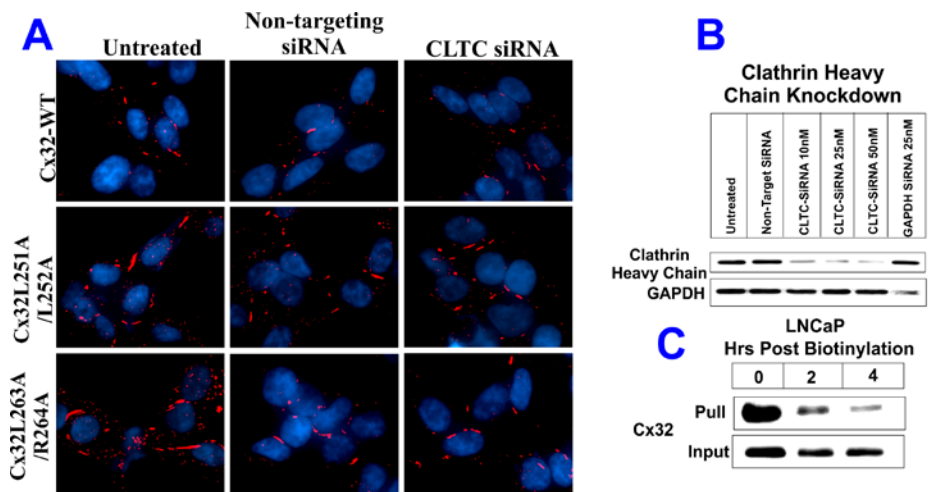


Figure 13. Clathrin knockdown has No Effect on Cx32 Degradation. Dileucine motifs have been shown to interact with clathrin via AP-2 to facilitate the internalization of membrane proteins. Hence, we knocked down the heavy chain of clathrin. We expected Cx32-WT to form larger GJs, similar to Cx32-L251A/L252A and Cx32-L263A/R264A if clathrin was involved in its endocytosis. Remarkably, clathrin knockdown had no effect on the size of GJs or its degradation (A), leaving open the mechanism by which Cx32 and the mutants are endocytosed. Western blot analysis showed that clathrin was knocked down efficiently (B). Knock down had no effect on the kinetics of degradation of Cx32 as assessed by cell surface biotinylation (C).

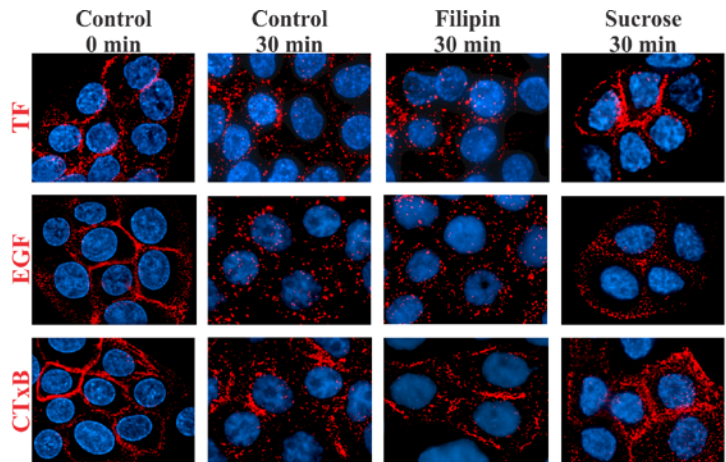


Figure 14. Filipin and hypertonic sucrose specifically inhibit lipid-raft and clathrin-mediated endocytosis in PC3 cells. Uptake of Alexa594-labeled transferrin (TF), epidermal growth factor (EGF) and Cholera toxin B (CTxB) was examined. Cells were treated with Filipin (7.5 μ g/ml) and hypertonic sucrose (0.45 M) for 5-30 minutes. Note that sucrose inhibited the uptake of only TF and EGF, while filipin inhibited the uptake of only CTxB. Chloropromazine had no effect on uptake of EGF, Cholera toxin B and transferrin in LNCaP and PC3 cells with a range of nontoxic concentrations tested (not shown).

studies showed that hypertonic sucrose inhibited the uptake of only transferrin and epidermal growth factor without affecting the uptake of cholera toxin while filipin inhibited the uptake of only cholera toxin without affecting the uptake of transferrin and EGF (**Figure 14, legend**). Consistent with the above studies, we found that hypertonic treatment caused the disappearance of Cx43 intracellular puncta whereas filipin had no effect. However, hypertonic treatment failed to induce discernible gap junction assembly (**Figure 15**). These findings hinted that the disappearance of intracellular puncta upon hypertonic treatment was likely caused by inhibition of clathrin-mediated endocytosis, which by itself was not sufficient to induce gap junction assembly.

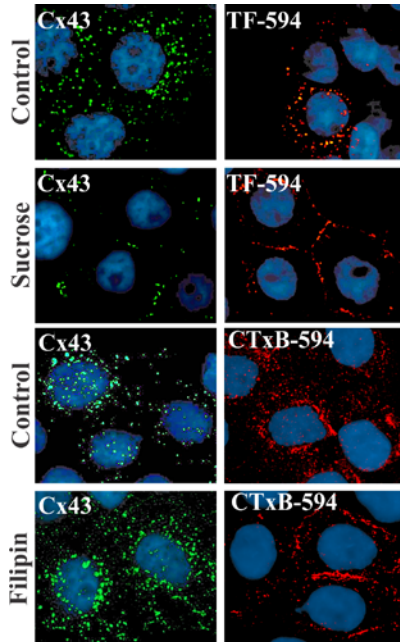


Figure 15. Effect of hypertonic sucrose and filipin on the intracellular accumulation of Cx43 in PC3 cells. PC3 cells, grown on glass cover slips in 6-well clusters, were treated with sucrose (0.45 M, 2 h) and Filipin (7.5 µg/ml, 1 h). Subcellular localization of Cx43 was examined immunocytochemically whereas the uptake of Alexa-594-conjugated transferrin (TF-594) and Alexa-594-conjugated cholera toxin B (CTxB-594) was measured as described in the text. Note that hypertonic sucrose inhibited the uptake of TF-594 and caused disappearance of intracellular Cx43 puncta. Note also that filipin inhibited the uptake of CTxB but had no effect on Cx43 localization.

Task 12. Develop as well as optimize methodology to knock down E-cadherin and N-cadherin in LNCaP and PC-3 cell lines using SiRNA and ShRNAs.

To explore whether the expression of E-cad and N-cad affects GJ assembly in a diametrically opposed way, we undertook two complementary experimental approaches. First, we designed ShRNAs to knock down N-cad. Second, because an independent approach to knock down E-cad using ShRNA was not successful as it failed to reduce the expression of E-cad (not shown), we introduced human N-cad in cells expressing E-cad to override E-cad-mediated cell-cell adhesion. We used recombinant retroviruses to express and knock down cadherins. Also, for these experiments both N-cad and E-cad were myc-tagged to distinguish them from their endogenously expressed counterparts. **Figures 16 and 17** show the representative data from three independent sets of experiments.

As assessed immunocytochemically and by the densitometric scanning of Western blots, ShN-cad decreased the expression level of N-cad by $80 \pm 7\%$ ($n=3$) (**Figure 16A**) with a concomitant decrease in the localization of N-cad at the areas of cell-cell contact (**Figure 16C**, compare top left panel with the bottom left panel), decrease in the intracellular accumulation of Cx43

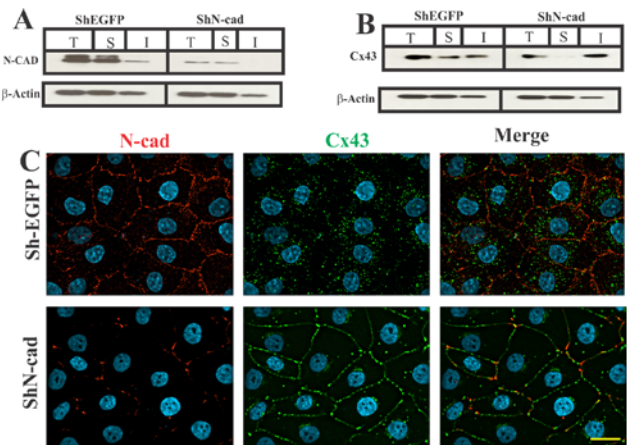


Figure 16. N-cad knockdown restores gap junction assembly in N-Cad expressing cells. Cells were infected with ShEGFP and ShN-Cad. Expression level of total (T), detergent-soluble (S) and detergent-insoluble (I) N-Cad (A) and Cx43 (B) were determined in cells infected with ShEGFP and ShN-Cad, respectively. Note that the N-Cad expression level is significantly reduced in ShN-Cad infected pooled polyclonal cultures (A), whereas the expression level of Cx43 (B) is not discernibly affected. Note also that knock down of N-Cad decreased the detergent soluble fraction, and increased the detergent-insoluble fraction, of Cx43. C. Pooled polyclonal cultures of N-cad expressing cells infected with ShEGFP and ShN-Cad were immunostained for Cx43 and N-Cad. Note the reduced expression of N-Cad at areas of cell-cell contact and in the intracellular pool, the disappearance of intracellular Cx43, and GJ formation in cells infected with ShN-Cad but not with control retrovirus (ShEGFP). Bar = 15 µm

Parmender P. Mehta, Ph.D.

and an increase in GJ assembly (**Figure 16C**, compare top middle and right panels with the corresponding bottom panels). Knock down of N-Cad had no discernible effect on the expression level of Cx43 but decreased the detergent-soluble fraction without affecting the detergent-insoluble fraction significantly (**Figure 16B**). These effects were not observed when cells were infected with ShEGFP (**Figure 16AB, left panels**) or ShP-Cad, an shRNA directed against placental cadherin (not shown).

In the next series of experiments, we introduced myc-tagged N-cad in E-cad expressing cells and myc-tagged E-cad in N-Cad cells. As assessed by quantitative immunocytochemical analysis, we found that the expression of E-cad in N-cad expressing cells induced GJ assembly and decreased intracellular Cx43 puncta (**Figure 17A**) whereas the expression of N-Cad in E-cad-expressing cells partially attenuated GJ assembly and caused intracellular accumulation of Cx43 (**Figure 17B**). Taken together, these our results document that the presence of N-cad at the cell surface is associated with the attenuation of GJ assembly, whereas the presence of E-cad with the facilitation of the assembly.

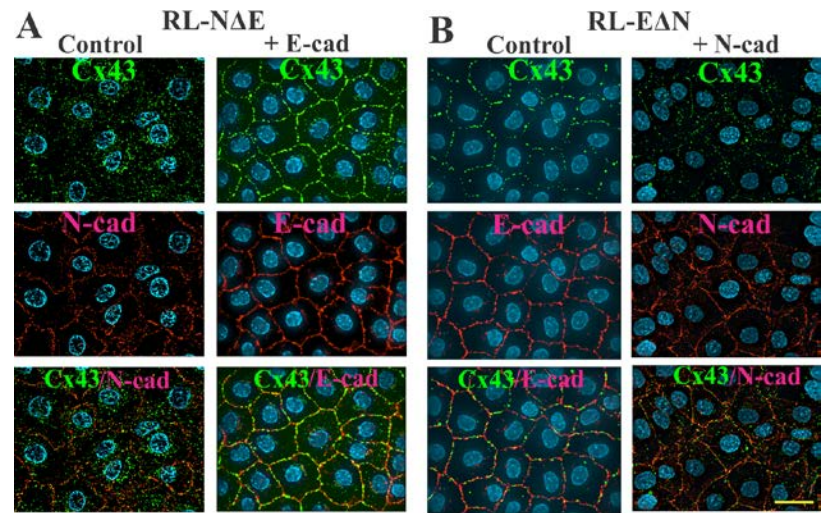


Figure 17. E-cadherin and N-cadherin have opposite effects on gap junction assembly. Myc-tagged N-Cad and E-Cad were introduced, respectively, into E-Cad expressing and N-Cad-expressing cells using recombinant retroviruses. Pooled polyclonal cultures were immunostained for Cx43 (green) and either endogenous cadherin or Myc (red). Note that E-Cad expression (+E-Cad) in N-cad expressing cells restores GJ formation (A) and N-Cad expression (+N-Cad) in E-cad expressing cells partially disrupts GJ assembly (B) and induces intracellular accumulation of Cx43. Bar = 20 μm.

Task 13. Generate recombinant retroviruses harboring shRNAs targeting various components of clathrin and lipid raft mediated endocytic pathways using retroviral packaging cell lines such as Amphotek and PTI67 (24-30 months).

These tasks were not initiated. Please see Figure 13 for clathrin knock down.

Task 14. Generate stable polyclonal cultures of LNCaP and PC-3 cells, using recombinant retroviruses, in which E-cadherin and N-cadherin has been knocked down or vice versa. (16-22 months).

This task was only partially accomplished. Please see Figure 16 for N-Cad knock down.

Task 15. Examine if knock down of E-cadherin or N-cadherin affects the trafficking of connexins and their subsequent assembly into gap junctions in E-cadherin expressing LNCaP cells and

N-cadherin expressing PC-3 cells (20-32 months).

This task was only partially accomplished. Please see Figure 10.

Task 16. Characterize organelle-specific markers for localizing connexins to different sorting compartments and ascertain, or rule out, if knock down or over-expression of E-cadherin and N-cadherin alters the subcellular fate of connexin32 and connexin43, or their subsequent assembly into gap junctions, as assessed by quantitative immunocytochemical and biochemical analyses in LNCaP and PC-3 cells (16-32 months).

Trafficking of Wild-type Cx32 and Its Mutants. To examine whether WT-Cx32 and its various mutants trafficked normally to the cell surface, we used cell-surface biotinylation as well as markers for the secretory and the endocytic compartments to assess their subcellular fate (**Figure 18A,B**). Using biotinylation of E-cad, a cell-surface protein, as a positive control, we found that WT-Cx32 and mutants L251A/L252A and L263A/R264A were biotinylated significantly whereas mutant L212A/I213A could not be significantly biotinylated (**Figure 18A**). These data suggested that despite abundant expression mutant L212A/I213A either trafficked poorly to the cell surface and/or was targeted to other subcellular compartments.

Connexins are Endocytosed non-canonically. Intriguingly, we also found that both WT-Cx32 and mutants L251A/L252A and L263A/R264A failed to co-localize with clathrin [74], with an early endocytic marker EEA1 [75], and with caveolin 1 (Cav 1) [76], which are the makers for the endocytic pathways (**Figure 19**). Also, no discernible co-localization was observed with GM130, a cis-Golgi-resident protein [77], Giantin, a Golgi-associated structural protein [78] and Caveolin 2 (Cav-2) [76], which are the makers for the secretory compartments (data not shown; but see **Figure 18B** for markers). In contrast, significant colocalization was observed with the lysosomal marker, Lamp2 [79;80] (not shown). Taken together, these data suggest that although the cytoplasmic tail of Cx32 harbors endocytic motifs that could potentially mediate its internalization by the clathrin-mediated pathway, the endocytic itinerary of both wild-type Cx32 and its various mutants seemed to be nonconventional compared to other transmembrane proteins at least in the cell

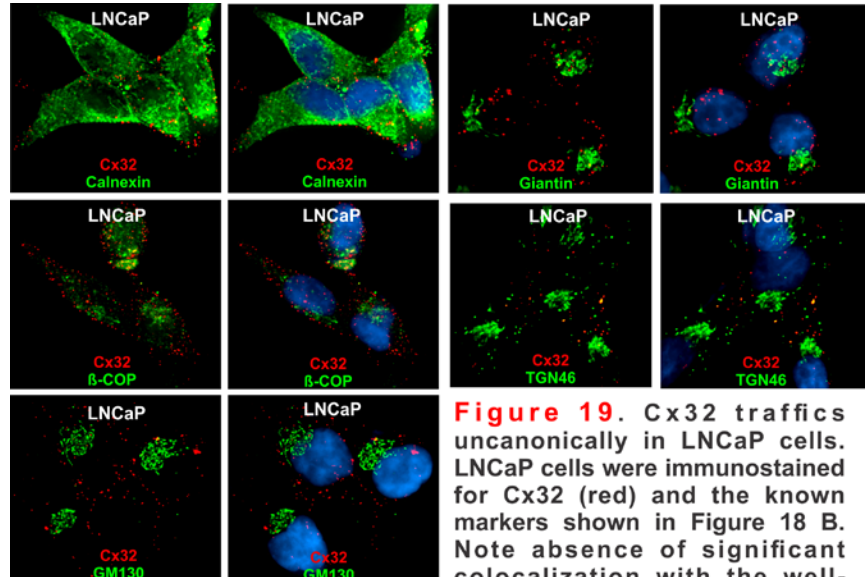
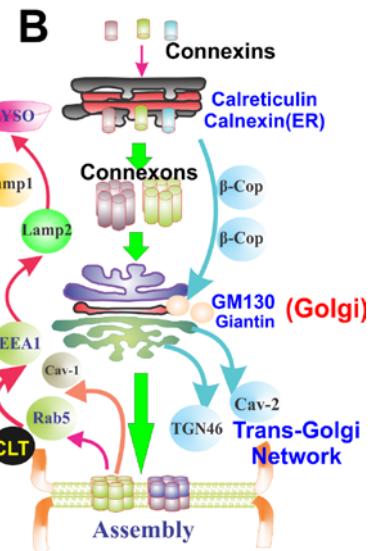
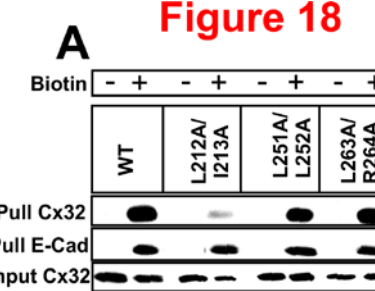


Figure 19. Cx32 traffics un canonically in LNCaP cells. LNCaP cells were immunostained for Cx32 (red) and the known markers shown in Figure 18 B. Note absence of significant colocalization with the well-characterized markers.

line used in the present study [81]. Also, these experiments identified a new dileucine-like motif in Cx32 that likely controls its trafficking to the cell surface and governs its assembly into GJs.

Task 17 Summarize and interpret data (12-36 months).

Miscellaneous

Live Cell Imaging of Gap Junctions. For determining the life-time of GJ plaques, we developed a procedure for the live cell imaging of LNCaP cells expressing fluorescently tagged Cxs. Cells were seeded on LabTek two well chamber slides and allowed to grow for 3 days. Cells containing GJ plaques (2-3 μm long) were chosen for live-cell imaging. After marking the positions of the plaques in X-Y plane, cells will be imaged every 15 min at 37°C for 8 h in an atmosphere of 5% CO₂/95% air in a live cell imaging chamber mounted on an Olympus IX81 motorized inverted microscope (Olympus America Inc; Center Valley, PA). The microscope is controlled by IX2-UCB U-HSTR2 motorized system with a focus drift compensatory device IX1-ZDC. Images will be captured using a Hamamatsu ORCA ER2 CCD camera and processed by imaging software Slide-book version 6.0 (Intelligent Imaging Innovations, Denver, CO). For each experimental condition, the life-time of 10 GJ plaques was determined. These procedures have also been described [45;82]. An example of the live cell imaging of a GJ plaque in LNCaP cells expressing EGFP-tagged Cx43 is shown in **Figure 20** (see legend for details). Our results showed that GJ plaques are long lived structures compared to short half-life of Cx43 and Cx32.

Knock down of Endogenous Cx43 in RWPE-1 and PZ-HPV-7 cell lines. To explore the role of GJs composed of Cx43 and Cx32 regulates the acinar differentiation of RWPE-1 and PZ-HPV-7 cells in 3-D cultures, we have knocked down the expression of endogenous Cx43 using Sh-Cx43RNA described in our previous studies [82]. As assessed by immunocytochemical and Western blot analysis, our results showed that Cx43

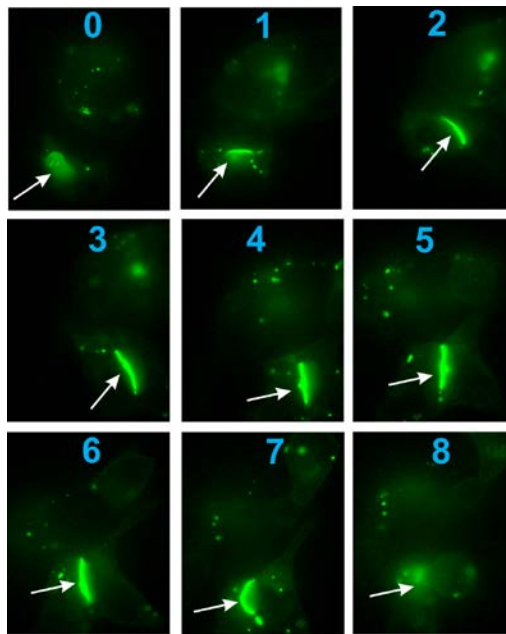


Figure 20. LNCaP cells expressing Cx43-EGFP were seeded on LabTek two well-chambers. After 48 h, the three GJ plaques, only one of which is in focus (indicated by the arrow) were imaged every 30 min at 37°C for 16 h on an Olympus IX81 motorized microscope. A GJ plaque is green and also changes position as the connected cells move within a few micrometers. The numbers in each panel indicate hours. Images were captured using a CCD camera and processed by imaging software Slidebook. Note that GJ plaque remains stable for at least 6 h and then collapsed suddenly within 1 h.

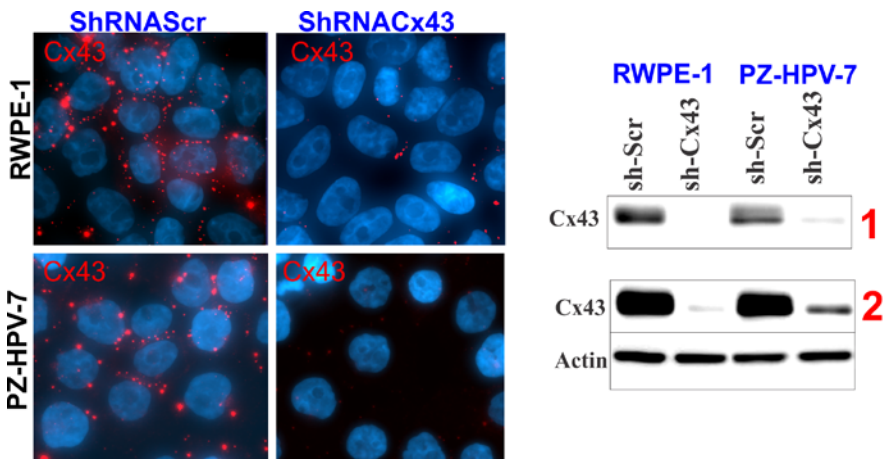


Figure 21. The expression of endogenous Cx43 was knocked down in RWPE-1 and PZ-HPV-7 cells using shRNACx43. ShRNA-Scr was used as a control. Note efficient knock down in both cell types. Knock down was assessed immunocytochemically and by Western blot analysis. Cx43 is in red. As assessed by Western blot analysis, the expression of Cx43 was reduced by more than 80%. Knock down was achieved through retroviral infection using pSuperRetro.puro. Shown are the pooled polyclonal cultures of both cell types after selection in puromycin. Numbers 1 and 2 represent low and high exposures of the blot.

Parmender P. Mehta, Ph.D.

expression was robustly reduced upon knock down in both cell types (**Figure 21, legend**). These knocked down cells will be used to express Cx43 and Cx32 and their mutants (described above) to assess their effect on acinar morphology in 3-D cultures.

3. Key Research Accomplishments

1. We have identified a key motif in the cytoplasmic tail of both Cx43 that regulates its endocytosis possibly by the clathrin-mediated pathway. The identified motif is —LSPMSPPG**YKLV**— which resides in the proline rich region encompassing amino acid 275 to 290 of Cx43.
2. Endocytosis of Cx43 is regulated through phosphorylation and dephosphorylation of serine 279 and 282 residing in this motif possibly via the clathrin-mediated pathway.
3. We have identified three dileucine-like motifs in the cytoplasmic tail of connexin32 that regulate its trafficking and endocytosis and control its assembly into GJs. The three dileucine [DE]XXXL[LI]-like motifs are the leucines 251 and 252, leucine 263 and arginine 264 and leucine 212 and isoleucine 213 in the cytoplasmic tail of Cx32. The motif **L212/I213** regulates trafficking whereas as motifs **L251/L252** and **L263/R264** regulate the endocytosis.
4. Retroviral-mediated expression of Cx43 and Cx32, in which motifs that regulate endocytosis have been mutated, in LNCaP cells results in the formation of large GJs.
5. ShRNAs to knock down N-cad and Cx43 were developed.

4. Reportable Outcomes:

1. The key research accomplishments supported by this award were reported at the following national and international meetings:
 - Johnson, K. E., Kelsey, L.K., and Mehta, PP (2008). Assembly of Connexin43 and Connexin32 is Regulated Differentially in a Human Cancer Cell lines. American Society For Cell Biology, Annual Meeting. San Diego, December 13-16.
 - Govindarajan, R., Chakraborty, S., Johnson, K.E., Kelsey, L.S., and Mehta, PP (2008). Assembly of Connexin43 into Gap Junctions is Differentially Regulated by E-cadherin and N-cadherin. American Society For Cell Biology, Annual Meeting. San Diego, December 13-16.
 - Johnson, KE., Kelsey, LS., Katoch, P., and Mehta, PP (2009). Trafficking and Assembly of connexins into gap junctions in human cancer cells. 2009 International conference on gap junctions, Sedona, Arizona, USA.
 - Mehta, PP (2010). Connexins and Chemoprevention of Prostate Cancer. Invited Speaker. 10th International Conference of Mechanism of Antimutagenesis and Anticarcinogenesis. September 26-29, Guaruja, Sao Paulo, Brazil.
 - Johnson, KE., Kelsey, LS., Katoch, P., and Mehta, PP (2011). Endocytosis of connexin43 and

Parmender P. Mehta, Ph.D.

the dynamics of gap junction assembly. American Society For Cell Biology, Annual Meeting. Denver, December 3-7.

- Katoch, P; Mitra, S., Johnson, KE., and Mehta, PP (2011). Cytoplasmic tail of connexin32 and the assembly of gap junctions. American Society For Cell Biology, Annual Meeting. Denver, December 3-7.
- Katoch, P., Ray, A., Kelsey, L., and Mehta, PP (2013). Two dileucine-like motifs govern the endocytosis of connexin32. International Meeting on Gap Junctions 2013, Charleston, SC. July 13-18.

2. The following key papers supported by this award have been published and are included as appendices. (see appendix).

- Chakraborty S, Mitra S, Falk, M, Caplan S, Wheelock MJ, Johnson K, and Mehta PP (2010). E-cadherin differentially regulates the assembly of connexin43 and connexin32 into gap junctions in human squamous carcinoma cells. *J Biol Chem* 285: 10761-10776.
- Govindarajan, R; Chakraborty, S; Johnson, KE; Falk, MM; Wheelock, MJ; Johnson, KR and Mehta, PP (2010). Assembly of connexin43 is differentially regulated by E-cadherin and N-cadherin in rat liver epithelial cells. *Mol Biol Cell* 21: 4089-4107.
- Kelsey, L; Katoch, P; Johnson, KE; Batra, SK; and Mehta, PP (2012). Retinoids regulate the formation and degradation of gap junctions in androgen-responsive human prostate cancer cells. *PLoS ONE*, 7: e32846
- Johnson, KJ; Mitra, S; Katoch, P; Kelsey, LS; Johnson, KR; and Mehta, PP (2013). Phosphorylation on Serines 279 and 282 of connexin43 regulates endocytosis and gap junction assembly in pancreatic cancer cells. *Mol Biol Cell*: 24, 715-733.

3. The following key paper supported by this award has been submitted for publication(see appendix).

Kelsey, L; Katoch, P; Ray, A; Mitra, S; Chakraborty, S; and Mehta, PP (2013). Vitamin D3 Regulates the Formation and Degradation of Gap Junctions in Androgen-Responsive Human Prostate Cancer Cells. *PLoS ONE*, Submitted.

4. The following student was supported in part by this award:

Parul Katoch: A sixth year graduate student. Expected date of graduation is May 2014.

Parmender P. Mehta, Ph.D.

5. Conclusions

The differentiated state of epithelial cells in normal prostate and in prostate tumors may depend on the assembly of Cx32 and Cx43 into gap junctions. During the progression of prostate cancer, pathways governing the trafficking and assembly of Cxs into gap junctions are impaired or altered. Cadherins regulate gap junction assembly and disassembly with metastasis-suppressing E-cad facilitating the assembly whereas metastasis-enhancing N-Cad facilitating disassembly. Both Cx43 and Cx32 are internalized by the clathrin-mediated endocytosis. However, both Cx43 and Cx32 traffic by the non-conventional endosomes. Our results also show that the defective assembly of both Cx43 and Cx32 is restored upon expressing sorting-motif mutants of these Cxs, which do not interact with the AP2 complex. For Cx43 our results have shown that phosphorylation of serine 279 and 282 targets it for endocytosis by the clathrin-mediated pathway. Thus, gap junctions composed of both Cx43 and Cx32 are internalized by clathrin-mediated endocytosis and are the targets of downstream signaling initiated by cadherins.

Reference List

1. Cunha GR, Donjacour AA, Cooke PS, Mee S, Bigsby RM, Higgins SJ, and Sugimura Y (1987) The endocrinology and developmental biology of the prostate. *Endocr Rev*, **8**, 338-362.
2. Arnold JT and Isaacs JT (2002) Mechanisms involved in the progression of androgen-independent prostate cancers: it is not only the cancer cell's fault. *Endocr.Relat Cancer*, **9**, 61-73.
3. Feldman BJ and Feldman D (2001) The development of androgen-independent prostate cancer. *Nature Rev.Cancer*, **1**, 34-45.
4. Goldstein,A.S., Huang,J., Guo,C., Garraway,I.P., and Witte,O.N. (2010) Identification of a Cell of Origin for Human Prostate Cancer. *Science*, **329**, 568-571.
5. Marker,P., Donjacour,A., Dahiya,R., and Cunha,G. (2003) Hormonal, cellular, and molecular control of prostatic development. *Dev.Biol*, **253**, 165-174.
6. Cunha,G., Donjacour,A., Cooke,P., Mee S, Bigsby,R., Higgins,S., and Sugimura,Y. (1987) The endocrinology and developmental biology of the prostate. *Endocr Rev*, **8**, 338-362.
7. Cunha GR, Alarid ET, Turner T, Donjacour AA, Boutin EE, and Foster BA (1992) Normal and abnormal development of the male urogenital tract.Role of androgens, mesenchymal-epithelial interactions, and growth factors. *J Androl*, **13**, 465-475.
8. Cunha GR, Foster BA, Donjacour AA, Rubin JS, Sugimura Y, Finch PW, Brody JR, and Aaronson SA (1994) Keratinocyte growth factor: a mediator of mesenchymal-epithelial interactions in the development of androgen target organs. In Motta M and Serio M (eds.) *Sex Hormones and Antihormones in Endocrine Dependent Pathology: Basic and Clinical Aspects*. Elsevier Science BV, pp 45-57.
9. Cunha GR (1994) Role of mesenchymal-epithelial interactions in normal and abnormal development of

Parmender P. Mehta, Ph.D.

the mammary gland and prostate. *Cancer*, **74**, 1030-1044.

10. Cunha GR, Hayward SW, Dahiya R, and Foster BA (1996) Smooth muscle-epithelial interactions in normal and neoplastic prostatic development. *Acta Anatomica*, **155**, 63-72.
11. Gumbiner,BM. (2005) Regulation of cadherin-mediated adhesion and morphogenesis. *Nat Rev Mol Cell Biol*, **6**, 622-634.
12. Nelson,W.J. (2008) Regulation of cell-to-cell adhesion by the cadherin-a-catenin complex. *Biochem Soc Trans*, **36**, 149-155.
13. Giepmans,B.N.G. and van IJzendoorn,S.C.D. (2009) Epithelial cell-cell junctions and plasma membrane domains. *Biochimica et Biophysica Acta (BBA) - Biomembranes*, **1788**, 820-831.
14. Laird,D.W. (2006) Life cycle of connexins in health and disease. *Biochem J*, **394**, 527-543.
15. Acevedo,V.D., Gangula,R.D., Freeman,K.W., Li,R., Zhang,Y., Wang,F., Ayala,G.E., Peterson,L.E., Ittmann,M., and Spencer,D.M. (2007) Inducible FGFR-1 Activation Leads to Irreversible Prostate Adenocarcinoma and an Epithelial-to-Mesenchymal Transition. *Cancer Cell*, **12**, 559-571.
16. Mosesson,Y., Mills,G.B., and Yarden,Y. (2008) Derailed endocytosis: an emerging feature of cancer. *Nat Rev Cancer*, **8**, 835-850.
17. Thiery,J.P., Acloque,H., Huang,R.Y.J., and Nieto,M.A. (2009) Epithelial-Mesenchymal Transitions in Development and Disease. *Cell*, **139**, 871-890.
18. Crespin,S., Defamie,N., Cronier,L., and Mesnil,M. (2009) Connexins and carcinogenesis. In Harris,A. and Locke,D. (eds.) *Connexinss: A Guide*., pp 529-42.
19. Mehta PP, Lokeshwar BL, Schiller PC, Bendix MV, Ostenson RC, Howard GA, and Roos BA (1996) Gap-junctional communication in normal and neoplastic prostate epithelial cells and its regulation by cAMP. *Molecular carcinogenesis*, **15**, 18-32.
20. Mehta,P.P., Perez-Stable,C., Nadji,M., Mian,M., Asotra,K., and Roos,B. (1999) Suppression of human prostate cancer cell growth by forced expression of connexin genes. *Dev Genetics*, **24**, 91-110.
21. Mehta,P.P. (2007) Introduction: A tribute to cell-cell channels. *J Membr.Biol*, **217**, 5-12.
22. Mehta,P., Bertram,J., and Loewenstein,W. (1986) Growth inhibition of transformed cells correlates with their junctional communication with normal cells. *Cell*, **44**, 187-196.
23. Naus,C.C. and Laird,D.W. (2010) Implications and challenges of connexin connections to cancer. *Nat Rev Cancer*, **10**, 435-441.
24. Saez,J.C., Berthoud,V.M., Branes,M.C., artinez,A.D., Bey., and Beyer,E.C. (2003) Plasma membrane

Parmender P. Mehta, Ph.D.

channels formed by connexins: their regulation and functions. *Physiol Rev*, **83**, 1359-1400.

25. Plante,I., Stewart,M.K.G., Barr,K., Allan,A.L., and Laird,D.W. (2010) Cx43 suppresses mammary tumor metastasis to the lung in a Cx43 mutant mouse model of human disease. *Oncogene*, **30**, 1681-1692.
26. McLachlan,E., Shao,Q., Wang,H.I., Langlois,S., and Laird,D.W. (2006) Connexins act as tumor suppressors in three dimensional mammary cell organoids by regulating differentiation and angiogenesis. *Cancer Res*, **66**, 9886-9894.
27. King TJ, Gurley KE, Prunty J, Shin JL, Kemp CJ, and Lampe PD (2005) Deficiency in the gap junction protein connexin32 alters p27Kip1 tumor suppression and MAPK activation in a tissue-specific manner. *Oncogene*, **24**, 1718-1726.
28. King,T.J. and Lampe,P.D. (2004) Mice deficient for the gap junction protein Connexin32 exhibit increased radiation-induced tumorigenesis associated with elevated mitogen-activated protein kinase (p44/Erk1, p42/Erk2) activation. *Carcinogenesis*, **25**, 669-680.
29. King,T.J. and Bertram,J.S. (2005) Connexins as targets for cancer chemoprevention and chemotherapy. *Biochimica et Biophysica Acta (BBA) - Biomembranes*, **1719**, 146-160.
30. Laird,D.W. (2010) The gap junction proteome and its relationship to disease. *Trends Cell Biol*, **20**, 92-101.
31. Bosco,D., Haefliger,J.A., and Meda,P. (2011) Connexins: Key Mediators of Endocrine Function. *Physiol.Rev.*, **91**, 1393-1445.
32. Govindarajan,R., Song,X.-H., Guo,R.-J., Wheelock,M.J., Johnson,K.R., and Mehta,P.P. (2002) Impaired trafficking of connexins in androgen-independent human prostate cancer cell lines and its mitigation by a-catenin. *J Biol Chem*, **277**, 50087-50097.
33. Kalra,J., Shao,Q., Qin,H., Thomas,T., aoui-Jamali,M.A., and Laird,D.W. (2006) Cx26 inhibits breast MDA-MB-435 cell tumorigenic properties by a gap junctional intercellular communication-independent mechanism. *Carcinogenesis*, **27**, 2528-2537.
34. Shao,Q., Wang,H., McLachlan,E., Veitch,G.I.L., and Laird,D.W. (2005) Down-regulation of Cx43 by Retroviral Delivery of Small Interfering RNA Promotes an Aggressive Breast Cancer Cell Phenotype. *Cancer Research*, **65**, 2705-2711.
35. Wang,M., BERTHOUD,V.M., and BEYER,E.C. (2007) Connexin43 increases the sensitivity of prostate cancer cells to TNF{alpha}-induced apoptosis. *Journal of Cell Science*, **120**, 320-329.
36. Kelsey,L., Katoch,P., johnson,K., Batra,S.K., and Mehta,P. (2012) Retinoids regulate the formation and degradation of gap junctions in androgen-responsive human prostate cancer cells. *PLoS ONE*, **7**, E32846.

Parmender P. Mehta, Ph.D.

37. Harris,A.L. (2007) Connexin channel permeability to cytoplasmic molecules. *Progress in Biophysics and Molecular Biology*, **94**, 120-143.
38. Beltramello,M., Piazza,V., Bukauskas,F.F., Pozzan,T., and Mammano,F. (2005) Impaired permeability to Ins(1,4,5)P₃ in a mutant connexin underlies recessive hereditary deafness. *Nature Cell Biology*, **7**, 63-69.
39. Chakraborty,S., Mitra,S., Falk,M.M., Caplan,S., Wheelock,M.J., Johnson,K.R., and Mehta,P.P. (2010) E-cadherin differentially regulates the assembly of connexin43 and connexin32 into gap junctions in human squamous carcinoma cells. *J Biol Chem*, **285**, 10761-10776.
40. Kojima,T., Kokai,Y., Chiba,H., Yamamoto,M., Mochizuki,Y., and Sawada,N. (2001) Cx32 but Not Cx26 Is Associated with Tight Junctions in Primary Cultures of Rat Hepatocytes. *Experimental Cell Research*, **263**, 193-201.
41. Kojima,T., Murata,M., Go,M., Spray,D.C., and Sawada,N. (2007) Connexins induce and maintain tight junctions in epithelial cells. *J Membr.Biol*, **217**, 13-19.
42. Mehta,P., Bertram,J., and Loewenstein,W. (1989) The actions of retinoids on cellular growth correlate with their actions on gap junctional communication. *J Cell Biol*, **108**, 1053-1065.
43. Mitra,S., Annamalai,L., Chakraborty,S., Johnson,K., Song,X., Batra,S.K., and Mehta,P.P. (2006) Androgen-regulated Formation and Degradation of Gap Junctions in Androgen-responsive Human Prostate Cancer Cells. *Mol Biol Cell*, **17**, 5400-5416.
44. VanSlyke,J.K. and Musil,L.S. (2000) Analysis of connexin intracellular transport and assembly. *Methods*, **20**, 156-164.
45. Govindarajan,R., Chakraborty,S., Falk,M.M., Johnson KR, Wheelock,M.J., and Mehta,P.P. (2010) Assembly of connexin43 is differentially regulated by E-cadherin and N-cadherin in rat liver epithelial cells. *Mol Biol Cell*, **21**, 4089-4107.
46. Habermann,H., Ray,V., and Prins,G. (2002) Alterations in gap junction protein expression in human benign prostatic hyperplasia and prostate cancer. *J Urol*, **167**, 655-660.
47. Wheelock,M.J., Shintani,Y., Maeda,M., Fukumoto,Y., and Johnson,K.R. (2008) Cadherin switching. *J Cell Sci*, **121**, 727-735.
48. Gravdal,K., Halvorsen,O.J., Haukaas,S.A., and Akslen,L.A. (2007) A Switch from E-Cadherin to N-Cadherin Expression Indicates Epithelial to Mesenchymal Transition and Is of Strong and Independent Importance for the Progress of Prostate Cancer. *Clin Cancer Res*, **13**, 7003-7011.
49. Shah,G.V., Muralidharan,A., Gokulgandhi,M., Soan,K., and Thomas,S. (2009) Cadherin Switching and Activation of a-Catenin Signaling Underlie Proinvasive Actions of Calcitonin-Calcitonin Receptor Axis in Prostate Cancer. *J.Biol.Chem.*, **284**, 1018-1030.

Parmender P. Mehta, Ph.D.

50. Kyprianou,N. (2010) ASK-ing EMT not to spread cancer. *PNAS*, **107**, 2731-2732.
51. Tomita,K., van Bokhoven,A., van Leenders,G.J.L.H., Ruijter,E.T.G., Jansen,C.F.J., Bussemakers,M.J.G., and Schalken,J.A. (2000) Cadherin Switching in Human Prostate Cancer Progression. *Cancer Research*, **60**, 3650-3654.
52. Drake,J.M., Strohbehn,G., Bair,T.B., Moreland,J.G., and Henry,M.D. (2009) ZEB1 Enhances Transendothelial Migration and Represses the Epithelial Phenotype of Prostate Cancer Cells. *Mol.Biol.Cell*, **20**, 2207-2217.
53. Chu,K., Cheng,C.J., Ye,X., Lee,Y.C., Zurita,A.J., Chen,D.T., Yu-Lee,L.Y., Zhang,S., Yeh,E.T., Hu,M.C.T., Logothetis,C.J., and Lin,S.H. (2008) Cadherin-11 Promotes the Metastasis of Prostate Cancer Cells to Bone. *Mol Cancer Res*, **6**, 1259-1267.
54. Jennbacken K, Tesan T, Wang W, Gustvasson,H., Damber J-E, and Welenm K (2010) N-cadherin increases after androgen deprivation and is associated with metastasis in prostate cancer. *Endocr Relat Cancer*, **17**, 469-479.
55. Huang,C.F., Lira,C., Chu,K., Bilen,M.A., Lee,Y.C., Ye,X., Kim,S.M., Ortiz,A., Wu,F.L.L., Logothetis,C.J., Yu-Lee,L.Y., and Lin,S.H. (2010) Cadherin-11 Increases Migration and Invasion of Prostate Cancer Cells and Enhances their Interaction with Osteoblasts. *Cancer Research*, **70**, 4580-4589.
56. Tanaka,H., Kono,E., Tran,C.P., Miyazaki,H., Yamashiro,J., Shimomura,T., Fazli,L., Wada,R., Huang,J., Vessella,R.L., An,J., Horvath,S., Gleave,M., Rettig,M.B., Wainberg,Z.A., and Reiter,R.E. (2010) Monoclonal antibody targeting of N-cadherin inhibits prostate cancer growth, metastasis and castration resistance. *Nat Med*, **16**, 1414-1420.
57. Thevenin,A.F., Kowal,T.J., Fong,J.T., Kells,R.M., Fisher,C.G., and Falk,M.M. (2013) Proteins and Mechanisms Regulating Gap-Junction Assembly, Internalization, and Degradation. *Physiology*, **28**, 93-116.
58. Thomas MA, Zosso N, Scerri I, Demaurex N, Chanson M, and Staub O (2003) A tyrosine-based sorting signal is involved connexin43 stability and gap junction turnover. *J Cell Sci*, **116**, 2213-2222.
59. Mehta PP, Hotz-Wagenblatt A, Rose B, Shalloway D, and Loewenstein WR (1991) Incorporation of the gene for a cell-to-cell channel proteins into transformed cells leads to normalization of growth. *Journal of Membrane Biology*, **124**, 207-225.
60. Mehta PP, Perez-Stable C, Nadji Mehrdad, Mian M, Asotra K, and Roos BA (1999) Suppression of human prostate cancer cell growth by forced expression of connexin genes. *Dev Genetics*, **24**, 91-110.
61. Falk,M.M., Baker,S.M., Gumpert,A., Segretain,D., and Buckheit,R.W. (2009) Gap junction turnover is achieved by the internalization of small endocytic double-membrane vesicles. *Mol Biol Cell*, **20**, 3342-3352.

Parmender P. Mehta, Ph.D.

62. Gumpert,A.M., Varco,J.S., Baker,S.M., Piehl,M., and Falk,M.M. (2008) Double-membrane gap junction internalization requires the clathrin-mediated endocytic machinery. *FEBS Letters*, **582**, 2887-2892.
63. Piehl,M., Lehmann,C., Gumpert,A., Denizot,J.P., Segretain,D., and Falk,M.M. (2007) Internalization of Large Double-Membrane Intercellular Vesicles by a Clathrin-dependent Endocytic Process. *Mol.Biol.Cell*, **18**, 337-347.
64. Nickel,B.M., DeFranco,B.H., Gay,V.L., and Murray,S.A. (2008) Clathrin and Cx43 gap junction plaque endoexocytosis. *Biochem.Biophys.Res.Commun.*, **374**, 679-682.
65. Langlois,S., Cowan,K.N., Shao,Q., Cowan,B.J., and Laird,D.W. (2008) Caveolin-1 and -2 Interact with Connexin43 and Regulate Gap Junctional Intercellular Communication in Keratinocytes. *Mol.Biol.Cell*, **19**, 912-928.
66. Schubert,A., Schubert,W., Spray,D.C., and Lisanti,M.P. (2002) Connexin family members target to lipid raft domains and interact with caveolin-1. *Biochemistry*, **41**, 5754-5764.
67. Lichtenstein,A., Minogue,P.J., BEYER,E.C., and BERTHOUD,V.M. (2011) Autophagy: a pathway that contributes to connexin degradation. *J Cell Sci*, **124**, 910-920.
68. Hesketh,G.G., Shah,M.H., Halperin,V.L., Cooke,C.A., Akar,F.G., Yen,T.E., Kass,D.A., Machamer,C.E., Van Eyk,J.E., and Tomaselli,G.F. (2010) Ultrastructure and Regulation of Lateralized Connexin43 in the Failing Heart. *Circ Res*, **106**, 1153-1163.
69. Bejiarno,E., Girao,H., Yuste,A., Patel,B., Marques,C., Spray,D., Pereira,P., and Cuervo,A. (2012) Autophagy modulates dyanimcs of connexons at the plasma membrane in an ubiquitin-dependent manner. *Mol Biol Cell*, **23**, 2156-2169.
70. Fong,J., Kells,R., Gumpert,A., Marzillier,J., Davidson,M., and Falk,M. (2012) Internalized gap junctions are degraded by autophagy. *Autophagy*, **8**, 738-755.
71. Heuser,J.E. and Anderson,R.G. (1989) Hypertonic media inhibit receptor-mediated endocytosis by blocking clathrin-coated pit formation. *J.Cell Biol.*, **108**, 389-400.
72. Schnitzer,J.E., Oh,P., Pinney,E., and Allard,J. (1994) Filipin-sensitive caveolae-mediated transport in endothelium: reduced transcytosis, scavenger endocytosis, and capillary permeability of select macromolecules. *J.Cell Biol.*, **127**, 1217-1232.
73. Orlandi,P.A. and Fishman,P.H. (1998) Filipin-dependent Inhibition of Cholera Toxin: Evidence for Toxin Internalization and Activation through Caveolae-like Domains. *J.Cell Biol.*, **141**, 905-915.
74. Roth,M.G. (2006) Clathrin-mediated endocytosis before fluorescent proteins. *Nat Rev Mol Cell Biol*, **7**, 63-68.

Parmender P. Mehta, Ph.D.

75. Mills,I.G., Jones,A.T., and Clague,M.J. (1998) Involvement of the endosomal autoantigen EEA1 in homotypic fusion of early endosomes. *Current Biol*, **8**, 881-884.
76. Parton,R.G. and Simons,K. (2007) The multiple faces of caveolae. *Nat Rev Mol Cell Biol*, **8**, 185-194.
77. Nakamura,N., Rabouille,C., Watson,R., Nilsson,T., Hui,N., Slusarewicz,P., Kreis,T.E., and Warren,G. (1995) Characterization of a cis-Golgi matrix protein, GM130. *J.Cell Biol.*, **131**, 1715-1726.
78. Jiang,S., Rhee,S.W., Gleeson,P.A., and Storrie,B. (2006) Capacity of the Golgi Apparatus for Cargo Transport Prior to Complete Assembly. *Mol.Biol.Cell*, **17**, 4105-4117.
79. Hunziker,W. and Geuze,H. (2011) Intracellular trafficking of lysosomal proteins. *EMBO J*, **18**, 379-389.
80. Rohrer,J., Schweizer,A., Russell,D., and Kornfeld,S. (1996) The targeting of Lamp1 to lysosomes is dependent on the spacing of its cytoplasmic tail tyrosine sorting motif relative to the membrane. *J.Cell Biol.*, **132**, 565-576.
81. Bonifacino,J.S. and Traub,L.M. (2003) Signals for sorting of transmembrane proteins to endosomes and lysosomes. *Ann Rev Biochem*, **72**, 395-447.
82. Johnson,K.E., Mitra,S., Katoch,P., Kelsey,L.S., Johnson,K.R., and Mehta,P.P. (2013) Phosphorylation on Ser-279 and Ser-282 of connexin43 regulates endocytosis and gap junction assembly in pancreatic cancer cells. *Mol.Biol.Cell*, **24**, 715-733.

Appendices:

4 published manuscripts and 1 submitted manuscript are appended.

Supporting Data:

None.

Abstract: 2008

Johnson, K. E., Kelsey, L.K., and Mehta, PP (2008). Assembly of Connexin43 and Connexin32 is Regulated Differentially in a Human Cancer Cell lines. American Society for Cell Biology, Annual Meeting. San Diego, December 13-16.

Kristen E. Johnson, Linda Kelsey, and Parmender P. Mehta

Department of Biochemistry and Molecular Biology University of Nebraska Medical Center, Omaha, NE, 68198

The trafficking and assembly of connexins (Cx) into gap junctions are defective in different cancers, however, the molecular basis of this defect has not yet been defined. In particular, the role of Cx in the pathogenesis of pancreatic cancer has not yet been explored. As a first step towards achieving this end, we have examined the expression and localization of Cx43, Cx26, Cx32 and Cx36 — the four Cx expressed in the normal pancreas, in various pancreatic cancer cell lines. In one model cell line, BxPC3, we found that Cx43 was inefficiently assembled into gap junctions despite adequate expression and remained intracellular. In contrast, exogenously-introduced Cx32 was assembled efficiently into gap junctions in BxPC3 cells. Immunocytochemical analyses revealed that Cx43 co-localized partially with both early secretory and with endocytic markers such as GM-130, EEA1, clathrin, caveolin-1 and Lamp-1. Cell surface biotinylation revealed that Cx43 trafficked normally to the cell surface, suggesting that it was endocytosed prior to its assembly into gap junctions. To determine the pathway by which Cx43 was endocytosed, we used chlorpromazine, which inhibits the clathrin-mediated pathway, and filipin and methyl-β-cyclodextrin (MβCD), which inhibit the lipid raft-mediated pathway. We found that both classes of inhibitors attenuated the endocytosis of Cx43 and facilitated its assembly into gap junctions. Our findings suggest that the assembly of Cx43 and Cx32 into gap junctions upon arrival at the cell surface is subject to Cx-specific distinct regulatory mechanisms at the site of cell-cell contact.

Abstract: 2008

Govindarajan, R., Chakraborty, S., Johnson, K.E., Kelsey, L.S., and Mehta, PP (2008). Assembly of Connexin43 into Gap Junctions is Differentially Regulated by E-cadherin and N-cadherin. American Society for Cell Biology, Annual Meeting. San Diego, December 13-16.

Assembly of Connexin43 into Gap Junctions is Differentially Regulated by E-cadherin and N-cadherin.

Rajgopal Govindarajan, Souvik Chakraborty, Kristen E. Johnson, Linda Kelsey and Parmender P. Mehta

Department of Biochemistry and Molecular Biology University of Nebraska Medical Center, Omaha, NE, 68198.

Loss of E-cadherin expression triggers dissemination of tumor cells, whereas gain of N-cadherin expression triggers motility. Hence, we investigated whether these cadherins affect the assembly of gap junctions differently. The assembly of connexin (Cx)43 into gap junctions was investigated in iso-genic clones, derived from rat liver clone9 (RL-CL9) cells, that express either E-cadherin or N-cadherin. We hypothesized that E-cadherin will facilitate the assembly whereas N-cadherin would disrupt it. The assembly of Cx43 into gap junctions was examined immunocytochemically and biochemically by detergent-solubility assay. In E-cadherin expressing clones, Cx43 was assembled into large, detergent-insoluble gap junctions whereas in N-cadherin expressing clones it remained intracellular as discrete puncta, which remained detergent-insoluble. Forced expression of N-cadherin in E-cadherin expressing clones disassembled gap junctions whereas shRNA-mediated knock down of N-cadherin induced gap junction assembly. Cell surface biotinylation revealed that Cx43 trafficked normally, and degraded with a similar kinetics, both in E-cadherin and N-cadherin clones, suggesting that the intracellular accumulation was not caused by impaired trafficking but by endocytosis prior to gap junction assembly. To test this notion, we investigated the pathway by which Cx43 was endocytosed. We used chlorpromazine to inhibit clathrin-mediated pathway and filipin and methyl- β -cyclodextrin (M β CD) to inhibit lipid raft- mediated pathway. Both filipin and M β CD increased gap junction assembly profoundly in N-cadherin expressing clones but had no effect on the assembly in E-cadherin clones. Immunocytochemical analyses revealed that Cx43 in N-cadherin expressing clones did not co-localize with early endocytic markers such as EEA1, clathrin and caveolin-1. These data suggest that N-cadherin disrupts gap junction assembly by inducing the endocytosis of Cx43 into detergent-resistant vesicles prior to its assembly into gap junctions. The diametrically opposed effect of E-cadherin and N-cadherin on gap junction assembly may rationally explain the intriguing and contrasting roles of these cadherins in regulating tumor cell motility.

Abstract: 2009

Johnson, KE., Kelsey, LS., Katoch, P., and Mehta, PP (2009). Trafficking and Assembly of connexins into gap junctions in human cancer cells. 2009 International conference on gap junctions, Sedona, Arizona, USA.

Cell-Cell Contact and the Determinants of Gap Junction Assembly and Growth

Kristen E. Johnson, Linda Kelsey, Parul Katoch and Parmender P. Mehta

Department of Biochemistry and Molecular Biology, University of Nebraska Medical Center, Omaha, NE 68198

It is as yet unknown how the trafficking and assembly of connexin(Cx)s into gap junction(GJ)s are initiated upon cell-cell contact. The importance of undertaking these studies is underscored by the fact that dysfunctional cell-cell adhesion and aberrant assembly of Cxs into GJs are the hallmarks of cancer progression. We investigated whether the assembly of Cx32 into GJs were contingent upon E-cadherin mediated cell-cell adhesion. We also examined the role of carboxyl terminus (CT) of these Cxs in initiating the formation of GJs and in determining the GJ size. Using cadherin and Cx null cells, and by introducing Cx43 and Cx32, either alone or in combination with E-cadherin, we demonstrated that cadherin-mediated cell-cell adhesion was neither essential nor sufficient to initiate GJ assembly *de novo*, and facilitated the assembly of only preformed GJs composed of Cx43 whereas the growth of cells on trans-well filters was required to initiate the assembly of Cx32. We also demonstrated that ZO-1 and the CT of Cx43 were required to initiate GJ assembly *de novo* or to stabilize them via direct or indirect interaction with the actin. To define motifs that determine the size of GJs composed of Cx32, a series of deletion mutants, with progressive truncation of 20 amino acids, was expressed in prostate cancer cell line, LNCaP, by recombinant retroviruses. The data showed that critical motifs that determined the size of GJs spanned between amino-acids 230-250 of Cx32CT, which contained two PKA phosphorylation sites RKGS and RLS, with putative phosphorylatable serine(S) residues at positions 233 and 240. To determine if phosphorylation of S233 and S240 of Cx32CT regulated GJ size, we substituted these residues with alanine and expressed the mutated Cxs by recombinant retroviruses in LNCaP cells. While a decrease in the frequency of larger GJs was seen in a double-mutant Cx32S233A-S240A, the most significant decrease was observed when two additional serines, S225 and S229, were substituted with alanine. These data suggest that phosphorylation of Cx32CT at these residues determines GJ size. Our findings suggest that the assembly of Cx32 and Cx43 into GJs is subject to regulatory mechanisms at cell-cell contact and that the assembly is governed by a complex interplay of E-cadherin, the carboxyl termini of Cxs and the actin cytoskeleton.

Abstract: 2010

Mehta, PP (2010). Connexins and Chemoprevention of Prostate Cancer. Invited Speaker. 10th International Conference of Mechanism of Antimutagenesis and Anticarcinogenesis. September 26-29, Guaruja, Sao Paolo, Brazil.

Connexins and Chemoprevention of Prostate Cancer

Parmender P. Mehta, Department of Biochemistry and Molecular Biology, University of Nebraska Medical Center, Omaha, NE 68198

Prostate cancer has been estimated to be the second leading cause of death among ageing men in the United States. Two hallmarks distinguish prostate cancer from other cancers: The first is the discrepancy between the high prevalence of latent cancer and the lower prevalence of clinical cancer. The second hallmark is its progression from a slow-growing, androgen-dependent state to a virulent, androgen-independent state. Thus, identification of molecular events that facilitate the clonal expansion and dissemination of organ-confined malignant prostate cancer cells to distant metastatic sites is crucial for designing strategies for the chemoprevention. Although it is well-established that the androgens and the natural and the synthetic analogs of vitamin A and D govern the proliferation and differentiation of normal and malignant prostate epithelial cells, the mechanisms involved have remained obscure. Our studies have shown that the expression of connexin connexin43 and connexin32 in an indolent, androgen-dependent prostate cancer cell line, LNCaP, retards growth, whereas that in an invasive, androgen-independent cell line, PC-3, results in their intracellular accumulation without significant effect on growth. Using connexin43 and connexin32 expressing LNCaP clones, we have examined the effect of Di-hydro testosterone (DHT), a synthetic androgen mibolerone (MB), 1, 25 (OH)2 vitamin D₃ (1,25 D), all-trans-retinoic acid (ATRA), and 9-Cis retinoic acid (9-CRA), either alone or in combination, on the formation and degradation of gap junctions. Treatment with DHT (10-100 nM), MB (1-5 nM), 1,25 D (10-100 nM), ATRA and 9 CRA (1µM) increased the assembly of both connexins into gap junctions as assessed immunocytochemically and biochemically by western blot analyses of Triton X-100-insoluble cell extracts. Androgen removal induced the degradation of gap junctions composed of connexin32 and the degradation was prevented by ATRA, 9-CRA and 1,25 D. The expression and degradation of E-cadherin and occludin, the constituent proteins of adherens and tight junctions, were not significantly affected. We also studied the effect of these agents on the formation and degradation of gap junctions in LNCaP clones expressing C-terminus deleted mutants of connexin32 and connexin43 to investigate if intact C-termini were required. Our findings suggest that one of the mechanisms by which these agents might maintain the differentiated state of prostate epithelial cells and act as chemopreventive agents may be related to their ability to control the formation and degradation of gap junctions.

Abstract: 2011

Johnson, KE., Kelsey, LS., Katoch, P., and Mehta, PP (2011). Endocytosis of connexin43 and the dynamics of gap junction assembly. American Society For Cell Biology, Annual Meeting. Denver, December 3-7.

Endocytosis of Connexin43 and the Dynamics of Gap Junction Assembly

Kristen E. Johnson, Parul Katoch, Linda Kelsey, and Parmender P. Mehta
Department of Biochemistry and Molecular Biology, University of Nebraska Medical Center, Omaha, NE 68198

Connexin(Cx)s, the constituent proteins of gap junctions, are expressed both in a tissue-specific manner as well as redundantly. Redundant and tissue-specific expression implies that distinct mechanisms must exist to regulate the assembly of each Cx into gap junctions. The importance of understanding this is underscored by the fact that the trafficking and assembly of Cxs into gap junctions are defective in different cancers. To explore how the assembly of Cxs is regulated upon arrival at the cell surface, we used two pancreatic cancer cell lines, BxPC3, in which Cx43 is inefficiently assembled and remains intracellular while Cx26 is efficiently assembled into gap junctions, and Capan-1, in which both Cxs are inefficiently assembled. Cell surface biotinylation showed that Cx43 trafficked normally to the cell surface and was endocytosed by the clathrin-mediated pathway in a Rab5-dependent manner before its assembly into gap junctions. Yeast two hybrid analysis showed that Cx43 interacted with the μ 2 subunit of the AP-2 complex via a consensus sorting signal, YKLV, residing in its cytoplasmic tail between amino acid residues 286-289. Retrovirus mediated transduction of mutant Cx43Y286A/V289D, but not of wild type Cx43, induced gap junction assembly in BxPC3 and Capan-1 cells. Phosphorylation of serines in the vicinity of YKLV has been shown to modulate the interaction between the cargo and the AP-2 complex. As assessed by immunocytochemical analysis, we found that transient transfection of mutants Cx43S279A and Cx43S282A, but not of Cx43S279D and Cx43S282D, also induced gap junction assembly in both cell lines. Transient transfection of mutants Cx43Y286/V289D, Cx43S279A and Cx43S282A also prevented endocytosis of Cx43 in single cells. Finally, retrovirally-introduced Cx32 was assembled efficiently into gap junctions in BxPC3 cells. Our findings document that the assembly of Cxs into gap junctions upon arrival at the cell surface is subject to regulatory mechanisms at the site of cell-cell contact that are likely to be Cx specific.

Abstract: 2011

Katoch, P; Mitra, S., Johnson, KE., and Mehta, PP (2011). Cytoplasmic tail of connexin32 and the assembly of gap junctions. American Society for Cell Biology, Annual Meeting. Denver, December 3-7.

The Cytoplasmic Tail of Connexin32 and the Assembly of Gap Junctions

Parul Katoch, Shalini Mitra, Kristen E. Johnson, and Parmender P. Mehta

Department of Biochemistry and Molecular Biology, University of Nebraska Medical Center, Omaha, NE 68198

The spatio-temporal events and cellular factors required for the de novo formation of a nascent gap junction plaque, its growth, and disassembly are poorly understood. The assembly of gap junctions is a multi-step process, and is initiated when six connexin(Cx)s oligomerize to form connexons, which dock with connexons on

contiguous cells to form intercellular channels. A gap junction plaque is formed when several intercellular channels cluster. We previously showed that the carboxyl tail (CT) of Cx32, a Cx highly expressed in well-differentiated and polarized cells, may be required to initiate the formation of a gap junction plaque and/or its subsequent growth. To explore the role of Cx32-CT further, a CT-truncated Cx32 (Cx32 Δ 220) as well as full length Cx32 (Cx32-FL) were retrovirally introduced in three separate cell-culture model systems. As assessed by quantitative immunocytochemical analyses, our results showed that Cx32 Δ 220 showed 2-3 fold decrease in gap junction size compared to Cx32-FL. Cell surface biotinylation showed that Cx32 Δ 220 trafficked normally to the cell surface, however, it was inefficiently assembled into gap junctions as assessed by detergent-solubility assay. Immunocytochemical analysis showed that Cx32 Δ 220 did not colocalize with markers of the secretory and endocytic pathway. Moreover, expression of Cx32-FL in cells stably expressing Cx32 Δ 220 increased the size of gap junctions, implying the direct involvement of Cx32-CT in this process. To define which domain of Cx32-CT determined the size of gap junctions, a series of deletion mutants, with progressive truncation of 20 amino acids, was retrovirally expressed in human prostate cancer cell line, LNCaP, in pancreatic cancer cell line, BxPC3, and in RL-CL9 cells. These experiments showed that the domain that determined the size of gap junctions lied between amino-acids 230-250 of Cx32-CT. A protein motif search identified two PKA phosphorylation motifs: RKGS and RLS, with putative serine residues at positions 233 and 240 that might be phosphorylated. Protein kinase A mediated phosphorylation has previously been shown to increase clustering of cell-cell channels. Our findings thus imply that the PKA phosphorylation motifs in Cx32-CT may regulate gap junction size and growth.

Abstract: 2013

Katoch, P., Ray, A., Kelsey, L., and Mehta, PP (2013). Two dileucine-like motifs govern the endocytosis of connexin32. International Meeting on Gap Junctions 2013, Charleston, SC. July 13-18.

Two dileucine-like motifs govern the assembly of connexin32 into gap junctions

Parul Katoch, Anuttoma Ray, Linda Kelsey and Parmender P. Mehta

Department of Biochemistry and Molecular Biology, University of Nebraska Medical Center, Omaha, NE

Connexin (Cx)32 is expressed in the polarized cells of pancreatic and prostatic acini yet little is known about how gap junction (GJ)s composed of it are assembled and disassembled. Earlier studies demonstrated that the impaired assembly of Cx43 in pancreatic tumor cells was corrected by expressing an endocytosis-defective mutant, which did not interact with AP2 complex. Our study also showed that the cytoplasmic-

tail of Cx32 regulated its assembly into GJs. To determine the motifs that govern Cx32 GJ assembly, we examined the role of two dileucine [DE]XXXL[LI]-like motifs present in its cytoplasmic tail, which have been known to mediate the clathrin-mediated endocytosis of many transmembrane proteins. Hence, we constructed the following Cx32 mutants in which the leucines and the arginine in the dileucine-like motifs were substituted with alanine: 1. L251A/L252A. 2. L263A/R264A. These mutants and the wild-type Cx32 (Cx32-WT) were expressed retrovirally in prostate and pancreatic cancer cell lines. The results showed that compared to Cx32-WT, the mutants formed significantly larger GJs. Cell surface biotinylation showed that both Cx32-WT and the mutants trafficked normally. Based on the kinetics of degradation of cell-surface biotinylated pool of Cx32-WT and the mutants, our results showed that the half-life of mutants was significantly prolonged, suggesting an increased residence time of mutants at the cell surface. However, clathrin-knock down had no effect on the internalization and the half-life of cell-surface associated Cx32-WT and the mutants. Remarkably, our results showed that neither Cx32-WT nor mutants co-localized with the known endocytic markers. To examine whether Rab5 was involved in the endocytosis of Cx32, we expressed EGFP-tagged wild-type Rab5 and its dominant-active mutant in cells expressing Cx32-WT and the mutants. We found that only Cx32-WT co-localized significantly in Rab5-positive vesicles. Thus, our findings point out a critical but intricate role of dileucine-like motifs in governing Cx32 GJ assembly.

E-cadherin Differentially Regulates the Assembly of Connexin43 and Connexin32 into Gap Junctions in Human Squamous Carcinoma Cells^{*§}

Received for publication, August 8, 2009, and in revised form, December 31, 2009. Published, JBC Papers in Press, January 19, 2010, DOI 10.1074/jbc.M109.053348

Souvik Chakraborty[†], Shalini Mitra[†], Matthias M. Falk[§], Steve H. Caplan[†], Margaret J. Wheelock[†], Keith R. Johnson[†], and Parmender P. Mehta^{†,1}

From the [†]Department of Biochemistry and Molecular Biology, Eppley Institute for Research in Cancer and Allied Diseases, Eppley Cancer Center, University of Nebraska Medical Center, Omaha, Nebraska 68198 and the [§]Department of Biological Sciences, Lehigh University, Bethlehem, Pennsylvania 18015

It is as yet unknown how the assembly of connexins (Cx) into gap junctions (GJ) is initiated upon cell-cell contact. We investigated whether the trafficking and assembly of Cx43 and Cx32 into GJs were contingent upon cell-cell adhesion mediated by E-cadherin. We also examined the role of the carboxyl termini of these Cxs in initiating the formation of GJs. Using cadherin and Cx-null cells, and by introducing Cx43 and Cx32, either alone or in combination with E-cadherin, our studies demonstrated that E-cadherin-mediated cell-cell adhesion was neither essential nor sufficient to initiate GJ assembly *de novo* in A431D human squamous carcinoma cells. However, E-cadherin facilitated the growth and assembly of preformed GJs composed of Cx43, although the growth of cells on Transwell filters was required to initiate the assembly of Cx32. Our results also documented that the carboxyl termini of both Cxs were required in this cell type to initiate the formation of GJs *de novo*. Our findings also showed that GJ puncta composed of Cx43 co-localized extensively with ZO-1 and actin fibers at cell peripheries and that ZO-1 knockdown attenuated Cx43 assembly. These findings suggest that the assembly of Cx43 and Cx32 into GJs is differentially modulated by E-cadherin-mediated cell-cell adhesion and that direct or indirect cross-talk between carboxyl tails of Cxs and actin cytoskeleton via ZO-1 may regulate GJ assembly and growth.

Gap junctions are conglomerations of intercellular channels that permit the direct exchange of ions, second messengers, and other molecules of less than 1500 Da between the cytoplasmic interiors of contiguous cells. The channels are composed of a family of proteins called connexins (Cx)² that are designated according to their molecular mass (1). The assembly of Cxs into

GJs is a multistep process. The newly synthesized Cxs are cotranslationally inserted into the endoplasmic reticulum, which oligomerize to form hexamers called connexons. The connexons are delivered to the cell surface via Golgi and trans-Golgi network in small vesicles and dock with the connexons in the contiguous cell membranes to form intercellular channels. A GJ plaque is formed when several intercellular channels cluster (2, 3). Because of the short half-life of Cxs (2–5 h), the plaque is in a dynamic state and is thought to model and remodel constantly through recruitment of newly synthesized connexons to the periphery and through endocytosis of moribund plaque components from the center or through the endocytosis of the plaque in its entirety (4–7). Although much has been learned about the intracellular transport of Cxs, the delivery of connexons to the cell surface, the formation of cell-to-cell channels, the spatio-temporal events and cellular factors required for the initial docking of connexons, the *de novo* formation of a nascent GJ plaque, its growth, and disassembly are poorly understood (2, 8).

The proximity between the plasma membranes of adjoining cells is, *a priori*, necessary for the formation of GJs, and cell-cell adhesion has been thought to facilitate this process. Cell-cell adhesion is mediated by cadherins, which belong to a large family of transmembrane proteins. Of all the cadherins, the most predominant isoform expressed in epithelial cells is the epithelial (E)-cadherin (9–11). Apart from controlling the formation of tight junctions and desmosomes, forced expression of E-cadherin has been shown to restore cell-cell adhesion and induce GJ assembly, and abolition of cadherin mediated cell-cell adhesion has been shown to disrupt the assembly (12–15). Despite these studies, the possible mechanism(s) by which cadherins might regulate GJ assembly have yet to be explored. The importance of undertaking these studies is underscored by the fact that dysfunctional E-cadherin-mediated cell-cell adhesion as well as aberrant assembly of Cxs into GJs are the hallmarks of cancer progression (16–18).

Here we sought to investigate if cell-cell adhesion mediated by E-cadherin expression was sufficient by itself to induce the assembly of Cxs into GJs or whether additional events were required. Because both cadherins and Cxs belong to a large family of related proteins, and most cells *in vivo* and *in vitro* are likely to express more than one family member (2, 10, 18), we thought to delineate these mechanisms in a cell culture model

* This work was supported, in whole or in part, by National Institutes of Health Grants RO-1 CA113903 (to P. P. M.), RO-1DE12308 (to K. R. J.), and RO-1GM074876 (to S. H. C.). This work was also supported by Department of Defense Grant PC081198 and Nebraska State Grant LB506 (to P. P. M.) and the Nebraska Center for Cellular Signaling graduate fellowship (to S. M. and S. C.).

§ The on-line version of this article (available at <http://www.jbc.org>) contains supplemental Figs. S1–S12.

¹ To whom correspondence should be addressed. Tel.: 402-559-3826; Fax: 402-559-6650; E-mail: pmehta@unmc.edu.

² The abbreviations used are: Cx, connexin; GJ, gap junction; PBS, phosphate-buffered saline; EYFP, enhanced yellow fluorescent protein; siRNA, small interfering RNA.

Assembly of Connexin32 and Connexin43

system that was Cx- and cadherin-null and where cadherins and Cxs could be introduced either alone or in combination (19, 20). Moreover, we rationalized that if the expression of a cadherin or cell-cell adhesion mediated by it *per se* was the sole determinant of the assembly of Cxs into GJs, then the assembly should be independent of the subtype of Cx introduced. Furthermore, because some Cxs are expressed in a tissue-specific manner (18), and have divergent carboxyl termini that might interact with the cadherins directly or indirectly to regulate GJ assembly (2, 18, 21, 22), we also assessed the role of these termini in initiating the formation of GJs in the presence and absence of E-cadherin.

Using cadherin- and Cx-null A431D cells, derived from human squamous carcinoma cell line A431(19, 20), and by introducing Cx43, a ubiquitously expressed Cx (22), and Cx32, a Cx preferentially expressed by the well differentiated and polarized cells (23), either alone or in combination with E-cadherin, we show that E-cadherin-mediated cell-cell adhesion facilitates the growth and assembly of only preformed GJs but is not sufficient to trigger the assembly of GJs *de novo*. We also show that in this cell system the carboxyl termini of Cx32 and Cx43 are required to initiate the formation of GJs *de novo*. Finally, our findings suggest a role for ZO-1 and actin filaments in initiating the formation or stabilization of GJs. Our data imply that the assembly of different Cxs into GJs is governed in a complex manner by E-cadherin, which in turn may depend on the motifs in the Cxs themselves and additional proteins that permit or impede docking of connexons and clustering of gap junctional channels.

MATERIALS AND METHODS

Cell Culture—The characterization of cadherin-null A431D and its E-cadherin-expressing counterpart, A431DE, has been described (19). These cells were grown in Dulbecco's modified Eagle's medium (Invitrogen) supplemented with 2.5% defined fetal bovine serum and 2.5% bovine growth serum (Hyclone, Salt Lake City, UT) in an atmosphere of 5% CO₂, 95% air. A431DE cells were maintained in complete medium containing puromycin (2 µg/ml). Connexin-expressing A431D and A431DE clones were isolated as described (see under "Retrovirus Production and Infection of Cells") and maintained, respectively, in complete medium containing G418 (200 µg/ml) and G418 plus puromycin. The retroviral packaging cell line Phoenix 293 was grown in RPMI 1640 medium containing 5% defined fetal bovine serum as described previously (24). HeLa cells were grown in Dulbecco's modified Eagle's medium containing 5% fetal bovine serum.

Plasmids, Retroviral Vectors, and Other Recombinant DNA Constructs—Retroviral vectors, LXSNCx32S, and LXSNCx43S, containing rat Cx32 and Cx43 cDNAs, respectively, were constructed as described previously (24–26). The carboxyl-terminally tagged pCx43-EYFP was constructed in the pEYFP-N1 vector as described previously (25). Carboxyl-terminally tagged pCx32-EYFP was constructed as described previously (27). Untagged carboxyl-terminally truncated pCxΔ233, pCxΔ257, and pCxΔ363 and carboxyl-terminally tagged truncated pCx43Δ233-EYFP and pCx43Δ257-EYFP were engineered in the pcDNA3.1 and pEYFP-N1 vector using

standard PCR-based cloning methods using LXSNCx43S as a template. The PCR amplifications were performed using the forward 5'-GCCTCGAGATGGGTGACTGGAGT-3' and the reverse primers 5'-CCGTGGATCCCTGAAGAAGACGTA-3' (for pCx43Δ233-EYFP), 5'-CCGTGGATCCCTTGATGG-GCTCAG-3' (for pCx43Δ257-EYFP), and 5'-CCGTGGATCC-ACTGCTGGAAGGTCGTTGGTCCA-3' (for pCx43Δ363). The forward and reverse primers, as underlined, were designed to contain XhoI and BamHI sites, respectively. The PCR products were first purified using QIAquick PCR purification kit (Qiagen, Valencia, CA) and, after digesting with XhoI and BamHI, were subcloned between XhoI- and BamHI-digested pEYFP-N1 vector. pCx32Δ220-EYFP was constructed by PCR using LXSNCx32S as a template. For PCR, the following primers were used: forward primer 5'-GCCGAATTCATGAAC-TGGACAGGTC-3' and the reverse primer 5'-CCGTGGATCC-CAACGGCGGGCACAG-3'. The forward and reverse primers contained EcoRI and BamHI sites, respectively, as underlined. The purified PCR products were cloned into EcoRI/BamHI-digested pEYFP-N1. The entire coding sequences of EYFP-tagged full-length and truncated Cx43 and Cx32 chimeras were then subcloned into retroviral vector LXSNCx32S using standard recombinant DNA methodology. All recombinant DNA constructs were verified by DNA sequencing.

Transient Transfection—Phoenix 293T cells (1×10^6) were seeded in 10-cm dishes in 10 ml of complete medium. HeLa cells were seeded at a density of 2.5×10^5 cells per well in 2 ml of complete medium on glass coverslips in 6-well clusters or at a density of 7.5×10^5 cells per 6-cm dish in 4 ml of complete medium. Twenty four hour post-seeding, cells were transfected with appropriate plasmids using FuGENE 6 Transfection Reagent (Roche Diagnostics) as per the manufacturer's instructions with DNA (in micrograms) to FuGENE (in µl) ratio of 1:3. The medium was replaced with fresh medium 8 h post-transfection.

Retrovirus Production and Infection of Cells—Control and recombinant retroviruses harboring full-length and mutant Cxs and their EYFP-tagged chimeras were produced in Phoenix 293T cells as described previously (24). A431D and A431DE cells were multiply infected with various recombinant retroviruses and selected in either G418 (400 µg/ml) or in puromycin (2 µg/ml) for 2–3 weeks in complete medium. Glass cylinders were used to isolate individual antibiotic-resistant clones, which were expanded, frozen, and maintained in G418 (200 µg/ml) and in G418 and puromycin (2 µg/ml).

Cell Surface Biotinylation Assay—Cells (5×10^5) were seeded in 6-cm dishes in 4 ml of complete medium and grown to 80–90% confluence. Cell surface biotinylation was performed at 4 °C. In brief, cells were incubated with freshly prepared EZ-Link™ Sulfo-NHS-SS biotin reagent (Pierce) at 0.5 mg/ml in phosphate-buffered saline (PBS) supplemented with 1 mM CaCl₂ and 1 mM MgCl₂ (PBS-PLUS) for 1 h. The reaction was quenched with PBS-PLUS supplemented with 20 mM glycine. Cell lysis and affinity precipitation of biotinylated proteins were performed as described previously (28) with the following modification. After cell lysis, 100 µg of total protein was incubated with 50 µl of streptavidin-agarose beads (Pierce) on a rotator overnight at 4 °C. The streptavidin-bound biotinylated proteins were eluted by incubating the beads for 30 min in 1×

SDS loading buffer. The samples were resolved by SDS-PAGE followed by Western blotting using appropriate antibodies. As an input, an equal amount of total protein (10 µg) was also subjected to SDS-PAGE and Western blot analysis. Protein concentration was determined using BCA reagent (Pierce).

Detergent Extraction and Western Blot Analysis of Connexin43 and Connexin32—Cell lysis, detergent solubility assay with Triton X-100, and Western blot analysis were performed as described previously (24, 28). In brief, 1×10^6 cells were seeded per 10-cm dish in 10 ml of complete medium and grown to confluence. Cells were then lysed in buffer SSK (10 mM Tris, 1 mM EGTA, 1 mM phenylmethylsulfonyl fluoride, 10 mM NaF, 10 mM *N*-ethylmaleimide, 10 mM Na₂VO₄, 10 mM iodoacetamide, 0.5% Triton X-100, pH 7.4) supplemented with the protease inhibitor mixture (Sigma). For the detergent solubility assay, the concentration of Triton X-100 was raised to 1% before ultracentrifugation at 100,000 $\times g$ for 60 min (35,000 rpm in analytical Beckman ultracentrifuge; model 17-65 using an SW50.1 rotor). The detergent-insoluble pellets were dissolved in buffer C (70 mM Tris/HCl, pH 6.8, 8 M urea, 10 mM *N*-ethylmaleimide, 10 mM iodoacetamide, 2.5% SDS, and 0.1 M dithiothreitol). Following normalization based on cell number, the total Triton X-100-soluble and -insoluble fractions were mixed with 4× SDS-loading buffer to a final concentration of 1× and boiled at 100 °C for 5 min (for Cx43) or incubated at room temperature for 1 h (for Cx32) before SDS-PAGE analysis.

Gene Knockdown by RNA Interference—SMARTpool siRNA against ZO-1 (TJP-1; catalogue no. L-007746-00) and DY-547-labeled siGLO RISC-free control siRNA (catalogue no. D-001600-01) were obtained from Thermo Fisher Scientific/Dharmacon RNA Interference Technologies. DY-547-labeled siGLO Lamin A/C siRNA (catalogue no. 001620-02) was used as a positive control. The 40 µM stock solution of the oligonucleotides was prepared using 1× siRNA buffer (Thermo Fisher Scientific). A431D-43 and A431DE-43 cells, seeded on glass coverslips in 12-well clusters, 8×10^4 cells/well, were transfected with the oligonucleotides using Oligofectamine (Invitrogen) as per the manufacturer's instructions. The final concentration of the oligonucleotides in each experiment was 130 nM. The efficiency of knockdown was assessed by immunoblotting and immunocytochemical analyses 72 h post-transfection. The final concentrations of the oligonucleotides as well as the duration of treatment were empirically determined from several pilot experiments.

Detergent (Triton X-100) Extraction of Cells *In Situ*—Live cells were extracted *in situ* with 1% Triton X-100 essentially as described previously (28). In brief, 2.5×10^5 cells were seeded per well in 6-well clusters containing glass coverslips. After 24 h, the cells were rinsed once in PBS and then incubated in isotonic medium (30 mM HEPES, pH 7.2, 140 mM NaCl, 1 mM CaCl₂, 1 mM MgCl₂, 300 mM sucrose) supplemented with the protease inhibitor mixture (Sigma) for 60 min at 4 °C in the presence and absence of 1% Triton X-100. The dishes were gently swirled intermittently. Following incubation, cells were fixed and immunostained with appropriate primary and secondary antibodies as described below.

Antibodies and Immunostaining—Rabbit polyclonal antibody against Cx43 and hybridoma M12.13 (a gift from Dr. Dan Goodenough, Harvard University) have been described earlier (26). Rabbit anti-EEA-1 (PA1-063) was obtained from Affinity BioReagents (Golden, CO). Mouse anti-occludin (clone OC-3F10) was from Zymed Laboratories Inc.. Rabbit anti- α -catenin, rabbit anti- β -catenin, rabbit anti-Cx32, and mouse anti- β -actin (clone C-15) antibodies were from Sigma. Mouse anti-ZO1 (610967) and mouse anti-GM130 (610822) antibodies were obtained from BD Transduction Laboratories. Rabbit anti-green fluorescent protein antibody (A6455) and Alexa Fluor 350-conjugated phalloidin were obtained from Invitrogen. Mouse anti-E-cadherin, mouse anti- α -catenin, and mouse anti- β -catenin antibodies have been described previously (19, 24, 29). We also used many other antibodies, both mouse monoclonal and rabbit polyclonal, against Cx43 to detect various phosphorylated forms. These antibodies are described in supplemental Fig. S3 legend.

Cells were immunostained after fixing with 2% paraformaldehyde for 15 min as described previously (24). In brief, 2.5×10^5 cells were seeded per well in 2 ml of complete medium in 6-well clusters containing glass coverslips. After 48 h, cells were fixed and immunostained at room temperature with various antibodies at appropriately calibrated dilutions. Secondary antibodies (rabbit or mouse) conjugated with Alexa Fluor 488 and Alexa Fluor 594 were used as appropriate. Images of immunostained cells were acquired with Leica DMRIE microscope (Leica Microsystems, Wetzler, Germany) equipped with Hamamatsu ORCA-ER CCD camera (Hamamatsu City, Japan) using 63× oil objective (NA 1.35). For co-localization studies, serial z-sections (0.3–0.5 µm) were collected and analyzed using image-processing software (Openlab 4.0 and Volocity 4.2.2, Improvision, Lexington, MA). SlowFade (Invitrogen) was used to mount cells on glass slides.

Cell Growth on Semi-permeable Filters—Approximately 4×10^4 cells were plated onto 12-mm Transwell filters (pore size, 0.4 µm; Corning Glass) in complete medium and grown for 3–6 days. Medium of the upper and lower filter chambers was changed on alternate days. The *in situ* detergent extraction and immunocytochemical analyses were performed directly on filters as described above for cells grown on glass coverslips. After immunostaining, the filters were cut with a sharp scalpel and mounted as follows. The filters were placed on glass slides with their cell side facing up and a drop of SlowFade was placed on top followed by a glass coverslip, which was pressed gently using a 50-g weight overnight. The edges were sealed with nail polish.

Cell Aggregation Assay—The hanging drop suspension culture method was used to test aggregation of parental and Cx-expressing A431D and A431DE cells as described previously (30). Cells were harvested with trypsin/EDTA and resuspended at 2.5×10^5 cells per ml in complete culture medium. A 20-µl drop of medium, containing 5×10^3 cells, was suspended as a hanging drop from the lid of a 10-cm² Petri dish (40 hanging drops per lid). The dish was filled with 10 ml of PBS to prevent drying of the drops. The cells were then allowed to aggregate in a humidified 5% CO₂ incubator at 37 °C for 14–16 h. At the end of the incubation, cells and aggregates were triturated 10 times

Assembly of Connexin32 and Connexin43

through a standard 200- μ l pipette tip to disperse loosely associated cells, and a coverslip was placed gently on top of the cells. The cells were visualized by phase-contrast light microscopy using a 5 \times objective, and images were captured using a CCD camera (Retiga 2000R, FAST 1394), mounted on Leica DMIRE2 microscope, with the aid of Volocity (Improvision, Lexington, MA). For quantifying the size, the outline of each aggregate was drawn using an ROI tool of the AlphaDigiDoc 1201 software, and the area of each aggregate was measured. All images were analyzed at the same magnification, and the area was recorded as “relative units” for each aggregate. The average area of the aggregates was considered as a measure of aggregate formation and was determined from 30–35 aggregates.

Gap Junctional Communication Assays—Gap junctional communication was measured by microinjecting the fluorescent tracers Alexa Fluor 488 (570 Da; A-10436) and Alexa Fluor 594 (760 Da; A-10438). The Alexa dyes were obtained from Invitrogen, and their stock solutions (10 mM) were prepared in water as described previously (24). These fluorescent tracers were microinjected into test cells using Eppendorf InjectMan and FemtoJet microinjection systems (models 5271 and 5242, Brinkmann Instrument, Westbury, NY) mounted on a Leica DMIRE2 microscope as described previously (24). The microinjected cells were viewed and images captured using a CCD camera (Retiga 2000R, FAST 1394) with the aid of Volocity (Improvision, Lexington, MA). The captured images were stored as TIFF files and processed using Corel Photopaint (Ottawa, Ontario, Canada). Gap junctional communication was quantified as described previously (24–26).

Cytochalasin B Treatment—The stock solution of cytochalasin B (Sigma) was prepared in ethanol at 10 mg/ml and was stored at –20 °C in small aliquots. Cells, seeded on glass cover-slips, were treated for 1–6 h at 37 °C with cytochalasin B at 1 μ g/ml, which was appropriately diluted in cell culture medium to give the desired concentration. Controls were treated with ethanol alone.

Gap Junction Size Measurement—The length and area of a GJ plaque were measured after *in situ* extraction of cells with 1% Triton X-100, which removes Cxs and connexons that are not incorporated into GJs (28), and immunostaining with Cx43 antibody as described above (see under “Detergent Extraction and Western Blot Analysis of Connexin43 and Connexin32”). Images of immunostained cells were acquired with a Leica DMRIE microscope (Leica Microsystems, Wetzler, Germany) equipped with Hamamatsu ORCA-ER CCD camera (Hamamatsu City, Japan) using a 63 \times oil objective (NA 1.35). Serial *z*-sections (0.5 μ m) were collected and subjected to iterative volume deconvolution using Volocity image-processing software (Improvision, Lexington, MA). Single optical section of the deconvolved image was used for measuring GJ size. Each distinct punctum seen at the cell-cell contact site was considered as one GJ plaque. The area of each GJ plaque was analyzed by drawing an ROI around each distinct punctum using the “magic wand” tool of the “Measurement” module of Volocity. The area of each GJ is represented as “pixel count,” and one pixel corresponds to 0.01 μ m². In each captured image, 3–5 puncta were randomly chosen for the measurement of area and length, and between 5 and 15 images were used. For the measurement of GJ

length, we used the “line” tool of the measurement module of Volocity to ascribe the farthest visible points along the long axis of each GJ punctum. The length is represented in relative units where “a unit” corresponds to 0.1 μ m. For determining the number of GJ plaques per cell-cell interface, we used the “merge planes” command of Volocity to merge all planes obtained during Z-sections. We then counted the number of distinct visible puncta along the cell-cell interfaces of two adjoining cells. Only distinct interfaces were chosen for these measurements at random to avoid ambiguity with regard to the localization of the puncta, and 60–70 interfaces were measured from three independent experiments.

Statistical Analysis—The statistical significance between groups was calculated by standard Student’s *t* test using means \pm S.E. and the entire sample size. These values were calculated using SigmaPlot 11 (Systat Software, Inc., San Jose, CA).

RESULTS

Differential Assembly of Connexin43 and Connexin32 into Gap Junctions—A431D cells, derived from human squamous carcinoma cell line A431, are devoid of E-cadherin or N-cadherin. Moreover, although the expression of desmosomal cadherins (desmocollins and desmogleins) was not affected, A431D cells do not form adherens junctions, desmosomes, and tight junctions and are devoid of cell-cell adhesion. Furthermore, the half-life of adherens junction-associated proteins, α - and β -catenin, is severely reduced (19, 20). We introduced Cx43 and Cx32 into cadherin-null (A431D) and E-cadherin-expressing (A431DE) cells using recombinant retroviruses LXSNCx43S and LXSNCx32S as described previously (24, 26). A431D cells do not express these Cxs detectably. Fig. 1 shows the expression level of Cx43 (*C*) and Cx32 (*D*) in representative clones derived from cadherin-null A431D (A431D-43 and A431D-32) and cadherin-expressing A431DE (A431DE-43 and A431DE-32) cells. These clones were chosen on the basis of equal expression of both Cxs and E-cadherin as assessed by the densitometric scanning of Western blots. For the sake of simplicity, these clones will be referred to as cells in subsequent studies. Immunocytochemical analysis showed that Cx43 assembled into GJs both in cadherin-null A431D-43 and E-cadherin-expressing A431DE-43 cells (Fig. 1*A*, *upper panels*), whereas Cx32 failed to assemble into GJs and appeared to form intracellular aggregates of variable size both in A431D-32 and A431DE-32 cells (Fig. 1*A*, *lower panels*).

In E-cadherin-expressing A431DE-43 cells, Cx43 clearly appeared to form larger GJs as compared with cadherin-null A431D-43 cells (Fig. 1*A*, compare the size of GJ puncta in *upper left panel* with the *right panel*). We therefore determined the size and area of 100–200 individual gap junctional puncta ([supplemental Fig. S1](#)) as well as the mean number of gap junctional puncta per cell-cell interface in A431D-43 and A431DE-43 cells ([supplemental Fig. S2](#)). The size of each fluorescent spot or punctum at the interface was presumed to represent a single GJ plaque (31). These measurements showed that the mean area and the length of GJ plaques increased nearly 2-fold ([supplemental Fig. S1](#)), and the mean number of GJ puncta per interface was decreased 2-fold ([supplemental Fig. S2](#)) in

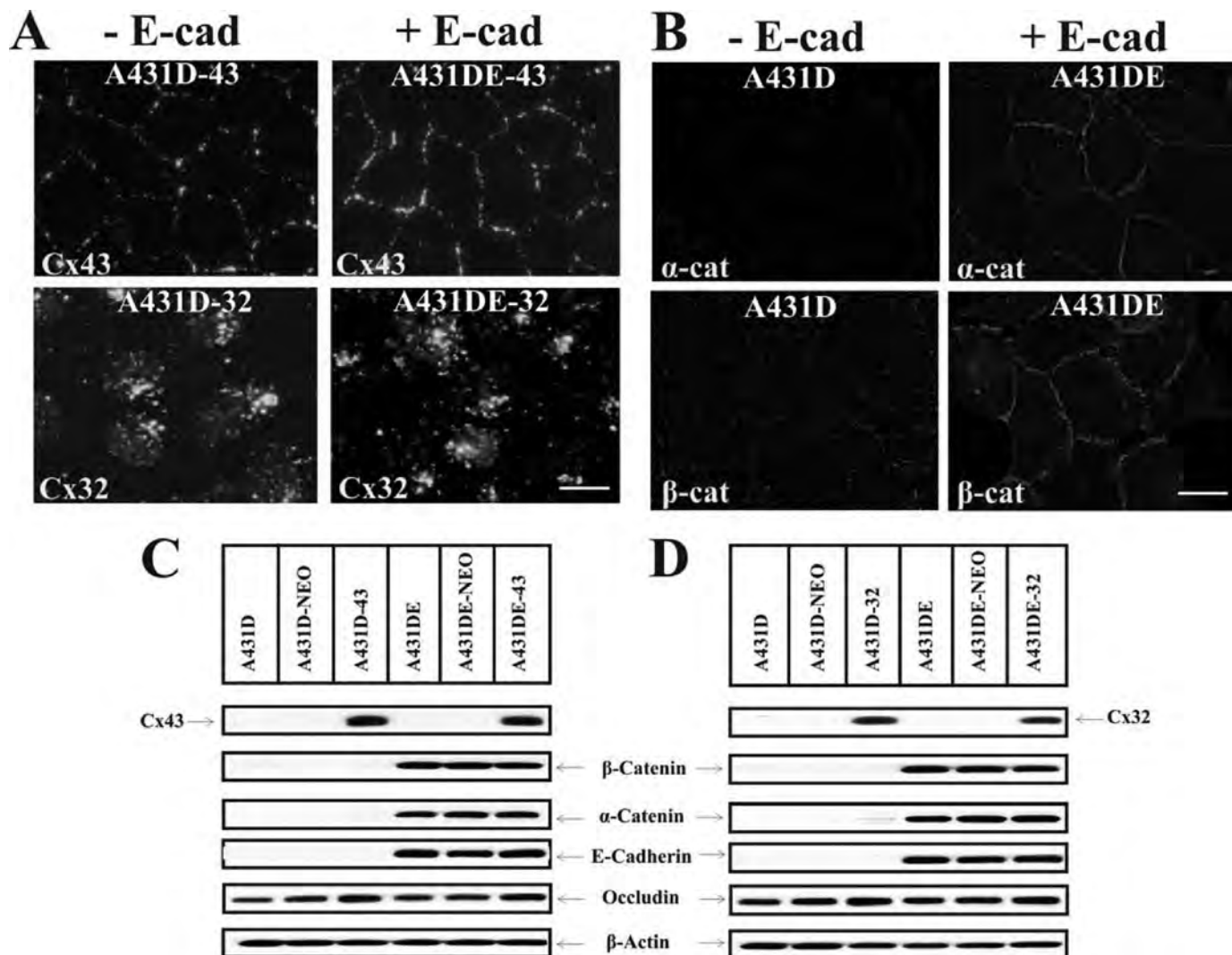


FIGURE 1. Isolation of A431D and A431DE clones expressing equal levels of connexin32 and connexin43. A431D and A431DE cells were infected with LXS, LXSNCx32S, and LXSNCx43S and selected as described (see under “Materials and Methods”). *A*, localization of Cx43 and Cx32 by immunocytochemical analyses. A431D-43, A431DE-43, A431D-32, and A431DE-32 cells were immunostained for Cx43 and Cx32. Note that Cx43 assembles into GJs in the absence (*-E-cad*) and in the presence (*+E-cad*) of E-cadherin (*E-cad*), whereas Cx32 remains intracellular and fails to assemble. Note also that Cx43 forms larger GJs in E-cadherin-expressing cells. *B*, E-cadherin expression recruits α -catenin (α -cat) and β -catenin (β -cat) to cell-cell contact areas. A431D and A431DE cells were immunostained for α - and β -catenins. Note localization of both catenins at cell-cell contact areas in A431DE but not in A431D cells. *C* and *D*, expression level of Cx43 (*C*) and Cx32 (*D*) and E-cadherin, β -catenin, α -catenin, and occludin in parental (A431D and A431DE) cells and in cells infected with LXS (A431D-NEO and A431DE-NEO), LXSNCx43S (A431D-43 and A431DE-43), and LXSNCx32S (A431D-32 and A431DE-32). Ten micrograms of total protein was resolved on 12% SDS-PAGE and immunoblotted for Cx32, Cx43, E-cadherin, β -catenin, α -catenin, and occludin. The blots were re-probed with β -actin to verify equal loading. Note that Cx43 (*C*) and Cx32 (*D*) are expressed only in clones infected with LXSNCx32S and LXSNCx43S, respectively. Note that expression of E-cadherin, α -catenin, and β -catenin is detected only in A431DE clones. Bar, 15 μ m.

A431DE-43 cells compared with A431D-43 cells. It is worth noticing that the polyclonal antibody used to probe these blots (catalogue no. 6219, Sigma) predominantly detected only one major form of Cx43 in A431D-43 and A431DE-43 cells and in other cell lines that differ widely in their capacity to form GJs used in our earlier studies (supplemental Fig. S3). However, both phosphorylated and nonphosphorylated bands were detected when the blots were probed with anti-Cx43 antibody raised against residues 252–271 (both monoclonal and polyclonal) or with other antibodies, some of which were phospho-specific (supplemental Fig. S3). Although the resolving power of the SDS-polyacrylamide gels did not permit us to establish a correlation between a specific phosphorylated form of Cx43 and its ability to assemble into GJs, the above data suggest that,

as is observed in several other cell lines that assemble GJs, Cx43 in A431D-43 and A431DE-43 cells is phosphorylated similarly before its assembly into GJs.

Consistent with the earlier studies (19), E-cadherin expression also stabilized adherens junction-associated proteins α - and β -catenins (Fig. 1, *C* and *D*), and recruited them to cell-cell contact areas (Fig. 1*B*, compare *left panels* with the *right panels*). Expression of Cx43 and Cx32 neither induced nor modulated E-cadherin-mediated cell-cell adhesion in cadherin-null and E-cadherin-expressing cells as assessed by conventional hanging drop assay (supplemental Fig. S4). This assay measures the rate and strength of cell-cell adhesion based on the sizes of cell aggregates formed over time from single cells as well as the resistance of the formed aggregates to a shearing force

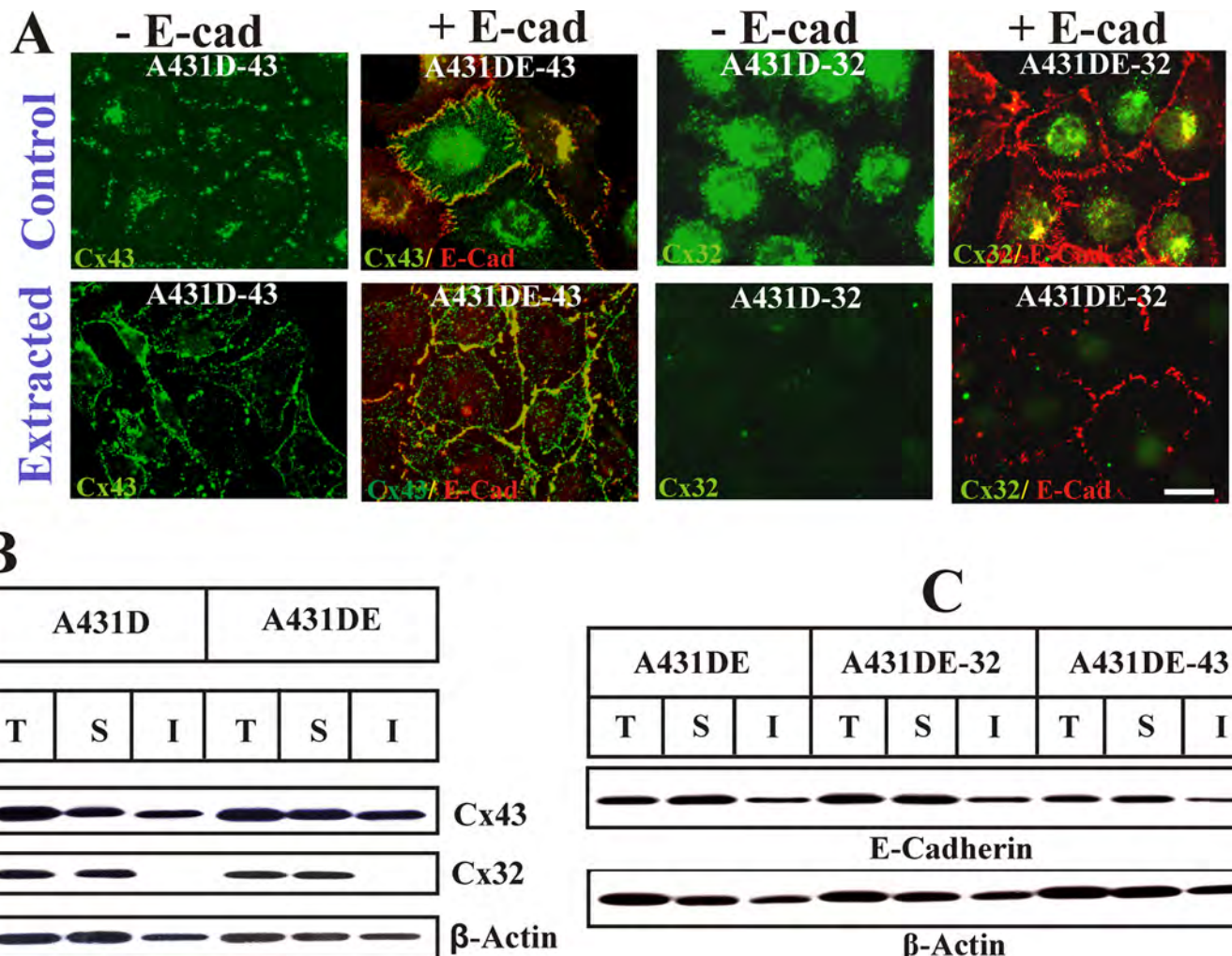


FIGURE 2. Detergent-solubility of connexin32 and connexin43 in A431D and A431DE cells. *A*, assembly of Cxs into GJs was examined in A431D-43, A431DE-43, A431D-32, and A431DE-32 cells upon *in situ* extraction with 1% Triton X-100 at 4 °C (see under “Materials and Methods”). Cells were immunostained for Cx32/Cx43 (green) and E-cadherin (red). Note the disappearance of intracellular, but not junctional, Cx43 and E-cadherin (*E-cad*) upon extraction. Note also the larger size of Cx43 puncta in A431DE-43 cells and their significant co-localization with E-cadherin under control and Triton X-100-extracted conditions. *B*, total (*T*), Triton X-100-soluble (*S*), and Triton X-100-insoluble (*I*) fractions from A431D-43, A431DE-43, A431D-32, and A431DE-32 were analyzed by Western blot analysis (see under “Materials and Methods”). Note that although Cx43 is detected in the both detergent-soluble and -insoluble fractions, Cx32 is detected only in the soluble fraction, and E-cadherin expression has no detectable effect on detergent solubility of Cx43. The blots were stripped and re-probed with anti-β-actin antibody as a loading control. *C*, connexin expression does not affect the detergent solubility of E-cadherin. Total, Triton X-100-soluble and -insoluble fractions from A431DE, A431DE-43, and A431DE-32 cells were analyzed by Western blot analysis (see under “Materials and Methods”). Note that similar levels of E-cadherin are detected in the detergent-insoluble fraction in all cells. The blots were stripped and re-probed with anti-β-actin to verify equal loading. Bar, 10 μm.

TABLE 1

Junctional communication of various fluorescent tracers in connexin43-expressing cells with or without E-cadherin

Tracer	Exp. no.	A431D-43	A431DE-43	p value
Lucifer Yellow (443 Da)	1	33 ± 4 ^a (22) ^b	32 ± 5 (24)	0.878
	2	29 ± 4 (30)	35 ± 4 (30)	0.301
Alexa Fluor 488 (570 Da)	1	18 ± 3 (28)	21 ± 4 (32)	0.560
	2	16 ± 3 (26)	19 ± 3 (40)	0.502
Alexa Fluor 594 (760 Da)	1	4 ± 1 (28)	5 ± 1 (29)	0.483
	2	6 ± 2 (34)	7 ± 2 (30)	0.726

^a Mean number of fluorescent cells 5 min after microinjection ± S.E. is shown.

^b Number of microinjection trials is shown.

(30, 32). Only E-cadherin-expressing cells aggregated efficiently (supplemental Fig. S4, *A*, lower panels; see also *B*), whereas cadherin-null cells with or without Cx expression did not (supplemental Fig. S4, *A*, upper panels; see also *B*).

E-Cadherin Expression and the Detergent Solubility of Connexin43 and Connexin32—To corroborate the immunocytochemical data, we measured the assembly of Cx43 and Cx32 into GJs biochemically (Fig. 2*B*), by detergent insolubility assay (28), and functionally, by measuring the junctional transfer of fluorescent tracer Alexa Fluor 488 (570 Da), Lucifer Yellow (443 Da) and Alexa Fluor 594 (760 Da) (supplemental Fig. S5 and Table 1). Moreover, we also examined the detergent solubility of both Cxs upon *in situ* extraction of live cells with 1% Triton X-100 (Fig. 2*A*). As expected, a significant proportion of Cx43 remained insoluble in 1% Triton X-100 in A431D-43 and A431DE-43 cells (Fig. 2*A*, compare control and extracted in *1st* and *2nd columns*, and *B*, top blot, *T* = total, *S* = soluble, and *I* = insoluble fractions), whereas no insoluble fraction of Cx32 was detected in cadherin-null A431D-32 or E-cadherin-expressing A431DE-32 cells (Fig. 2*A*, compare control and extracted in

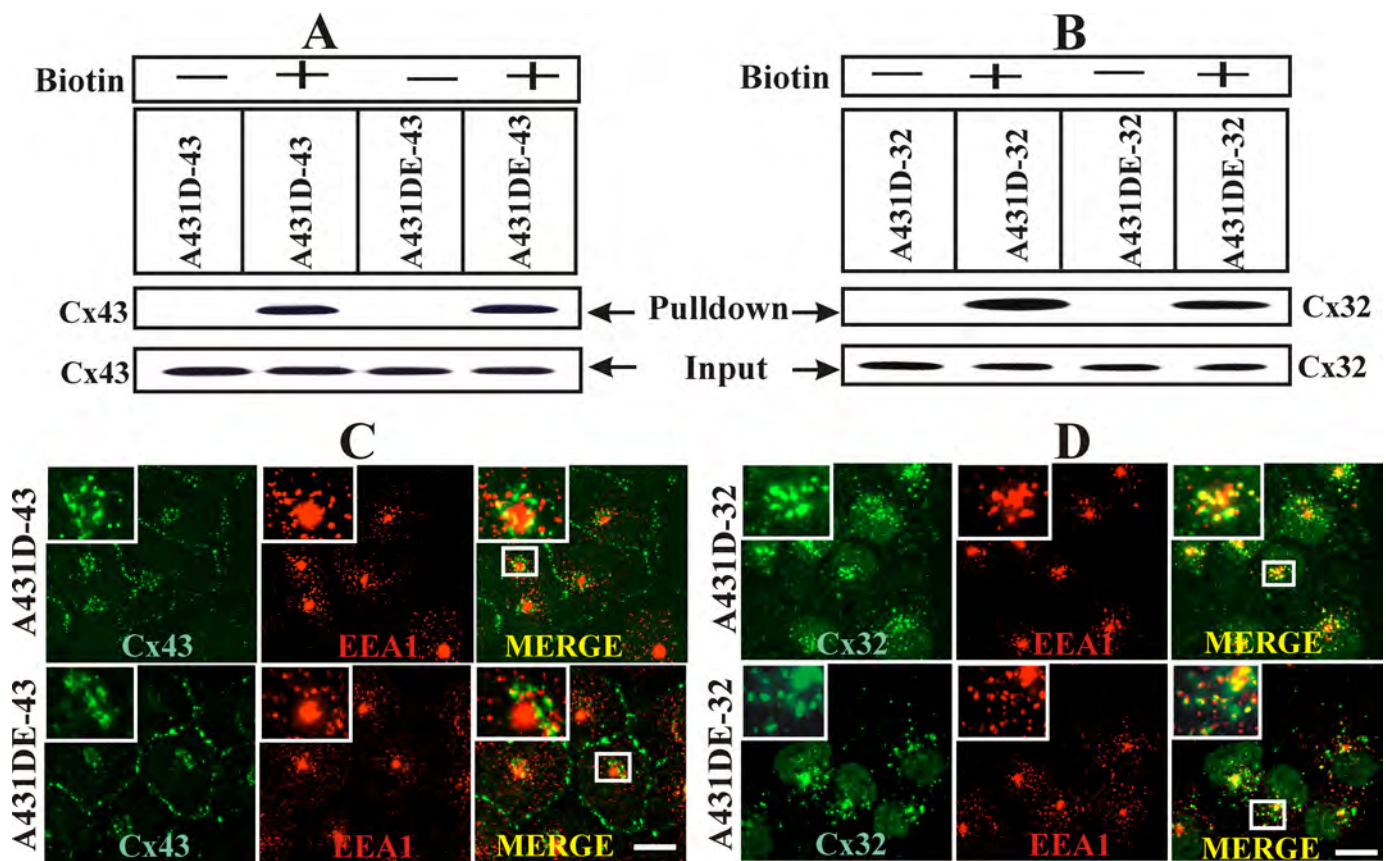


FIGURE 3. E-cadherin expression does not affect trafficking and subcellular localization of connexin43 and connexin32. *A* and *B*, cell-surface biotinylation of Cx43 and Cx32 in A431D and A431DE cells. Confluent A431D-43 (*A*) and A431DE-43 and A431D-32 and A431DE-32 cells (*B*) were biotinylated with sulfo-NHS-SS-biotin at 4 °C, and biotinylated Cxs from 100 µg of total protein were detected by streptavidin pulldown followed by Western blotting (see under “Materials and Methods”). As an input, 10 µg of total protein was used and probed for Cx43 or Cx32. Note that in both A431D-43 and A431DE-43 cells (*A*; labeled as + Biotin) and A431D-32 and A431DE-32 cells (*B*; labeled as + Biotin), similar levels of Cx43 and Cx32 were detected in the streptavidin Pulldown lanes, respectively. A nonbiotinylated dish (labeled as – Biotin) was used as a negative control. *C* and *D*, co-localization of Cx43 and Cx32 with EEA1 in A431D-43 and A431DE-32 and A431DE-43 and A431DE-32 cells. Note the co-localization of both Cx43 (*C*) and Cx32 (*D*, green) with EEA1 (red) in all cells. Note extensive co-localization of Cx32 with EEA1. The boxed region is magnified and shown in the inset. Bar, 15 µm.

2nd and 4th columns, and *B, middle blot*). Under similar conditions, the detergent solubility of E-cadherin was not significantly affected as assessed by *in situ* extraction (Fig. 2*A*, compare control and extracted, 2 and 4 columns) and by Western blot analysis (Fig. 2*C*). In agreement with the immunocytochemical data, no junctional communication of Alexa Fluor 488 was detected in cadherin-null A431D and A431D-32 and E-cadherin-expressing A431DE and A431DE-32 cells (supplemental Fig. S5). On the other hand, Cx43-expressing cells communicated extensively, and cadherin expression had little effect on junctional communication (supplemental Fig. S5, bottom panels, and Table 1). Altogether, the data shown in Figs. 1 and 2 and supplemental Figs. S1–S4 suggest the following. 1) Cx43 is able to assemble into GJs in the absence of E-cadherin, but Cx32 is not. 2) E-cadherin-mediated cell-cell adhesion facilitates the assembly and growth of GJs composed of Cx43. 3) E-cadherin expression alone is not sufficient to induce the assembly of Cx32 into GJs *de novo*.

Trafficking and Subcellular Localization of Connexin43 and Connexin32 in the Presence and the Absence of E-cadherin—We next examined whether failure of Cx32 to form GJs was due to its impaired trafficking to the cell surface or a result of endocytosis prior to its assembly into GJs. We used cell-surface biotin-

ylation to determine the trafficking of Cx43 and Cx32 to the cell surface and markers specific for the secretory and the endocytic pathways to examine their subcellular localization in cadherin-null and E-cadherin-expressing cells. As shown in Fig. 3, both Cx43 (Fig. 3*A*) and Cx32 (Fig. 3*B*) were biotinylated significantly in cadherin-null and cadherin-expressing cells. Connexin43 co-localized only partially with the early endocytic marker, EEA1 (Fig. 3*C*) (33), whereas Cx32 co-localized extensively (Fig. 3*D*). Both Cx43 and Cx32 co-localized with GM130 (supplemental Fig. S6), a marker for cis-Golgi (34) and Lamp-1 (data not shown), in cadherin-null and E-cadherin-expressing cells. Taken together, these data suggest that a significant fraction of Cx32 traffics to the cell surface both in the presence and absence of E-cadherin but in contrast to Cx43 is likely endocytosed prior to its assembly into GJs.

Assembly of Connexin32 into Gap Junctions Is Induced in A431D and A431DE Cells When Grown on Trans-Well-permeable Membrane Supports—In contrast to ubiquitous expression of Cx43, the expression of Cx32 is preferentially observed in well differentiated and polarized cells, such as hepatocytes and the secretory cells of exocrine glands (23). Permeable membrane supports have been widely used as surrogate substrates to mimic the milieu encountered by epithelial cells in

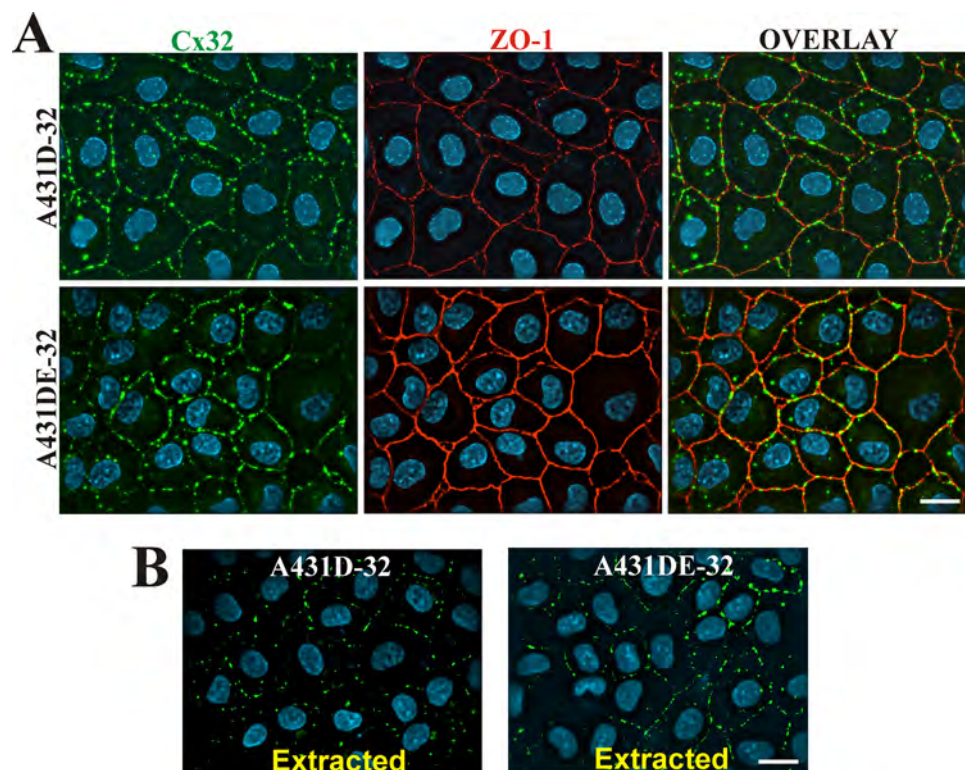


FIGURE 4. Connexin32 assembles into gap junctions in A431D-32 and A431DE-32 cells grown on Transwell filters. *A*, A431D-32 and A431DE-32 cells, seeded on clear Transwell filters, were grown for 5 days and immunostained for Cx32 (green) and ZO-1 (red) as described under “Materials and Methods.” Note the formation of distinct GJ puncta at the cell-cell contact sites as delineated by ZO-1. Note lack of significant difference in the size and number of Cx32 puncta at the cell-cell contact sites between A431D-32 and A431DE-32 cells. Note also that the GJ puncta remain detergent-resistant (*B*). Bar, 15 μ m.

TABLE 2

Junctional communication of various fluorescent tracers in cells grown on Transwell filters expressing connexin43 and connexin32 with or without E-cadherin

A431D-43, A431DE-43, A431D-32, and A431DE-32 cells were grown on 35-mm Transwell filters in replicate at a density of 2×10^5 cells per dish and allowed to grow to confluence for 5 days. Junctional communication was measured by microinjection of different fluorescent tracers as described under “Materials and Methods.”

Cell line	Lucifer Yellow	Alexa Fluor 488	Alexa Fluor 594
A431D-32	0 ± 0 ^a (52) ^b	0 ± 0 (39)	0 ± 0 (32)
A431DE-32	0 ± 0 (53)	0 ± 0 (47)	0 ± 0 (49)
A431D-43	31 ± 5 (22) ^c	16 ± 4 (27) ^d	6 ± 2 (26) ^e
A431DE-43	34 ± 7 (25) ^c	17 ± 5 (23) ^d	7 ± 2 (32) ^e

^a Mean number of fluorescent cells 5 min after microinjection ± S.E. is shown.

^b Number of microinjection trials is shown. There was no statistically significant difference in junctional communication between A431D-43 and A431DE-43 cells.

^c Data are not significant; $p = 0.735$ for Lucifer Yellow.

^d Data are not significant; $p = 0.875$ for Alexa Fluor 488.

^e Data are not significant; $p = 0.728$ for Alexa Fluor 594.

vivo and to induce polarized and differentiated cell states (35). Hence, we investigated if the assembly of Cx32 into GJs could be induced upon growing cadherin-null A431D-32 and E-cadherin-expressing A431DE-32 cells on Transwell filters. When grown on Transwell filters for 3–6 days (see under “Materials and Methods”), A431D and A431DE cells became more columnar, as assessed by a 2-fold increase in cell height compared with cells grown on plastic or glass coverslips (supplemental Fig. S7, *A* and *B*), but failed to attain a fully polarized state as assessed by the random orientation of Golgi stacks (GM130 staining), distribution of $\beta 1$ -integrin, and Na-K-

ATPase (supplemental Fig. S7*B*), and ZO-1 (supplemental Fig. S7*A*, *red*) at the apical and basolateral domains (35). However, despite incomplete polarization, Cx32 assembled into discrete GJ puncta (Fig. 4*A*), which remained Triton X-100-insoluble upon *in situ* extraction (Fig. 4*B*). Such puncta were not observed in cells grown on glass coverslips in parallel (supplemental Fig. S8*A*). As assessed visually, E-cadherin expression seemed to have little effect on the number and size of Cx32 GJs assembled in filter-grown A431D and A431DE cells (Fig. 4*A*).

We also found that the assembly of Cx43 into GJs appeared to be slightly enhanced when cadherin-null A431D-43 cells were grown on Transwell filters (supplemental Fig. S8*B*) as compared with cells grown on glass coverslips in parallel experiments (supplemental Fig. S8*C*); however, E-cadherin expression had no further effect (supplemental Fig. S8*B*). Also, neither the expression of E-cadherin in A431D cells nor punctate immunostaining characteristics of GJs were observed

in parental A431D and A431DE cells grown on Transwell filters (data not shown). To assess if the detergent-resistant puncta represented functional GJs, we measured the junctional transfer of fluorescent tracers, Lucifer Yellow (443 Da), Alexa Fluor 488 (570 Da), and Alexa Fluor 594 (760 Da) by microinjection. Intriguingly, we found that filter-grown A431D-32 and A431DE-32 cells did not communicate (Table 2). These findings suggest that the filter-grown A431D-32 and A431DE-32 cells acquire a partially polarized physiological state that is conducive for the assembly of Cx32 into GJs, but the junctional channels stay closed and do not permit the passage of molecules ≥ 443 Da. Moreover, the data also suggest that assembly of Cx43 is enhanced upon partial polarization independent of E-cadherin expression when cells acquire a columnar phenotype.

Carboxyl Termini of Connexin43 and Connexin32 Are Required to Initiate Gap Junction Assembly in A431D Cells—The findings reported above showed that Cx43 was assembled into GJs in cadherin-null cells in the absence of measurable cell-cell adhesion, and E-cadherin-mediated cell-cell adhesion enhanced the assembly further. On the other hand, the assembly of Cx32 into GJs was contingent upon acquisition of partially polarized state. Because the carboxyl termini of Cx43 and Cx32 have been shown to interact with many proteins (21, 22, 36), we examined if they were required for GJ assembly in A431D and A431DE cells. To test this notion, we generated the following EYFP-tagged chimeras of Cx43 and Cx32: 1) Cx43-EYFP, which does

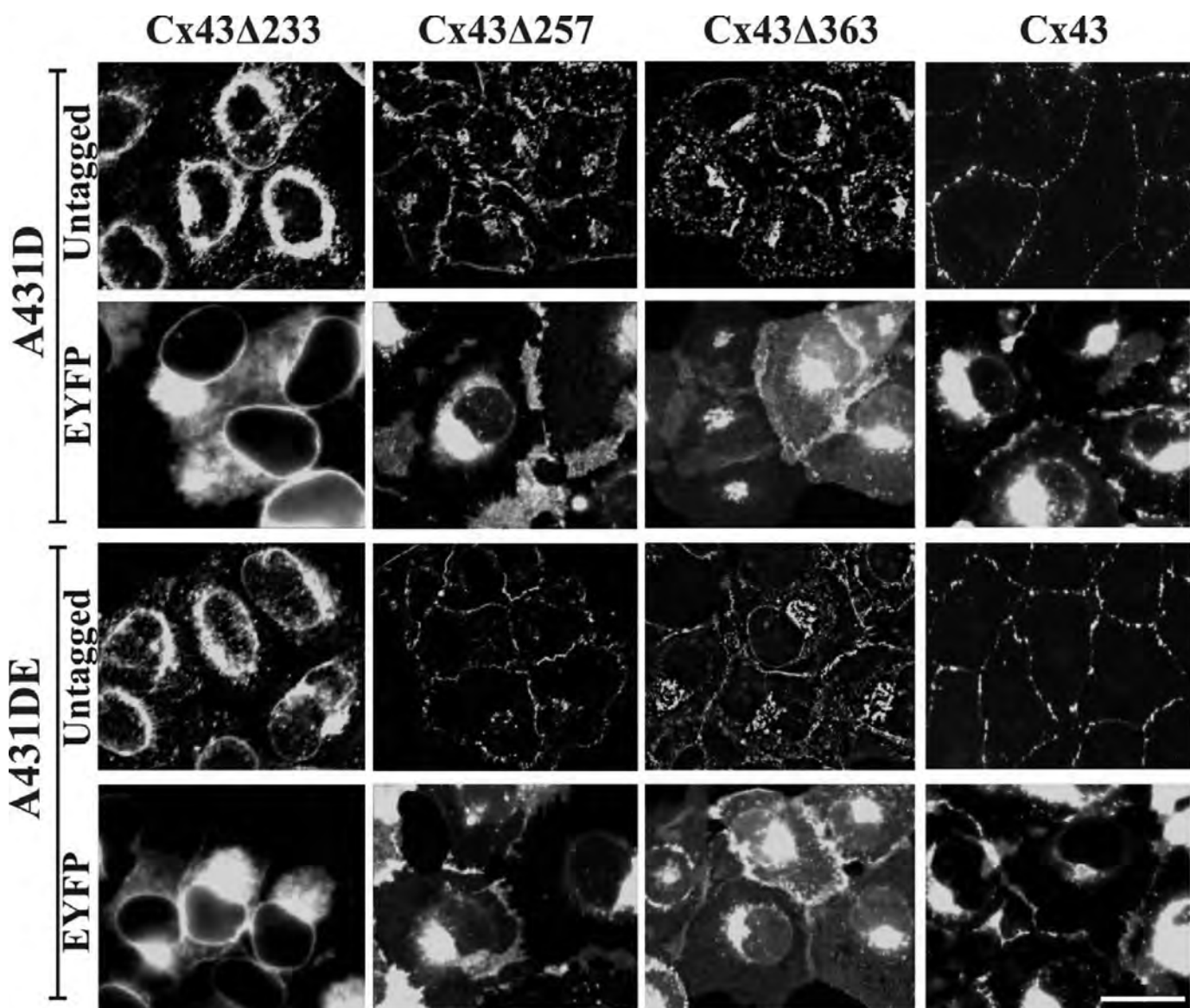


FIGURE 5. Carboxyl-terminally truncated untagged and EYFP-tagged chimeras of Cx43 fail to assemble into gap junctions. Polyclonal cultures of A431D and A431DE cells expressing Cx43Δ233, Cx43Δ233-EYFP, Cx43Δ257, Cx43Δ257-EYFP, Cx43Δ363, Cx43Δ363-EYFP, Cx43, and Cx43-EYFP were grown on glass coverslips. Cells expressing untagged Cx43 and truncated mutants were immunostained with polyclonal antibody raised against amino acid residues 252–271 of Cx43 (see under “Materials and Methods”). Note that all truncated and EYFP-tagged chimeras of Cx43 remain intracellular, whereas untagged Cx43 is assembled into GJs in cadherin-null (A431D) and E-cadherin-expressing (A431DE) cells. Note that the localization pattern of untagged *versus* EYFP-tagged full-length and mutant Cx chimeras appears to be different partly due to the brighter diffuse EYFP fluorescence of tagged Cx mutants compared with untagged Cx mutants, which were detected immunocytochemically. All EYFP-tagged and carboxyl-terminally truncated mutants are lost upon *in situ* extraction (data not shown). Bar, 10 μ m.

not bind to the second PDZ domain of ZO-1 (37); 2) Cx43Δ363, from which ZO-1 binding domain has been deleted (38, 39); 3) Cx43Δ257, from which 135 amino acids that harbor most of the potential phosphorylation sites and the known interacting motifs, including the ZO-1-binding site, have been deleted; 4) Cx43Δ257-EYFP; 5) Cx43Δ233, from which 159 amino acids comprising the entire carboxyl terminus have been deleted, including the tubulin-binding site (38, 39); 6) Cx43Δ233-EYFP; 7) Cx32-EYFP; 8) Cx32Δ220, which assembles into GJs but is devoid of most of the carboxyl terminus (24); and 9) Cx32Δ220-EYFP.

Cadherin-null A431D and E-cadherin-expressing A431DE cells were infected with the recombinant retroviruses harboring these chimeras, along with the untagged Cx43 and Cx32,

and the formation of GJs was investigated immunocytochemically in polyclonal cultures, pooled from 50 to 100 clones, within four to six population doublings. In addition, the same chimeras were also introduced into HeLa cells, which have been widely used to examine the assembly of various Cxs into GJs (7, 40, 41), and into LNCaP prostate cancer cells used in our laboratory (24). We found that chimeras Cx43-EYFP, Cx43Δ363, Cx43Δ257, Cx43Δ257-EYFP, Cx43Δ233, and Cx43Δ233-EYFP failed to assemble into GJs in A431D and A431DE cells seeded on glass coverslips and remained either intracellularly or diffusely distributed at the regions of cell-cell contact (Fig. 5) as compared with untagged Cx43 (Fig. 5, 4th column; see also Figs. 1–3). Moreover, all truncated, untagged, and EYFP-tagged mutants and chimeras of Cx43 could be extracted with 1% Tri-

Assembly of Connexin32 and Connexin43

ton X-100, suggesting that they had not assembled into GJs (data not shown). Functional studies showed that these cells did not permit the transfer of fluorescent tracer Alexa Fluor 488, Lucifer Yellow, and Alexa Fluor 594 (Table 3). We also found that, when grown on Transwell filters, Cx32Δ220 and Cx32Δ220-EYFP formed intracellular aggregates of variable size that appeared to be distributed throughout the cytoplasm both in A431D and A431DE cells (Fig. 6, *top panels*). Moreover, these aggregates or puncta were lost upon *in situ* extraction with 1% Triton X-100 (Fig. 6, *bottom panels*) as compared with full-length Cx32 (Fig. 4) and Cx32-EYFP which formed GJs (data not shown).

TABLE 3

Junctional communication of various fluorescent tracers in cells expressing wild-type and EYFP-tagged connexin43 chimeras with or without E-cadherin

A431D-43, A431DE-43, A431D-32, and A431DE-32 cells were grown on 35-mm Transwell filters in replicate at a density of 2×10^5 cells per dish and allowed to grow to confluence for 5 days. Junctional communication was measured by microinjecting different fluorescent tracers as described under "Materials and Methods."

Cell line	Lucifer Yellow	Alexa Fluor 488	Alexa Fluor 594
A431D-43	24 ± 5 ^a (22) ^b	16 ± 3 (19)	7 ± 2 (20)
A431DE-43	26 ± 4 (21) ^c	17 ± 3 (29) ^d	8 ± 3 (18) ^e
A431D-43-EYFP	0 ± 0 (36)	0 ± 0 (37)	0 ± 0 (18)
A431D-43Δ257	0 ± 0 (23)	0 ± 0 (27)	0 ± 0 (23)
A431D-43Δ363	0 ± 0 (33)	0 ± 0 (42)	0 ± 0 (44)
A431DE-43-EYFP	0 ± 0 (20)	0 ± 0 (17)	0 ± 0 (22)
A431DE-43Δ257	0 ± 0 (24)	0 ± 0 (20)	0 ± 0 (18)
A431DE-43Δ363	0 ± 0 (23)	0 ± 0 (22)	0 ± 0 (24)

^a Mean number of fluorescent cells 5 min after microinjection ± S.E. of the mean is shown.

^b Number of microinjection trials is shown. There was no statistically significant difference in junctional communication between A431D-43 and A431DE-43 cells.

^c Data are not significant; $p = 0.758$ for Lucifer Yellow.

^d Data are not significant; $p = 0.823$ for Alexa Fluor 488.

^e Data are not significant; $p = 0.779$ for Alexa Fluor 594.

Next, we investigated whether the assembly of these Cx43 chimeras could be induced upon growing cells on Transwell filters. We found that these chimeras failed to form GJs, remained intracellular or diffusely localized at the areas of cell-cell contact, and were lost upon *in situ* extraction with 1% Triton X-100 ([supplemental Fig. S9](#), compare control and extracted). In contrast, Cx43-EYFP and Cx43Δ257-EYFP formed large GJs in HeLa and LNCaP cells ([supplemental Fig. S10A](#)), and Western blotting performed in HeLa cells confirmed that chimeric Cxs were stable and migrated at the predicted size ([supplemental Fig. S10B](#)). Consistent with the earlier studies (39), we found that Cx43Δ233-EYFP, in which the tubulin-binding site had been deleted, remained intracellular in HeLa cells ([supplemental Fig. S10A, left panels](#)). Moreover, in LNCaP cells, Cx32, Cx32-EYFP, Cx32Δ220, and Cx32Δ220-EYFP were expressed appropriately and formed GJs ([supplemental Fig. S10D](#)) (24). These data suggest that carboxyl terminus of Cx43 and Cx32 is required to form GJs in A431D cells.

Connexin43, ZO-1, and Actin Co-localize as Discrete Puncta at Cell-Cell Contact Sites—Previous studies showed that Cx43 interacted with the second PDZ domain of ZO-1 (39, 42). Addition of EYFP tag to full-length Cx43 has been shown to abolish its interaction with ZO-1 (37). Moreover, the interaction of ZO-1 with Cx43 has been shown to influence GJ assembly and dynamics (22). Because chimeras Cx43-EYFP and Cx43Δ257-EYFP failed to form GJs in A431D-43 and A431DE-43 cells, but formed larger GJs in HeLa and LNCaP cells, we studied the subcellular localization of ZO-1 and Cx43 in cells expressing full-length Cx43 and EYFP-tagged chimeras in A431D-43 and

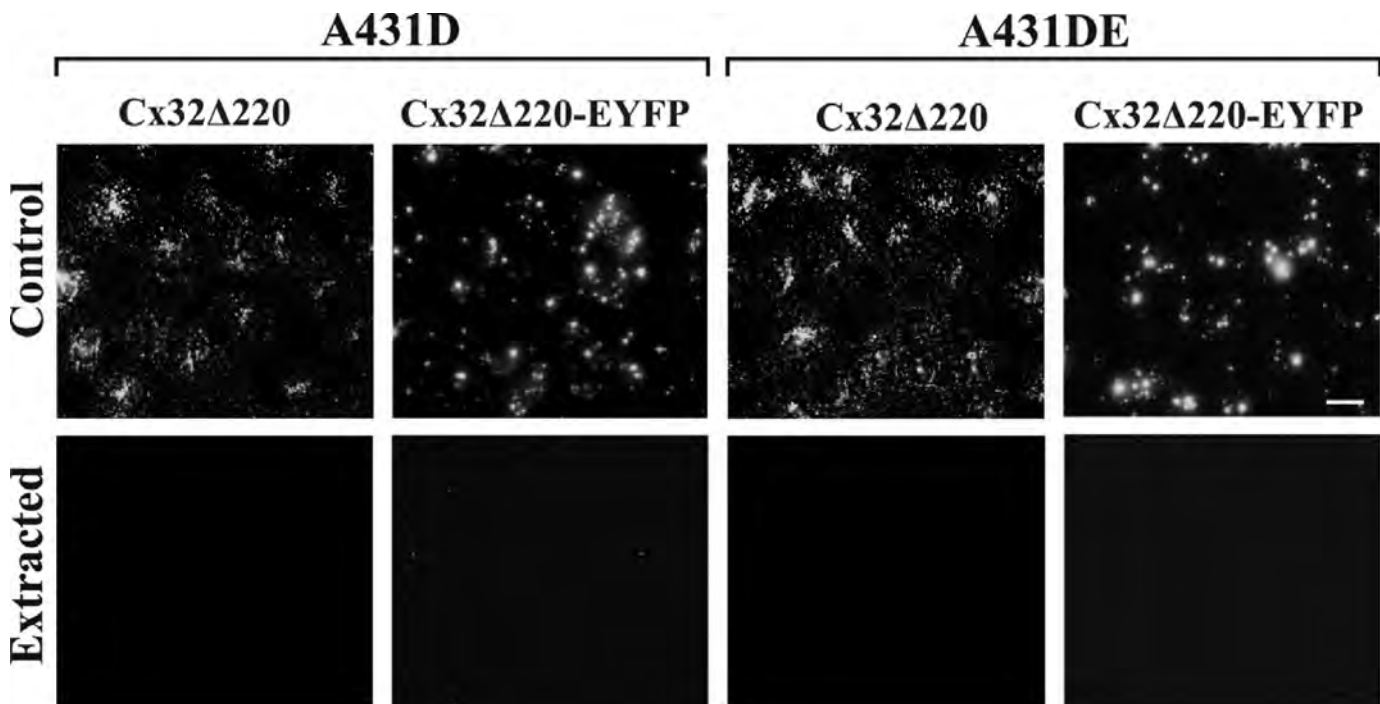


FIGURE 6. Carboxyl-terminally truncated untagged and EYFP-tagged chimera of Cx32 fail to assemble into gap junctions. Polyclonal cultures of A431D and A431DE cells expressing Cx32Δ220 and Cx32Δ220-EYFP were grown on Transwell filters and were extracted *in situ* with 1% Triton X-100 (see under "Materials and Methods"). Note that both Cx32Δ220 and Cx32Δ220-EYFP remain as scattered intracellular puncta or aggregates that are lost upon detergent extraction. Note that the localization pattern of untagged versus EYFP-tagged full-length and mutant Cx chimeras appears to be different partly due to the brighter diffuse EYFP fluorescence of tagged Cx mutants compared with untagged Cx mutants, which were detected immunocytochemically. Bar, 20 μ m.

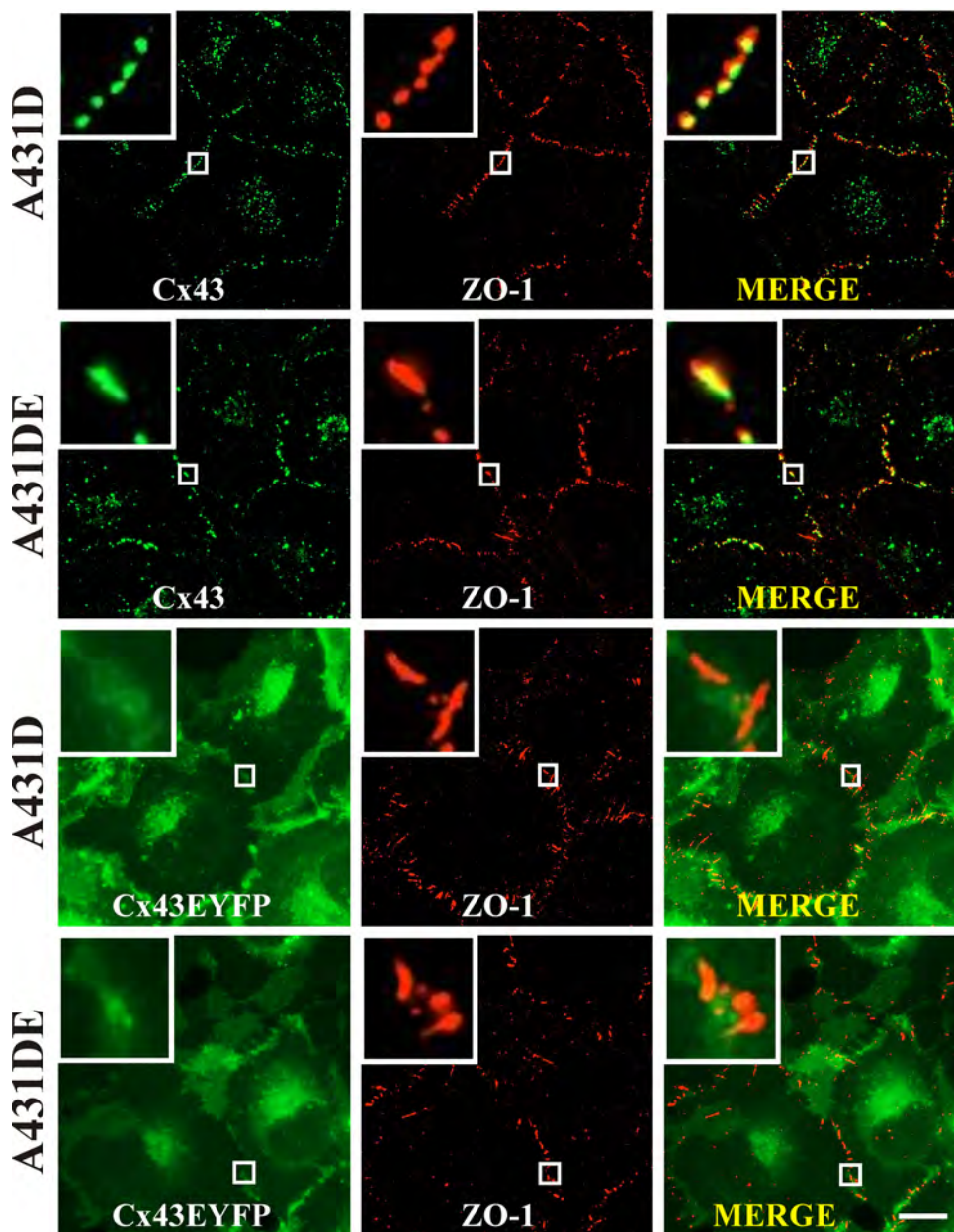


FIGURE 7. Gap junction assembly-dependent co-localization of connexin43 and ZO-1. Polyclonal cultures of A431D-43 and A431DE-43 cells, seeded on glass coverslips, were fixed, permeabilized, and immunostained for Cx43 (green) and ZO-1 (red), whereas those of Cx43-EYFP were immunostained for ZO-1 (see under “Materials and Methods”). The insets show the magnified images of co-localized Cx43 and ZO-1 puncta. Note that only untagged Cx43 is assembled into GJs and is co-localized with ZO-1. Note also that ZO-1 and Cx43-EYFP do not co-localize significantly. Bar, 10 μ m.

A431DE-43 cells. First, we found that ZO-1 was localized as discrete puncta at cell-cell contact regions (Fig. 7, top row, middle panels). Second, ZO-1 co-localized extensively with untagged Cx43 (Fig. 7, rows 1 and 2) at the areas of cell-cell contact and not at intracellular sites. Third, as expected, ZO-1 did not co-localize with Cx43-EYFP (Fig. 7, rows 3 and 4) or with Cx43 Δ 257 and Cx43 Δ 363 (data not shown). Fourth, there was no noticeable difference in the pattern and the extent of co-localization of Cx43 and ZO-1 between A431D-43 and A431DE-43 cells.

Apart from binding to α -catenin, occludin, and claudins, ZO-1 has also been shown to bind actin (43, 44). Because Cx43

and ZO-1 co-localized extensively at the areas of cell-cell contact, and the fact that actin has been documented to play a critical role in the establishment and/maintenance of adherens and tight junctions (35, 45, 46), we examined the role of actin in GJ assembly. To test this notion, we immunostained Alexa Fluor 350-conjugated phalloidin-labeled A431D-43 and A431DE-43 cells for Cx43 and ZO-1 using Alexa Fluor 594- and Alexa Fluor 488-conjugated secondary antibodies. Fig. 8 shows that Cx43 and ZO-1 puncta appeared to associate with the actin fibers lining the cell peripheries.

To explore further the relationship between Cx43, ZO-1 and actin, we examined the effect of disrupting actin filaments on GJ assembly. Cells were treated with cytochalasin B (1 μ g/ml) for 1–6 h, and the localization of F-actin, Cx43, and ZO-1 was examined as described above. Fig. 9 shows that in cadherin-null A431D-43 cells, cytochalasin B disrupted cortical F-actin and GJ puncta, which were displaced to subcellular compartments. These changes were observed as early as 1 h after treatment (Fig. 9, compare rows 1 and 2). On the other hand, in cadherin-expressing A431DE-43 cells, cytochalasin B failed to disrupt gap junctional plaques noticeably, and Cx43 and ZO-1 persisted as puncta at cell-cell contact areas (Fig. 9, compare rows 3 and 4) even up to 6 h (supplemental Fig. S11). Moreover, the depolymerization of actin itself appeared to have been delayed in A431DE-43 cells (supplemental Fig. S11). Also, we found that in cytochalasin B-treated A431D-43

cells, Cx43 and ZO-1 puncta appeared to co-localize in subcellular compartments, suggesting that they might have internalized together. Altogether, the above data suggest that intimacy between Cx43 and F-actin via ZO-1 may be required to maintain or stabilize GJ plaques. Moreover, the data also suggest that E-cadherin might facilitate the stabilization of gap junctional plaques via the direct or indirect interaction of plaque components with actin filaments.

ZO-1 Knockdown Attenuates Gap Junction Formation—To test directly if ZO-1 was required for the formation and/or maintenance of GJs, we silenced its expression by siRNAs in A431D-43 and A431DE-43 cells. For these experiments, we

Assembly of Connexin32 and Connexin43

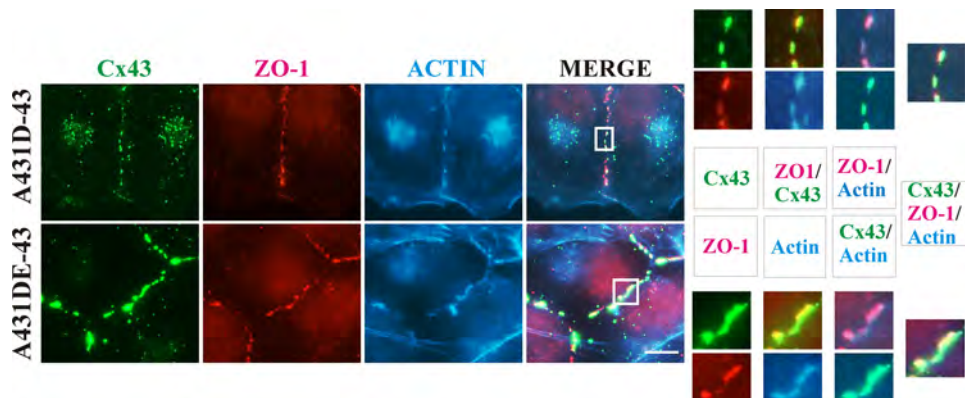


FIGURE 8. Connexin43 and ZO-1 puncta are formed on F-actin at cell-cell contact. A431D-43 (top row) and A431DE-43 (bottom row) cells, seeded on glass coverslips, were immunostained for Cx43 (green) and ZO-1 (red). F-actin (blue) was detected using Alexa Fluor 350-conjugated phalloidin. The magnified images of co-localized Cx43, ZO-1, and F-actin are shown on the right, and the key describing the corresponding images in color is shown in the middle. Note that significant co-localization of Cx43, ZO-1, and F-actin is observed only at puncta and at the regions of cell-cell contact. Bar, 5 μ m.

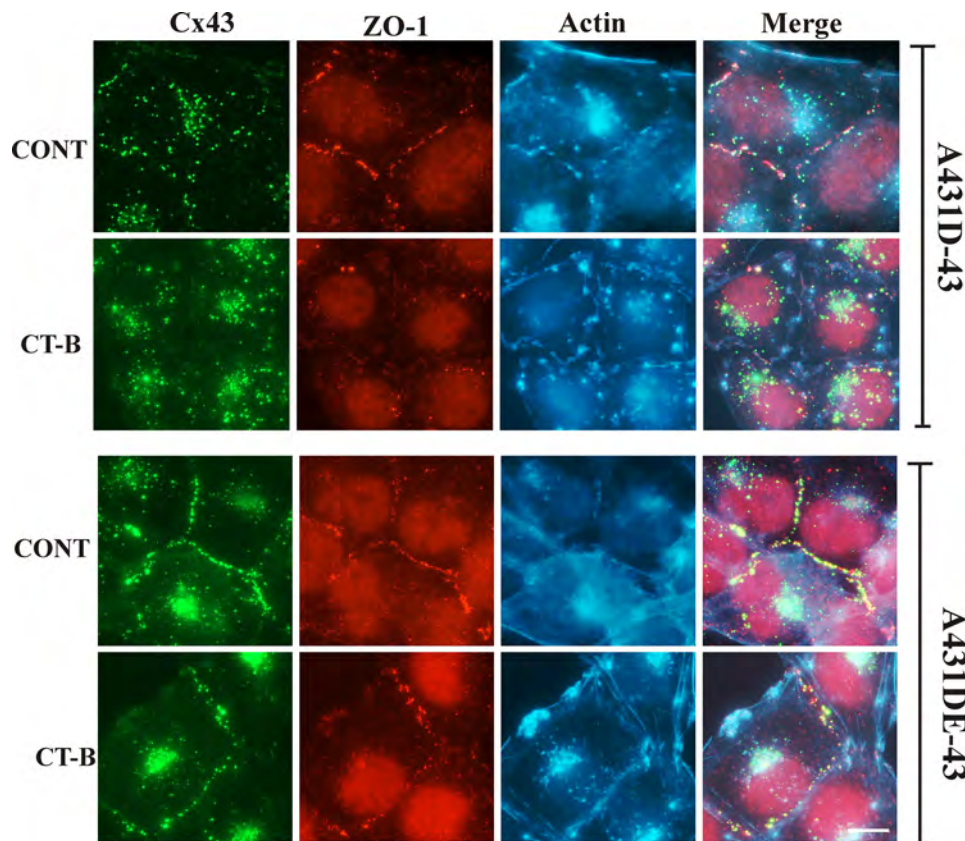


FIGURE 9. E-cadherin delays gap junction disassembly. A431D-43 and A431DE-43 cells, seeded on glass coverslips, were treated with cytochalasin B at 1 μ g/ml (labeled CT-B) for 1–6 h and immunostained for Cx43 and ZO-1. F-actin was detected with Alexa Fluor 350-conjugated phalloidin. Note that co-localized GJ puncta of Cx43 and ZO-1 are disrupted/internalized within 1 h in A431D-43 cells, whereas no detectable disruption/internalization is noticed in A431DE-43 cells within 1 h and even until 6 h (supplemental Fig. S11). Bar, 5 μ m. CONT, control.

used Dharmacon control siGLO and Smart Pool ZO-1 siRNAs. We first optimized experimental conditions, both duration and concentration of siRNAs, to achieve near 100% transfection efficiency in A431D-43 and A431DE-43 cells (supplemental Fig. S12A, and see “Materials and Methods”). As assessed by Western blot analysis of the total cell lysates, we

consistently observed a robust 80–90% knockdown of ZO-1 (Fig. 10A). Immunocytochemical analysis showed that ZO-1 knockdown drastically diminished the preponderance of GJ puncta at the areas of cell-cell contact (Fig. 10B, *1st column*, compare *1st* and *2nd rows* with *3rd* and *4th rows*) and enhanced accumulation of Cx43 in the cytosol both in A431D-43 and A431DE-43 cells (Fig. 10B, *2nd* and *4th rows*, *right* and *left panels*). Knockdown of lamin A/C, a nuclear membrane-associated protein (data not shown), or mock transfection of control siRNAs (SiGLO) had no discernible effect on the formation of GJs (supplemental Fig. S12B). These findings suggest that ZO-1 is required to initiate and/or stabilize the formation of gap junctional plaques both in cadherin-null (A431D) and E-cadherin-expressing (A431DE) cells.

DISCUSSION

It is as yet unknown how the docking of connexons and the clustering of gap junctional channels are initiated upon cell-cell contact. Cadherins have been thought to facilitate the assembly of GJs by enhancing cell-cell contact; however, the molecular mechanisms involved in this process have remained unexplored. Here, we investigated whether E-cadherin expression was sufficient to facilitate the assembly of connexons into GJs via triggering cell-cell adhesion or whether additional events were required. To further explore the molecular mechanisms, we also examined the role of the carboxyl tail of Cx43, a ubiquitously expressed Cx (2, 18, 22), and of Cx32, a Cx expressed preferentially by the well differentiated and polarized cells (23), in controlling the formation of GJs in the presence and absence of E-cadherin. The ration-

ale behind undertaking these studies was that the carboxyl termini of Cxs are highly divergent, are phosphorylated by several kinases, and interact with several proteins (21, 22), which might allow assembly to be regulated promiscuously by cadherins in a Cx-specific manner. For our studies, we utilized cadherin-null A431D cells, which have been used to examine adherens junc-

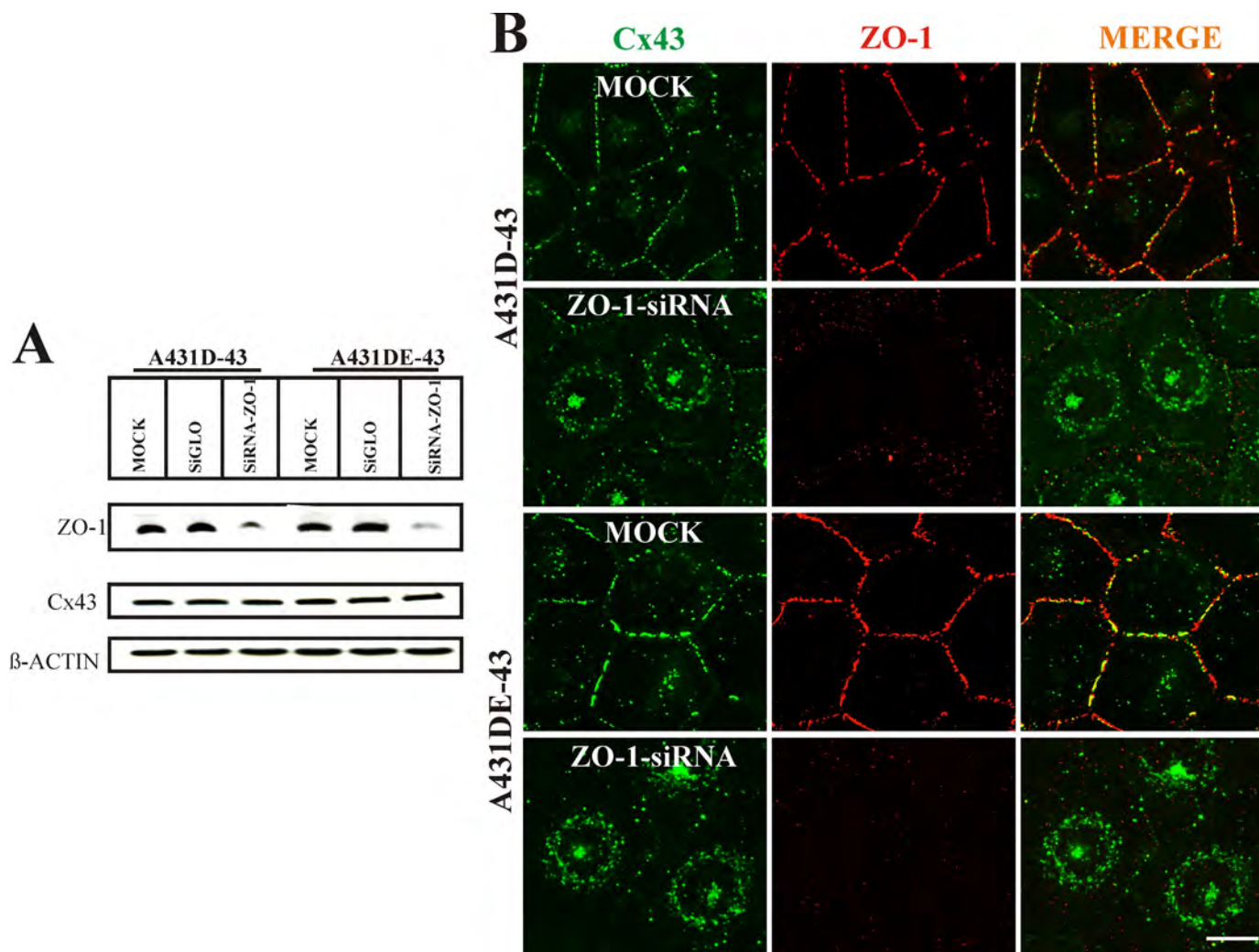


FIGURE 10. ZO-1 knockdown disrupts gap junction assembly. A431D-43 and A431DE-43 cells were either mock-transfected with Oligofectamine (labeled *MOCK*) or transfected with 130 nm ZO-1 SMARTpool siRNA (labeled *siRNA*) or DY-547-labeled control RISC-free siGLO RNA (labeled *SIGLO*) as described under “Materials and Methods.” *A*, expression of ZO-1 and Cx43 was determined by immunoblotting 10 μ g of total protein. The blots were re-probed with anti- β -actin antibody to verify equal loading. Note that ZO-1 expression is reduced significantly in cells transfected with ZO-1 SMARTpool siRNAs. *B*, cells were immunostained for Cx43 and ZO-1 together. Note that ZO-1 staining (red) is significantly reduced in ZO-1 SMART pool siRNA-transfected cells compared with MOCK-transfected cells. Note significant loss of gap junction puncta (green), with a concomitant increase in the intracellular Cx43 staining, in ZO-1 siRNA-transfected cells compared with MOCK-transfected cells. Bar, 10 μ m.

tion assembly in previous studies (19, 20). Our findings documented that E-cadherin-mediated cell-cell adhesion was neither essential nor sufficient to initiate the formation of GJs *de novo* in A431D cells and facilitated the growth and assembly of only preformed GJs composed of Cx43. Growth of cells on Transwell filters was required to initiate the assembly of Cx32. Our findings also demonstrate a novel and an essential role of the carboxyl termini of Cx43 and Cx32 in initiating the formation of GJs *de novo* in A431D cells. Moreover, our studies further document that ZO-1 is required to initiate or stabilize GJs composed of Cx43 and that direct or indirect cross-talk between Cxs and the actin cytoskeleton via ZO-1 may be essential for GJ assembly.

Our biotinylation data showed that even though both Cxs trafficked normally to the cell surface (Fig. 3), only Cx43 was able to assemble into GJs (Fig. 1A). Moreover, E-cadherin expression facilitated the assembly of only Cx43 and failed to induce the assembly of Cx32 (Fig. 1A). These data suggest

that the assembly of Cxs into GJs upon arrival at the cell surface is subject to regulatory mechanisms at the site of cell-cell contact that are likely to be Cx-specific and that cell-cell adhesion by itself is not sufficient to initiate the assembly. Because expression of Cx32 and Cx43 by itself neither triggered nor augmented E-cadherin-mediated cell-cell adhesion (*supplemental Fig. S4*), these regulatory mechanisms are likely to be cell-cell adhesion-independent, at least with regard to the type of adhesion measured by cell-cell aggregation assay, which has been widely used to document cell-cell adhesion mediated by cadherins (19, 32) as well as by Cxs (47, 48). Although previous studies have demonstrated an important role of cell-cell adhesion in facilitating GJ assembly (12–15), our findings do not rule out the causative role played by other cell-cell adhesion mechanisms that are independent of E-cadherin and connexins. Notwithstanding that such cell-cell adhesion systems likely exist in A431D cells, for example those mediated by nectins, NCAM, and JAMS, etc. (9, 10), they were insuffi-

Assembly of Connexin32 and Connexin43

cient to trigger the assembly of Cx32 in monolayer cultures, which suggests that the assembly was regulated promiscuously in a Cx-specific manner both in the presence and absence of E-cadherin.

With regard to the assembly of Cx43, E-cadherin expression not only increased the mean size of the GJs but also decreased the mean number of puncta per interface by 2-fold (*supplemental Fig. S1* and *Fig. S2*). One plausible explanation for these data might be that formation of cadherin trans-dimers, or adherens junctions, initiates a signaling pathway that facilitates the coalescence of smaller puncta, which are highly dynamic and unstable (49, 50), into larger ones without affecting the frequency of plaque initiation, possibly via altering actin dynamics at the site of cell-cell contact (45). This explanation is in accord with the findings, which showed that expression of E-cadherin not only induced cell-cell adhesion in A431D cells (*supplemental Fig. S4*) but also stabilized expression and recruited α - and β -catenins to the site of cell-cell contact (*Fig. 1, B* and *D*). Moreover, this explanation is also in congruence with the findings that formation of cadherin trans-dimers appears to leave a distance of 20–25 nm between contiguous plasma membranes (10, 51), which is likely to hinder the docking of connexons that can protrude from the cell surface at the most by a few nanometers. Our findings with A431D cells showed that the assembly was triggered in the absence of measurable cell-cell adhesion, which had been presumed to be necessary.

Our data with cadherin-null A431D cells have unveiled a previously unrecognized essential role of the carboxyl tails of Cxs in initiating the assembly of GJs. In congruence with the findings reported in other studies, the carboxyl tail-deleted Cxs and the EYFP-tagged chimeras used in this study formed GJs in HEK293, HeLa, and the human prostate cancer cell line LNCaP. One possible explanation for these data is that in cadherin-null A431D cells, the linkage of Cxs to actin via carboxyl termini may be required to prime the initiation of GJ plaques before their maturation into larger plaques, as has been demonstrated during the genesis of adherens junctions (52–54), and that the requirement for this linkage is either bypassed or compensated by alternative pathway(s) used to assemble GJs when cadherins are present such as in N-cadherin-expressing HeLa and HEK293 cells and E-cadherin-expressing LNCaP cells (24, 55).

The carboxyl termini of Cxs interact with several proteins, such as ZO-1 and ZO-2, which are thought to form scaffolding complexes that link Cxs to the cytoskeleton (21, 22). Our findings showed that GJs were formed on actin-rich fibers at the areas of cell-cell contact where ZO-1 and Cx43 co-localized extensively (*Fig. 8*). Moreover, ZO-1 did not co-localize with Cx43-EYFP, Cx43 Δ 363, Cx43 Δ 257, and Cx43 Δ 257-EYFP, which failed to assemble into GJs in A431D cells (*Fig. 7*). Furthermore, GJs were disassembled within 1 h after cytochalasin B treatment in cadherin-null A431D43 cells, and the disassembly was delayed in E-cadherin-expressing A431DE-43 cells. Although the interaction of ZO-1 with Cx43 has been shown to modulate GJ assembly and disassembly, the mechanisms have not yet been elucidated. Our data imply that, at least in A431D and A431DE cells, a direct or indirect interaction between Cx43 and actin via ZO-1 may be required to initiate the formation of nascent GJ plaques or to stabilize them, and this interaction

might be further strengthened by E-cadherin via α -catenin as has been observed during the formation of adherens junctions (52, 54). This explanation is in accord with our data, which showed that junctional plaques were more stable in E-cadherin-expressing A431DE-43 cells compared with cadherin-null A431D-43 cells. This notion is further substantiated by our data, which show that ZO-1 knockdown attenuated GJ assembly both in A431D-43 and A431DE-43 cells (*Fig. 10*), and by our findings demonstrating the failure of Cx43-EYFP, Cx43 Δ 363, Cx43 Δ 257, and Cx43 Δ 257-EYFP (which do not bind ZO-1) to assemble into GJs. This line of thought is further supported by the studies, which showed that the specific interaction between the PDZ2 domain of ZO-1 and Cx43 was required for GJ assembly but not for trafficking to the cell surface (56, 57). Our data also support the conclusions drawn from earlier studies, which showed that the clustering of cell-cell channels to form nascent GJ puncta and their incorporation into the plaques, but not the maintenance of matured GJ plaques, was dependent on an intact actin cytoskeleton (58–60).

The above arguments may also apply to the assembly of Cx32 into GJs in cells grown on Transwell filters. For example, Cx32 is predominantly expressed by well differentiated and polarized cells (23), and it is likely that its assembly into GJs might also be governed by the appropriate expression of proteins that maintain or are induced upon partial polarization and that allow it to interact with the cytoskeletal proteins via its carboxyl terminus. The acquisition of the polarized state is accompanied not only by extensive remodeling of cytoskeletal elements but also by recruitment of several protein complexes to the areas of cell-cell contact such as Crumbs complex and the partitioning defective complex (35, 46, 61–63). Connexin32, apart from interacting with caveolin-1 and Cx26, has been shown to interact with occludin, a tight junction-associated protein that binds ZO-1 (21), and with Discs Large Homolog-1 (64), a protein with multiple PDZ binding domains expressed in well differentiated and polarized cells. Moreover, this line of thought is consistent with the failure of carboxyl tail-deleted Cx32 Δ 220 and Cx32 Δ 220-EYFP to assemble into GJs in cadherin-null and E-cadherin-expressing cells (*Fig. 6*).

An intriguing aspect of the data with respect to the assembly of Cx32 on Transwell filters is that despite robust formation of GJ puncta and their detergent insolubility (*Fig. 4*), the channels did not permit the transfer of GJ-permeable fluorescent tracers, such as Lucifer Yellow, Alexa Fluor 488, and Alexa Fluor 594 (*Table 2*), which are known to pass through these channels (3). In this regard our data showed that when grown on Transwell filters for 3–6 days, A431D and A431DE cells, while becoming more columnar as assessed by a 2-fold increase in cell height compared with cells grown on plastic (*supplemental Fig. S7*), failed to attain a fully polarized state as assessed by the random orientation of Golgi stacks and distribution of β 1-integrin, ZO-1, and Na-K-ATPase at the apical and basolateral domains (*supplemental Fig. S7*). Although there may be several explanations for these findings, one plausible explanation is that additional physiological stimuli or acquisition of a fully polarized state may be required to open these channels. Alternatively, GJs may serve yet another function independent of communication

when cells have acquired a polarized state, which is known to last from minutes to days or even years (46, 62, 63). The role of gap junctional communication in maintaining the polarized and the differentiated state of epithelial cells has not yet been investigated. Recent studies have shown that formation of GJs is required to induce the assembly of tight junctions or to maintain them (65). The fact that cell polarization also enhanced the assembly of Cx43 into gap junctions in cadherin-null A431D-43 cells, and E-cadherin expression had no further effect, suggests that its assembly might also be regulated by proteins that are induced upon polarization and that may allow maturation of gap junctional puncta in the absence of E-cadherin expression. Although the molecular mechanisms involved in the assembly of Cx32 into GJs in cells grown on Transwell filters remain to be investigated, our findings imply that distinct regulatory mechanisms are utilized to initiate its formation into nascent gap junctional plaques, the choice of which is likely dictated by the physiological state of the cells.

What might be the possible physiological relevance of E-cadherin-mediated facilitation of GJ assembly with regard to increase in plaque size, stability, and function of cell-cell channels? The number of channels in a given GJ plaque may range from 50 to over 10,000, and there is a wide range of variation in the size of GJs formed between two adjacent cells (3, 66). Moreover, clustering of cell-cell channels and increase in GJ size and function in response to polypeptide hormones is frequently observed (67). Furthermore, it has been demonstrated that clustering of cell-cell channels is a prerequisite for the opening of cell-cell channels and that larger GJ plaques have more open channels compared with smaller plaques in which most channels remain closed (68). Although our data showed that E-cadherin expression had no discernible effect on the permeability of fluorescent tracers, such as Lucifer Yellow, Alexa Fluor 488, and Alexa Fluor 594, it is possible that permeability to physiologically relevant molecules or to smaller molecules less than 443 Da was enhanced upon E-cadherin expression, which increases the frequency of larger GJ plaques in A431DE-43 cells. Alternatively, E-cadherin-mediated increase in GJ plaque size and stability may facilitate the assembly of other junctional complexes, which are required to maintain the polarized and differentiated state of epithelial cells (62, 63). More elaborate studies with a variety of cell-cell adhesion molecules are needed to assess further the physiological significance of our findings with respect to the functional role of gap junctional communication.

In essence, our studies with human A431D squamous carcinoma-derived cells have shown that the assembly of Cx43 and Cx32 upon arrival at the cell surface is regulated differently both in the absence and presence of E-cadherin, although the molecular nature of the mechanisms involved remains to be elaborated. We have also shown that E-cadherin-mediated cell-cell adhesion facilitates the assembly of GJs composed of Cx43 but is not sufficient to induce the assembly of Cx32. Using A431D and A431DE cells, we have uncovered a role for the carboxyl tails of Cx43 and Cx32 in initiating the *de novo* formation of GJs, which had remained previously unrecognized. Our

data also imply that direct or indirect cross-talk between carboxyl tails of Cxs and actin cytoskeleton via ZO-1 may regulate GJ assembly and growth. The fact that our findings pertaining to the role of E-cadherin and ZO-1 in regulating the assembly of Cxs into GJs in A431D cell culture model systems are different from those reported in other cell culture models implies that multiple regulatory mechanisms are likely utilized in a physiological state, cell context, and internal and external milieu-dependent manner to control GJ size, dynamics, and growth. Future studies will be needed to fully understand and elaborate the molecular mechanism by which E-cadherin expression facilitates the assembly of Cx43 into GJs, how cross-talk between Cx43 and actin via ZO-1 regulates plaque dynamics and assembly, and how cell growth on Transwell filters facilitates the assembly of Cx32 into GJs.

Acknowledgments—We thank Kristen Johnson, Linda Kelsey, and Parul Katoch for technical help and friendship.

REFERENCES

1. Beyer, E. C., and Berthoud, V. M. (2009) in *Connexins: A Guide* (Harris, A., and Locke, D., eds) pp. 3–26, Springer, Humana Press, NY
2. Laird, D. W. (2006) *Biochem. J.* **394**, 527–543
3. Sosinsky, G. E., and Nicholson, B. J. (2005) *Biochim. Biophys. Acta* **1711**, 99–125
4. Falk, M. M., Baker, S. M., Gumpert, A. M., Segretain, D., and Buckheit, R. W., 3rd (2009) *Mol. Biol. Cell* **20**, 3342–3352
5. Gaietta, G., Deerinck, T. J., Adams, S. R., Bouwer, J., Tour, O., Laird, D. W., Sosinsky, G. E., Tsien, R. Y., and Ellisman, M. H. (2002) *Science* **296**, 503–507
6. Jordan, K., Chodock, R., Hand, A. R., and Laird, D. W. (2001) *J. Cell Sci.* **114**, 763–773
7. Piehl, M., Lehmann, C., Gumpert, A., Denizot, J. P., Segretain, D., and Falk, M. M. (2007) *Mol. Biol. Cell* **18**, 337–347
8. Musil, L. S. (2009) in *Connexins: A Guide* (Harris, A., and Locke, D., eds) pp. 225–240, Springer, Humana Press, NY
9. Nelson, W. J. (2008) *Biochem. Soc. Trans.* **36**, 149–155
10. Teppas, U., Trunong, K., Godt, D., Ikura, M., and Peifer, M. (2000) *Nat. Rev. Cell Mol. Biol.* **1**, 91–100
11. Wheelock, M. J., and Johnson, K. R. (2003) *Annu. Rev. Cell Dev. Biol.* **19**, 207–235
12. Hernandez-Blazquez, F. J., Joazeiro, P. P., Omori, Y., and Yamasaki, H. (2001) *Exp. Cell Res.* **270**, 235–247
13. Jongen, W. M., Fitzgerald, D. J., Asamoto, M., Piccoli, C., Slaga, T. J., Gros, D., Takeichi, M., and Yamasaki, H. (1991) *J. Cell Biol.* **114**, 545–555
14. Meyer, R. A., Laird, D. W., Revel, J. P., and Johnson, R. G. (1992) *J. Cell Biol.* **119**, 179–189
15. Musil, L. S., Cunningham, B. A., Edelman, G. M., and Goodenough, D. A. (1990) *J. Cell Biol.* **111**, 2077–2088
16. Crespin, S., Defamie, N., Cronier, L., and Mesnil, M. (2009) in *Connexins: A Guide* (Harris, A., and Locke, D., eds) pp. 529–542, Springer, Humana Press, NY
17. Thiery, J. P., and Sleeman, J. P. (2006) *Nat. Rev. Mol. Cell Biol.* **7**, 131–142
18. Wei, C. J., Xu, X., and Lo, C. W. (2004) *Annu. Rev. Cell Dev. Biol.* **20**, 811–838
19. Lewis, J. E., Wahl, J. K., 3rd, Sass, K. M., Jensen, P. J., Johnson, K. R., and Wheelock, M. J. (1997) *J. Cell Biol.* **136**, 919–934
20. Sobolik-Delmaire, T., Katafiasz, D., and Wahl, J. K., 3rd (2006) *J. Biol. Chem.* **281**, 16962–16970
21. Hervé, J. C., Bourmeyster, N., Sarrouilhe, D., and Duffy, H. S. (2007) *Prog. Biophys. Mol. Biol.* **94**, 29–65
22. Solan, J. L., and Lampe, P. D. (2009) *Biochem. J.* **419**, 261–272
23. Bavamian, S., Klee, P., Allagnat, F., Haefliger, J. A., and Meda, P. (2009) in *Connexins: A Guide* (Harris, A., and Locke, D., eds) pp. 511–527, Springer,

Assembly of Connexin32 and Connexin43

Humana Press, NY

24. Mitra, S., Annamalai, L., Chakraborty, S., Johnson, K., Song, X. H., Batra, S. K., and Mehta, P. P. (2006) *Mol. Biol. Cell* **17**, 5400–5416
25. Govindarajan, R., Zhao, S., Song, X. H., Guo, R. J., Wheelock, M., Johnson, K. R., and Mehta, P. P. (2002) *J. Biol. Chem.* **277**, 50087–50097
26. Mehta, P. P., Perez-Stable, C., Nadji, M., Mian, M., Asotra, K., and Roos, B. A. (1999) *Dev. Genet.* **24**, 91–110
27. Lauf, U., Lopez, P., and Falk, M. M. (2001) *FEBS Lett.* **498**, 11–15
28. VanSlyke, J. K., and Musil, L. S. (2000) *Methods* **20**, 156–164
29. Shintani, Y., Fukumoto, Y., Chaika, N., Svoboda, R., Wheelock, M. J., and Johnson, K. R. (2008) *J. Cell Biol.* **180**, 1277–1289
30. Rudnicki, J. A., and McBurney, M. W. (1987) in *Teratocarcinomas and Embryonic Stem Cells: A Practical Approach* (Robertson, E. J., ed) pp. 19–49, IRL Press at Oxford University Press, Oxford
31. Gourdie, R. G., Green, C. R., and Severs, N. J. (1991) *J. Cell Sci.* **99**, 41–55
32. Kim, S. H., Li, Z., and Sacks, D. B. (2000) *J. Biol. Chem.* **275**, 36999–37005
33. Mills, I. G., Jones, A. T., and Clague, M. J. (1998) *Curr. Biol.* **8**, 881–884
34. Nakamura, N., Rabouille, C., Watson, R., Nilsson, T., Hui, N., Slusarewicz, P., Kreis, T. E., and Warren, G. (1995) *J. Cell Biol.* **131**, 1715–1726
35. Rodriguez-Boulan, E., Kreitzer, G., and Müsch, A. (2005) *Nat. Rev. Mol. Cell Biol.* **6**, 233–247
36. Solan, J. L., and Lampe, P. D. (2009) in *Connexins: A Guide* (Harris, A., and Locke, D., eds) pp. 263–286, Springer, Humana Press, NY
37. Hunter, A. W., Barker, R. J., Zhu, C., and Gourdie, R. G. (2005) *Mol. Biol. Cell* **16**, 5686–5698
38. Giepmans, B. N., Verlaan, I., Hengeveld, T., Janssen, H., Calafat, J., Falk, M. M., and Moolenaar, W. H. (2001) *Curr. Biol.* **11**, 1364–1368
39. Giepmans, B. N., and Moolenaar, W. H. (1998) *Curr. Biol.* **8**, 931–934
40. Elfgang, C., Eckert, R., Lichtenberg-Fraté, H., Butterweck, A., Traub, O., Klein, R. A., Hülser, D. F., and Willecke, K. (1995) *J. Cell Biol.* **129**, 805–817
41. Lauf, U., Giepmans, B. N., Lopez, P., Braconnor, S., Chen, S. C., and Falk, M. M. (2002) *Proc. Natl. Acad. Sci. U.S.A.* **99**, 10446–10451
42. Giepmans, B. N., Hengeveld, T., Postma, F. R., and Moolenaar, W. H. (2001) *J. Biol. Chem.* **276**, 8544–8549
43. Fanning, A. S., Jameson, B. J., Jesaitis, L. A., and Anderson, J. M. (1998) *J. Biol. Chem.* **273**, 29745–29753
44. Fanning, A. S., Ma, T. Y., and Anderson, J. M. (2002) *FASEB J.* **16**, 1835–1837
45. Mège, R. M., Gavard, J., and Lambert, M. (2006) *Curr. Opin. Cell Biol.* **18**, 541–548
46. Li, R., and Gundersen, G. G. (2008) *Nat. Rev. Mol. Cell Biol.* **9**, 860–873
47. Cotrina, M. L., Lin, J. H., and Nedergaard, M. (2008) *Glia* **56**, 1791–1798
48. Lin, J. H., Takano, T., Cotrina, M. L., Arcuino, G., Kang, J., Liu, S., Gao, Q., Jiang, L., Li, F., Lichtenberg-Frate, H., Haubrich, S., Willecke, K., Goldman, S. A., and Nedergaard, M. (2002) *J. Neurosci.* **22**, 4302–4311
49. Holm, I., Mikhailov, A., Jillson, T., and Rose, B. (1999) *Eur. J. Cell Biol.* **78**, 856–866
50. Jordan, K., Solan, J. L., Dominguez, M., Sia, M., Hand, A., Lampe, P. D., and Laird, D. W. (1999) *Mol. Biol. Cell* **10**, 2033–2050
51. Miyaguchi, K. (2000) *J. Struct. Biol.* **132**, 169–178
52. Adams, C. L., Chen, Y. T., Smith, S. J., and Nelson, W. J. (1998) *J. Cell Biol.* **142**, 1105–1119
53. Itoh, M., Nagafuchi, A., Moroi, S., and Tsukita, S. (1997) *J. Cell Biol.* **138**, 181–192
54. Vasioukhin, V., Bauer, C., Yin, M., and Fuchs, E. (2000) *Cell* **100**, 209–219
55. Shaw, R. M., Fay, A. J., Putthenveedu, M. A., von Zastrow, M., Jan, Y. N., and Jan, L. Y. (2007) *Cell* **128**, 547–560
56. Chen, J., Pan, L., Wei, Z., Zhao, Y., and Zhang, M. (2008) *EMBO J.* **27**, 2113–2123
57. Hunter, A. W., and Gourdie, R. G. (2008) *Cell Commun. Adhes.* **15**, 55–63
58. Johnson, R. G., Meyer, R. A., Li, X. R., Preus, D. M., Tan, L., Grunewald, H., Paulson, A. F., Laird, D. W., and Sheridan, J. D. (2002) *Exp. Cell Res.* **275**, 67–80
59. Thomas, T., Jordan, K., and Laird, D. W. (2001) *Cell Commun. Adhes.* **8**, 231–236
60. Wang, Y., and Rose, B. (1995) *J. Cell Sci.* **108**, 3501–3508
61. Bornens, M. (2008) *Nat. Rev. Mol. Cell Biol.* **9**, 874–886
62. Bryant, D. M., and Mostov, K. E. (2008) *Nat. Rev. Mol. Cell Biol.* **9**, 887–901
63. Mellman, I., and Nelson, W. J. (2008) *Nat. Rev. Mol. Cell Biol.* **9**, 833–845
64. Duffy, H. S., Iacobas, I., Hotchkiss, K., Hirst-Jensen, B. J., Bosco, A., Dandachi, N., Dermietzel, R., Sorgen, P. L., and Spray, D. C. (2007) *J. Biol. Chem.* **282**, 9789–9796
65. Kojima, T., Murata, M., Go, M., Spray, D. C., and Sawada, N. (2007) *J. Membr. Biol.* **217**, 13–19
66. Sosinsky, G. E., Gaietta, G., and Giepmans, B. N. (2009) in *Connexins: A Guide* (Harris, A., and Locke, D., eds) pp. 241–261, Springer, Humana Press, NY
67. Stagg, R. B., and Fletcher, W. H. (1990) *Endocr. Rev.* **11**, 302–325
68. Bukauskas, F. F., Jordan, K., Bukauskienė, A., Bennett, M. V., Lampe, P. D., Laird, D. W., and Verselis, V. K. (2000) *Proc. Natl. Acad. Sci. U.S.A.* **97**, 2556–2561
69. Deleted in proof

Assembly of Connexin43 into Gap Junctions Is Regulated Differentially by E-Cadherin and N-Cadherin in Rat Liver Epithelial Cells

Rajgopal Govindarajan,* Souvik Chakraborty,† Kristen E. Johnson,†
Matthias M. Falk,‡ Margaret J. Wheelock,† Keith R. Johnson,† and
Parmender P. Mehta†

†Department of Biochemistry and Molecular Biology, Eppley Institute for Research in Cancer and Allied Diseases, Eppley Cancer Center, University of Nebraska Medical Center, Omaha, NE 68198; and ‡Department of Biological Sciences, Lehigh University, Bethlehem, PA, 18015

Submitted May 7, 2010; Revised September 15, 2010; Accepted September 22, 2010

Monitoring Editor: Asma Nusrat

Cadherins have been thought to facilitate the assembly of connexins (Cxs) into gap junctions (GJs) by enhancing cell–cell contact, however the molecular mechanisms involved in this process have remained unexplored. We examined the assembly of GJs composed of Cx43 in isogenic clones derived from immortalized and nontransformed rat liver epithelial cells that expressed either epithelial cadherin (E-Cad), which curbs the malignant behavior of tumor cells, or neuronal cadherin (N-Cad), which augments the invasive and motile behavior of tumor cells. We found that N-cad expression attenuated the assembly of Cx43 into GJs, whereas E-Cad expression facilitated the assembly. The expression of N-Cad inhibited GJ assembly by causing endocytosis of Cx43 via a nonclathrin-dependent pathway. Knock down of N-Cad by ShRNA restored GJ assembly. When both cadherins were simultaneously expressed in the same cell type, GJ assembly and disassembly occurred concurrently. Our findings demonstrate that E-Cad and N-Cad have opposite effects on the assembly of Cx43 into GJs in rat liver epithelial cells. These findings imply that GJ assembly and disassembly are the down-stream targets of the signaling initiated by E-Cad and N-Cad, respectively, and may provide one possible explanation for the disparate role played by these cadherins in regulating cell motility and invasion during tumor progression and invasion.

INTRODUCTION

The cell–cell and cell–matrix adhesion molecules and their associated proteins often assemble into large macromolecular complexes, such as adherens junctions, desmosomes, tight junctions, and hemi-desmosomes and maintain the polarized and differentiated state of epithelial cells (Bryant and Mostov, 2008). Most cells in a polarized epithelium are also interconnected by another class of junctions, called GJs, which permit the direct passage of small molecules (≤ 1 kDa) between adjoining cells (Goodenough and Paul, 2009). Gap junctions are ensembles of several cell–cell channels that are formed by a family of ~ 20 related proteins, called

Cxs, which have been designated according to their molecular mass. A gap junctional cell–cell channel is formed when Cxs first oligomerize as hexamers to form a connexon, which, upon reaching the cell surface, docks with a connexon displayed by an adjacent cell (Segretain and Falk, 2004; Laird, 2006). Cell–cell communication mediated by gap junctional channels has been shown to regulate the proliferation and differentiation of epithelial cells and thus to fulfill a homeostatic role (Saez *et al.*, 2003; Goodenough and Paul, 2009). Impaired, or loss of, Cx expression has been implicated in the pathogenesis of several forms of neoplasia as evidenced by *in vitro* and *in vivo* studies showing induction of cellular differentiation and attenuation of the malignant phenotype upon forced expression of Cxs in tumor cells and by gene knock out studies in transgenic mice (Wei *et al.*, 2004; Crespin *et al.*, 2009). Mutations in several Cx genes have been characterized in inherited diseases associated with aberrant cellular proliferation and differentiation (Laird, 2010).

In contrast to the well-established role of tight and adherens junctions, the role of GJs in initiating and maintaining the polarized and differentiated state of epithelial cells is not understood and remains yet to be explored. The importance of investigating this is underscored by the fact that loss of the polarized and differentiated state of epithelial cells is the hallmark of a variety of carcinomas as they progress from an indolent to an invasive state as well of epithelial to mesenchymal transformation (EMT) in which tumor cells become more migratory and motile (Thiery *et al.*, 2009). It is thought that these changes are induced upon disruption of several

This article was published online ahead of print in *MBoC in Press* (<http://www.molbiolcell.org/cgi/doi/10.1091/mbc.E10-05-0403>) on September 29, 2010.

*Department of Pharmaceutical and Biomedical Sciences, University of Georgia, Athens, GA 30602.

Address correspondence to: Parmender P. Mehta (pmehta@unmc.edu).

Abbreviations used: Cx, connexin; GJ, gap junction; Cad, cadherin; EMT, epithelial mesenchymal transformation.

© 2010 R. Govindarajan *et al.* This article is distributed by The American Society for Cell Biology under license from the author(s). Two months after publication it is available to the public under an Attribution–Non-commercial–Share Alike 3.0 Unported Creative Commons License (<http://creativecommons.org/licenses/by-nc-sa/3.0/>).

junctional complexes (Mosesson *et al.*, 2008). Moreover, recent studies have shown that forced expression of Cxs partially reverses EMT-like characteristics acquired by breast cancer cells (McLachlan *et al.*, 2006) and that maintenance of tight junctions may be dependent on the formation of GJs in some cell types (Kojima *et al.*, 2007).

A first step toward elucidation of the role of GJs in maintaining the polarized and differentiated state of epithelial cells is to examine their assembly and disassembly upon loss or alteration of this state. Because bidirectional signaling between cadherins and Cxs has been implicated in the assembly of GJs (Musil *et al.*, 1990; Jongen *et al.*, 1991; Meyer *et al.*, 1992; Hernandez-Blazquez *et al.*, 2001; Wei *et al.*, 2005), and because cadherins have been shown to play an important role in tumor progression and EMT (Wheelock and Johnson, 2003; Wheelock *et al.*, 2008; Thiery *et al.*, 2009), we explored the role of E-Cad, a cadherin expressed widely by epithelial cells, and N-Cad, a cadherin expressed by neuronal and mesenchymal cells (Tepass *et al.*, 2000; Gumbiner, 2005), in controlling the assembly and disassembly of GJs. We chose these cadherins because they have been shown to affect the behavior of epithelial tumor cells in a diametrically opposed way, although both mediate cell-cell adhesion in cells in which they are normally expressed. For example, loss of, or dysfunctional, E-Cad mediated cell-cell adhesion facilitates the dissemination of tumor cells and confers upon them a more invasive state. On the other hand, it is the gain of N-Cad by the tumor cells that augments the dissemination of tumor cells and increases their migration and motility (Cavallaro and Christofori, 2004; Wheelock *et al.*, 2008). Also, several studies have shown that one of the hallmarks of tumor progression and EMT is the gain of N-Cad expression by tumor cells, which may or may not be accompanied by the concomitant loss of E-Cad expression (Cavallaro and Christofori, 2004; Wheelock *et al.*, 2008; Thiery *et al.*, 2009).

Based on the well-documented role of Cxs in suppressing tumor formation and the fact that Cx expression and GJ assembly are compromised in advanced stages of carcinomas (Mehta *et al.*, 1999; King and Lampe, 2004; Crespin *et al.*, 2009), as well as prompted by studies that showed inhibition of GJ assembly by N-Cad (Wang and Rose, 1997), we reasoned that the two cadherins could have opposite effects on the assembly of GJs, with E-Cad facilitating and N-Cad inhibiting the assembly. To test this notion, we studied the assembly of GJs composed of Cx43 in isogenic clones derived from rat liver clone 9 (RL-CL9) cells that expressed either E-Cad or N-Cad. We show here that N-Cad expression attenuates GJ assembly by triggering endocytosis of Cx43 by a nonclathrin dependent pathway upon arrival at the cell surface, whereas knock down of N-Cad, or expression of E-Cad, facilitates the assembly. Our findings document that GJ assembly is one of the downstream targets of signaling initiated by these cadherins and may rationally explain some of the intriguing and at times contrasting roles of E-Cad and N-Cad in regulating cell adhesion, migration, and motility of tumor cells.

MATERIALS AND METHODS

Cell Culture

Immortalized and nontransformed rat liver clone 9 (RL-CL9) epithelial cells were purchased from ATCC and have been described earlier (Mehta *et al.*, 1986; Mehta *et al.*, 1992). Stock cultures were maintained by seeding 10^5 cells per 10-cm dish in DMEM (GIBCO, Grand Island, NY) supplemented with 5% defined fetal bovine serum (Hyclone, Salt Lake City, UT) in an atmosphere of 5% CO₂/95% air. Cells were passaged once a week and used between passages 3–12. New stock cultures were initiated every month from frozen vials. This schedule was strictly maintained. The retroviral packaging cell lines,

Phoenix 293T, PA317, and PTi67 were grown as described previously (Mitra *et al.*, 2006). RL-CL9 cells were infected with various recombinant retroviruses, and pooled cultures were grown and maintained in complete medium containing G418 (200 µg/ml), puromycin (2 µg/ml), and G418 plus puromycin (see retroviruses and retrovirus infection).

Isolation of Isogenic Subclones from RL-CL9 Cells Expressing E-Cadherin and N-Cadherin

One hundred RL-CL9 cells from passages 4 and 30 were seeded in 10-cm dishes in complete culture medium and allowed to grow into colonies. Between 63–100 clones from early and late passage cells were isolated using glass cylinders and expanded and frozen. Each clone was analyzed separately by Western blot and immunocytochemical analysis for the expression of E-Cad, N-Cad, Cx43 as well as for subcellular localization. Subclones that expressed only E-Cad and no detectable level of N-Cad were designated as RL-EΔN cells whereas subclones that expressed N-Cad and no detectable level of E-Cad were designated as RL-NΔE cells. Further characterization of these clones is described in Results.

Plasmids, Retroviral Vectors, and Other Recombinant DNA Constructs

We used the following retroviral vectors for our studies. 1. LXSNC32 harboring rat Cx32. 3. LXSNE-Cad (human), which was constructed by subcloning E-Cad into the EcoR1 and BamHI sites of LXSNC32. 4. LZRS-E-Cad-Myc and LZRS-N-Cad-Myc expressing Myc-tagged human E-Cad and N-Cad. 5. ShN-Cad, ShP-Cad, and ShEGFP in pSuper.Retro.puro. The construction of these retroviral vectors has been described (Mehta *et al.*, 1999; Nieman *et al.*, 1999; Kim *et al.*, 2000a; Govindarajan *et al.*, 2002; Maeda *et al.*, 2005; Maeda *et al.*, 2006; Mitra *et al.*, 2006; Shintani *et al.*, 2008). GFP-tagged Rab5 and Rab7 and their constitutively active mutants, Rab5Q-L and Rab7Q-L, were kind gifts from Dr. Caplan. These retroviral vectors were used to produce recombinant retroviruses in HEK293T, PA317 and PTi67 amphotropic packaging cell lines as described (Mitra *et al.*, 2006; Chakraborty *et al.*, 2010). RL-CL9 cells were multiply (2–4 times) infected with various recombinant retroviruses and selected in either G418 (400 µg/ml) or puromycin (2 µg/ml) for 2–3 wk in complete medium. Pooled cultures from 1000–2000 colonies obtained from three to four dishes were expanded, frozen, and maintained in G418 (200 µg/ml) and in G418 and puromycin (2 µg/ml). Pooled polyclonal cultures were used within two to three passages for immunocytochemical and biochemical analyses.

Cell Surface Biotinylation Assay

Cells (2×10^5) were seeded in 6-cm dishes in 4 ml of complete medium and grown to confluence. Cell surface biotinylation was performed at 4°C by incubation with freshly prepared EZ-Link Sulfo-NHS-SS Biotin reagent (Pierce, Rockford, IL) at 0.5 mg/ml in phosphate buffered saline (PBS) supplemented with 1 mM CaCl₂ and 1 mM MgCl₂ (PBS-PLUS) for 1 h as described (Van Slyke and Musil, 2000; Chakraborty *et al.*, 2010). The reaction was quenched with PBS-PLUS containing 20 mM glycine and cell lysis and affinity precipitation of biotinylated proteins were performed with 100 µg of total protein using 50 µl of streptavidin agarose beads (Pierce, Rockford, IL) on a rotator overnight at 4°C. The streptavidin-bound biotinylated proteins were eluted by incubating the beads for 30 min in 1× SDS loading buffer and resolved by SDS-PAGE followed by Western blotting. As an input, equal amount of total protein (10 µg) was also subjected to SDS-PAGE and Western blot analysis. To determine the kinetics of degradation of cell-surface associated Cx43, cells were biotinylated at 4°C as described above and, after washing and quenching biotin, were chased at 37°C for various times before affinity precipitation of the biotinylated proteins with streptavidin. The protein concentration was determined using BCA reagent (Pierce).

Detergent Extraction and Western Blot Analysis of Cx43 and Cx32

Cell lysis, detergent solubility assay with 1% Triton X-100 (TX-100), and Western blot analysis were performed as described (Van Slyke and Musil, 2000; Mitra *et al.*, 2006; Chakraborty *et al.*, 2010). Briefly, 5×10^5 RL-EΔN and RL-NΔE cells were seeded per 10-cm dish in 10 ml of complete medium and grown to confluence. Cells were then lysed in buffer SSK (10 mM Tris, 1 mM EGTA, 1 mM PMSF, 10 mM NaF, 10 mM NEM, 10 mM Na₂VO₄, 10 mM iodoacetamide, 0.5% TX-100, pH 7.4) supplemented with the protease inhibitor cocktail (Sigma, St. Louis, MO). To determine the detergent solubility of Cx43, the concentration of TX-100 was raised to 1% before ultracentrifugation at 100,000 × g for 60 min (35,000 rpm in analytical Beckman ultracentrifuge; Model 17–65 using a SW50.1 rotor). The detergent-insoluble pellets were dissolved in buffer C (70 mM Tris/HCl, pH 6.8, 8 M urea, 10 mM NEM, 10 mM iodoacetamide, 2.5% SDS, and 0.1 M DTT). After normalization based on cell number, the total, TX-100-soluble, and -insoluble fractions were mixed with 4× SDS-loading buffer to a final concentration of 1× and boiled at 100°C for 5 min (for Cx43) or incubated at room temperature for 1 h (for Cx32) before SDS-PAGE analysis.

Detergent (TX-100) Extraction of Cells In Situ

RL-EΔN and RL-NΔE cells were extracted *in situ* with 1% TX-100 essentially as described previously (Govindarajan *et al.*, 2002; Chakraborty *et al.*, 2010). In brief, 2.5×10^5 cells were seeded per well in six-well clusters containing glass cover slips and were grown for 2–3 d when they attained confluence. The cells were rinsed once in PBS and then incubated in isotonic medium (30 mM HEPES, pH 7.2; 140 mM NaCl; 1 mM CaCl₂; 1 mM MgCl₂) supplemented with the protease inhibitor cocktail (Sigma, MO) for 45 min at 4°C in the presence and absence of 1% TX-100. The dishes were swirled gently and intermittently. After incubation, cells were fixed and immunostained with appropriate primary and secondary antibodies as described below. The detergent-solubility of Cxs in single RL-EΔN and RL-NΔE cells was examined 24–36 h after seeding between 1 and 2×10^3 cells per well in six-well clusters. Under these conditions between 50 and 60% of seeded cells remained single and well-spread.

Antibodies and Immunostaining

Rabbit polyclonal and mouse monoclonal antibodies against Cx43 and Cx32 have been described earlier (Mehta *et al.*, 1999). Rabbit anti-EEA-1 (PA1-063) was obtained from Affinity BioReagents (Golden, CO). Rabbit anti-caveolin-1 and anti-caveolin-2 were purchased from BD Transduction laboratories (San Jose, CA). Mouse anti-occludin (clone OC-3F10) was from Zymed Laboratories (South San Francisco, CA). Rabbit anti- α -catenin, rabbit anti- β -catenin, rabbit anti-Cx32 (loop and tail), and mouse anti- β -actin (clone C-15) antibodies were from Sigma (St. Louis, MO). Mouse anti-ZO1 (610967) and mouse anti-GM130 (610822) antibodies were obtained from BD Transduction laboratories (San Jose, CA). Mouse anti-clathrin heavy chain (MA1-065) was purchased from Affinity Bioreagents (Rockford, IL). Mouse anti-N-Cad, mouse anti-E-Cad, mouse anti- α -catenin, and mouse anti- β -catenin antibodies have been previously described (Maeda *et al.*, 2005; Mitra *et al.*, 2006; Shintani *et al.*, 2008; Chakraborty *et al.*, 2010). We also used rabbit anti-E-Cad antibody for immunostaining rat E-Cad. The production of this antibody has been described (Wheelock *et al.*, 1987). Alexa-488 and Alexa-594 phalloidins as well as Alexa-488 and Alexa-594 conjugated cholera toxin, transferrin, and EGF were purchased from Invitrogen (Molecular Probes/Invitrogen, Eugene, OR).

RL-EΔN and RL-NΔE cells (see Results), seeded in six-well clusters at a density of 2.5×10^4 /well and allowed to grow to confluence, were immunostained at room temperature with various antibodies at appropriately calibrated dilutions after fixing with 2% para-formaldehyde for 15 min as described previously (Mitra *et al.*, 2006; Chakraborty *et al.*, 2010). Secondary antibodies (rabbit or mouse) conjugated with Alexa-488 and Alexa-594 were used as appropriate. Images of immunostained cells were acquired with a Leica DMRIE microscope (Leica Microsystems, Wetzler, Germany) equipped with Hamamatsu ORCA-ER CCD camera (Hamamatsu City, Japan). For colocalization studies, serial z sections (0.5 μ m) were collected and analyzed after iterative deconvolution using image-processing software (Volocity; Improvision, Lexington, MA). SlowFade antifade (Molecular Probes/Invitrogen) was used to mount cells on glass slides.

Cell Growth on Transwell Filters

RL-CL9, RL-EΔN, and RL-NΔE cells (2×10^4) were plated onto 12-mm transwell filters (pore size, 0.4 μ m; Corning Life Sciences, MA) and grown for 7–21 d as described (Chakraborty *et al.*, 2010). Medium of the upper and lower filter chambers was changed on alternate days. The immunocytochemical analyses were performed directly on filters, after which the filters were cut with a sharp scalpel and mounted on glass slides with their cell side facing up. A drop of SlowFade antifade was placed on top followed by a glass coverslip, which was pressed gently using a 50 gm weight overnight. The edges were sealed with nail polish.

Cell Aggregation Assay

The hanging drop suspension culture method was used to test aggregation of RL-EΔN and RL-NΔE cells as described (Chakraborty *et al.*, 2010). After harvesting with trypsin/EDTA, cells were resuspended at 2.5×10^5 cells per ml in complete culture medium and a 20- μ l drop of medium containing 5×10^3 cells was suspended as a hanging drop from the lid of a 10 cm² Petri dish (40 hanging drops per lid) filled with PBS to prevent drying of the drops. The cells were then allowed to aggregate in a humidified 5% CO₂ incubator at 37°C for 16–20 h after which cells and aggregates were triturated five times with a standard 200 μ l pipette tip to disperse loosely associated cells and a coverslip was placed gently on top of the cells. The cells were visualized by phase-contrast light microscopy at $\times 5$ magnification and images captured using a CCD camera (Retiga 2000R, FAST 1394) mounted on a Leica DMRIE2 microscope with the aid of Volocity software (Improvision, Lexington, MA). For quantifying the size, the outline of each aggregate was drawn using an ROI tool and the area of each aggregate was measured. All images were analyzed at the same magnification and the area was recorded as “relative units” for each aggregate. The average area of the aggregates was considered as a measure of aggregate formation.

Cell Migration Assay

RL-EΔN and RL-NΔE cells were seeded on LabTek two-well chamber slides and allowed to grow to confluence. Confluent monolayers of cells were wounded by manually scratching with a pipette tip. We chose scratch areas of equal width for these assays. After marking the positions of the wounds in the X-Y plane, cells were imaged every 30 min at 37°C in an atmosphere of 5% CO₂/95% air for 24 h in a live cell imaging chamber mounted on an Olympus IX81 motorized inverted microscope (Olympus America Inc; Center Valley, PA). The microscope was controlled by IX2-UCB U-HSTR2 motorized system with a focus drift compensatory device IX1-ZDC. Images were captured using a Hamamatsu ORCA ER2 CCD camera and processed by imaging software Slidebook version 5.0 (Intelligent Imaging Innovations, Denver, CO).

Gap Junctional Communication Assays

Gap junctional communication was measured by microinjecting fluorescent tracers, Alexa Fluor 488 (MW 570 Da; A-10436) and Alexa Fluor 594 (MW 760 Da; A-10438), and by scrape loading as described (Govindarajan *et al.*, 2002; Chakraborty *et al.*, 2010). Fluorescent tracers were microinjected with an Eppendorf InjectMan and FemtoJet microinjection systems (Models 5271 and 5242, Brinkmann Instrument, Westbury, NY) mounted on a Leica DMRIE2 microscope. The images of microinjected cells were captured using a CCD camera (Retiga 2000R, FAST 1394) with the aid of Volocity software (Improvision, Lexington, MA) one and five minutes after microinjection for RL-EΔN and RL-NΔE cells, respectively, and the number of fluorescent cells, excluding the microinjected one, was counted from the captured images that were stored as TIFF files as described previously (Govindarajan *et al.*, 2002; Chakraborty *et al.*, 2010).

Cells were scrape-loaded as described (Govindarajan *et al.*, 2002; Chakraborty *et al.*, 2010). Briefly, RL-EΔN and RL-NΔE cells were seeded in six-well clusters at a density of 2.5×10^4 /well and allowed to grow to confluence. Cell culture medium from freshly confluent cells was removed and replaced with 1 ml of medium containing rhodamine-conjugated fluorescent dextrans (10 kDa, 1 mg/ml; fixable) and Lucifer yellow (0.5%). Cells were scrape-loaded using a sterile scalpel by two longitudinal scratches and incubated for one minute at room temperature. Cells were washed quickly two to three times with warm PBS containing calcium and magnesium and returned to the incubator for five minutes, after which the medium was removed, cells were washed two times with PBS and fixed with 3.7% buffered Formalin at room temperature. The autofluorescence of cells was quenched with 0.1 M glycine and after washing once with PBS, the cover slips were mounted on glass slides in a droplet of SlowFade. Images of the scrape-loaded cells were captured as described above.

Treatments

Stock solutions of brefeldin (BIOMOL) and monensin (Calbiochem) were prepared in ethanol at 10 mM and stored at -80°C in small aliquots. Stock solution of chlorpromazine (BIOMOL) was prepared at 50 mg/ml in ethanol and those of filipin and methyl- β -cyclodextrin were prepared in cell culture medium at 20 mM each and stored frozen at -80°C for up to 1 mo. All solutions were appropriately diluted in the cell culture medium at the time of treatment.

RESULTS

Characteristics of Rat Liver Clone 9 (RL-CL9) Cells

We used an immortalized, nontransformed rat epithelial cell line, called RL-CL9, to examine GJ assembly and disassembly (Mehta *et al.*, 1986; Mehta *et al.*, 1992). RL-CL9 cells have a typical epithelial morphology (Figure S-1A) and express adherens junction-associated proteins E-Cad and α - and β -catenins, and tight junction associated proteins, occludin and ZO-1; moreover, these cells form cortical actin bundles and form GJs composed of Cx43 (Figure 1A). Furthermore, when grown on transwell filters, these cells grow as a monolayer, continue to express Cx43 and ZO-1 (Figure 1B), and acquire a partially polarized state as assessed by increased height of these cells and apical distribution of Na-K ATPase (not shown). Finally, these cells express both mesenchymal markers, such as vimentin, and epithelial markers, such as cytokeratin 8 (data not shown).

Altered Cadherin Expression and Gap Junction Assembly

We fortuitously observed that upon serial propagation of RL-CL9 cells from passage 4 to greater than passage 20, a population of cells emerged that began to lose typical cob-

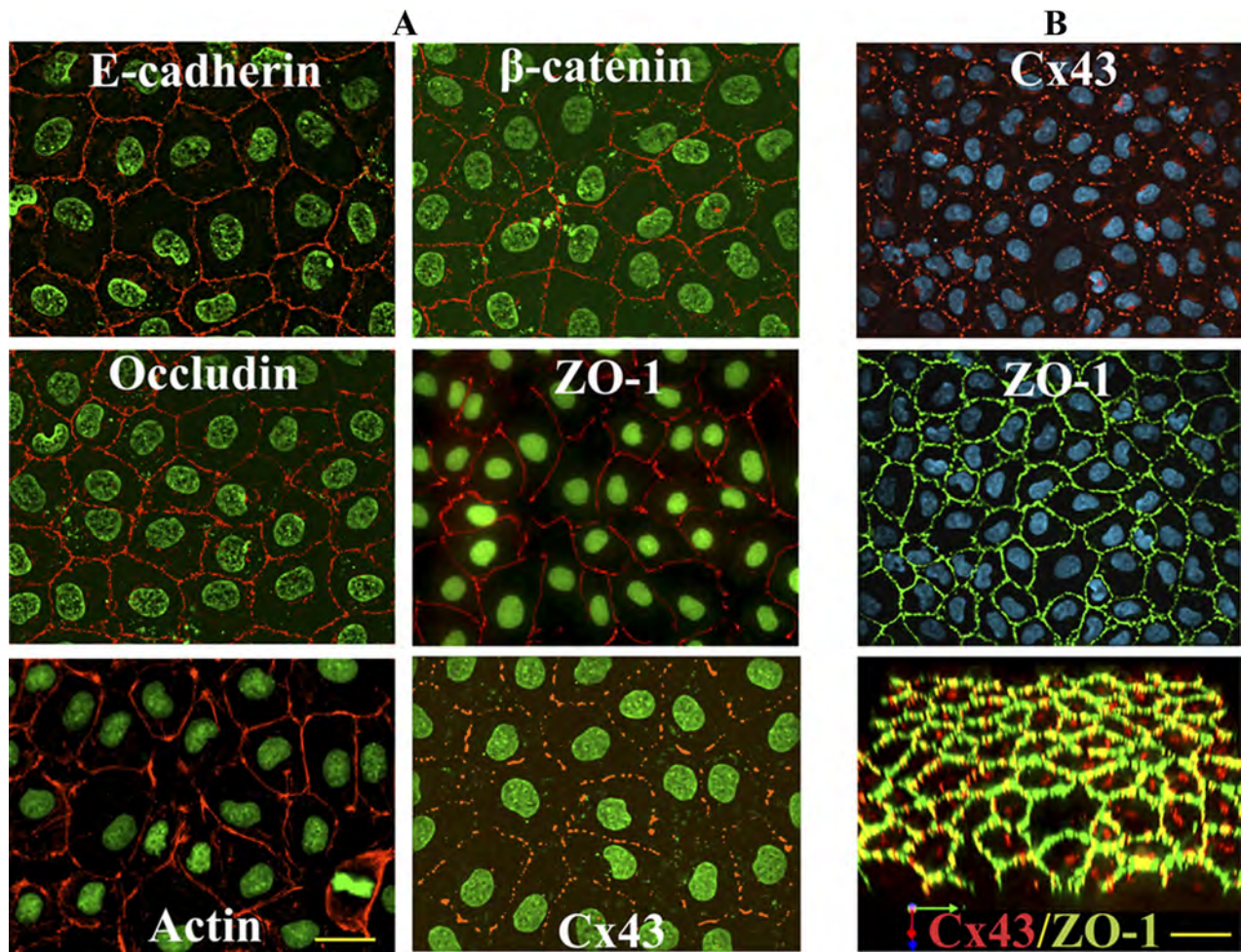


Figure 1. Expression of cell junction-associated proteins and Cx43 in RL-CL9 cells. (A) RL-CL9 cells, seeded in six-well clusters on glass coverslips, were immunostained for E-Cad and β -catenin, occludin and ZO-1, and actin and Cx43. Note robust expression of these proteins at cell-cell contact areas. (B) RL-CL9 cells were grown for 21 d on transwell filters and immunostained for Cx43 and ZO-1. Note that these cells form a uniform monolayer and continue to express Cx43 and ZO-1 robustly. Bottom image in B is the three-dimensional merged image of the top two images, which was volume rendered using Volocity. Nuclei (Green) were stained with DAPI. Bar = 20 μ m in A and 10 μ m in B.

blestone-like epithelial morphology (Figure S-1, top row). Moreover, immunocytochemical analysis showed that this population of cells began to express N-Cad (Figure S-1, middle row, left panel) in addition to E-Cad (Figure S-1, bottom row, middle panel). Furthermore, in this population of cells Cx43 was not assembled into GJs and was retained in the cytoplasm (Figure S-1, middle row). In addition, E-Cad expression at the areas of cell-cell contact of these cells appeared to be less robust and at times discontinuous (Figure S-1, bottom row, arrows). On systematic examination, we found that serial propagation of early passage RL-CL9 cells for 4–6 mo was gradually accompanied by an increase in the expression level of N-Cad (Figure S-2A, lower panels; Figure S-2C, blots) and vimentin (Figure S-2B, upper panels; Figure S-2C, blot), an increase in the proportion of cells in which actin was organized into stress fibers (Figure S-2B, bottom panels), and an increase in the proportion of cells in which Cx43 remained intracellular and failed to form GJs (not shown). Moreover, the expression level of E-Cad was not significantly altered (Figure S-2C), although some E-Cad began to accumulate in the cytoplasm (Figure S-2A, upper panels).

Gap Junction Assembly in E-Cadherin and N-Cadherin Expressing RL-CL9 Isogenic Subclones

To test whether gain of N-Cad expression was associated with the loss of GJ forming ability, we isolated between 63 and 92 clones from early and late passage RL-CL9 cells and examined the expression level and localization of Cx43, E-Cad, and N-Cad by immunocytochemical and Western blot analyses in each clone. We found that 70% of clones isolated from early passage (passage 4) RL-CL9 cells expressed only E-Cad and no detectable level of N-Cad, whereas 79% of clones isolated from late passage (passage 20) cells expressed only N-Cad and no detectable levels of E-Cad (Table S-1). Moreover, as assessed immunocytochemically, 61% of clones isolated from early passage RL-CL9 cells formed GJs whereas only 25% of clones isolated from late passage cells formed GJs (Table S-1). Furthermore, in clones in which both N-Cad and E-Cad were expressed to varying level, a fraction of Cx43 remained intracellular whereas a fraction was assembled into GJs (data not shown). For further study, we selected two E-Cad expressing clones lacking N-Cad expression, designated as RL-EΔN, and two

N-Cad expressing clones lacking E-Cad expression, designated as RL-NΔE, from early passage RL-CL9 cells to minimize the phenotypic and epigenetic changes that might have ensued upon serial propagation of early passage cells in vitro and which might have occurred in late passage RL-CL9 cells. Qualitatively similar data were obtained with both clones selected from each category and data from only one representative clone are shown in subsequent studies.

Gap Junction Assembly and Function in RL-EΔN and RL-NΔE Cells

As assessed by Western blot analysis, RL-EΔN cells expressed only E-Cad and no N-Cad, whereas RL-NΔE cells expressed only N-Cad and no E-Cad; moreover, the expression level of Cx43, α - and β -catenins, occludin and ZO-1, and cytokeratin 8 and vimentin was not significantly different (Figure 2, A and B). In RL-EΔN cells, Cx43 was assem-

bled into GJs, whereas in RL-NΔE cells it was predominantly intracellular as discrete puncta although small puncta, which were barely detectable immunocytochemically, were also observed at cell-cell contact regions (Figure 2 B). Although no discernible difference in the expression level of actin was observed between RL-EΔN and RL-NΔE cells, actin was organized into cortical bundles in RL-EΔN cells whereas it was organized into more stress fibers in RL-NΔE cells as was observed in early passage and late passage RL-CL9 cells (data not shown, but see Figure 1 and Figure S-2B). Moreover, as was observed in early passage RL-CL9 cells, when grown on transwell filters, RL-EΔN cells grew as a monolayer, became columnar, and expressed ZO-1 robustly at the areas of cell-cell contact (Figure 2C, top row), whereas RL-NΔE cells formed a monolayer in which cell borders seemed to partially overlap. Furthermore, the pattern of localization of ZO-1 at areas of cell-cell contact was

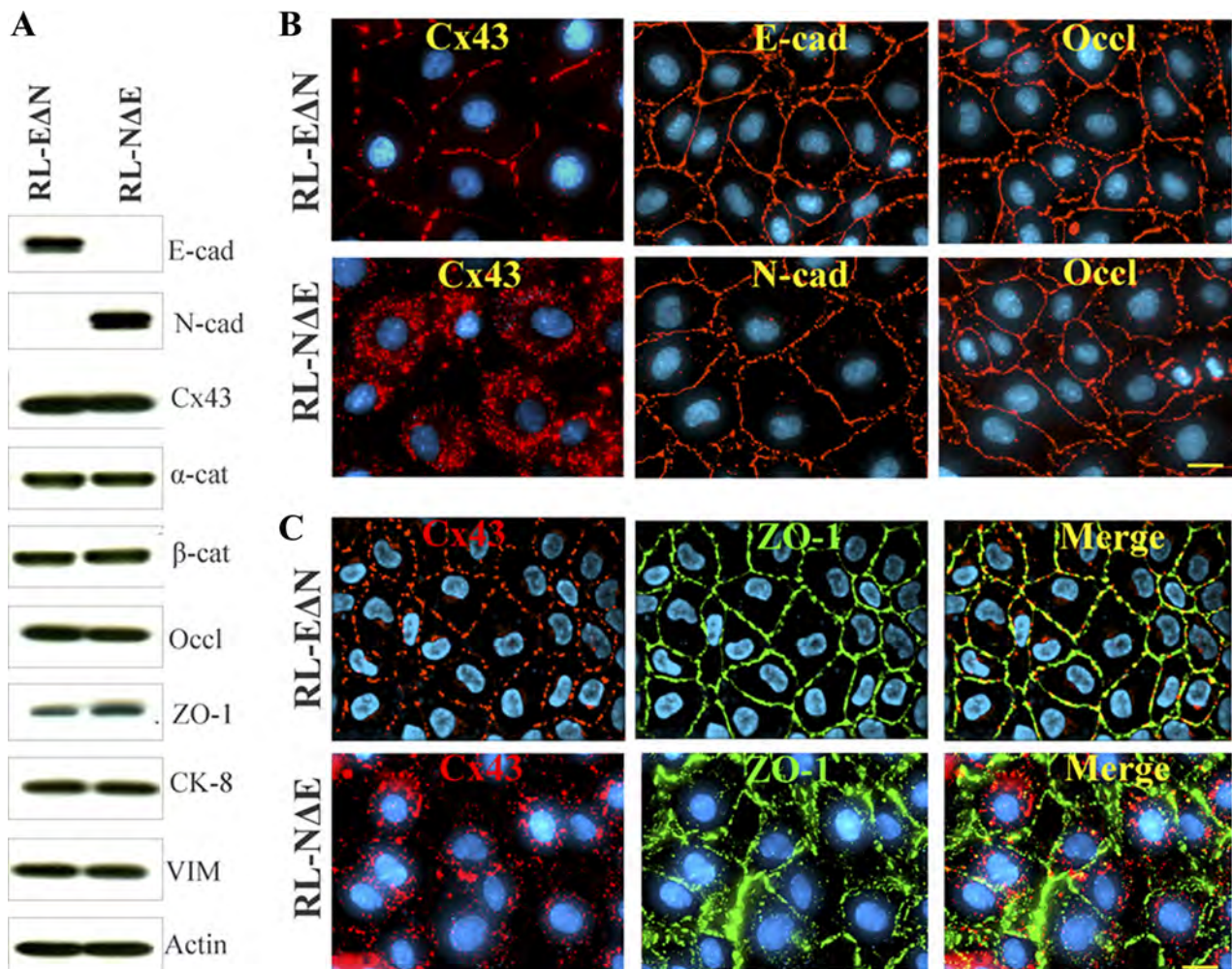


Figure 2. Localization and expression of Cx43, adherens and tight junction proteins, and cytoskeletal proteins in RL-EΔN and RL-NΔE cells. (A) Western blot analysis of the expression level of E-Cad (E-cad) and N-Cad (N-cad), Cx43, α - and β -catenins, occludin and ZO-1, cytokeratin 8 and vimentin and actin. Note that RL-EΔN cells express only E-Cad, but no detectable level of N-Cad, whereas RL-NΔE cells express only N-Cad but no E-Cad. Note also that the expression level of Cx43 and other proteins is not discernibly different in the two cell lines. (B) RL-EΔN and RL-NΔE cells were seeded on glass coverslips and immunostained for Cx43, E-Cad (E-cad), N-Cad (N-cad), and occludin (Occl). Note that Cx43 is assembled into GJs in RL-EΔN cells, whereas it remains intracellular as vesicular puncta in RL-NΔE cells. Note also that E-Cad, N-Cad, and occludin are localized at the areas of cell-cell contact in both cell types. (C) RL-EΔN and RL-NΔE cells were seeded on transwell filters for 5 d and immunostained for Cx43 and ZO-1. Note a more robust expression of ZO-1 at cell-cell contact areas in RL-EΔN cells compared with RL-NΔE cells. Note also partial overlap of cell boundaries in RL-NΔE cells as well as GJ like punctate structures. Nuclei (Blue) were stained with DAPI. Bar = 10 μ m in B and 15 μ m in C.

discontinuous and diffuse (Figure 2C, bottom row). In addition, although Cx43 appeared to have formed GJ like puncta due to partial overlap of the cell peripheries of the adjacent cells, such puncta were rarely observed at the areas of cell-cell contact upon careful examination (Figure 2C, bottom row). Compared with RL-EΔN cells which became columnar and could be maintained as a monolayer on filters for 2–3 mo, RL-NΔE cells became moribund and died within 10 d after attaining confluence. To corroborate the immunocytochemical data, we measured the junctional transfer of fluorescent tracer, Lucifer Yellow (MW 443), by scrape-loading (Figure 3A), and of Alexa 488 (MW 570) and Alexa 594 (MW 760), by microinjection (Figure 3B), in cells grown on glass cover slips and transwell filters. We found that RL-EΔN cells communicated extensively whereas RL-NΔE cells did not communicate either on plastic or on transwell filters (Figure 3 and Table 1).

Because in contrast to RL-NΔE cells, Cx43 was assembled into GJs in RL-EΔN cells, we also investigated whether cell–cell adhesion mediated by E-Cad and N-Cad remained functional in both cell types. A hanging drop assay, which measures the rate and strength of cell–cell adhesion based on the size of cell aggregates formed over time as well as the resistance of the formed aggregates to a shearing force was used (Kim *et al.*, 2000b). As shown in Table S-2 both RL-EΔN and RL-NΔE cells aggregated efficiently as assessed by the mean area of the aggregates. We also found that RL-EΔN and RL-NΔE cells failed to invade in a standard Matrigel invasion assay (data not shown). Standard scratch (wound) assays were performed to determine whether RL-NΔE cells were more motile compared with RL-EΔN cells. Live cell imaging of the scratches of equal width in three independent experiments showed that wounds were filled within 14 ±

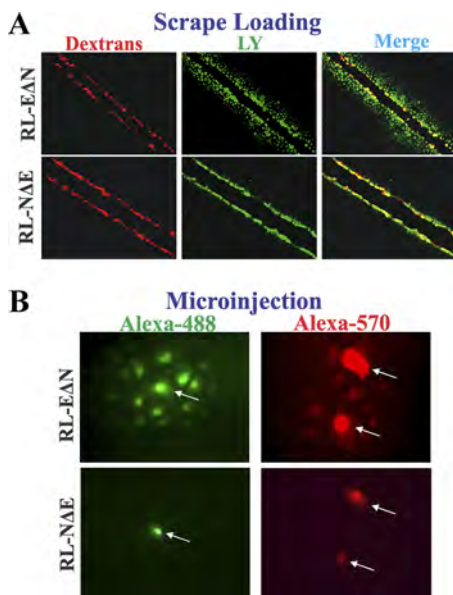


Figure 3. Gap junctional communication in RL-EΔN and RL-NΔE cells. (A) Cells were grown on glass coverslips and scrape-loaded with Lucifer Yellow and Alexa-594 conjugated dextrans. (B) Cells were microinjected with the indicated tracers as described in Materials and Methods. Note that in RL-EΔN cells, Lucifer Yellow was transferred from scrape-loaded (red) cells to neighboring cells, whereas no transfer is observed in RL-NΔE cells. Note also that the transfer of Alexa-488 and Alexa-570 from microinjected cells (indicated by arrows) to neighboring cells is observed only in RL-EΔN cells.

Table 1. Junctional communication of various fluorescent tracers in RL-EΔN and RL-NΔE cells*

Tracer	Exp. #	RL-EΔN	RL-NΔE	RL-NΔE (on filters)
Lucifer Yellow	1	24 ± 4 ^a (20) [‡]	0 ± 0 (32)	0 ± 0 (21)
	2	22 ± 4 (20)	0 ± 0 (40)	0 ± 0 (20)
Alexa-488	1	13 ± 4 (20)	0 ± 0 (36)	0 ± 0 (33)
	2	12 ± 3 (20)	0 ± 0 (40)	0 ± 0 (44)
Alexa-594	1	4 ± 1 (20)	0 ± 0 (20)	0 ± 0 (29)
	2	6 ± 2 (20)	0 ± 0 (30)	0 ± 0 (38)

*Number of fluorescent cells 5 min after microinjection.

^aMean ± SE.

[‡]Number of microinjection trials. RL-EΔN and RL-NΔE cells were seeded in 6-cm Nunc dishes in replicate at a density of 2×10^5 cells per dish and allowed to grow to confluence for 4 days. Junctional communication was measured by microinjecting different fluorescent tracers as described in Materials and Methods.

2 h in RL-NΔE cells whereas 22 ± 2 h were required to fill the wounds in RL-EΔN cells (Figure S-3). The mean (\pm SE) rate of migration was significantly faster in RL-NΔE cells as compared with RL-EΔN cells ($p = 0.04$).

Taken together, the data presented in Figures 2, 3, and S-3 and in Tables 1 and S-1 suggest that a switch in expression from E-Cad to N-Cad is associated with the attenuation of assembly and/or maintenance of GJs and their function, while the expression of E-Cad is associated with the facilitation of assembly and function. Moreover, these data also suggest that in RL-NΔE cells GJ assembly was not disrupted because of lack of cell–cell adhesion but by some other defect. Furthermore, these findings suggest that in RL-NΔE cells, N-Cad expression is more closely related with increased motility and with the loss of ability to grow and sustain a polarized monolayer on transwell filters than with invasion in Matrigel.

Detergent-Solubility of Cx43 in RL-EΔN and RL-NΔE Cells

To substantiate the immunocytochemical and functional data, and to elucidate the possible mechanism of attenuation of GJ assembly in RL-NΔE cells, we determined the assembly of Cx43 into GJs biochemically by Western blot analysis of total and Triton X (TX)-100-soluble and TX-insoluble cell fractions (VanSlyke and Musil, 2000). Intriguingly, a significant proportion of Cx43 was detected in detergent-insoluble fractions in both RL-EΔN and RL-NΔE cells (Figure 4A). Detergent solubility of live RL-NΔE and RL-EΔN cells by *in situ* extraction with 1% TX-100 showed that intracellular Cx43 puncta in RL-NΔE cells and intercellular gap junctional puncta in RL-EΔN cells were detergent-insoluble (Figure 4B). We also found that in RL-NΔE cells small intercellular puncta at areas of cell–cell contact, which were barely detectable immunocytochemically, remained detergent-resistant. The solubility of β-catenin, an adherens junction-associated protein, was not significantly affected in RL-EΔN and RL-NΔE cells (Figure 4B), whereas EEA1, a marker for the early endosomes, was lost upon *in situ* extraction (data not shown). These data suggest that a significant proportion of Cx43 in RL-NΔE cells is detergent-insoluble and that the detergent-insoluble fraction corresponds to discrete puncta that lie scattered throughout the cytoplasm, as well as to very small puncta that are seen at areas of cell–cell contact.

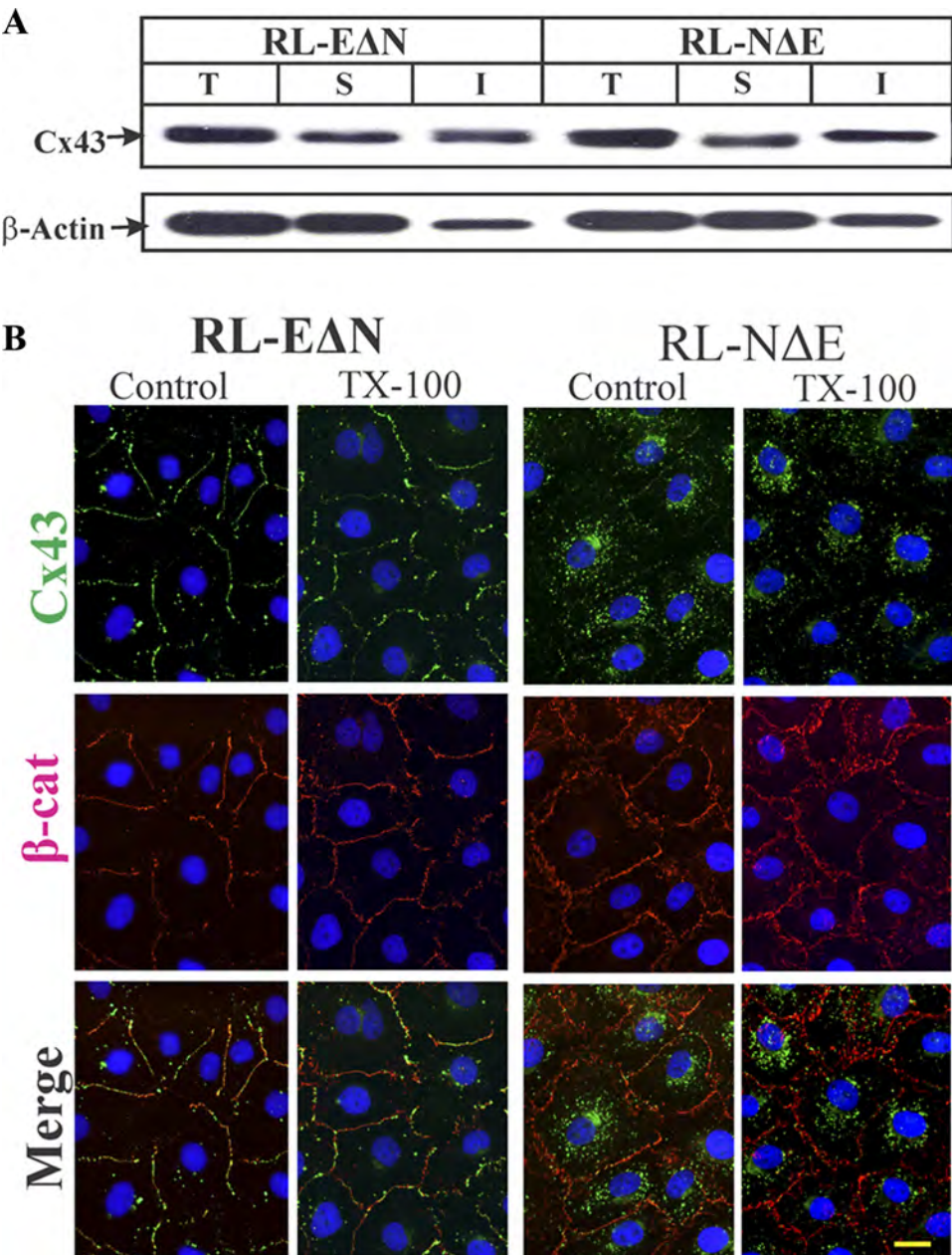


Figure 4. Detergent-solubility of Cx43 in RL-E Δ N and RL-N Δ E cells. (A) Total (T), TX-100-soluble (S), and TX-insoluble (I) fractions from cells were analyzed by Western blot analysis as described in Materials and Methods. The blots were stripped and reprobed with anti-β-actin antibody to verify equal loading. Note that Cx43 is detected in both detergent-soluble and detergent-insoluble fractions in both cell types. (B) Detergent solubility of Cx43 was examined in cells upon *in situ* extraction with 1% Triton X-100 at 4°C as described in Materials and Methods. Cells were immunostained for Cx43 (green) and β-catenin (red). Note that both junctional Cx43 in RL-E Δ N cells and intracellular Cx43 in RL-N Δ E cells were detergent-insoluble. Note also that the intensity of β-catenin at the areas of cell-cell contact is not significantly affected by the detergent treatment. Bar = 15 μ m.

Opposing Effects of E-Cadherin and N-Cadherin on Gap Junction Formation

To explore further whether the expression of E-Cad and N-Cad affects GJ assembly in a diametrically opposed way, we undertook two complementary experimental approaches. First, we knocked down N-Cad in RL-N Δ E cells using ShRNA. Second, we introduced human N-Cad in RL-E Δ N cells and E-Cad in RL-N Δ E cells. We used recombinant retroviruses to express and knock down cadherins. Also, for these experiments both N-Cad and E-Cad were myc-tagged to distinguish

them from their endogenously expressed rat counterparts. An independent approach to knock down E-Cad using SiRNA was not successful as it failed to reduce the expression of E-Cad in RL-E Δ N cells (unpublished). To minimize clonal heterogeneity, GJ assembly and cellular localization of Cx43 were examined in pooled polyclonal cultures within 1–3 passages after G418 or puromycin selection (see Materials and Methods). Figures 5 and 6 show the representative data from three independent sets of experiments and Table 2 provides the summary of the quantitative data.

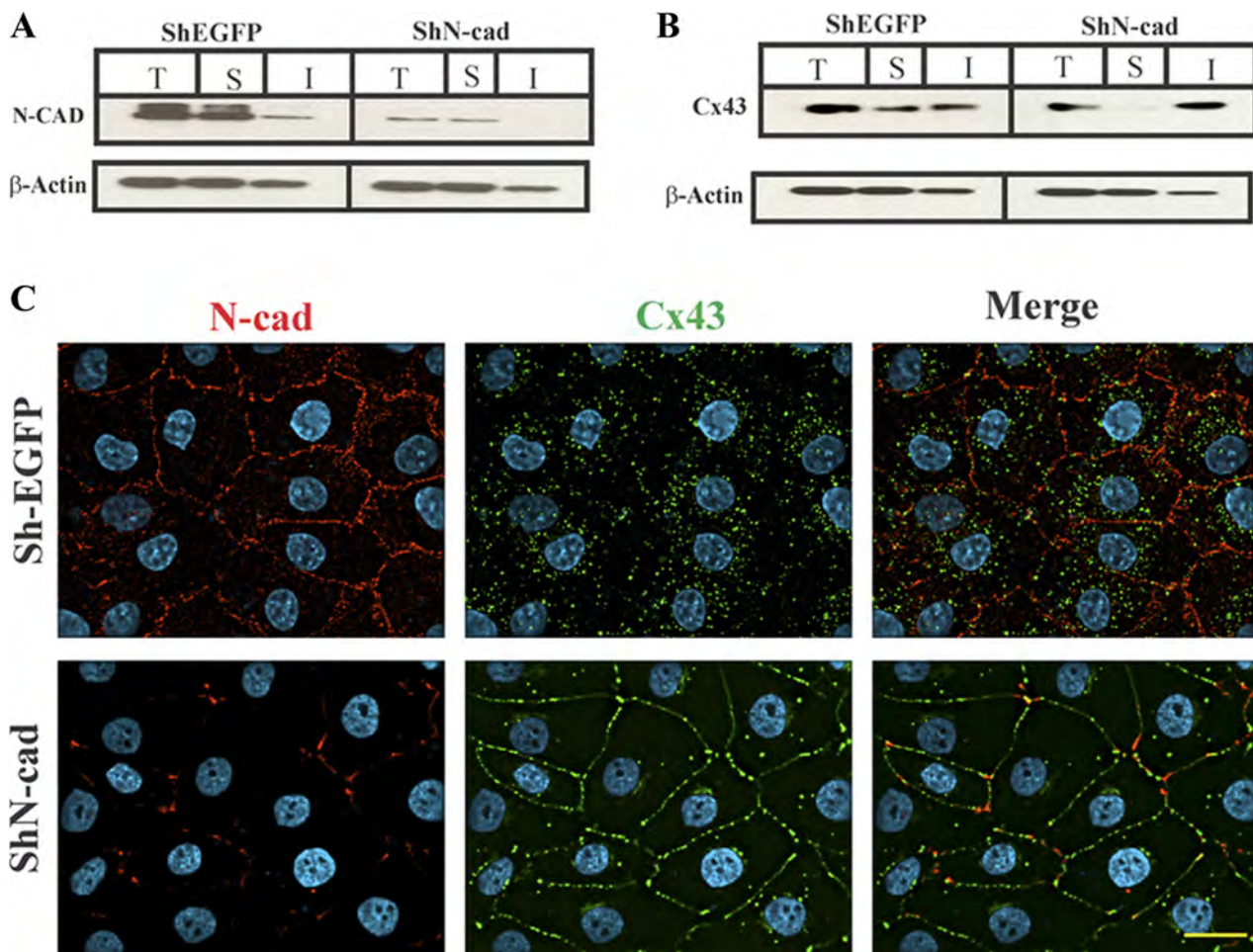


Figure 5. N-cadherin knockdown restores gap junction assembly in RL-NΔE cells. Cells were infected with ShEGFP and ShN-Cad and selected as described in Materials and Methods. Expression level of total (T), detergent-soluble (S), and detergent-insoluble (I) N-Cad (A) and Cx43 (B) were determined in cells infected with ShEGFP and ShN-Cad, respectively. Ten micrograms of total protein and normalized soluble and insoluble fractions were resolved on 12% SDS-PAGE and immunoblotted for Cx43 and N-Cad. The blots were reprobed with β-actin to verify equal loading. Note that the N-Cad expression level is significantly reduced in ShN-Cad infected pooled RL-NΔE polyclonal cultures (A), whereas the expression level of Cx43 (B) is not discernibly affected. Note also that knock down of N-Cad decreased the detergent soluble fraction, and increased the detergent-insoluble fraction, of Cx43. (C) Pooled polyclonal cultures of RL-NΔE cells infected with ShEGFP and ShN-Cad were immunostained for Cx43 and N-Cad. Note the reduced expression of N-Cad at areas of cell-cell contact and in the intracellular pool, the disappearance of intracellular Cx43, and GJ formation in cells infected with ShN-Cad but not with control retrovirus (ShEGFP). Bar = 15 μm.

As assessed immunocytochemically and by the densitometric scanning of Western blots, ShN-cad decreased the expression level of N-Cad by $80 \pm 7\%$ ($n = 3$) in RL-NΔE cells (Figure 5 A) with a concomitant decrease in the localization of N-Cad at the areas of cell-cell contact (Figure 5C, compare top left panel with the bottom left panel), decrease in the intracellular accumulation of Cx43 and an increase in GJ assembly (Figure 5C, compare top middle and right panels with the corresponding bottom panels). Knock down of N-Cad had no discernible effect on the expression level of Cx43 but decreased the detergent-soluble fraction without affecting the detergent-insoluble fraction significantly (Figure 5B). These effects were not observed when RL-NΔE cells were infected with ShEGFP (Figure 5, A and B, left panels) or ShP-Cad, an shRNA directed against placental cadherin (not shown). Moreover, knock down of N-Cad neither induced E-Cad expression nor affected the expression level of ZO-1 and α- and β-catenins (data not shown).

In the next series of experiments, we introduced myc-tagged N-Cad in RL-EΔN cells and myc-tagged E-Cad in

RL-NΔE cells. As assessed by immunocytochemical and Western blot analyses, E-Cad (Figure S-4A, bottom right panel; Figure S-4C) and N-Cad (Figure S-4B, bottom right panel; Figure S-4D) were expressed robustly and appropriately at the areas of cell-cell contact when introduced into RL-NΔE and RL-EΔN cells, respectively. As assessed by quantitative immunocytochemical analysis, we found that the expression of E-Cad in RL-NΔE cells induced GJ assembly and decreased intracellular Cx43 puncta (Figure 6A, Table 2), whereas the expression of N-Cad in RL-EΔN cells partially attenuated GJ assembly and caused intracellular accumulation of Cx43 (Figure 6B, Table 2). The expression of E-Cad in RL-NΔE cells had no discernable effect on the expression level of N-Cad and its localization (Figure S-4, A and C). Similarly, the expression of N-Cad had no detectable effect on the expression level of E-Cad and its localization in RL-NΔE cells (Figure S-4, B and D). Taken together, these data document that the presence of N-Cad at the cell surface is associated with the attenuation of GJ assembly, whereas the presence of E-Cad with the facilitation of the assembly.

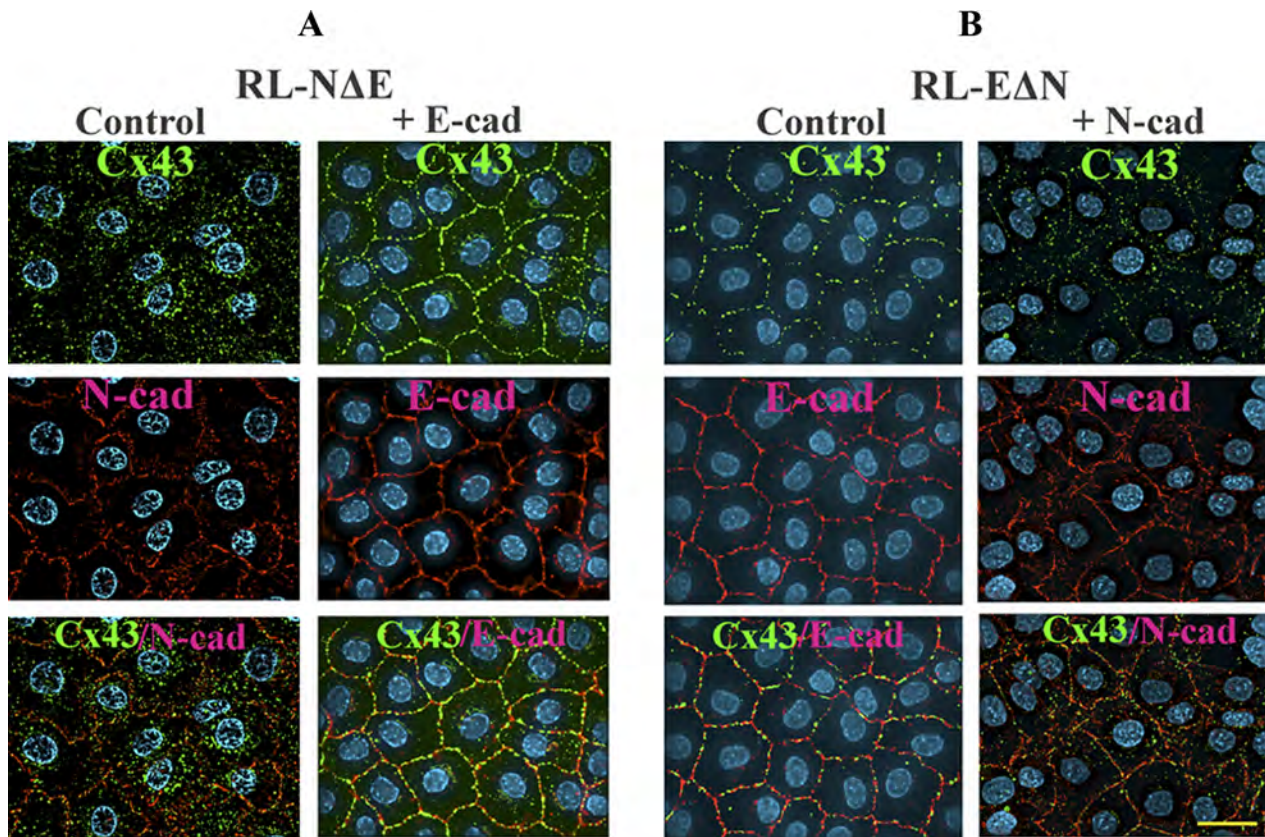


Figure 6. E-cadherin and N-cadherin have opposite effects on gap junction assembly. Myc-tagged N-Cad and E-Cad were introduced, respectively, into RL-EΔN and RL-NΔE cells as described in Materials and Methods. Pooled polyclonal cultures were immunostained for Cx43 (green) and either endogenous cadherin or Myc (red). Note that E-Cad expression (+E-Cad) in RL-NΔE cells restores GJ formation (A) and N-Cad expression (+N-Cad) in RL-EΔN cells partially disrupts GJ assembly (B) and induces intracellular accumulation of Cx43. Bar = 20 μ m.

Cx43 Traffics Normally to Cell Surface in RL-NΔE and RL-EΔN Cells

We next explored the molecular basis of attenuation of GJ assembly and intracellular accumulation of Cx43 in RL-NΔE

Table 2. Effect of E-cadherin and N-cadherin expression on intracellular accumulation of connexin43 in RL-EΔN and RL-NΔE cells

Exp. #	RL-EΔN	RL-EΔN +N-Cadherin	RL-NΔE	RL-NΔE +E-Cadherin
1	5 \pm 2	14 \pm 6	24 \pm 7	10 \pm 4
2	7 \pm 3	23 \pm 7	33 \pm 9	15 \pm 5
3	4 \pm 2	27 \pm 9	37 \pm 11	17 \pm 11

N-cadherin and E-cadherin were introduced, respectively, into RL-EΔN and RL-NΔE cells (see Materials and Methods). Pooled polyclonal cultures were immunostained for Cx43 and E-cadherin and N-cadherin. Images were captured using 0.5- μ m Z-steps and deconvolved. After merging all the deconvolved image stacks into a single plane, the number of intracellular puncta were counted in 10 randomly selected cells. E-cadherin or N-cadherin immunostaining was used to delineate cell boundaries. The mean number of puncta per cell \pm SE was then calculated. Note that N-cadherin expression in RL-EΔN cells increased the number of intracellular puncta, whereas expression of E-cadherin in RL-NΔE cells had the opposite effect.

cells. Attenuation of GJ assembly and/or intracellular accumulation of Cx43 could be caused either by its impaired trafficking or by its endocytosis before GJ assembly upon arrival at the cell surface or by the endocytosis of minuscule GJs that remain very small. We used cell surface biotinylation to examine whether Cx43 trafficked normally to the cell surface in RL-NΔE and RL-EΔN cells. Figure 7A shows that Cx43 was biotinylated significantly in both RL-NΔE and RL-EΔN cells. To determine whether cell surface-associated Cx43 was degraded more rapidly in RL-NΔE cells compared with RL-EΔN cells, we determined the kinetics of its degradation after biotinylation. We found that cell surface biotinylated Cx43 degraded with a similar kinetics in both cell types (Figure 7, B–D). These findings suggest that intracellular accumulation of Cx43 in N-Cad expressing RL-NΔE cells is neither caused by impaired trafficking nor by altered kinetics of its degradation at the cell surface, but by some undefined mechanism that interferes with its assembly into GJs upon arrival at the cell surface resulting in its accumulation in intracellular vesicles or minuscule annular GJs.

Cx43 Is Endocytosed by Nonclathrin-Mediated Pathway in RL-NΔE Cells

In RL-NΔE cells, Cx43 trafficked to the cell surface based on cell surface biotinylation, but failed to form functional GJs; moreover, a significant proportion of Cx43 remained detergent-insoluble as discrete intracellular puncta as assessed biochemically and immunocytochemically upon *in situ* ex-

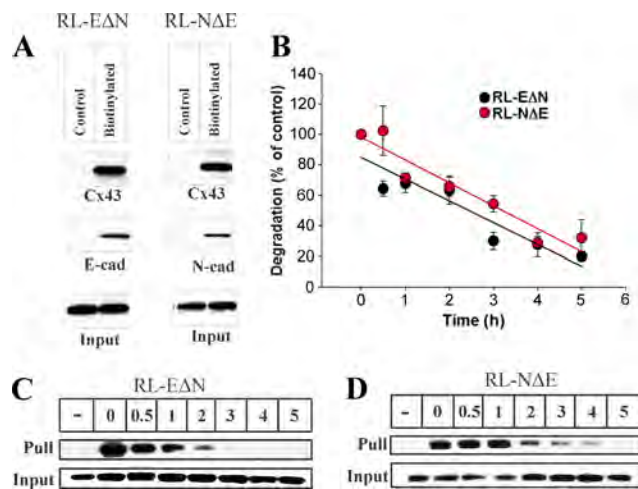


Figure 7. Cx43 traffics to cell surface in RL-EΔN and RL-NΔE cells. Confluent cultures of RL-EΔN and RL-NΔE cells (A) were biotinylated with sulfo-NHS-SS-biotin at 4°C, and biotinylated proteins from 100 µg of total cell lysate were detected by Streptavidin pull down followed by Western blotting for Cx43, E-Cad, and N-Cad (see Materials and Methods). In the lanes labeled Input, 10 µg of total protein was used and probed for Cx43. Note that in both RL-EΔN and RL-NΔE cells (A; labeled as Biotinylated), nearly the same amount of Cx43 was detected in the Streptavidin “Pull down” lanes. Note also that E-Cad and N-Cad were pulled down, respectively, only in RL-EΔN cells and RL-NΔE cells. A nonbiotinylated dish (labeled as Control) was used as a negative control. (B–D). Cell surface associated Cx43 degrades with similar kinetics in RL-EΔN and RL-NΔE cells. Cells were biotinylated at 4°C and were incubated for various times at 37°C before Streptavidin pull down and Western blotting as described in Materials and Methods. A nonbiotinylated dish was kept as a control (−). The blots were quantified after normalization of the input for each time point, and the values from three independent experiments were plotted graphically using Sigma plot as described in Materials and Methods. Note that cell surface associated biotinylated Cx43 degrades with similar kinetics in both RL-EΔN and RL-NΔE cells.

traction with 1% TX-100 (Figures 2–4). This raised the possibility that N-Cad expression attenuated GJ assembly either

by triggering the endocytosis of connexons into detergent-insoluble puncta before their assembly into GJs or by triggering endocytosis of nascent, minuscule, and nonfunctional GJ plaques before their maturation into immunocytochemically detectable, larger, and functional plaques (Jordan *et al.*, 2001; Piehl *et al.*, 2007; Falk *et al.*, 2009). Hence, we investigated whether Cx43 was endocytosed by a clathrin-mediated pathway or a nonclathrin-mediated pathway. We used chlorpromazine and hypertonic medium, which prevent the formation of clathrin coated pits, to block the clathrin-mediated pathway (Heuser and Anderson, 1989; Wang *et al.*, 1993), and filipin and methyl-β-cyclodextrin (MβCD), which impair the structure and function of sphingolipid-cholesterol-rich membrane microdomains (lipid rafts), to inhibit non-clathrin-mediated pathway (Subtil *et al.*, 1994; Orlandi and Fishman, 1998; Skretting *et al.*, 1999). Moreover, the specificity of these drugs in inhibiting each pathway was assessed by measuring the uptake of Alexa-594- or Alexa-488-labeled transferrin and cholera toxin, which are predominantly endocytosed by clathrin-mediated and nonclathrin-mediated pathways, respectively (Wang *et al.*, 1993; Subtil *et al.*, 1994; Orlandi and Fishman, 1998). For these experiments, RL-EΔN and RL-NΔE cells were treated with chlorpromazine (5 µg/ml), filipin (2.5 µg/ml), and MβCD (5 mM) for 2 h. These concentrations were determined based on several pilot experiments in which the dose and the duration of treatment were varied while the internalization of Alexa-488/594-labeled transferrin and cholera toxin was monitored microscopically. We found that both in RL-EΔN and RL-NΔE cells, chlorpromazine and hypertonic media inhibited the uptake of only Alexa-488/594-labeled transferrin but did not affect the uptake of Alexa-488/594-labeled cholera toxin. Similarly, filipin and MβCD inhibited the uptake of only Alexa-488/594-labeled cholera toxin but did not affect the uptake of Alexa-488/594-labeled transferrin (data not shown). Consistent with the effect of filipin and MβCD on the inhibition of uptake of cholera toxin, we found that they induced GJ assembly profoundly in RL-NΔE cells (Figure 8, bottom row, compare panel 1 with panels 3 and 4) but had no discernible effect on the assembly in RL-EΔN

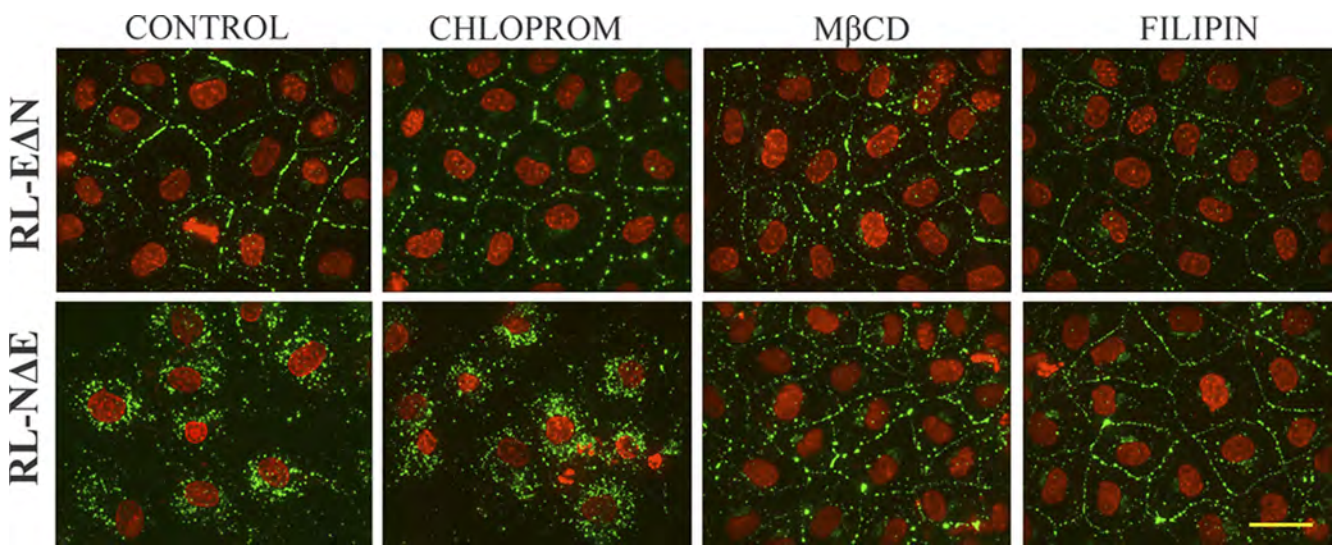


Figure 8. Inhibition of nonclathrin-dependent endocytosis restores gap junction assembly in RL-NΔE cells. RL-EΔN and RL-NΔE cells, seeded on glass cover slips in six-well clusters and allowed to grow to confluence, were treated with chlorpromazine (Chlorprom; 5 µg/ml), filipin (2.5 µg/ml), or methyl-β-cyclodextrin (MβCD, 5 mM) for 60 min. After washing and fixation, cells were immunostained for Cx43. Note that treatment with filipin and MβCD restored GJ assembly in RL-NΔE cells but had no significant effect on RL-EΔN cells. Bar = 20 µm.

cells (Figure 8, upper row, compare panel 1 with panels 3 and 4). On the other hand, chlorpromazine had no effect on GJ assembly in RL-NΔE cells (Figure 8, bottom row, compare panel 1 and 2) but appeared to decrease the preponderance of intracellular puncta in RL-EΔN cells as assessed visually (Figure 8, top row, compare panels 1 and 2). A rigorous quantitative analysis has to be performed to assess if chloropromazine enhanced GJ assembly in RL-EΔN cells. Similar data were obtained when RL-NΔE and RL-EΔN cells were treated with hypertonic medium (data not shown).

To further define the subcellular fate of intracellular puncta, we immunostained RL-NΔE cells with the markers specific for the endocytic pathway and examined whether they colocalized with Cx43. These analyses showed that Cx43 did not detectably colocalize with clathrin, a major structural component of clathrin-coated vesicles, with the early endosome marker, EEA-1, and with caveolin-2 (Figure 9) although some colocalization was observed with caveolin-1 both in the perinuclear region and at the cell surface consistent with what has been reported in earlier studies (Langlois *et al.*, 2008). Because none of the commercially available antibodies recognized rat Rab5 and Rab7, we transiently expressed GFP-tagged, constitutively active, Rab5 and Rab7

in RL-NΔE cells and immunostained cells for Cx43 to examine whether it colocalized with these markers. We found that Cx43 did not colocalize with Rab5-GFP-positive vesicles, however some colocalization was observed with Rab7-GFP positive late endosomes (Figure S-5). Moreover, significant colocalization of Cx43 was observed with Lamp-1 (Figure S-5, bottom row), which is localized on lysosomes (Rohrer *et al.*, 1996). Taken together, the above data suggest that in RL-NΔE cells connexons that arrive at the cell surface are either internalized before their docking and assembly into GJs or are assembled into minuscule GJs, which are endocytosed by nonclathrin dependent pathway into detergent-resistant puncta that eventually are targeted to lysosomes for degradation.

On the Origin of Detergent-Insoluble Intracellular Puncta in RL-EΔN and RL-NΔE Cells

In the next series of experiments, we explored the possible mechanisms by which detergent-resistant intracellular puncta might be generated. To test whether these puncta arose from the endocytosis of connexons that failed to dock with the adjacent connexons or from the formation of minuscule GJs, which acquired resistance to detergent extrac-

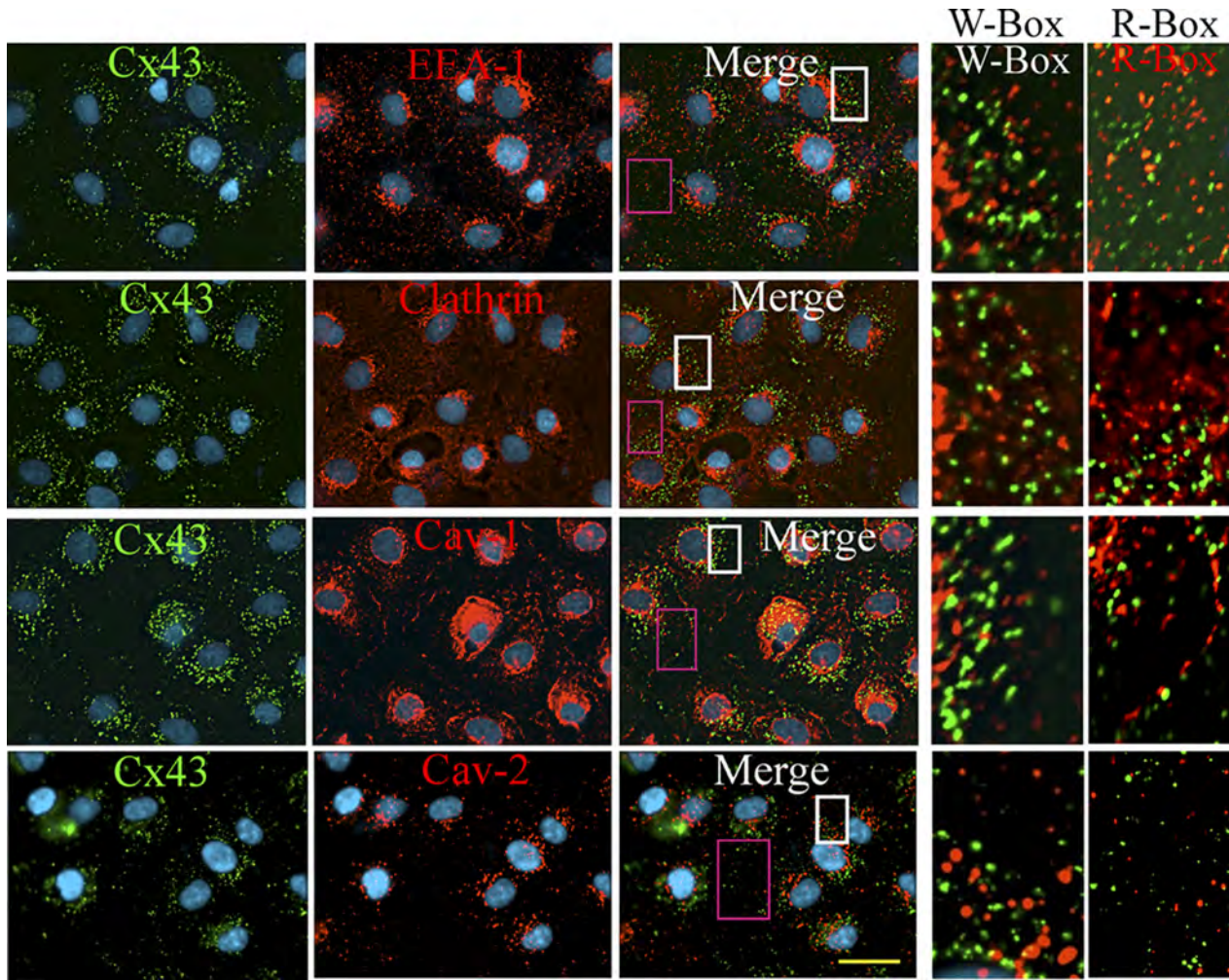


Figure 9. Cx43 does not colocalize with known endocytic markers in RL-NΔE cells. RL-NΔE cells, seeded as described in Figure 8 legend, were immunostained for Cx43 (green) and endocytic markers, EEA-1, clathrin, caveolin-1, and caveolin-2 (red). Note that Cx43 does not colocalize with any of these markers as shown in the enlarged images of the marked boxes on the right. W-Box = white box; R-Box = Red box. Bar = 20 μm.

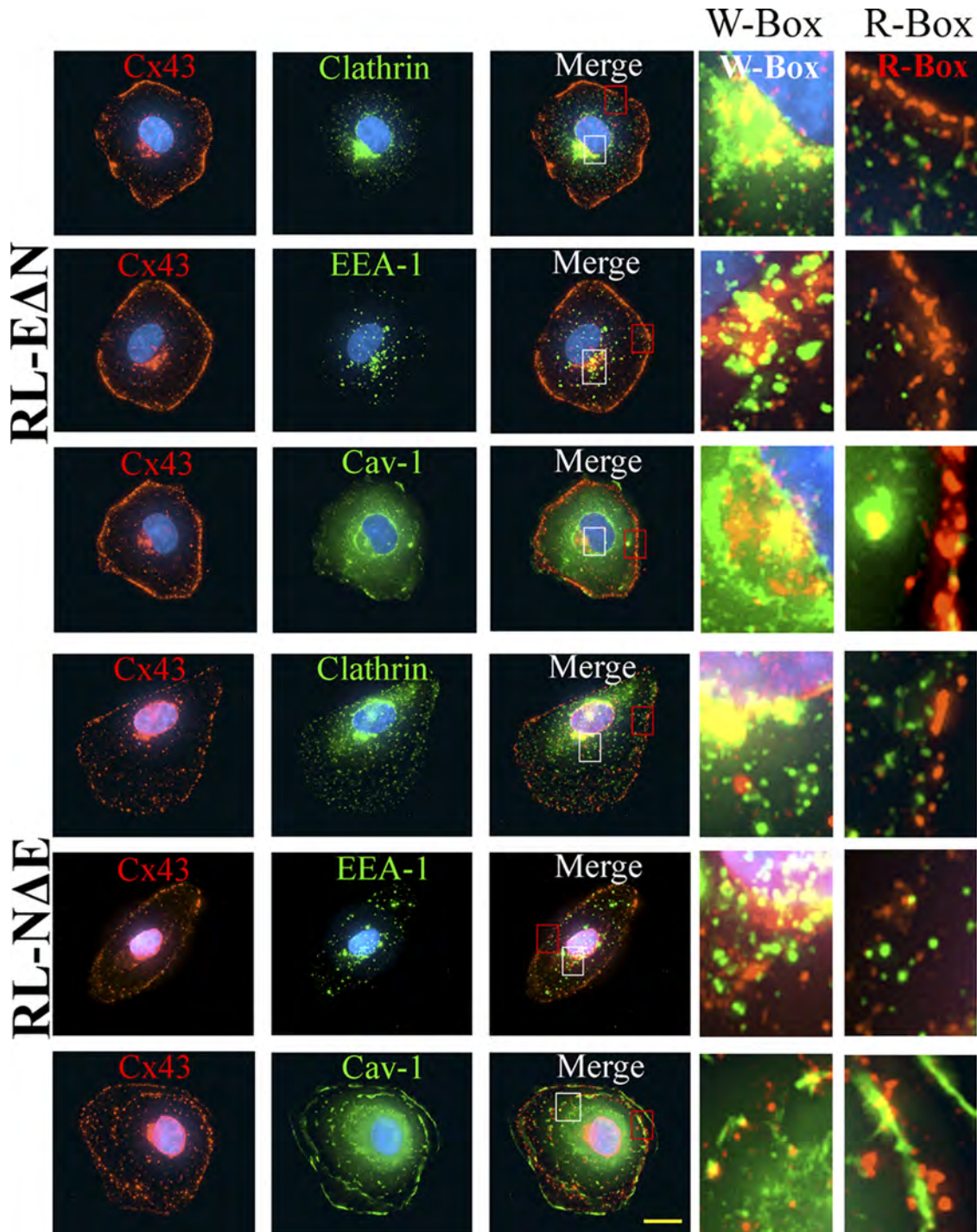


Figure 10. Cx43 is endocytosed into detergent-soluble puncta in RL-NΔE and RL-EΔN single cells. Between $1-2 \times 10^3$ RL-EΔN and RL-NΔE cells were seeded on six-well clusters containing glass cover slips. The subcellular fate of Cx43 was examined in single cells upon *in situ* extraction with 1% Triton X-100 at 4°C as described in Materials and Methods. Cells were immunostained for Cx43 (green) and clathrin, EEA-1 and caveolin-1 (red). Enlarged images marked by the white boxes (W-box) and red boxes (R-box) are shown on the right. Note that significant colocalization with all the markers is observed in the perinuclear regions in both cell types, while partial localization to a variable extent is observed in the cell peripheries. All, punctate and nonpunctate, immunostaining was lost upon detergent extraction (not shown). Bar = 7 μm.

tion, as has been observed during the formation of adherens junctions (Adams *et al.*, 1996), we examined the subcellular fate of intracellular puncta in single RL-NΔE and RL-EΔN cells 24–36 h after seeding and determined their detergent solubility upon *in situ* extraction with 1% TX-100 in 3 inde-

pendent experiments. We rationalized that given the short half-life of Cx43 (2–5 h), intracellular puncta in single cells plausibly represent endocytosed undocked connexons that trafficked to the cell surface or vesicles along the secretory pathway. We found that in RL-NΔE and RL-EΔN single

cells, Cx43 was localized as discrete puncta both at the cell periphery and in the cytoplasm; moreover, as shown in representative images in Figure 10, these puncta colocalized with clathrin, EEA-1 and Cav-1 albeit to a variable extent. The extent of colocalization appeared to be more robust at the perinuclear region as compared with cell periphery. However, we found that in contrast to what was observed in confluent cells, all puncta—both intracellular and at the cell periphery—were lost upon *in situ* extraction with 1% TX-100 as assessed immunocytochemically (data not shown).

To rule out the possibility that the detergent-resistant puncta arose during the transit of Cx43 along the secretory pathway, we blocked ER to Golgi transport with brefeldin (Klausner *et al.*, 1992; Chardin and McCormick, 1999) and *cis*-Golgi to *medial*-Golgi transport with monensin (Tartakoff, 1983). For these experiments, confluent RL-NΔE and RL-EΔN cells were treated with brefeldin (10 μM) and monensin (10 μM) for 30 min to 4 h and immunostained for Cx43 and GM130, a *cis*-Golgi resident protein (Marra *et al.*, 2007). We found that in RL-NΔE cells, treatment with brefeldin for 1–4 h disrupted Golgi structure but did not diminish the number of Cx43 puncta discernibly (Figure 11A, compare panels in the top row with the middle row). Moreover, these puncta neither colocalized with GM130 (Figure 11A, middle row) nor with calreticulin, an ER-resident protein (Caramelo and Parodi, 2008) (data not shown). We also found that treatment of RL-NΔE cells with monensin for 2–4 h blocked the transport of Cx43 in the *cis*-Golgi, as assessed by its extensive colocalization with GM130 in the perinuclear regions, but did not appear to diminish the number of intracellular puncta. Moreover, these puncta still persisted when brefeldin and monensin treated RL-NΔE cells were extracted *in situ* with 1% TX-100 although the perinuclear staining specific for Cx43 and GM130 was lost (data not shown).

Intriguingly, treatment of RL-EΔN cells with brefeldin for 1–4 h also fragmented Golgi, but, in contrast to N-Cad expressing RL-NΔE cells, seemed to enhance GJ assembly or stabilize GJ plaques as assessed visually by the appearance of larger puncta at areas of cell-cell contact. As has been observed by others, in untreated RL-EΔN cells, Cx43 appeared to colocalize with GM130 near the perinuclear regions (Figure 11B, top row). Also, treatment of RL-EΔN cells with monensin not only caused accumulation of Cx43 in perinuclear regions, as assessed by its extensive colocalization with GM130 but also appeared to increase the number of intracellular puncta in some cells, which possibly represent endocytosed or degraded GJs (Figure 11B, compare panels in top row with the bottom row). We also found that when RL-EΔN cells were treated with brefeldin and monensin for more than 4 h GJ assembly was drastically disrupted, with concomitant increase in the number of intracellular puncta (data not shown). Taken together, the data shown in Figures 10 and 11, combined with those shown in Figures 4, 8, and 9, suggest that detergent resistant intracellular puncta in N-Cad expressing RL-NΔE cells are likely generated at the site of cell-cell contact—and not en route from ER to cell surface via Golgi and trans-Golgi network—and possibly represent minuscule annular GJs, which become detergent-insoluble and eventually degrade in the lysosomes. The data obtained from single cells suggest that undocked connexons in both RL-NΔE and RL-EΔN cells most likely are endocytosed by both a clathrin-dependent and nonclathrin-dependent pathway.

Cadherin Expression and Assembly of Cx32 into Gap Junctions in RL-EΔN and RL-NΔE Cells

To investigate whether the assembly of other Cxs into GJs was also regulated differentially by E- and N-Cad, we introduced rat Cx32 into RL-EΔN and RL-NΔE cells, which do not express this Cx, by recombinant retroviruses and examined its subcellular fate in pooled polyclonal cultures within 2–3 passages after selection in G418. We chose Cx32 because it is expressed only by well-differentiated and polarized cells (Bavamian *et al.*, 2009). We found that Cx32 was assembled efficiently into GJs in RL-EΔN cells but not in RL-NΔE cells where it remained intracellular as discrete puncta that also remained detergent-insoluble as assessed immunocytochemically upon *in situ* extraction with 1% TX-100 (Figure 12A) and biochemically by the detergent insolubility assay (Figure 12B) similar to what was observed with Cx43. Moreover, we found that both junctional and nonjunctional Cx43 and Cx32 did not appear to colocalize significantly in RL-EΔN and RL-NΔE cells. Taken together, these data suggest that N-Cad expression also prevents the assembly of Cx32 into GJs, possibly by triggering its endocytosis into detergent-insoluble puncta.

Cadherin Expression and Gap Junction Assembly in Mouse Mammary Tumor Cell Line

To assess the relevance of our findings in RL-CL9 cells further, we examined whether E-Cad and N-Cad expression also regulated the assembly of Cx43 into GJs differentially in other cell culture model systems, such as in the mouse mammary epithelial cell line (NMuMG), which has been widely used to study EMT (Maeda *et al.*, 2005). These cells express E-Cad and N-Cad and undergo EMT in response to transforming growth factor β (Maeda *et al.*, 2005). We found that in parental NMuMG cells that expressed nearly equal levels of both E-Cad and N-Cad, Cx43 was localized both at areas of cell-cell contact and in the cytosol (Figure S-6, top row). In a subclone of NMuMG that expressed a higher level of E-Cad compared with N-Cad (clone E9), Cx43 was predominantly assembled into GJs (Figure S-6, middle row), whereas in a clone that expressed only N-Cad and undetectable levels of E-Cad (clone 11), Cx43 remained intracellular just like in RL-NΔE cells (Figure S-6, bottom row). These data suggest that the expression of N-Cad also disrupts the assembly of Cx43 into GJs in NMuMG cells.

DISCUSSION

Our findings demonstrate that E-Cad and N-Cad have distinct effects on the assembly of Cx43 into GJs in isogenic subclones of RL-CL9 cells that express either one or the other cadherin. A key conclusion of our study is that Cx43 undergoes a profoundly different subcellular fate dependent on the type of cadherin expressed. When only E-Cad is expressed, Cx43 is preponderantly assembled into large GJs and when only N-Cad is expressed, Cx43 is endocytosed by a nonclathrin-mediated pathway before its assembly into functional GJs. Moreover, when both cadherins are simultaneously expressed in the same cell type, GJ assembly and disassembly seemed to occur concurrently. This conclusion is based on the screening of 60–92 isogenic E-Cad and N-Cad expressing clones and performing a systematic analysis of junctional and nonjunctional fate of Cx43 in selected clones. This analysis showed that intracellular localization of Cx43 as discrete vesicular puncta always coincided with the cell surface expression of N-Cad, whereas junctional localization coincided with the cell surface expression of E-Cad.

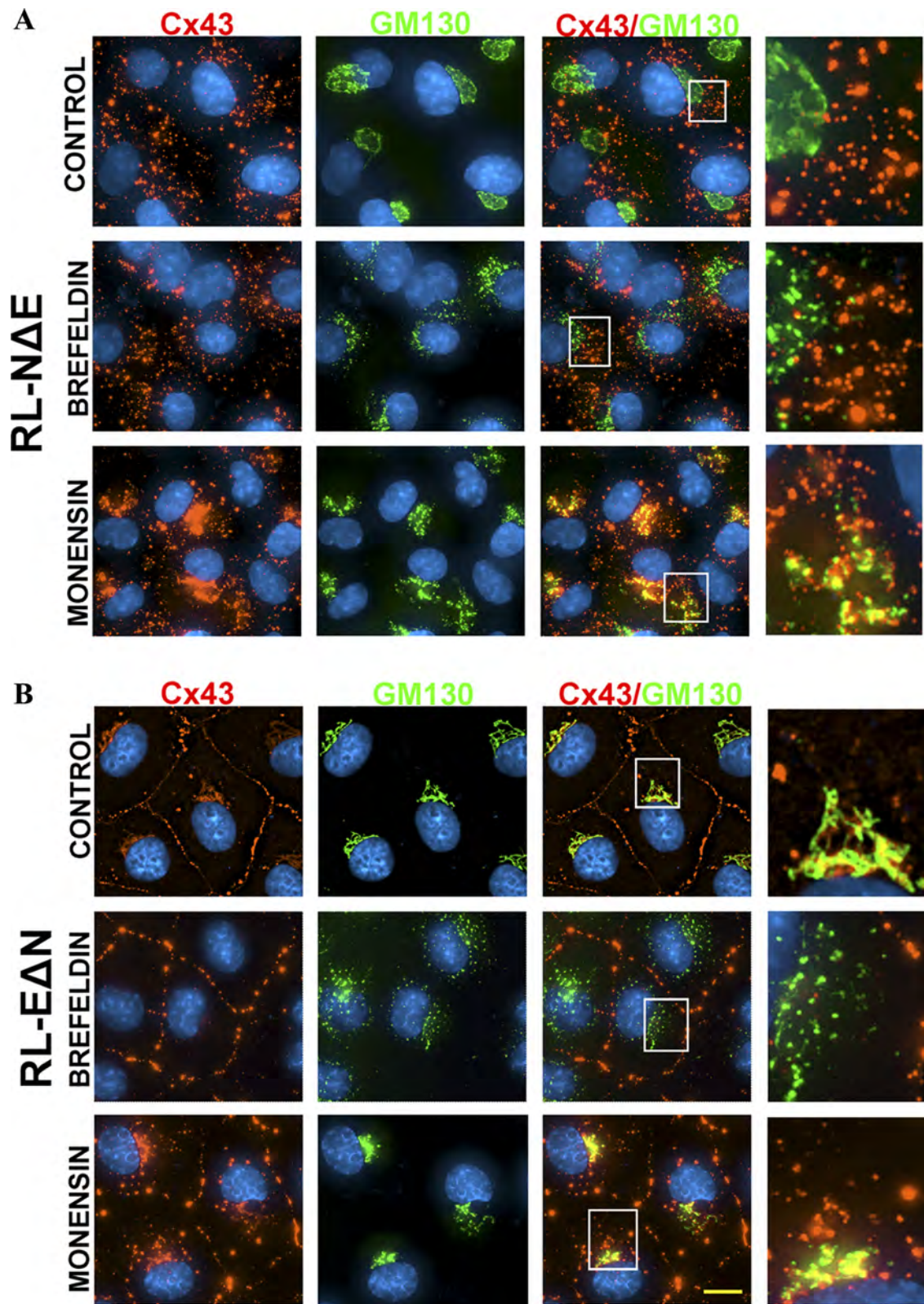


Figure 11. Detergent-resistant intracellular puncta are not generated along the secretory pathway in RL-N Δ E cells. RL-N Δ E (A) and RL-E Δ N (B) cells were seeded in 6-cm Petri dishes and allowed to attain confluence. Cells were treated with brefeldin or monensin (10 μ M) for 2 h and immunostained for Cx43 and GM130, a *cis*-Golgi resident protein (see Materials and Methods). Enlarged images marked by the white boxes are shown on the right. Note that both in RL-N Δ E cells (A) and RL-E Δ N cells (B), brefeldin disrupted the Golgi. Note also that brefeldin did not decrease the number of Cx43 puncta in RL-N Δ E (A) cells but seemed to have stabilized or increase GJ plaques in RL-E Δ N cells (B). Note a significant colocalization of Cx43 with GM130 due to the blockade of intraGolgi transport by monensin. Note also that monensin did not decrease the number of Cx43 puncta in RL-N Δ E cells. Bar = 8 μ m.

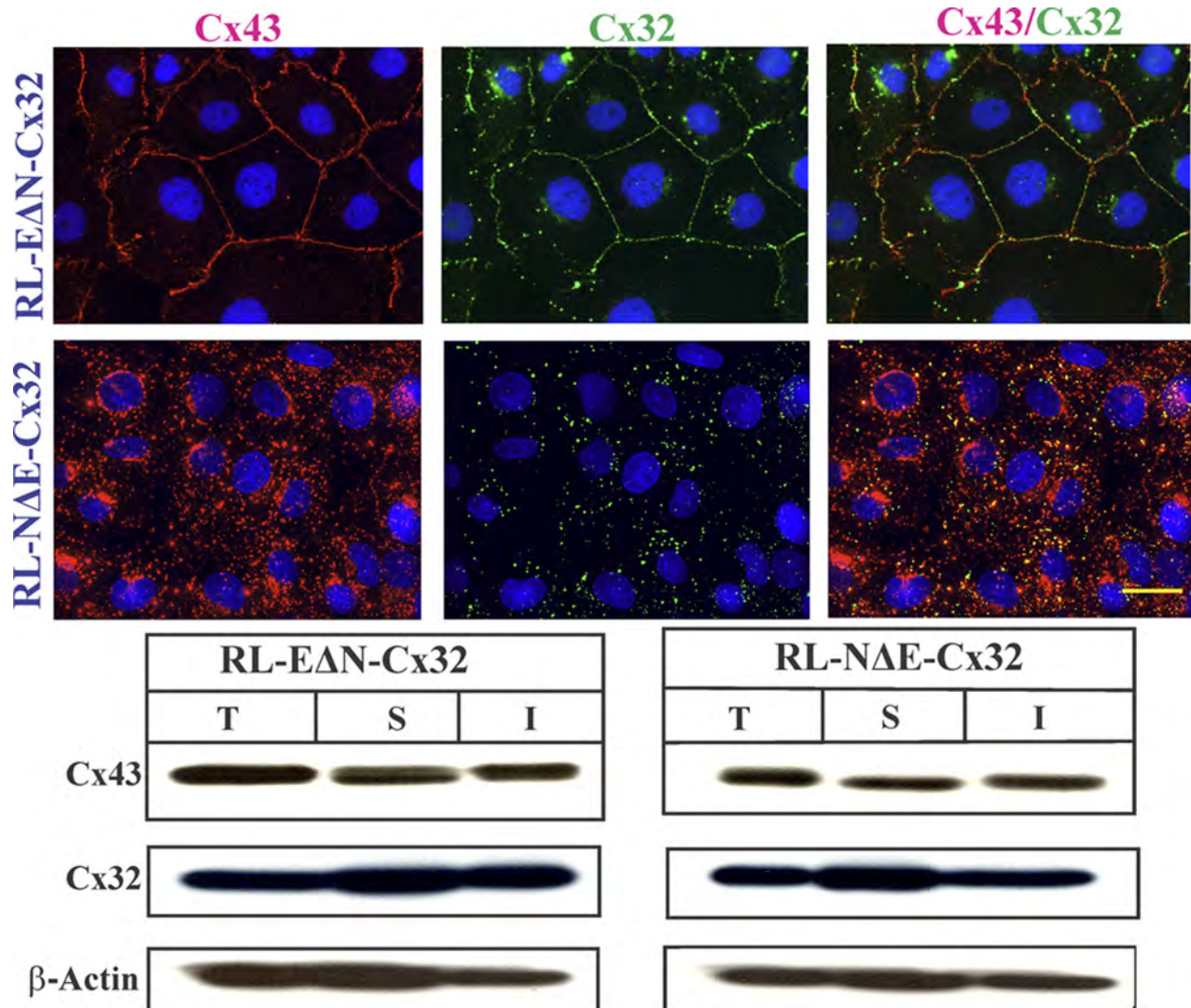


Figure 12. Differential assembly of Cx32 in RL-E Δ N and RL-N Δ E cells. (A) RL-E Δ N and RL-N Δ E cells were infected with recombinant retrovirus harboring rat Cx32 and pooled polyclonal cultures were immunostained for Cx43 and Cx32 after *in situ* extraction with 1% TX-100. Note that both Cxs assemble into GJs in RL-E Δ N cells but remain intracellular in RL-N Δ E cells. (B) Cell lysates prepared from pooled polyclonal cultures were analyzed by the detergent-solubility assay. Total (T), TX-100-soluble (S), and TX-insoluble (I) fractions were analyzed by Western blot analysis as described in Materials and Methods. The blots were stripped and reprobed with anti- β -actin antibody to verify equal loading. Note that both Cx43 and Cx32 are detected in detergent-soluble and detergent-insoluble fractions in both cell types. Bar = 20 μ m.

Thus, through the dissection of the relative contributions of E-Cad and N-Cad, we have discovered a distinct role of each cadherin in regulating the assembly of Cx43 into GJs in RL-CL9 cells. Our studies show that GJ assembly and disassembly are the down-stream targets of the signaling initiated by E-Cad and N-Cad, respectively, and may provide one possible explanation for the disparate role played by these cadherins in regulating cell motility and invasion during tumor progression and EMT.

Our biotinylation data showed that intracellular accumulation of Cx43 was not caused by impaired trafficking because Cx43 trafficked normally to the cell surface and was degraded with similar kinetics in both RL-E Δ N and RL-N Δ E cells (Figure 7). However, GJ assembly was attenuated only in cells that expressed N-Cad and was recuperated only in those cells in which the expression of N-Cad was knocked down (Figure 5). Moreover, our biochemical and immunochemical data showed that a significant proportion of

Cx43 remained detergent-insoluble both in RL-E Δ N and RL-N Δ E cells despite the fact that no functional GJs were assembled in the latter (Figures 3 and 4). These findings were intriguing because acquisition of detergent insolubility had been generally attributed to the incorporation of Cxs into GJs—and not to their intracellular and nonjunctional localization (VanSlyke and Musil, 2000; Musil, 2009). On the basis of these findings, we rationalized that the detergent-resistant intracellular vesicular puncta in N-Cad expressing RL-N Δ E cells arose because of endocytosis of Cx43 in a nonclathrin-dependent manner. This notion was corroborated by our subsequent data, which showed that inhibition of clathrin-independent endocytosis by filipin and M β CD, which disrupt lipid rafts and endocytosis mediated by them, not only caused the disappearance of these intracellular puncta but also restored GJ formation robustly in N-Cad expressing RL-N Δ E cells, confirming the requirement for the productive endocytosis in the generation of detergent-resis-

tant vesicular puncta and its inhibition for the formation of GJs. The lack of colocalization of these detergent-resistant intracellular Cx43 containing vesicular puncta with EEA-1, Rab5, caveolin-1, caveolin-2 suggests that Cx43 in RL-N Δ E cells is endocytosed in a Rab5-independent manner into Rab5-negative vesicles that mature into Rab7-positive late endosomes, which are then targeted to the lysosomes for degradation (Figures 9 and S-5).

Because the kinetics of degradation of cell-surface associated Cx43 was not appreciably different in RL-E Δ N and RL-N Δ E cells (Figure 7), we rationalized that the detergent-resistant intracellular puncta in the latter arose at areas of cell-cell contact upon arrival of Cx43 (connexons) at the cell surface—and not en route to the cell surface along the secretory pathway. The lack of colocalization of these detergent-resistant intracellular Cx43 containing vesicles with conventional early endocytic markers further raised the possibility that the puncta did not arise by a canonical endocytic route and thus might be minuscule annular GJs which were endocytosed before maturing into larger functional GJ plaques and which incidentally became detergent-insoluble. Minuscule annular GJs of <0.5 μ m have been observed in earlier studies (Jordan *et al.*, 2001; Baker *et al.*, 2008) and smaller GJ plaques have also been found to be extremely unstable (Holm *et al.*, 1999; Jordan *et al.*, 1999). The notion that detergent-resistant intracellular vesicular puncta arose at cell-cell contacts was substantiated by our experimental data with single cells, which showed that Cx43 puncta, both intracellular as well as at the cell peripheries, colocalized with clathrin, EEA-1, and Cav-1 and remained detergent soluble (Figure 10 and data not shown). Moreover, inhibition of ER to Golgi transport with brefeldin and inhibition of Golgi to cell surface transport with monensin had no discernible effect on the number of intracellular puncta in RL-N Δ E cells (Figure 11A), which suggests that the intracellular puncta are not generated along the secretory pathway due to impaired trafficking but arise at sites of cell-cell contact upon arrival of Cx43 at the cell surface. TX-100 insoluble immunofluorescent E-Cad puncta, barely resolvable by standard microscopy, have been observed during the early stages of adherens junction formation at sites of cell-cell contact before they coalesce to form larger plaques (Yonemura *et al.*, 1995; Adams *et al.*, 1996). Although it is at present unclear at what stage of maturation a GJ plaque becomes detergent-insoluble, and in general what is the molecular basis of acquisition of detergent-insolubility by macromolecular complexes, it seems likely that the expression of N-Cad triggers the formation of these detergent-resistant intracellular puncta in RL-N Δ E by preventing the coalescence of minuscule GJs, and triggering their endocytosis by a non-clathrin-dependent pathway before they form large GJs.

E-Cad is predominantly expressed in epithelial cells whereas N-Cad is expressed in neuronal and mesenchymal cells (Tepass *et al.*, 2000; Gumbiner, 2005), and both cadherins have been shown to facilitate the assembly of Cx43 into GJs (Wei *et al.*, 2005; Li *et al.*, 2008; Chakraborty *et al.*, 2010). It is of note that N-Cad is the main cadherin expressed in cardiac myocytes where it is required for the assembly of Cx43 into GJs (Li *et al.*, 2005; Li *et al.*, 2008). Although cell-cell adhesion mediated by cadherins has been shown to control the assembly of several junctional complexes, including GJs, it is as yet unknown how they signal (Gumbiner, 2005; Nelson, 2008; Wheelock *et al.*, 2008; Sepniak *et al.*, 2009). As assessed by cell-cell aggregation assays, our results showed that cell-cell adhesion mediated by both E-Cad and N-Cad remained intact in RL-E Δ N and RL-N Δ E cells (Table S-2). Thus, attenuation of junction formation in

N-Cad expressing cells was not the result of absent cell-cell adhesion, although our data do not exclude the possibility that the distinct effects were caused by the quantitative and qualitative difference in the strength of cell-cell adhesion mediated by these cadherins. Our data also showed that GJ assembly was partially restored in N-Cad expressing RL-N Δ E cells upon expression of E-Cad and was partially disrupted upon expression of N-Cad in E-Cad expressing RL-E Δ N cells. Thus, when both cadherins were expressed simultaneously in the same cell, both assembly and disassembly seemed to occur concurrently.

What might be the possible molecular explanation for the diametrically opposite effects of E-Cad and N-Cad on the assembly of Cx43 into GJs in these cells? One plausible explanation for these data is that engagement of E-Cad and N-Cad triggers distinct signaling pathways, or recruits a distinct set of proteins to sites of cell-cell contact, or both, which affect GJ assembly differently. N-Cad, which is normally expressed in mesenchymal cells, has been shown to facilitate or enhance fibroblast growth factor receptor mediated signaling by preventing ligand-induced internalization of the receptor and through activation of sustained MAPK-ERK signaling cascade when expressed in tumor cells of epithelial origin (Hazan *et al.*, 2000; Suyama *et al.*, 2002; Hultit *et al.*, 2007). Similarly, E-Cad has also been shown to interact or associate with receptors for fibroblast growth factor and epidermal growth factor, leading to the attenuation of signaling as well as to modulation of MAPK-ERK signaling cascade (Pece *et al.*, 1999; Pece and Gutkind, 2000; Perrais *et al.*, 2007). Thus, E-Cad and N-Cad engagement may have several distinct downstream molecular targets that might facilitate or attenuate GJ assembly differently independent of cell-cell adhesion and dependent upon the signaling pathway initiated upon expression. As Cx43 has been shown to be endocytosed in response to growth factors, such as epidermal growth factor, this may be one possible explanation for the disparate effect of E-Cad and N-Cad on GJ assembly in RL-E Δ N and RL-N Δ E cells. Further studies using the constitutively active mutants of epidermal growth factor receptor as well as knock down studies with fibroblast growth factor receptors will be required to substantiate this notion.

As GJ assembly and disassembly occurred concurrently when both cadherins were simultaneously expressed in the same cell type, it is also possible that the assembly of Cx43 is independently regulated by E-Cad and N-Cad, locally, through recruitment of separate sets of proteins to the site of cell-cell contact or through their segregation into distinct membrane microdomains, which determines junctional versus nonjunctional fate of Cx43 upon arrival at the cell surface. This explanation is in accord with the findings that Cxs lie in the vicinity of cadherins and their associated proteins α - and β -catenins during GJ assembly and disassembly and may also associate with them transiently either directly or indirectly (Fujimoto *et al.*, 1997; Wei *et al.*, 2005; Xu *et al.*, 2006). In mesenchyme-derived NIH3T3 cells, which express N-Cad, interaction between Cx43 and N-Cad was required for GJ assembly and turnover at the cell surface (Wei *et al.*, 2005). Moreover, when coexpressed in the same cells, E-Cad and N-Cad are likely to exist in separate complexes as their interaction is not heterophilic (Tepass *et al.*, 2000; Gumbiner, 2005). Furthermore, N-Cad and Cxs have been found to be concentrated in lipid rafts and interaction between N-Cad and p120 catenin, which also interacts with Cx43 (Wei *et al.*, 2005), occurs in cholesterol-rich environment (Locke *et al.*, 2005; Taulet *et al.*, 2009). Finally, it is also possible that the expression of N-Cad could squelch away components which

otherwise would have been used by E-Cad to form mature adherens junctions to facilitate assembly. Because knockdown of N-Cad in RL-NΔE cells, which lack detectable level of E-Cad, restored GJ assembly, it is likely that other mechanisms, which are not mediated by these classical cadherins, or are induced upon knock down of cadherins, exist to restore and regulate the assembly of GJs. One possible mechanism is that cell-cell adhesion generated by the docking of connexons by themselves is sufficient to induce assembly in the absence of classical cadherins and it is utilized only when no other mechanism is active. This notion is corroborated by our recent studies, which showed that the assembly of Cx43 was induced in the absence of E-Cad mediated cell-cell adhesion in cadherin null human squamous carcinoma cells (Chakraborty *et al.*, 2010) and by other studies in which expression of Cx43 induced cell-cell adhesion of its own (Lin *et al.*, 2002; Cotrina *et al.*, 2009).

While the molecular mechanism(s) by which E-Cad and N-Cad affect the assembly of Cx43 into GJs in an opposite manner remains to be elucidated, regulation of endocytosis of minuscule GJ puncta at the areas of cell-cell contact before they mature into larger plaques seems to be the determining factor that dictates the assembly of GJs in RL-CL9 cells. Alternatively, because raft component proteins are expected to have decreased lateral mobility (Lingwood and Simons, 2010), attenuation of junction assembly may result from the decreased lateral mobility of docked connexons due to their entrapment in lipid rafts. This notion is in agreement with our data, which showed that the stability of cell-surface associated Cx43 remained unaffected, although it remains to be seen whether the surface residence time of connexons was also significantly reduced, which either prevented their recruitment to nascent minuscule GJ plaques or permitted their endocytosis before docking in N-Cad expressing RL-NΔE cells compared with E-Cad expressing RL-EΔN cells. Because the assembly of Cx32 into GJs was also regulated in diametrically opposed ways in RL-EΔN and RL-NΔE cells, it appears that the effect of N-Cad expression on junction assembly is not Cx specific. Hence, expression of N-Cad in epithelial cells, which normally do not express it, creates a milieu at the areas of cell-cell contact that is nonconducive for the assembly of larger GJ plaques. Moreover, the findings that the assembly of Cx43 into GJs appeared to be similarly affected in the mouse mammary epithelial cell line, NuMuG, which is widely used for studying EMT (Maeda *et al.*, 2005), suggests that the differential effect of E-Cad and N-Cad in regulating GJ assembly and disassembly may be a general feature of tumor epithelial cells that express both cadherins.

What might be the physiological significance of these findings? E-Cad and N-Cad have been shown to play opposite role in controlling cell migration, motility, and invasion of tumor cells *in vitro* and *in vivo* (Cavallaro and Christofori, 2004; Thiery *et al.*, 2009). Also, a switch in N-Cad expression with or without concomitant loss of E-Cad expression—commonly referred to as cadherin switching—is often observed in cells during EMT and during the progression of carcinomas from an indolent state to a more invasive state (Wheelock *et al.*, 2008). N-Cad has been found to be at the invasive front of several tumors (Cavallaro and Christofori, 2004) and the expression of Cx43 in some tumor cell lines has also been associated with the acquisition of invasive potential (Olk *et al.*, 2009). Recent studies showed that knock down of Cx43 disrupted cell-cell adhesion, reduced cell polarity and focal adhesion plaques, but increased speed of migration and cell protrusive activity in cells derived from epicardium and in neural crest cells that express N-

Cad (Xu *et al.*, 2006; Rhee *et al.*, 2009). Disruption of several junctional complexes is a hallmark of tumor progression and invasion as well as of EMT(Mosesson *et al.*, 2008; Thiery *et al.*, 2009). Tumor cells have now been shown to migrate and invade both as single cells and collectively (Friedl and Gilmour, 2009). Moreover, endocytosis has emerged as an important process that orchestrates cell motility and migration by regulating the spatial distribution of signaling molecules, such as cell surface receptors and their downstream effectors (Lanzetti and Di Fiore, 2008; Sorkin and von Zastrow, 2009). In the light of these studies, it is tempting to speculate that bidirectional signaling between Cxs and cadherins in normal and tumor cells is fine-tuned to control the assembly of GJs as well as other junctional complexes to modulate the polarized and differentiated state and to modulate cell motility and invasion under normal and pathological states.

ACKNOWLEDGMENTS

We thank Linda Kelsey for her expert technical help. We thank Tom Dao for help with live cell imaging. We thank Drs. S. Caplan and Naava Naslavsky for helpful suggestions and discussion throughout the course of this study. This research was supported by National Institutes of Health Grant CA113903, Department of Defense Prostate Cancer Research Program Grant 081198, and Nebraska State Grant LB506 (to P.P.M.) and RO-1DE12308 (to K.R.J.). We gratefully acknowledge support from the Nebraska Center for Cellular Signaling and Cancer Graduate Research Training Program of Eppley Institute in the form of fellowships (to S.C. and K.E.J., respectively).

REFERENCES

- Adams, C., Nelson, J. W., and Smith, S. J. (1996). Quantitative analysis of cadherin-catenin-actin reorganization during development of cell-cell adhesion. *J. Cell Biol.* 135, 1899–1911.
- Baker, S. M., Kim, N., Gundersen, G. G., Segretain, D., and Falk, M. M. (2008). Acute internalization of gap junctions in vascular endothelial cells in response to inflammatory mediator-induced G-protein coupled receptor activation. *FEBS Letters* 582, 4039–4046.
- Bavamian, S., Klee, P., Allagnat, F., Haefliger J.-A., and Meda, P. (2009). Connexins and Secretion. In: *Connexins: A Guide*, ed. A. Harris and D. Locke Springer, 511–528.
- Bryant, D. M., and Mostov, K. E. (2008). From cells to organs: building polarized tissue. *Nat. Rev. Mol. Cell Biol.* 9, 887–901.
- Caramelo, J. J., and Parodi, A. J. (2008). Getting in and out from calnexin/calreticulin cycles. *J. Biol. Chem.* 283, 10221–10225.
- Cavallaro, U., and Christofori, G. (2004). Cell adhesion and signalling by cadherins and Ig-CAMs in cancer. *Nat. Rev. Cancer* 4, 118–132.
- Chakraborty, S., Mitra, S., Falk, M. M., Caplan, S., Wheelock, M. J., Johnson, K. R., and Mehta, P. P. (2010). E-cadherin differentially regulates the assembly of connexin43 and connexin32 into gap junctions in human squamous carcinoma cells. *J. Biol. Chem.* 285, 10761–10776.
- Chardin, P., and McCormick, F. (1999). Brefeldin A: the advantage of being uncompetitive. *Cell* 97, 153–155.
- Cotrina, M. L., Lin, J. H., and Nedergaard, M. (2009). Adhesive properties of connexin hemichannels. *Glia* 56, 1791–1798.
- Crespin, S., Defamie, N., Cronier, L., and Mesnil, M. (2009). Connexins and carcinogenesis. In: *Connexinss: A Guide*, ed. A. Harris and D. Locke 529–542.
- Falk, M. M., Baker, S. M., Gumpert, A., Segretain, D., and Buckheit, R. W. (2009). Gap junction turnover is achieved by the internalization of small endocytic double-membrane vesicles. *Mol. Biol. Cell* 20, 3342–3352.
- Friedl, P., and Gilmour, D. (2009). Collective cell migration in morphogenesis, regeneration and cancer. *Nat. Rev. Mol. Cell Biol.* 10, 445–457.
- Fujimoto, K., Nagafuchi, A., Tsukita, S., Kuraoka, A., Ohkuma, A., and Shibata, Y. (1997). Dynamics of connexins, E-cadherin and a- catenin on cell membranes during gap junction formation. *J. Cell Sci.* 110, 311–322.
- Goodenough, D. A., and Paul, D. L. (2009). Gap junctions. *Cold Spring Harb. Perspect. Biol.* 1, a002576
- Govindarajan, R., Song, X.-H., Guo, R.-J., Wheelock, M. J., Johnson, K. R., and Mehta, P. P. (2002). Impaired trafficking of connexins in androgen-independent human prostate cancer cell lines and its mitigation by a-catenin. *J. Biol. Chem.* 277, 50087–50097.

Gumbiner, B. M. (2005). Regulation of cadherin-mediated adhesion and morphogenesis. *Nat. Rev. Mol. Cell Biol.* 6, 622–634.

Hazan, R. B., Phillips, G. R., Qiao, R. F., and Norton, L. (2000). Exogenous expression of N-cadherin in breast cancer cells induces cell migration, invasion, and metastasis. *J. Cell Biol.* 148, 779–790.

Hernandez-Blazquez, F., Joazeiro, P., Omori, Y., and Yamasaki, H. (2001). Control of intracellular movement of connexins by E-cadherin in murine skin papilloma cells. *Exp. Cell Res.* 270, 235–247.

Heuser, J. E., and Anderson, R. G. (1989). Hypertonic media inhibit receptor-mediated endocytosis by blocking clathrin-coated pit formation. *J. Cell Biol.* 108, 389–400.

Holm, I., Mikhailov, A., Jilson, T., and Rose, B. (1999). Dynamics of gap junctions observed in living cells with connexin43-GFP chimeric protein. *Euro J. Cell Biol.* 78, 856–866.

Hulit, J., *et al.* (2007). N-cadherin signaling potentiates mammary tumor metastasis via enhanced extracellular signal-regulated kinase activation. *Cancer Res.* 67, 3106–3116.

Jongen, W., Fitzgerald, D., Asamoto, M., Piccoli, C., Slaga, T., Gros, D., Takeichi, M., and Yamasaki, H. (1991). Regulation of connexin 43-mediated gap junctional intercellular communication by Ca^{2+} in mouse epidermal cells is controlled by E-cadherin. *J. Cell Biol.* 114, 545–555.

Jordan, K., Solan, J. L., Dominguez, M., Sia, M. A., Hand, A., Lampe, P. D., and Laird, D. W. (1999). Trafficking, assembly, and function of a connexin43-green fluorescent protein chimera in live mammalian cells. *Mol. Biol. Cell* 10, 2033–2050.

Jordan, K., Chodock, R., Hand, A., and Laird, D. W. (2001). The origin of annular junctions: a mechanism of gap junction internalization. *J. Cell Sci.* 114, 763–773.

Kim, J.-B., Islam, S., Kim, Y. J., Prudoff, R. S., Sass, K. M., Wheelock, M. J., and Johnson, K. R. (2000a). N-cadherin extracellular repeat 4 mediates epithelial to mesenchymal transition and increased motility. *J. Cell Biol.* 151, 1193–1205.

Kim, S. H., Li, Z., and Sacks, D. B. (2000b). E-cadherin-mediated cell-cell attachment activates Cdc42. *J. Biol. Chem.* 275, 36999–37005.

King, T. J., and Lampe, P. D. (2004). The gap junction protein connexin32 is a mouse lung tumor suppressor. *Cancer Res.* 64, 7191–7196.

Klausner, R. D., Donaldson, J. G., and Lippincott-Schwartz, J. (1992). Brefeldin A: Insights into the control of membrane traffic and organelle structure. *J. Cell Biol.* 116, 1071–1080.

Kojima, T., Murata, M., Go, M., Spray, D. C., and Sawada, N. (2007). Connexins induce and maintain tight junctions in epithelial cells. *J. Membr. Biol.* 217, 13–19.

Laird, D. W. (2006). Life cycle of connexins in health and disease. *Biochem. J.* 394, 527–543.

Laird, D. W. (2010). The gap junction proteome and its relationship to disease. *Trends Cell Biol.* 20, 92–101.

Langlois, S., Cowan, K. N., Shao, Q., Cowan, B. J., and Laird, D. W. (2008). Caveolin-1 and -2 interact with connexin43 and regulate gap junctional intercellular communication in keratinocytes. *Mol. Biol. Cell* 19, 912–928.

Lanzetti, L., and Di Fiore, P. (2008). Endocytosis and cancer: an “insider” network with dangerous liaisons. *Traffic* 9, 2011–2021.

Li, J., Levin, M. D., Xiong, Y., Petrenko, N., Patel, V. V., and Radice, G. L. (2008). N-cadherin haploinsufficiency affects cardiac gap junctions and arrhythmic susceptibility. *J. Mol. Cell Cardiol.* 44, 597–606.

Li, J., Patel, V. V., Kostetskii, I., Xiong, Y., Chu, A. F., Jacobson, J. T., Yu, C., Morley, G. E., Molkentin, J. D., and Radice, G. L. (2005). Cardiac-specific loss of N-cadherin leads to alteration in connexins with conduction slowing and arrhythmogenesis. *Circ. Res.* 97, 474–481.

Lin, J. H., *et al.* (2002). Connexin 43 enhances the adhesivity and mediates the invasion of malignant glioma cells. *J. Neurosci.* 22, 4302–4311.

Lingwood, D., and Simons, K. (2010). Lipid rafts as a membrane-organizing principle. *Science* 327, 46–50.

Locke, D., Liu, J., and Harris, A. L. (2005). Lipid rafts prepared by different methods contain different connexin channels, but gap junctions are not lipid rafts. *Biochemistry* 44, 13027–13042.

Maeda, M., Johnson, K. R., and Wheelock, M. J. (2005). Cadherin switching: essential for behavioral but not morphological changes during an epithelium-to-mesenchyme transition. *J. Cell Sci.* 118, 873–887.

Maeda, M., Shintani, Y., Wheelock, M. J., and Johnson, K. R. (2006). Src activation is not necessary for transforming growth factor (TGF)- β -mediated epithelial to mesenchymal transitions (EMT) in mammary epithelial cells: PP1 directly inhibits TGF- β receptors I and II. *J. Biol. Chem.* 281, 59–68.

Marra, P., Salvatore, L., Mironov, A., Jr., Di Campli, A., Di Tullio, G., Trucco, A., Beznousenko, G., Mironov, A., and De Matteis, M. A. (2007). The biogenesis of the Golgi ribbon: the roles of membrane input from the ER and of GM130. *Mol. Biol. Cell* 18, 1595–1608.

McLachlan, E., Shao, Q., Wang, H. L., Langlois, S., and Laird, D. W. (2006). Connexins act as tumor suppressors in three dimensional mammary cell organoids by regulating differentiation and angiogenesis. *Cancer Res.* 66, 9886–9894.

Mehta, P. P., Perez-Stable, C., Nadji, M., Mian, M., Asotra, K., and Roos, B. (1999). Suppression of human prostate cancer cell growth by forced expression of connexin genes. *Dev. Genetics* 24, 91–110.

Mehta, P. P., Yamamoto, M., and Rose, B. (1992). Transcription of the gene for the gap junctional protein connexin43 and expression of functional cell-to-cell channels are regulated by cAMP. *Mol. Biol. Cell* 3, 839–850.

Mehta, P., Bertram, J., and Loewenstein, W. (1986). Growth inhibition of transformed cells correlates with their junctional communication with normal cells. *Cell* 44, 187–196.

Meyer, R., Laird, D., Revel, J.-P., and Johnson, R. (1992). Inhibition of gap junction and adherens junction assembly by connexin and A-CAM antibodies. *J. Cell Biol.* 119, 179–189.

Mitra, S., Annamali, L., Chakraborty, S., Johnson, K., and Mehta, P. P. (2006). Androgen-regulated formation and degradation of gap junctions in androgen-responsive human prostate cancer cells. *Mol. Biol. Cell* 17, 5400–5417.

Mosesson, Y., Mills, G. B., and Yarden, Y. (2008). Derailed endocytosis: an emerging feature of cancer. *Nat. Rev. Cancer* 8, 835–850.

Musil, L. S. (2009). Biogenesis and degradation of gap junctions. In: *Connexins: A Guide*, ed. A. Harris and D. Locke Springer, 225–240.

Musil, L., Cunningham, B. A., Edelman, G., and Goodenough, D. (1990). Differential phosphorylation of the gap junction protein connexin43 in junctional communication-competent and -deficient cell lines. *J. Cell Biol.* 111, 2077–2088.

Nelson, W. J. (2008). Regulation of cell-to-cell adhesion by the cadherin- α -catenin complex. *Biochem. Soc. Trans.* 36, 149–155.

Nieman, M. T., Kim, J.-B., Johnson, K. R., and Wheelock, M. J. (1999). Mechanism of extracellular domain-deleted dominant negative cadherins. *J. Cell Sci.* 112, 1621–1632.

Olk, S., Zoidl, G., and Dermietzel, R. (2009). Connexins, cell motility, and the cytoskeleton. *Cell Motil. Cytoskeleton* 66, 1–17.

Orlandi, P. A., and Fishman, P. H. (1998). Filipin-dependent inhibition of cholera toxin: evidence for toxin internalization and activation through caveolae-like domains. *J. Cell Biol.* 141, 905–915.

Pece, S., Chiariello, M., Murga, C., and Gutkind, J. S. (1999). Activation of the protein kinase Akt/PKB by the formation of E-cadherin-mediated cell-cell junctions. *J. Biol. Chem.* 274, 19347–19351.

Pece, S., and Gutkind, J. S. (2000). Signaling from E-cadherins to the MAPK pathway by the recruitment and activation of epidermal growth factor receptors upon cell-cell contact formation. *J. Biol. Chem.* 275, 41227–41233.

Perrais, M., Chen, X., Perez-Moreno, M., and Gumbiner, B. M. (2007). E-cadherin homophilic ligation inhibits cell growth and epidermal growth factor receptor signaling independently of other cell interactions. *Mol. Biol. Cell* 18, 2013–2025.

Piehl, M., Lehmann, C., Gumpert, A., Denizot, J. P., Segretain, D., and Falk, M. M. (2007). Internalization of large double-membrane intercellular vesicles by a clathrin-dependent endocytic process. *Mol. Biol. Cell* 18, 337–347.

Rhee, D. Y., Zhao, X. Q., Francis, R. J. B., Huang, G. Y., Mably, J. D., and Lo, C. W. (2009). Connexin 43 regulates epicardial cell polarity and migration in coronary vascular development. *Development* 136, 3185–3193.

Rohrer, J., Schweizer, A., Russell, D., and Kornfeld, S. (1996). The targeting of Lamp1 to lysosomes is dependent on the spacing of its cytoplasmic tail tyrosine sorting motif relative to the membrane. *J. Cell Biol.* 132, 565–576.

Saez, J. C., Berthoud, V. M., Branes, M. C., Artinez, A. D., Bey, E., and Beyer, E. C. (2003). Plasma membrane channels formed by connexins: their regulation and functions. *Physiol. Rev.* 83, 1359–1400.

Segretain, D., and Falk, M. M. (2004). Regulation of connexin biosynthesis, assembly, gap junction formation, and removal. *Biochim. Biophys. Acta* 1662, 3–21.

Sepniak, E., Radice, G. L., and Vasioukhin, V. (2009). Adhesive and signaling functions of cadherins and catenins in vertebrate development. *Cold Spring Harb. Perspect. Biol.* 1, 1–13.

Shintani, Y., Fukumoto, Y., Chaika, N., Svoboda, R., Wheelock, M. J., and Johnson, K. R. (2008). Collagen I-mediated up-regulation of N-cadherin requires cooperative signals from integrins and discoidin domain receptor 1. *J. Cell Biol.* **180**, 1277–1289.

Skretting, G., Torgersen, M. L., van Deurs, B., and Sandvig, K. (1999). Endocytic mechanisms responsible for uptake of GPI-linked diphtheria toxin receptor. *J. Cell Sci.* **112**, 3899–3909.

Sorkin, A., and von Zastrow, M. (2009). Endocytosis and signalling: intertwining molecular networks. *Nat. Rev. Mol. Cell Biol.* **10**, 609–622.

Subtil, A., Hemar, A., and Dautry-Varsat, A. (1994). Rapid endocytosis of interleukin 2 receptors when clathrin-coated pit endocytosis is inhibited. *J. Cell Sci.* **107**, 3461–3468.

Suyama, K., Shapiro, I., Guttman, M., and Hazan, R. B. (2002). A signaling pathway leading to metastasis is controlled by N-cadherin and the FGF receptor. *Cancer Cell* **2**, 301–314.

Tartakoff, A. (1983). Perturbation of vesicular traffic with the carboxylic ionophore monensin. *Cell* **32**, 1026–1028.

Taulet, N., Comunale, F., Favard, C., Charrasse, S., Bodin, S. p., and Gauthier-Rouvière, C. +. (2009). N-cadherin/p120 catenin association at cell-cell contacts occurs in cholesterol-rich membrane domains and is required for rhoA Activation and myogenesis. *J. Biol. Chem.* **284**, 23137–23145.

Tepass, U., Trunong, K., Godt, D., Ikura, M., and Peifer, M. (2000). Cadherins in embryonic and neural morphogenesis. *Nature Rev. Cell Mol. Biol.* **1**, 91–100.

Thiery, J. P., Acloque, H., Huang, R.Y.J., and Nieto, M. A. (2009). Epithelial-mesenchymal transitions in development and disease. *Cell* **139**, 871–890.

VanSlyke, J. K., and Musil, L. S. (2000). Analysis of connexin intracellular transport and assembly. *Methods* **20**, 156–164.

Wang, L. H., Rothberg, K. G., and Anderson, R. G. (1993). Mis-assembly of clathrin lattices on endosomes reveals a regulatory switch for coated pit formation. *J. Cell Biol.* **123**, 1107–1117.

Wang, Y., and Rose, B. (1997). An inhibition of gap-junctional communication by cadherins. *J. Cell Sci.* **110**, 301–309.

Wei, C. J., Francis, R., Xu, X., and Lo, C. W. (2005). Connexin43 associated with an N-cadherin-containing multiprotein complex is required for gap junction formation in NIH3T3 cells. *J. Biol. Chem.* **280**, 19925–19936.

Wei, C. J., Xu, X., and Lo, C. W. (2004). Connexins and cell signaling in development and disease. *Ann. Rev. Cell Dev. Biol.* **20**, 811–838.

Wheelock, M. J., Buck, C., Bechtol, K., and Damsky, C. (1987). Soluble 80 Kd fragment of cell-CAM 120/180 disrupts cell-cell adhesion. *J. Cell. Biochem.* **34**, 187–202.

Wheelock, M. J., and Johnson, K. R. (2003). Cadherins as modulators of cellular phenotype. *Annu. Rev. Cell Dev. Biol.* **19**, 207–235.

Wheelock, M. J., Shintani, Y., Maeda, M., Fukumoto, Y., and Johnson, K. R. (2008). Cadherin switching. *J. Cell Sci.* **121**, 727–735.

Xu, X., Francis, R., Wei, C. J., Linask, K. L., and Lo, C. W. (2006). Connexin 43-mediated modulation of polarized cell movement and the directional migration of cardiac neural crest cells. *Development* **133**, 3629–3639.

Yonemura, S., Itoh, M., Nagafuchi, A., and Tsukita, S. (1995). Cell-to-cell adherens junction formation and actin filament organization: similarities and differences between non-polarized fibroblasts and polarized epithelial cells. *J. Cell Sci.* **108**, 127–142.

Supplementary Figure Legends

Figure S-1. Serial propagation of RL-CL9 cells and the expression of Cx43, E-cadherin and N-cadherin.

A. RL-CL9 cells were passaged serially for 6-8 months and imaged at passage 3 (early), 14 (middle) and 28 (late). Note the typical epithelial appearance of early passage cells and appearance of cells that have begun to lose this morphology, marked by red arrows, with serial passage. **B.** RL-CL9 cells at passage 22 were immunostained for N-Cad (red) and Cx43 (green). Note intracellular localization of Cx43 only in cells that express N-Cad (delineated by dotted line) and junctional localization in cells that lack N-Cad. **C.** RL-CL9 cells at passage 14 were immunostained for Cx43 (red) and E-Cad (green). Note the appearance of cells in which Cx43 is intracellular despite the expression of E-Cad (arrows).

Figure S-2. Localization and expression of E-cadherin, N-cadherin, vimentin and actin in RL-CL9 cells at early and late passages. RL-CL9 cells were passaged serially and immunostained at passage 7 (Early) and 25 (Late) for E-Cad and N-Cad (**A**), for vimentin and actin (**B**). Note the emergence of cells that express N-Cad (red) heterogeneously. Note also that some E-Cad shows increased localization at intracellular sites in late passage cells. Note also the increases in the expression level and the altered patterns of localization of vimentin and actin in early versus late passage cells. **C.** Western blot analysis of expression of E-Cad, N-Cad, vimentin and actin in early and late passage cells. Two lanes represent cell lysates independently obtained from early and late passage RL-CL9 cells. Note that the expression level of E-Cad and actin remains unchanged whereas that of N-Cad and vimentin increases.

Figure S-3. Directional migration of RL-NΔE and RL-EΔN cells. RL-EΔN and RL-NΔE cells were seeded in LabTek two well chamber slides and allowed to grow to confluence. Confluent monolayers of cells were wounded and cells imaged as described in “Materials and Methods”. Both cell types were imaged in parallel (see Materials and Methods). Shown are the live cell images of the corresponding time points that were converted to TIFF files. The numbers refer to time in hours and represent the corresponding captured frames. Note that the scratches in the RL-NΔE cultures were filled earlier compared to RL-EΔN cultures. The wounds were filled within 14 ± 2 h in RL-NΔE cells whereas 22 ± 2 h were required to fill the wounds in RL-EΔN cells

(n=3). The meant (\pm SE) rate of migration in RL-N Δ E cells was significantly faster than that of RL-E Δ N cells (P=0.04). A two tailed Student's *t* test was used to calculate P value assuming unequal variance.

Figure S-4. Expression level and localization of myc-tagged E-cadherin and N-cadherin in RL-E Δ N and RL-N Δ E cells upon retroviral infection. Myc tagged N-Cad and E-Cad were introduced, respectively, into RL-E Δ N and RL-N Δ E cells as described in Materials and Methods. Pooled polyclonal cultures were immunostained with antibody against Myc for detecting E-Cad in RL-N Δ E cells (**A**) and N-Cad in RL-E Δ N cells (**B**). Note that myc tagged E-Cad and N-Cad are expressed robustly at the area of cell-cell contact. **C.D.** Western blot analysis of E-Cad and N-Cad expression in RL-N Δ E and RL-E Δ N cells after retroviral infection. Note robust expression of E-Cad in RL-N Δ E cells and N-Cad in RL-E Δ N cells upon retroviral transduction of myc-tagged cadherins as detected by anti-myc antibody.

Figure S-5. Cx43 co-localizes with Rab7 and Lamp-1 but not with Rab5 in RL-N Δ E cells. RL-N Δ E cells were seeded on glass cover slips at a density of 3×10^5 cells in six well clusters and transfected with Rab5-GFP (Q-L) and Rab7-GFP (Q-L) after 16 h. Cells were fixed after 36 h and immunostained for Cx43 (red, rows 1 and 2) and for Cx43 and Lamp-1 (Bottom row). Note that Cx43 co-localizes partially with Rab7 and extensively with Lamp-1 in as shown in the enlarged images of the marked boxes on the right.

Figure S-6. Expression of E-cadherin and N-cadherin and the junctional and non-junctional fate of Cx43 in NMuMG rat mammary cells. Localization of E-Cad, N-Cad and Cx43 was examined in NMuMG cells that express both E-Cad and N-Cad (top row, NMuMG), in NMuMG derived subclone, Clone E9, that expresses nearly equal levels of both E-Cad and N-Cad (middle row), and in NMuMG derived subclone, Clone E11, that expresses high level of N-Cad and no detectable level of E-Cad (bottom row). Note that in parental NMuMG cells, cells that express high levels of E-Cad assemble GJs. Note also that in Clone E9 cells, both junctional and non-junctional localization of Cx43 is observed whereas in Clone E11, Cx43 remains intracellular and is not assembled into GJs.

Table S-1. Expression of E-cadherin and N-cadherin in isogenic clones derived from early and late passage RL-CL9 cells and the junctional and non-junctional localization of Cx43.

	RL-EARLY	RL-LATE
Number of clones	92	63
E-Cadherin +ve (% +ve) ^a	30/43 (70)	5/30 (17)
N-Cadherin +ve (% +ve) ^a	14/49 (30)	20/33 (79)
Junctional(Intercellular) Cx43 (% +ve) ^a	56/92 (61)	16/63 (25)
Non-junctional (Intracellular) Cx43 (% +ve) ^a	0/92 (0)	32/63 (51)
Junctional and Non-junctional Cx43 (% +ve) ^a	36/92 (32)	15/63 (24)

One hundred RL-CL9 cells at passage 4 and 30 were seeded in replicate 10 cm dishes in 10 ml complete medium and allowed to grow into colonies for 3-4 weeks. Individual clones were picked using glass cylinders, expanded and frozen. Each clone was examined for the expression of E-Cad and N-Cad and for the junctional versus non-junctional localization of Cx43 by immunocytochemical analysis as described in Materials and Methods. **a** = Number of positive clones versus total number of clones analyzed. In parenthesis = % of positive clones.

Table S-2 Cell-cell adhesion remains intact in RL-EΔN and RL-NΔE cells.

Cell Line	Exp #	Mean Area (SE)	# Aggregates
RL-EΔN	1	1775 ± 322	40
	2	1910 ± 378	32
RL-NΔE	1	1940 ± 415	39
	2	2165 ± 445	33

Five thousand cells, suspended in a 20 μ l of complete medium and placed on the lids of petri dishes, were allowed to aggregate as described in Materials and Methods. The size of aggregates from four random snapshots obtained from two independent experiments was measured and the average aggregate size was calculated and plotted as described (see Methods). As assessed visually, aggregates formed of RL-EΔN cells appeared to be more compact and regular compared to RL-NΔE cells. The differences in the mean sizes of the aggregates among RL-EΔN and RL-NΔE cells were not statistically significant ($P \geq 0.8$).

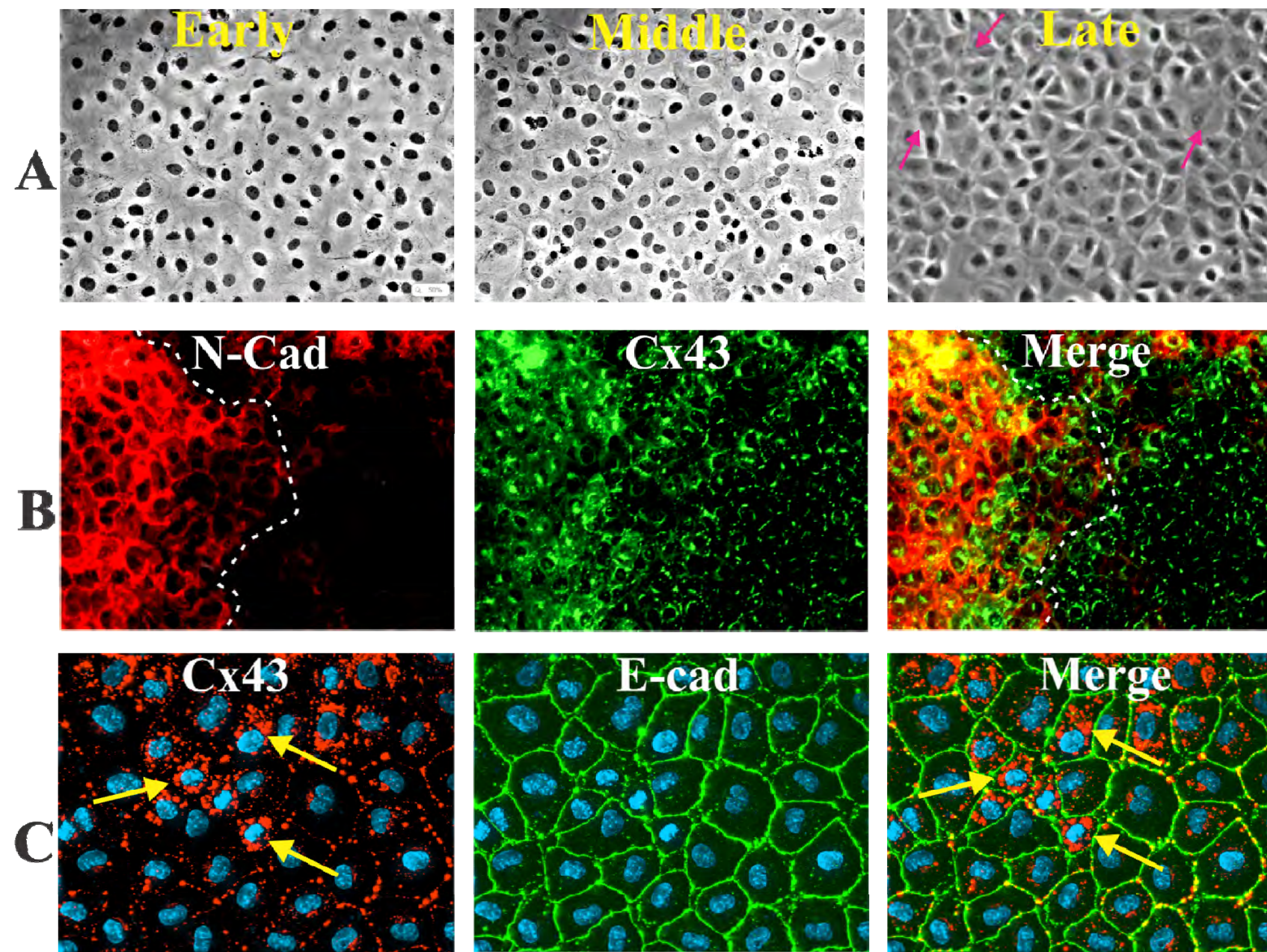


Figure S-1

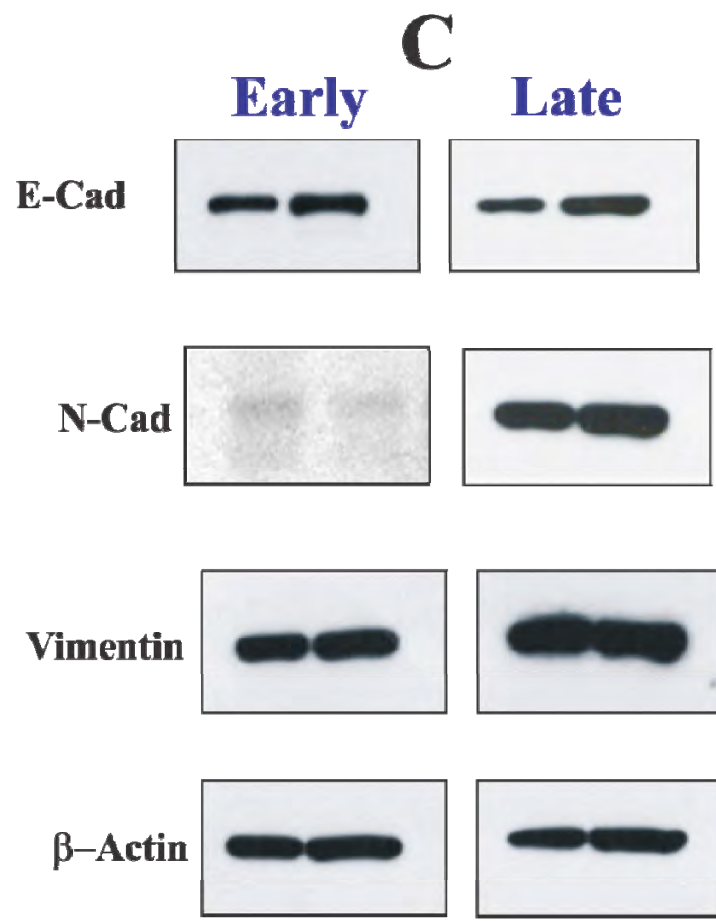
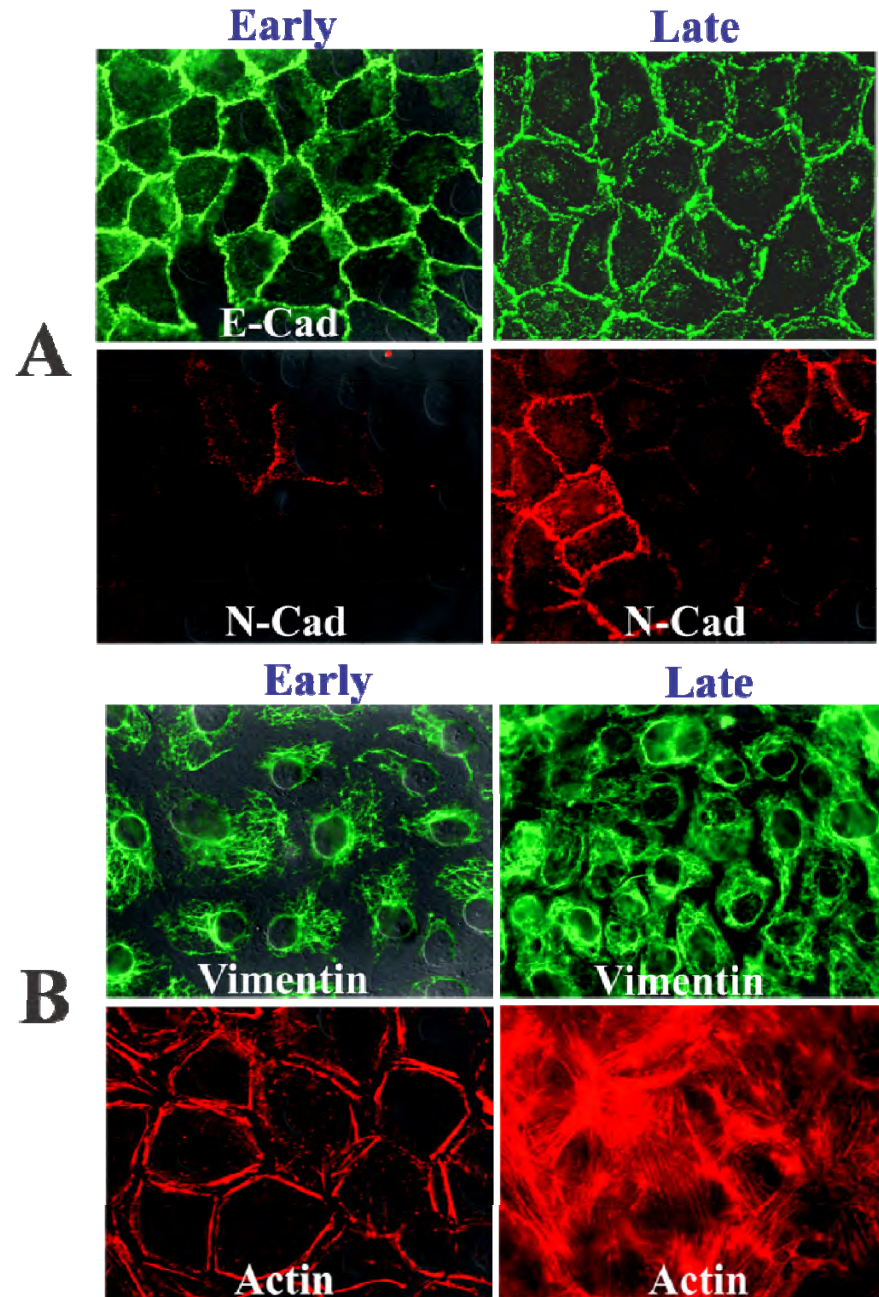


Figure S-2

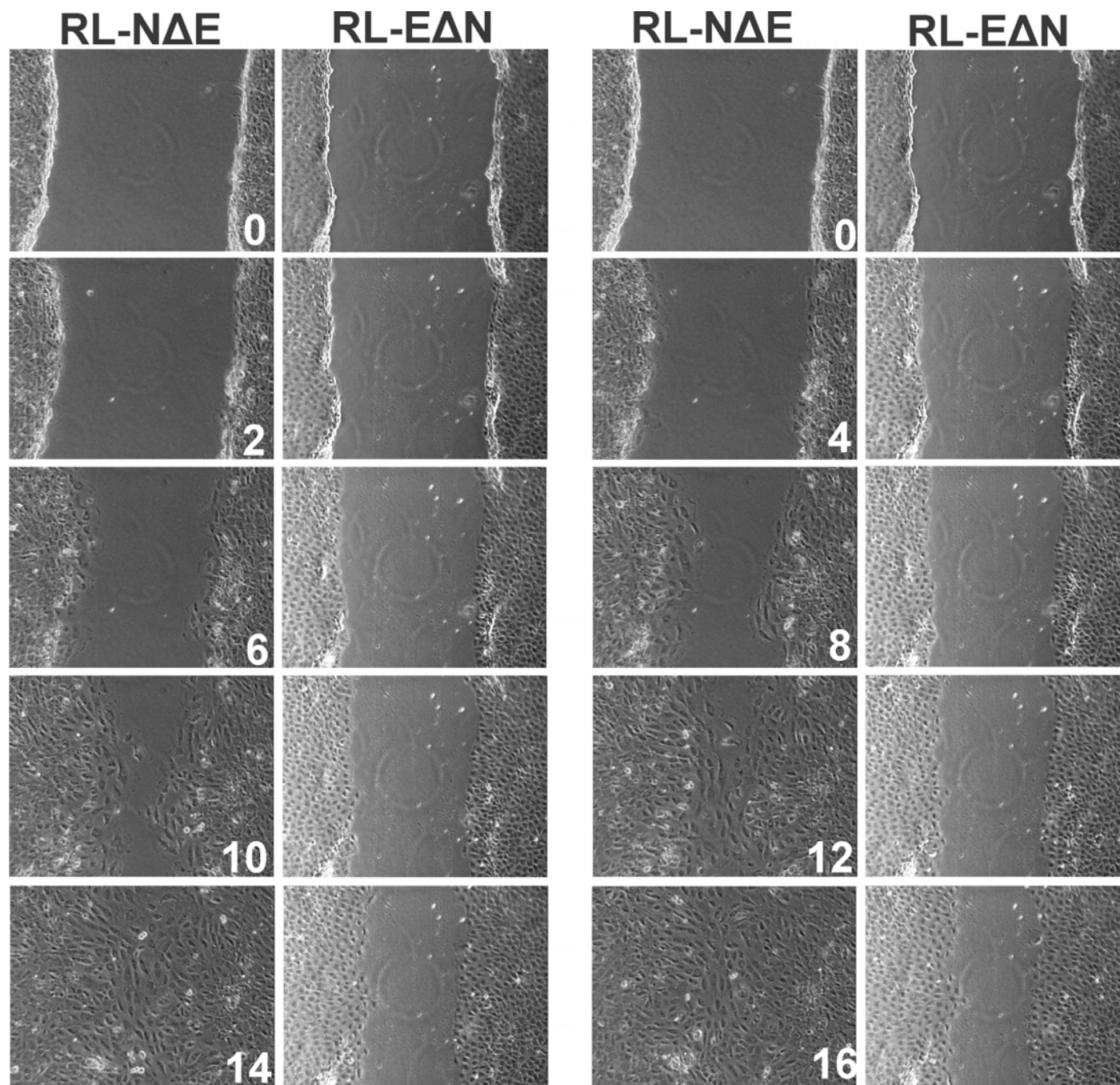


Figure S-3

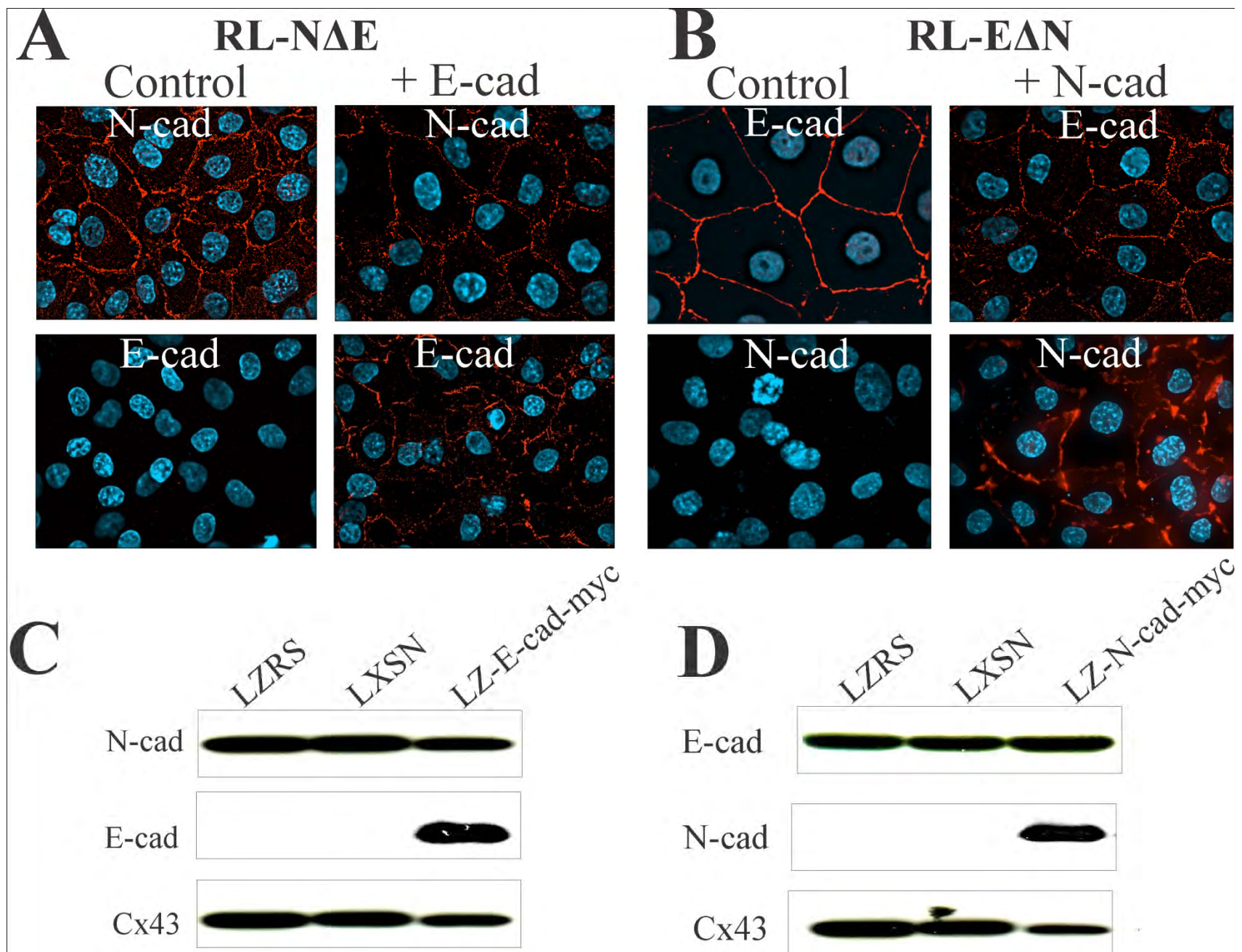


Figure S-4

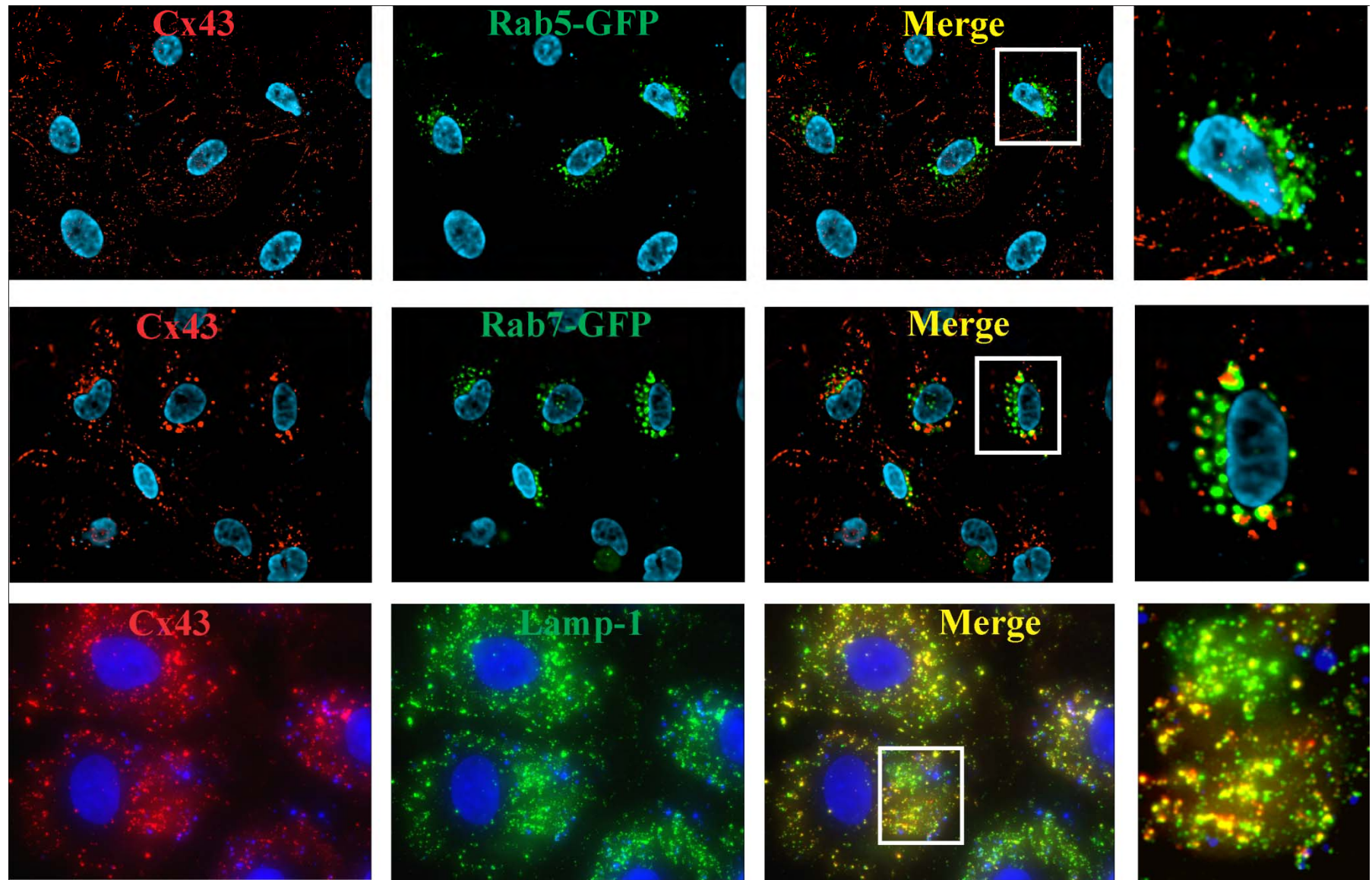


Figure S-5

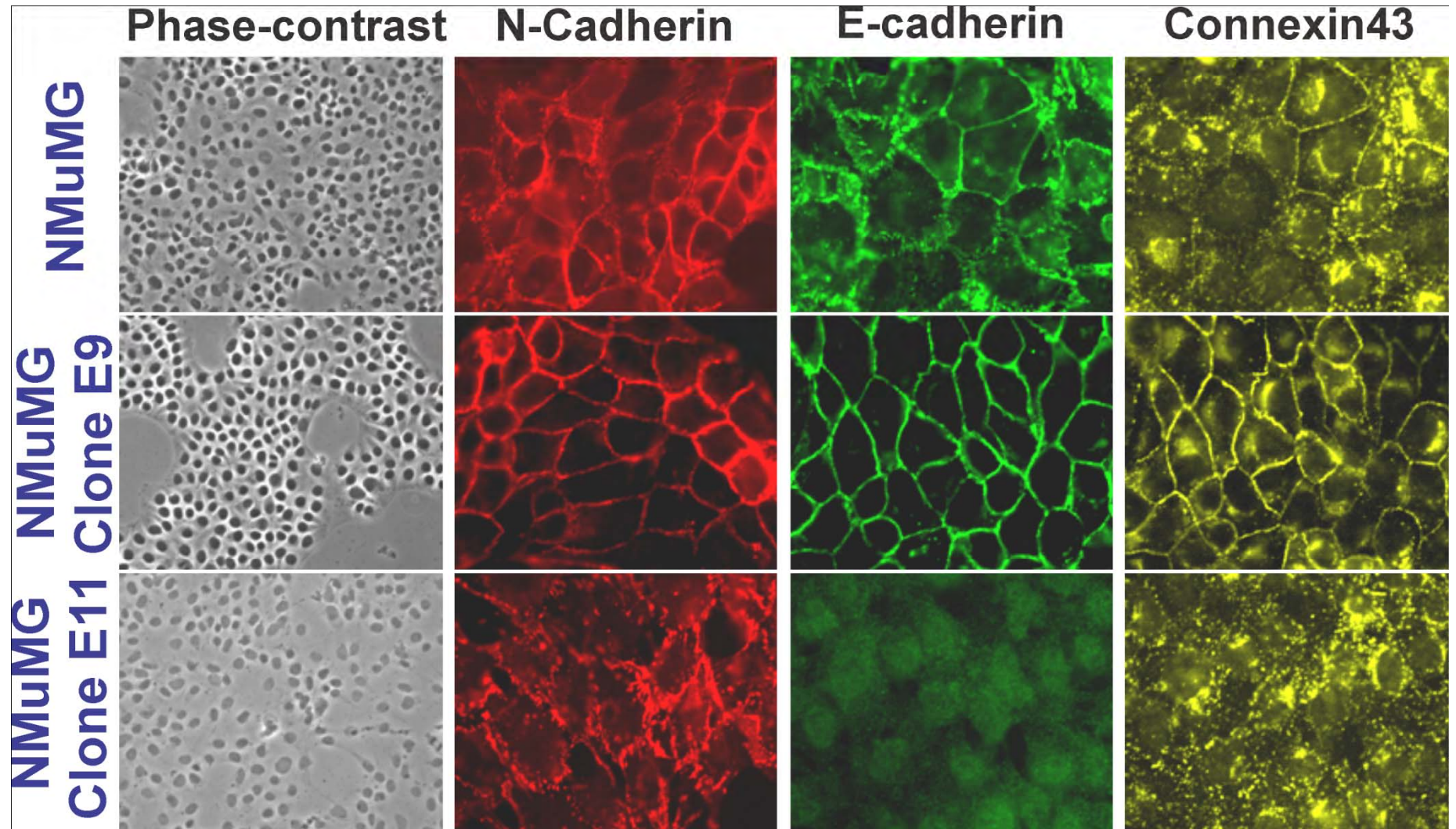


Figure S-6

Retinoids Regulate the Formation and Degradation of Gap Junctions in Androgen-Responsive Human Prostate Cancer Cells

Linda Kelsey, Parul Katoch, Kristen E. Johnson, Surinder K. Batra, Parmender P. Mehta*

Department of Biochemistry and Molecular Biology, University of Nebraska Medical Center, Omaha, Nebraska, United States of America

Abstract

The retinoids, the natural or synthetic derivatives of Vitamin A (retinol), are essential for the normal development of prostate and have been shown to modulate prostate cancer progression *in vivo* as well as to modulate growth of several prostate cancer cell lines. 9-cis-retinoic acid and all-trans-retinoic acid are the two most important metabolites of retinol. Gap junctions, formed of proteins called connexins, are ensembles of intercellular channels that permit the exchange of small growth regulatory molecules between adjoining cells. Gap junctional communication is instrumental in the control of cell growth. We examined the effect of 9-cis-retinoic acid and all-trans retinoic acid on the formation and degradation of gap junctions as well as on junctional communication in an androgen-responsive prostate cancer cell line, LNCaP, which expressed retrovirally introduced connexin32, a connexin expressed by the luminal cells and well-differentiated cells of prostate tumors. Our results showed that 9-cis-retinoic acid and all-trans retinoic acid enhanced the assembly of connexin32 into gap junctions. Our results further showed that 9-cis-retinoic acid and all-trans-retinoic acid prevented androgen-regulated degradation of gap junctions, post-translationally, independent of androgen receptor mediated signaling. Finally, our findings showed that formation of gap junctions sensitized connexin32-expressing LNCaP cells to the growth modifying effects of 9-cis-retinoic acid, all-trans-retinoic acid and androgens. Thus, the effects of retinoids and androgens on growth and the formation and degradation of gap junctions and their function might be related to their ability to modulate prostate growth and cancer.

Citation: Kelsey L, Katoch P, Johnson KE, Batra SK, Mehta PP (2012) Retinoids Regulate the Formation and Degradation of Gap Junctions in Androgen-Responsive Human Prostate Cancer Cells. PLoS ONE 7(4): e32846. doi:10.1371/journal.pone.0032846

Editor: Natasha Kyriyanou, University of Kentucky College of Medicine, United States of America

Received October 19, 2011; **Accepted** January 31, 2012; **Published** April 13, 2012

Copyright: © 2012 Kelsey et al. This is an open-access article distributed under the terms of the Creative Commons Attribution License, which permits unrestricted use, distribution, and reproduction in any medium, provided the original author and source are credited.

Funding: This research was supported by NIH CA113903, DOD PCRP (Department of Defense Prostate Cancer Research Program) 081198, and Nebraska State Grant LB506 (PPM). We gratefully acknowledge support from the Nebraska Center for Cellular Signaling and NCI training fellowship to Kristen Johnson. The funders had no role in study design, data collection and analysis, decision to publish, or preparation of the manuscript.

Competing Interests: The authors have declared that no competing interests exist.

* E-mail: pmehta@unmc.edu

Introduction

Retinoids, the natural or synthetic derivatives of vitamin A, regulate not only embryonic development but also organogenesis in adult tissues [1]. A requirement for vitamin A for proliferation, differentiation has been demonstrated in many studies in which a deficiency of this vitamin resulted in multiple developmental defects [1–3]. All trans-retinoic acid (ATRA) and 9-Cis-Retinoic Acid (9-CRA) are the two most important metabolites of vitamin A (retinol) with diverse physiological functions [1]. Retinoids are members of the nuclear-receptor superfamily of transcription factors and exert their pleiotropic effects by regulating the expression of several target genes [3–5]. There are six retinoid receptors, namely RAR α , β , γ , which bind to ATRA and 9-CRA, and RXR α , β , γ , which bind only to 9-CRA. Retinoid initiated signaling regulates several homeostatic control mechanisms during embryonic development and in adult tissues and one such control mechanism likely to be regulated is the direct cell-cell communication mediated by a special class of cell junctions called gap junctions (GJs) [6–8]. Gap junctions are ensembles of intercellular channels that signal by permitting the direct exchange of small molecules (≤ 1500 Da) between contiguous cells. The constituent proteins of GJs, called connexins (Cx), are coded by 21 genes,

which have been designated according to their molecular mass [9]. Cell-cell channels are bicellular structures formed by the collaborative effort of two cells. To form a GJ cell-cell channel, Cxs first oligomerize as hexamers, called connexons, which dock with the connexons displayed on contiguous cells [10]. Multiple lines of evidence lends credence to the notion that gap junctional communication is an important homeostatic control mechanism for regulating cell growth and differentiation. For example, impaired Cx expression, or loss of function, has been implicated in the pathogenesis of several types of cancers, and mutations in several Cx genes have been detected in genetic disorders characterized by aberrant cellular proliferation and differentiation [8,10–12].

Our previous studies showed that prostate luminal cells expressed Cx32 and its expression coincided with the acquisition of the differentiated state of these cells [13,14]. We showed that progression of prostate cancer (PCA) from an androgen-dependent state to an invasive, androgen-independent state was characterized by the failure of Cx32 to assemble into GJs [14,15]. We have further shown that reintroduction of Cx32 into androgen-responsive human PCA cell line, LNCaP, retards cell growth *in vivo* and *in vitro* [14,16]. Subsequently, we demonstrated that androgens regulated the formation and degradation of GJs by altering the expression level of Cx32, posttranslationally. In the

absence of androgens, a major fraction of Cx32 was degraded by endoplasmic reticulum associated degradation (ERAD) whereas in their presence this fraction was rescued from degradation [17]. The significance of these findings is underscored by the fact that androgens play a major role in the survival and maintenance of the secretory (differentiation-related) function of luminal epithelial cells of normal prostate as well as of tumor cells as androgen ablation induces apoptosis or dedifferentiation of these cells [18,19].

Like androgens, retinoids are also essential for the normal development of the prostate and modulate PCA progression in certain mouse models as well as suppress the growth of androgen-dependent and -independent human PCA cell lines. Squamous metaplasia of the prostate was observed among the offsprings of vitamin A-deficient [20] and RAR γ knock out mice [21]. Moreover, tissue-specific inactivation of RAR α in prostate resulted in multi-focal intraepithelial hyperplasia [22]. Epidemiological studies have shown that decreased vitamin A serum levels increase PCA incidence and progression, and that restoration of retinoid levels might have a role in the reversal of the malignant phenotype [23,24]. Several studies, including ours, have shown that the ability of retinoids to suppress tumor cell growth and induce differentiation is contingent upon their ability to enhance gap junctional communication [25–28]. Because Cx32 is expressed by luminal epithelial cells of normal prostate where it is assembled into GJs and by epithelial cells of prostate tumors in which it is inefficiently assembled into GJs [13–15] and because formation of GJs has been implicated in maintaining the polarized and differentiated state of epithelial cells [29], we reasoned that chemopreventive, growth inhibitory and pro-differentiating effects of 9-CRA and ATRA might result from their ability to control formation and degradation of GJs. Therefore, we investigated whether the formation and degradation of GJs composed of Cx32 were regulated by 9-CRA and ATRA in human PCA cells. Because retinoids have been shown to increase the expression of androgen receptor (AR) in androgen-responsive human PCA cell lines [30], we rationalized that they might modulate androgen-regulated formation and degradation of GJs and affect growth of androgen-responsive PCA cells that express Cx32. By using androgen-responsive LNCaP cells, which express retrovirally introduced Cx32 whose degradation is androgen-regulated [17], we show that 9-CRA and ATRA, like androgens, enhance the expression of Cx32 and its subsequent assembly into GJs. Moreover, we further show here that in this cell culture model, ATRA and 9-CRA prevent androgen-regulated degradation of GJs, independent of AR mediated signaling. Finally, our findings show that expression of Cx32 and formation of GJs sensitizes these cells to growth modifying effects of 9-CRA, ATRA and androgens.

Materials and Methods

Cell Culture

Androgen-responsive LNCaP cells were a gift from Dr. Lin [31]. One of the several clones of LNCaP cells expressing retrovirally transduced rat Cx32, hereafter referred to as LNCaP-32 cells, and one of the several control clones selected in G418 after infection with control retrovirus, hereafter referred to as LNCaP-N cells, were isolated as described [17] and were used in the present study along with the parental LNCaP cells, hereafter referred to as LNCaP-P cells. LNCaP-P cells were grown in RPMI containing 5% fetal bovine serum in an atmosphere of 5% CO₂/95% air and stock cultures were maintained weekly as previously described. LNCaP-N and LNCaP-32 cells were maintained in RPMI containing 5% fetal bovine serum and G418 at 200 µg/ml as describe [17]. During the course of these studies, we used two

separate lots of fetal bovine sera obtained from Sigma and HyClone Laboratories, with nearly similar effect on the growth of LNCaP cells. Steroid-depleted (charcoal-stripped) serum was obtained from HyClone Laboratories (Salt Lake City, UT). We also used phenol red free RPMI for experiments in which charcoal-stripped serum was used [17].

Antibodies and Immunostaining

Hybridoma M12.13 (a gift from Dr. Dan Goodenough, Harvard University) has been described earlier [14,16,17,32,33]. Mouse anti-occludin (clone OC-3F10) was from Zymed laboratories Inc. (South San Francisco, CA). Rabbit anti- α -catenin, rabbit anti- β -catenin, rabbit anti-Cx32, and mouse anti- β -actin (clone C-15) were from Sigma (St. Louis, MO). Mouse anti-E-cadherin, mouse anti- α -catenin, mouse anti- β -catenin antibodies were generously provided by Drs. Johnson and Wheelock (Eppley Institute) and have been described [17,32,33]. A rabbit polyclonal anti-AR receptor antibody was from Santa Cruz Biotech (sc-13062, San Diego, CA). Cells were immunostained after fixing with 2% para-formaldehyde for 15 min as described previously [17,32,33]. Briefly, cells (1.5×10^5), seeded in six well clusters containing glass cover slips and allowed to grow to approximately 50–70% confluence, were immunostained at room temperature with various antibodies at appropriately calibrated dilutions. Secondary antibodies (rabbit or mouse) conjugated with Alexa 488 and Alexa 594 were used as appropriate. Images of immunostained cells were acquired with Leica DMRIE microscope (Leica Microsystems, Wetzler, Germany) equipped with Hamamatsu ORCA-ER CCD camera (Hamamatsu-City, Japan). For co-localization studies, serial z-sections (0.5 µm) were collected and analyzed using image processing software (Velocity; Improvision, Inc; Perkin Elmer).

Stock Solutions

Stock solutions of various reagents were prepared as follows: 9-CRA and ATRA (BIOMOL, Plymouth, PA) were prepared in ethanol at 3 mM each and stored in aliquots at -80°C protected from light. All experiments pertaining to 9-CRA and ATRA were performed in yellow light as described [26,27]. Stock solutions of a synthetic androgen, mibolerone (MB), (BIOMOL), and of a natural androgen, dihydro-testosterone (DHT), were prepared at 1 mM in ethanol and stored at -20°C in small aliquots protected from light. They were appropriately diluted with the medium at the time of treatment.

Androgen Depletion and Other Treatments

Cells were seeded in six well clusters containing glass cover slips (1.5×10^5 cells per well) and in 6-cm (2×10^5 cells per dish) or in 10-cm dishes (3.5×10^5 cells per dish) in 2, 4 and 10 ml complete culture medium, respectively. Cells were treated when approximately 50% confluent, by replenishing with fresh medium containing various reagents at the desired concentration added from stock solutions so that the final concentration of the solvent did not exceed 0.3%. To grow cells under androgen-depleted medium, normal cell culture medium was replaced with androgen-depleted cell culture medium (phenol red-free RPMI containing 5% charcoal-stripped serum). The controls received fresh medium containing normal serum.

Western Blot Analysis and Detergent Solubility of Connexin32

Cell lysis, detergent solubility assay with 1% Triton X-100 (TX-100) and the expression level of Cx32 were analyzed by Western

blot analysis as described [17,32,33]. Briefly, 5×10^5 LNCaP-P, LNCaP-N and LNCaP-32 cells were seeded per 10 cm dish in 10 ml of complete medium and grown to confluence, after which cells were lysed in buffer SSK (10 mM Tris, 1 mM EGTA, 1 mM PMSF, 10 mM NaF, 10 mM NEM, 10 mM Na_2VO_4 , 10 mM iodoacetamide, 0.5% TX-100, pH 7.4) supplemented with the protease inhibitor cocktail (Sigma, St. Louis, MO). Total, detergent-soluble and -insoluble extracts were separated by ultracentrifugation at $100,000 \times g$ for 60 min (35,000 rpm in analytical Beckman ultracentrifuge; Model 17-65 using a SW50.1 rotor). The detergent-insoluble pellets were dissolved in buffer C (70 mM Tris/HCl, pH 6.8, 8 M urea, 10 mM NEM, 10 mM iodoacetamide, 2.5% SDS, and 0.1 M DTT). Following normalization based on cell number, the total, TX-100-soluble and -insoluble fractions were mixed with $4 \times$ SDS-loading buffer to a final concentration of 1 \times and incubated at room temperature for 1 h (for Cx32) before SDS-PAGE analysis.

Communication Assays

Gap junctional communication was assayed by microinjecting the following fluorescent tracers: Lucifer Yellow (MW 443 Da; Lithium salt); Alexa Fluor 488 (MW 570 Da; A-10436), and Alexa Fluor 594 (MW 760 Da; A-10438). Stock solutions of Alexa dyes, obtained as hydrazide sodium salts from Molecular Probes (Carlsbad, CA), were prepared in water at 10 mM. Lucifer yellow was microinjected as 2.5% aqueous stock solution. Eppendorf InjectMan and FemtoJet microinjection systems (models 5271 and 5242, Brinkmann Instrument, Inc. Westbury, NY), mounted on Leica DMIRE2 microscope as described previously, were used to microinject fluorescent tracers. The images of microinjected cells were captured with the aid of CCD camera (Retiga 2000R, FAST 1394) using QCapture (British Columbia, Canada) and stored as TIFF files. Junctional transfer of fluorescent tracer was quantitated by scoring the number of fluorescent cells (excluding the injected one) from the captured TIFF images either at 1 min (Lucifer Yellow), 3 min (Alexa 488) and 15 min (Alexa 594) after microinjection into test cell as described [14,17,32,34].

Colony Formation and Cell Growth Assays

Cell growth was assessed either by colony forming assay or by counting cells as described [14,34]. For colony forming assay, 2×10^3 cells were seeded in 6 cm dishes in triplicate in 3 ml culture medium. After 24 h, one ml medium containing MB, 9-CRA and ATRA was added to the dishes to give the desired final concentration. Cells were grown for 3–4 weeks (with a medium change every 4–5 days containing the appropriate concentration of MB, DHT, 9-CRA and ATRA) when they formed visible colonies. Colonies in dishes were fixed with 3.7% buffered formaldehyde, stained with 0.025% solution of crystal violet in PBS, and photographed. For measuring cell growth, 5×10^4 cells were seeded in 6 cm dishes in replicate and treated with MB, 9-CRA and ATRA either alone or in combination as described above. Cells were allowed to grow for 9–11 days with a medium change at day 5. Cells were trypsinized and counted in a hemocytometer.

Results

Retinoids Enhance Cx32 Expression Level

We used LNCaP-32 cells that express retrovirally transduced rat Cx32 [17] because parental LNCaP-P and LNCaP-N cells are devoid of detectable levels of known Cxs and do not form functional GJs (See Materials and Methods). Earlier studies

showed that in LNCaP-32 cells androgens regulated the formation and degradation of GJs by controlling the expression level of Cx32 posttranslationally, by rescuing its ERAD-mediated degradation [17]. Based on the rationale described above (see introduction) and on our experience with other cell lines [26,27], LNCaP-32 cells were treated with 9-CRA and ATRA for 48 h to examine if they affect Cx32 expression level. We found that 9-CRA and ATRA increased Cx32 expression level in a dose-dependent manner (Figure 1, A). Significant enhancement, however, was observed only at concentration of 1 μM or higher. As assessed by the colony formation assay, concentrations higher than 1 μM were toxic to these cells (data not shown) and hence we chose 1 μM of 9-CRA and ATRA for subsequent studies. Time course studies showed that enhancement with both retinoids occurred as early as 24 h post-treatment and reached a plateau at 72 h (Figure 1, B). The effect of 9-CRA and ATRA on Cx32 expression level was comparable to that observed with a synthetic androgen, mibolerone (MB), and was not observed with RAR-specific ligands, 13-CRA and tetrahydrotetramethyl-naphthalenylpropenylbenzoic acid (TTNPB), or with 4-hydroxy-phenretinamide (4-HPR)(Figure 1 C). We also examined whether 9-CRA and ATRA increased the expression level of other cell junction associated proteins. We found that both 9-CRA and ATRA had no significant affect on the expression level of adherens junction proteins E-cadherin and α - and β -catenins, however, the expression level of tight junction associated protein, occludin, was enhanced to some extent (Figure 1D). Moreover, 9-CRA and ATRA neither induced the expression of endogenous Cx32 in parental LNCaP cells nor altered the expression level of retrovirally transcribed Cx32 mRNA in LNCaP-32 cells as measured by semi-quantitative RT-PCR analysis (data not shown).

Retinoids Enhance Gap Junction Assembly and Junctional Communication

We next examined the effect of 9-CRA and ATRA on the assembly of Cx32 into GJs and on junctional communication. Concomitant with an increase in the expression level of Cx32, 9-CRA and ATRA increased GJ assembly as assessed immunocytochemically (Figure 2 A) and biochemically by Western blot analysis of total and Triton X (TX)-100-insoluble extracts [16,17,35] prepared at various times after treatment (Figure 2 B). Moreover, as shown in Table 1, enhancement of GJ assembly was accompanied by parallel increase in junctional communication as measured by the junctional transfer of three GJ permeable fluorescent tracers, Lucifer Yellow (MW 443), Alexa 488 (MW 570), and Alexa 594 (MW 760). For example, 9-CRA and ATRA increased junctional transfer of Alexa 594 (MW 760) 2–3 folds compared to controls (Table 1). Because E-cadherin has been shown to facilitate the assembly of Cxs into GJs [32,33], and Cx expression has been shown to facilitate the assembly of tight junctions [29], we also examined whether 9-CRA and ATRA increased the expression level of Cx32 and its assembly into GJs indirectly by facilitating the assembly of other cell junctions as assessed by the detergent-insolubility of their constituent and associated proteins. We found that both 9-CRA and ATRA had no significant affect on the expression level of adherens junction protein E-cadherin, however, the assembly of tight junction protein, occludin, but not its associated protein ZO-1, appeared to have been enhanced (Figure 2 B). Taken together, these data suggest that 9-CRA and ATRA, like androgens, enhance the expression level of Cx32, and its subsequent assembly into GJs, without significantly altering the expression of E-cadherin, which has been shown to modulate the assembly of GJs [32,33,36,37]. As

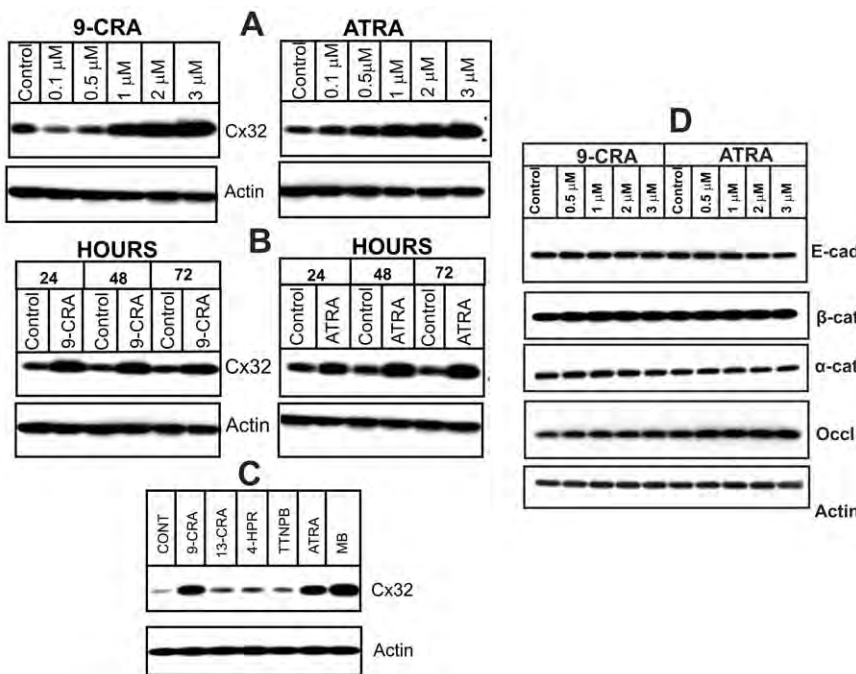


Figure 1. Retinoids increase Cx32 expression level. Cx32-expressing LNCaP-32 cells were treated with the 9-CRA, ATRA, MB and other retinoids as indicated. **A.** Dose-dependent enhancement of Cx32 expression level upon 9-CRA and ATRA treatment for 48 h. Note that significant enhancement is observed only at concentrations above 0.5 μ M. **B.** Kinetics of enhancement of Cx32 expression level upon treatment with 9-CRA and ATRA (1 μ M) for the indicated times. Note that enhancement is observed as early as 24 h. **C.** Only 9-CRA and ATRA and MB increase Cx32 expression level. Note that RAR-specific retinoids, TTNPB (tetrahydrotetramethyl-nephthalenylpropenylbenzoic acid), and 13-CRA (13-cis-retinoic acid) and the other unrelated retinoid, 4-HPR, are ineffective. Note that MB (2.5 nM) is at least 300–500 times more potent than 9-CRA and ATRA on equimolar basis. **D.** Effect of 9-CRA and ATRA on adherens and tight junction associated proteins. Expression of adherens junction associated proteins E-cadherin and α - and β -catenins, and tight junction associated protein, occludin, was analyzed by Western blot analysis of total cell lysate (5 μ g). Note that only the expression of occludin appears to change noticeably.

doi:10.1371/journal.pone.0032846.g001

was observed in our earlier studies with androgens, the assembly of Cx32 and occludin into cell junctions, or vice versa, appears to be regulated coordinately [17,29,38,39].

Retinoids Modulate Androgen-regulated Formation and Degradation of Gap Junctions

Our previous studies showed that Cx32 was degraded upon androgen depletion by ERAD, and that androgens enhanced GJ formation by re-routing the ERAD-targeted pool of Cx32 to the cell surface [17]. Prompted by the data shown in Figures 1 and 2, we next examined the expression level of Cx32 and its junctional and non-junctional fate upon androgen depletion in the presence and absence of 9-CRA and ATRA. For these studies, cells were grown in androgen-depleted (charcoal-stripped), phenol-red free cell culture medium. Consistent with earlier studies [17], we found that androgen depletion decreased Cx32 expression level, which was prevented upon addition of MB and DHT (Figure 3 A). However, we found that the decrease in the expression level of Cx32 was also prevented when androgen-depleted medium was replenished with 9-CRA and ATRA (Figure 3 A). Moreover, combined treatment with MB and 9-CRA or ATRA was neither synergistic nor additive with respect to Cx32 expression level (Figure 3 A). To substantiate the above data, we assessed the formation of GJs immunocytochemically (Figure 3 B), biochemically by detergent insolubility assay (Figure 3 C), and functionally by measuring the junctional transfer of Lucifer Yellow (MW 443 Da), Alexa 488 (MW 570 Da), and Alexa 594 (MW 760 Da) (Table 2). As shown in Figure 3B, androgen depletion reduced the

number of GJs drastically as Cx32-specific immunostaining was rarely observed at cell-cell contact areas, while GJs were readily detected in cells when androgen-depleted medium was supplemented with 9-CRA and ATRA and with MB and DHT (Figure 3 B). Consistent with the immunocytochemical data, junctional transfer of Lucifer Yellow decreased significantly upon androgen depletion, which was prevented upon replenishing androgen-depleted medium with MB, ATRA and 9-CRA (Table 2). The detergent insolubility assay further corroborated the immunocytochemical and junctional transfer data (Figure 3 C). As was observed in our earlier studies, depletion of androgens had no significant effect on the detergent solubility of E-cadherin and β -catenin and tight junction associated protein, ZO-1 (Figure 3 C). As a control, depletion or addition of androgens, 9-CRA and ATRA to parental LNCaP-P and G418-resistant LNCaP-N cells neither induced GJ assembly nor had any effect on the junctional transfer (data not shown). Collectively, these data suggest that 9-CRA and ATRA prevent androgen-regulated degradation of Cx32 and enhance GJ formation in LNCaP-32 cells. Because combined treatment with androgens and retinoids was neither synergistic nor additive, the data further suggest that GJ formation is enhanced by rescuing the same pool of Cx32 which is targeted for ERAD upon androgen depletion.

Retinoids Enhance Gap Junction Formation Independent of Androgen Receptor Function

Treatment of LNCaP cells with 9-CRA has been shown to enhance AR expression level [30]. To test if 9-CRA and ATRA

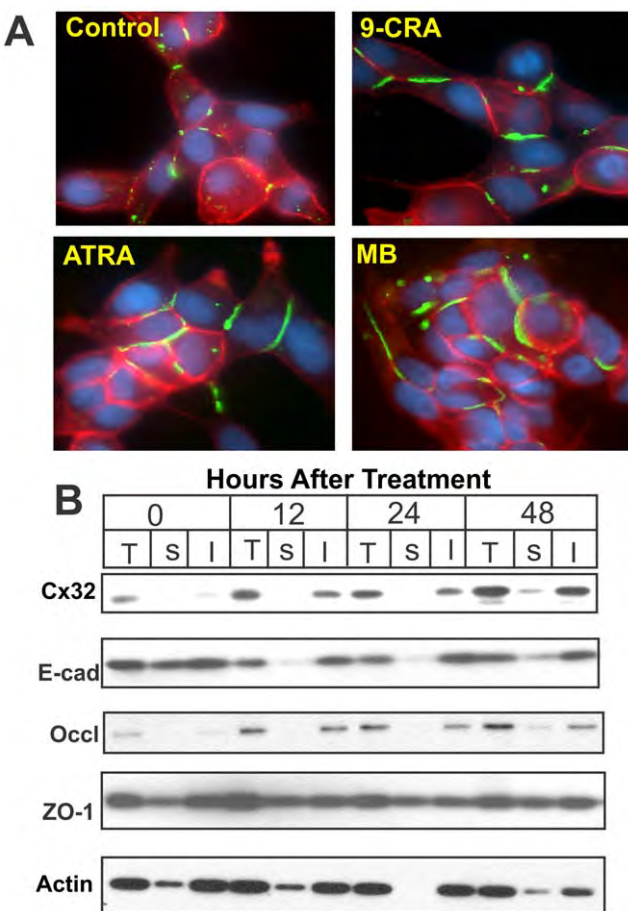


Figure 2. Retinoids enhance the assembly of Cx32 into gap junctions. **A.** LNCaP-32 cells, grown either in six well clusters or 10-cm dishes, were treated with 9-CRA and ATRA for various times. Assembly of Cx32 (green) into GJs was assessed immunocytochemically. E-cadherin is shown in red. Note that GJ formation was enhanced with 9-CRA and ATRA and MB treatment. **B.** Assembly of Cx32 into GJs, of tight junction associated protein, occludin and ZO-1, and adherens junction protein, E-cadherin, was assessed biochemically by TX100 insolubility assay as described in Materials and methods. Note also that both the total level and the detergent-insoluble fraction of Cx32 increased significantly. Note also that the detergent-solubility of adherens junction associated proteins, E-cadherin, is not significantly affected whereas that of tight junction associated protein, occludin, is marginally enhanced. In (A), the nuclei (blue) are stained with DAPI.

doi:10.1371/journal.pone.0032846.g002

enhanced AR expression in normal and androgen-depleted medium, we grew LNCaP-32 cells in control, androgen-depleted, and androgen-depleted plus 9-CRA, ATRA and MB containing medium for 48 h. As assessed by Western blot analysis, we found that androgen depletion reduced both the expression level of AR and Cx32, which was prevented upon replenishment with MB, DHT, 9-CRA and ATRA (Figure 4 A). These data raised the possibility that 9-CRA and ATRA enhanced GJ assembly in an AR-dependent manner — and not independently. To test this notion, we treated LNCaP-32 cells with Casodex (Bicalutamide), which blocks androgen action by competing with androgens for binding to the AR and inhibiting function [40,41], and examined the expression level of Cx32 and GJ formation upon treatment with 9-CRA, ATRA and MB in the presence and absence of Casodex in normal and androgen-depleted medium. Consistent

with previous studies, we found that treatment with Casodex caused degradation of AR (Figure 4 B) as well as abolished the effect of MB and DHT on Cx32 expression as was observed in our earlier studies [17]. However, degradation of AR was also observed with Casodex in the presence of 9-CRA and ATRA both in androgen-depleted and normal medium. Despite robustly decreasing AR expression level, we found that Casodex had no effect on 9-CRA- and ATRA-mediated enhancement of Cx32 expression level. To substantiate that decrease and increase in Cx32 expression was accompanied by parallel changes in GJ formation, we examined the formation of GJs immunocytochemically in Casodex-treated cells in the presence and absence of MB, 9-CRA and ATRA. GJs were not formed when cells were treated with casodex in normal serum or in androgen-depleted medium containing MB or DHT (Figure 5). On the other hand, we found that GJs were abundant when cells were treated with casodex along with 9-CRA or ATRA (Figure 5). These data suggest that the mechanism by which 9-CRA and ATRA prevent the degradation of Cx32 and enhance GJ formation upon androgen depletion is independent of AR expression level and/or function or both.

Connexin32 Expression Alters the Response of LNCaP Cells to Growth Modulatory Effect of Retinoids and Androgens

To test if Cx32 expression potentiates the growth inhibitory effect of 9-CRA, ATRA and androgens, we measured cell growth by treating LNCaP-32, along with LNCaP-P and LNCaP-N cells, with various non-toxic concentrations of these agents. Cell growth was determined by the colony forming assay (Figures 6 and 7) and by counting the number of cells (Tables 3 and 4). As assessed visually by the size of the colonies, we found that the growth of LNCaP-32 cells was profoundly inhibited by MB, 9-CRA and ATRA whereas the growth of LNCaP-P and LNCaP-N cells was not substantially affected (Figure 6). We also found that while combined treatment with MB and 9-CRA or ATRA inhibited growth more drastically compared to treatment with either agent alone in LNCaP-P and LNCaP-N cells, these effects were more pronounced in LNCaP-32 cells (Figure 7). For example, in order to see visible colonies, dishes of LNCaP-32 cells treated with MB and 9-CRA or ATRA had to be fixed 10–13 days later compared with the dishes of LNCaP-P and LNCaP-N cells. The data shown in Figures 6 and 7 were substantiated by counting the number of cells in replicate cultures in two independent experiments (Table 3 and 4). For example, the growth of LNCaP-P and LNCaP-N cells was inhibited by only 20–25% upon treatment with 9-CRA, ATRA and MB whereas the growth of LNCaP-32 cells was inhibited by 40–55% (Table 3). Similarly, the growth of LNCaP-32 cells was more profoundly inhibited with the combined treatment with MB and 9-CRA or ATRA compared with LNCaP-P and LNCaP-N cells (Table 4). Moreover, in agreement with our previous findings [14], we found that LNCaP-32 cells formed more compact colonies with smooth edges compared with LNCaP-P and LNCaP-N cells which formed colonies with scattered edges (Figure 8). Furthermore, we also observed that 9-CRA and ATRA treated LNCaP-P and LNCaP-N cells became flatter and more tightly packed compared to untreated cells and these changes were more robustly pronounced in LNCaP-32 cells (Figure 8). Finally, the morphological changes similar to those observed upon treatment with 9-CRA and ATRA were not as pronounced when cells were treated with MB (not shown) although growth was inhibited.

Table 1. Effect of 9-CRA, ATRA, and androgen on junctional transfer in LNCaP-32 cells.

Junctional Tracer	Expt #	Junctional Transfer ^a			
		NS	NS+9-CRA ^b	NS+ATRA ^b	NS+MB ^b
Lucifer Yellow	1	14.5±4.1(14)	34.4±6.3(18)	24.7±6.5(19)c	32±6.3.7(22)
	2	16.1±3.6(17)	28.7±4.5(14)	22.1±5.1(17)	38.9±7.1(20)
Alexa-488	1	12.8±4.2(19)	24.3±4.7(25)	22.5.±5.2(29)	30.7±7.1(22)
	2	10.2±3.3 (21)	25.8±2.3(22)	20.2±4.8(26)	29.8±8.2(27)
Alexa-594	1	7.7±2.3(25)	17.1±2.9(25)	14.9±3.7(25)	14.1±3.9(27)
	2	5.3±1.7(20)	14.8±4.1(22)	13.3±3.9(22)	15.1±5.7 (22)

LNCaP-32 cells, seeded in 6 cm dishes, were grown to 70% confluence. Junctional transfer was measured after microinjecting fluorescent tracers as described in Materials and Methods.

^a: The number of fluorescent cell neighbors (mean ± SE) 1 min (Lucifer Yellow), 3 min (Alexa-488) and 15 min (Alexa-594) after microinjection into test cell. The total number of injection trials is shown in parentheses.

^b: Cells were treated for 48 h with 9-CRA and ATRA (1 μM) and MB (2.5 nM).

doi:10.1371/journal.pone.0032846.t001

Discussion

Our findings demonstrate that retinoids enhance the expression level of Cx32 and formation of functional GJs in androgen-responsive human PCA cell line, LNCaP, which expresses retrovirally introduced Cx32. Earlier studies with these cells had shown that androgens enhanced GJ formation by controlling the expression level of Cx32 posttranslationally in a novel way — by rescuing the ERAD-targeted pool of Cx32 and rerouting it to the cell surface for GJ formation [17]. A key feature of our findings is that, apart from enhancing GJ assembly in normal medium, 9-CRA and ATRA also enhanced assembly by preventing degradation of Cx32, which is triggered upon androgen depletion in LNCaP-32 cells, independently of AR expression level or function. Only the assembly of Cx32 into GJs appeared to be significantly facilitated by 9-CRA and ATRA as neither the assembly nor degradation of adherens junction associated proteins, E-cadherin and α and β catenin, were significantly affected although the assembly of tight junction associated protein, occludin, appeared to be enhanced. The significance of these findings is further underscored by the fact that both androgens and retinoids have been documented to maintain the polarized and differentiated state of epithelial cells of normal prostate and prostatic tumors [19,42–45], and all have been shown to have pleiotropic effects by acting as transcription factors [1,3,5,46]. Our findings also showed that Cx32 expression potentiated the growth inhibitory effect of androgens and retinoids in LNCaP-32 cells, which indicates that their growth inhibitory and chemopreventive effects in prostate might be related to their ability to induce GJ formation.

Several independent lines of inquiry prompted us to undertake these studies. First, the expression of Cx32 had generally been found to coincide with the differentiated state of cells in the prostate as well as in other well-differentiated and polarized cells of several other organs [14,38,47–52]. Second, both androgens and retinoids had previously been shown to affect prostate morphogenesis and oncogenesis in animal models and in cell lines, including LNCaP [18,19,42–45,53–56]. Third, previous studies had shown that retinoids enhanced GJ formation in several *in vivo* and *in vitro* model systems, indicating that their chemopreventive and pro-differentiating actions might be related to their ability to enhance GJ assembly [7,25–27,57–59]. Fourth, Cx32 has been documented to be a tumor suppressor in tissues in which it is expressed [60–62] and it seemed reasonable that its expression and

assembly into GJs might be regulated by retinoids either alone or in conjunction with androgens.

How might retinoids enhance GJ assembly and prevent disassembly in LNCaP-32 cells? Our earlier studies with LNCaP-32 cells had shown that androgen-depletion attenuated GJ assembly by triggering the degradation of Cx32 by ERAD and not by modulating the transcription of the endogenous Cx32 gene or affecting Cx32 mRNA level driven by the retroviral promoter [17]. Because 9-CRA and ATRA neither induced the expression of the endogenous Cx32 in parental LNCaP and LNCaP-32 cells nor affected retroviral driven Cx32 mRNA transcripts, it seems likely that they enhanced GJ assembly by preventing the androgen-regulated pool of Cx32, posttranslationally, both under normal culture conditions as well as under androgen depleted condition [17]. It is well-established that AR is degraded upon androgen removal [63] and the expression level of AR in LNCaP cells has been known to be enhanced by 9-CRA and ATRA [30]. Our previous studies [17] had shown that AR-mediated signaling was the predominant factor in maintaining Cx32 expression level and preventing its degradation, posttranslationally, under androgen-depleted conditions in LNCaP-32 cells or in androgen-containing medium in the presence of anti-androgen, Casodex, which inhibits AR-function [64]. While our data showed that both 9-CRA and ATRA enhanced the expression level of AR under androgen-depleted conditions (Figure 4 A), GJ assembly was also robustly enhanced in the presence of Casodex despite low level of AR (Figure 4 B). It is possible that under androgen-depleted conditions, degradation of Cx32 is prevented by 9-CRA and ATRA by modulating the expression level of AR, leading to enhanced GJ assembly (Figure 4). However, our data also showed that when AR function was inhibited with anti-androgen, Casodex, androgen-mediated enhancement of Cx32 expression was annulled in normal serum as well as in androgen-depleted medium supplemented with MB, but the enhancement of GJ assembly mediated by 9-CRA and ATRA was not affected despite low AR expression. One possible explanation for these data is that 9-CRA and ATRA enhance GJ assembly by an AR-dependent mechanism under androgen-depleted conditions by rescuing the same pool of Cx32 which normally is ERAD targeted, yet activate another signaling pathway to enhance GJ assembly when AR function is inhibited by casodex under normal conditions. Further studies are required to explore this possibility.

Cadherins have previously been shown to facilitate the trafficking and assembly of Cxs into GJs and their loss has been

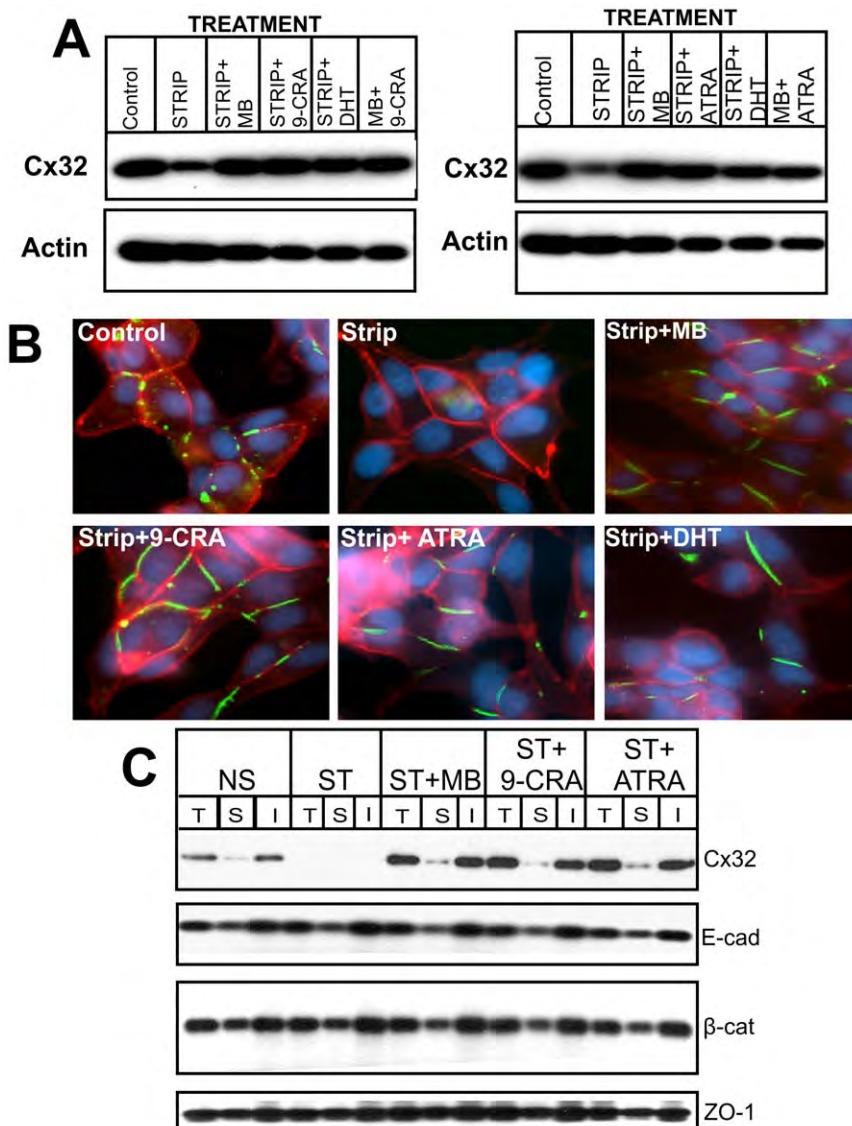


Figure 3. Retinoids block androgen-regulated formation and degradation of gap junctions. LNCaP-32 cells, grown to 70% confluence either in six well clusters or 10-cm dishes, were switched to charcoal-stripped, androgen-depleted (Strip) medium. Expression level of Cx32 and formation of GJs were analyzed by Western blot (**A**) and immunocytochemical analysis (**B**) after 48 h in the presence and absence of 9-CRA and ATRA (1 μ M) and MB (2.5 nM) and DHT (10 nM). **C.** Formation of GJs was also analyzed by Western blot analysis of total, detergent-soluble and -insoluble fractions as described in Materials and Methods. Note that Cx32 and GJs are degraded in androgen-depleted medium and degradation is blocked upon replenishment with 9-CRA, ATRA, MB and DHT. Note also that only the expression level of Cx32 and its detergent solubility changed significantly whereas that of E-cadherin (E-cad), β -catenin (β -cat) and ZO-1 was not significantly affected. In (B), the nuclei (green) were stained with DAPI. In A, 10 μ g of total protein was analyzed.

doi:10.1371/journal.pone.0032846.g003

shown to have the opposite effect on GJ assembly [32,33,37,65]. However, our data documented that 9-CRA and ATRA had no significant effect on the degradation of adherens junction associated proteins E-cadherin or α and β catenins both under normal and androgen-depleted conditions (Figures 2 and 3). Therefore, it seems less likely that the degradation of Cx32, and GJs composed of it, was triggered indirectly by the loss of E-cadherin. Previous studies in other cells [29,38,39], and our earlier studies with LNCaP-32 cells [17], had shown that the trafficking of occludin to the cell surface and its detergent solubility was controlled by the assembly of Cx32 into GJs as androgen-depletion caused its internalization into intracellular stores [17]. In this regard, it is worth noticing that 9-CRA and ATRA increased both

the total level of occludin as well as its detergent insolubility, although not robustly, which suggests that the assembly of Cx32 and occludin might be coordinately regulated by retinoids, and that this might be one of the mechanisms by which retinoids act as chemopreventive agents and maintain the polarized and differentiated state of epithelial cells. Further studies are required to substantiate this notion.

A salient feature of the data presented here is that the expression of Cx32 potentiated the growth inhibitory effect of androgens, 9-CRA and ATRA in LNCaP-32 cells as compared with their effect on LNCaP-P and LNCaP-N cells (Figure 6, Table 3). Moreover, combined treatment with the androgens and 9-CRA and ATRA was more potent than treatment with the either agent alone

Table 2. Effect of 9-CRA, ATRA and androgen on junctional transfer in LNCaP-32 cells under androgen-depleted conditions.

Treatment	Exp #	Junctional Tracer		
		LY	Alexa488	Alexa-594
NS	1	14.5±4.1(21)	27.4±4.7(24)	15.4±3.3(22)
	2	16.1±3.6(27)	24.8±5.2(27)	16.1±6.1(18)
Strip	1	2.4±0.7(24)	2.1±0.6(24)	0(11)
	2	1.8±0.6(22)	2.8±0.6(27)	0(13)
Strip+MB	1	29.4±5.7(32)	26±4.1(21)	13.3±2.47(23)
	2	32.9±6.3(28)	30.1±5.2(20)	14.4±3.1(19)
Strip+9-CRA	1	27.4±5.1(24)	29.2±8.1(21)	12.5±2.1(22)
	2	33.8±7.4(28)	34.9±6.1(25)	15.9±4.1(18)
Strip+ATRA	1	22.4±3.7(23)	23.7±4.6(24)	13.2±3.3(32)
	2	28.2±4.1(29)	28.9±5.7(24)	15.9±7.1(30)

LNCaP-32 cells, seeded in 6 cm dishes, were grown to 70% confluence, after which they were switched to charcoal-stripped, androgen-depleted medium (Strip) for 48 h in the presence and absence of 9-CRA, ATRA, and MB. Junctional transfer was quantified as described in Table 1 legend and in Materials and Methods.

doi:10.1371/journal.pone.0032846.t002

(Figure 7, Table 4). Treatment of LNCaP cells with androgens, 9-CRA and ATRA has had complex effects on growth, with some concentrations inhibiting growth and others enhancing growth [66–73]. In our studies, the concentrations of MB, 9-CRA and ATRA chosen were only marginally growth inhibitory to Cx-null LNCaP-P and LNCaP-N cells, but were profoundly growth inhibitory to Cx32-expressing LNCaP-32 cells. It is worth mentioning that in agreement with our earlier studies in other cell culture model systems [26], but in contrast to the complexity of the effect of MB, 9-CRA and ATRA on cell growth [66–73], these agents consistently enhanced the expression level of Cx32 and its assembly into GJs both in normal serum and under androgen-depleted condition in LNCaP-32 cells.

What might be the possible explanation for these findings? It is as yet unknown which signaling pathways are activated or suppressed upon formation and degradation of GJs [8,10,74] and how they are causally linked to the growth inhibitory effect [28,58,59]. Because androgens, 9-CRA and ATRA also inhibited the growth of Cx-null cells, and inhibition was potentiated upon expression of Cx32, it seems more likely that the formation of GJs either modulates a signaling pathway different from that activated by androgens and 9-CRA and ATRA or amplifies a pathway(s) activated by them or both. In previous studies we had shown that expression of Cx32 in LNCaP cells not only inhibited growth in vivo and in vitro but also induced differentiation as assessed by the ability to synthesize prostatic specific antigen, which is expressed by the well-differentiated luminal cells of the prostate [14]. Moreover, these studies also showed that serial propagation of Cx32-expressing LNCaP sub-clones caused selection of cells in which the capacity to assemble GJs was lost as only few sub-clones could be established that retained the ability to form GJs and in which the growth suppressing effect of junction formation was compensated by other growth-modulatory mechanisms [14]. In this regard, it is noteworthy that transient expression of Cx43 in LNCaP cells via adenoviruses sensitizes these cells to apoptosis induced by tumor necrosis factor α , TRAIL, and anti-Fas antibodies to which Cx-null LNCaP cells are resistant. Because

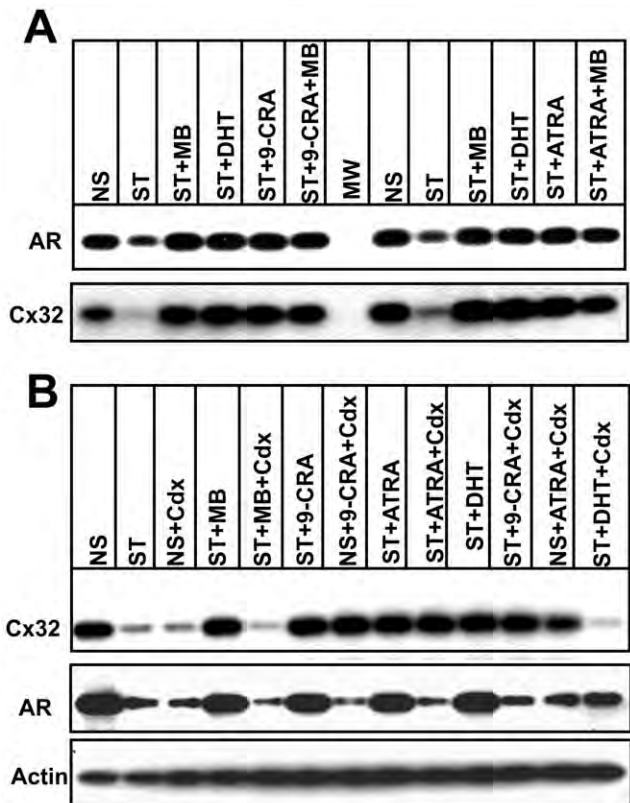


Figure 4. Effect of 9-CRA, ATRA and androgens on the expression level of Cx32 and AR. **A.** LNCaP-32 cells were grown to 70–80% confluence in 6 cm dishes. Cells were switched to charcoal-stripped, androgen-depleted medium (ST) containing 9-CRA and ATRA (1 μ M) and MB (2.5 nM) and DHT (10 nM) for 24 h. Cells in androgen-containing medium (NS) or androgen-depleted medium (ST) were used as controls. Expression level of Cx32 and AR was analyzed by Western blotting. Note that the expression level of both Cx32 and AR decreases upon androgen depletion and the decrease is blocked upon treatment with 9-CRA, ATRA, MB and DHT. **B.** LNCaP-32 cells, seeded as above, were treated with 9-CRA and ATRA (1 μ M) and MB (2.5 nM) and DHT (10 nM) in the presence and absence of Casodex (10 μ M) in normal and androgen-depleted medium. Expression level of Cx32 and AR was examined after Western blotting. Note that in Casodex containing medium, the expression level Cx32 does not decrease in the presence of 9-CRA and ATRA (1 μ M) in charcoal-stripped medium despite low level of AR expression. This is not observed with MB and DHT.

doi:10.1371/journal.pone.0032846.g004

formation of functional GJs was required for sensitization and Cx expression had no effect on TNF- α receptor number, Wang et al. have proposed that transmission of some small molecules from cell-to-cell acted as an apoptotic trigger [75]. It is at present difficult to envisage how chemopreventive, pro-differentiating and growth-inhibitory effects of 9-CRA and ATRA are tied to the formation of GJs as the expression of several classes of genes has been shown to be altered by them [11,12,28,59,76,77].

The incidence of PCA escalates dramatically at ages when men confront other competing causes of mortality. Prostate cancer is a slow growing tumor with a long latency period and while the incidence of histologically detectable PCA is high, the incidence of clinically detectable disease is low and is influenced by dietary factors [19,71,78]. Moreover, this long latency period affords opportunities for intervention with therapies that are designed to delay disease initiation and/or progression. Although retinoids have been considered as one of the candidate dietary factors in

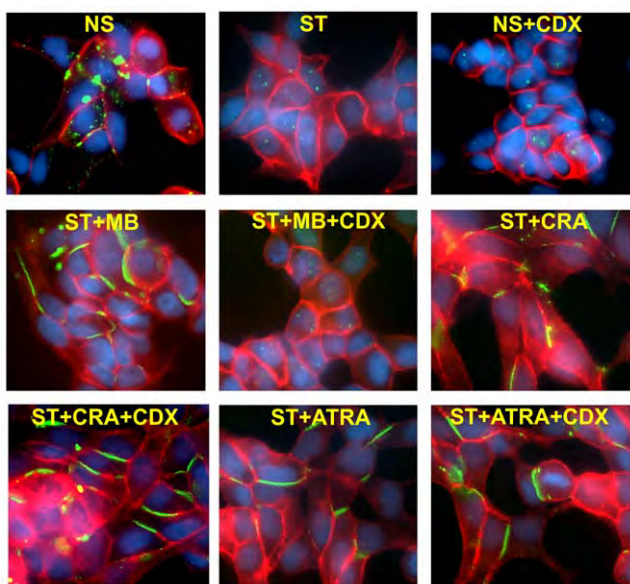


Figure 5. Effect of 9-CRA, ATRA, and androgens on the formation of gap junctions in the presence and the absence of casodex. LNCaP-32 cells, seeded in six well clusters containing glass cover slips, were allowed to grow to 70% confluence. Cells were then grown for additional 24 h in normal medium (NS), in charcoal-stripped, androgen-depleted medium alone (ST), in normal serum containing casodex (NS+CDX), and in androgen-depleted medium supplemented with MB (ST+MB), with MB and casodex (ST+MB+CDX), with 9-CRA (ST+CRA), 9-CRA and CDX (ST+CRA+CDX), with ATRA (ST+ATRA), and with ATRA and CDX (ST+ATRA+CDX). Degradation and subcellular localization of Cx32 were analyzed immunocytochemically as described in Materials and methods. Note that GJs (green) are not degraded in cells treated with 9-CRA and ATRA both in the presence and absence of casodex whereas they are degraded in normal serum and androgen-depleted but MB supplemented medium containing casodex. E-cadherin is shown in red and the nuclei (blue) were stained with DAPI. doi:10.1371/journal.pone.0032846.g005

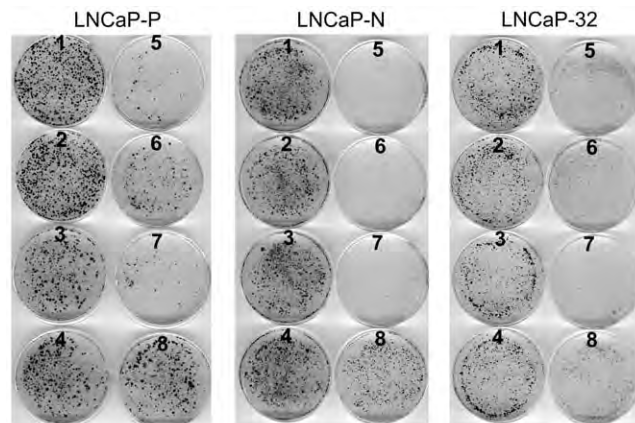


Figure 7. Connexin expression and junction formation accentuates the growth inhibitory effect of 9-CRA, ATRA and androgens in LNCaP cells. LNCaP-P, LNCaP-N and LNCaP-32 cells were seeded at clonal density in 6 cm dishes in triplicate as described in Figure 6 legend. After 24 h, cells were treated with 9-CRA, ATRA and MB either alone or in combination. Cells were grown until they formed visible colonies (21 d for LNCaP-P and LNCaP-N and 28 d for LNCaP-32). Medium was changed every 4 d. Colonies were fixed with formalin and stained with crystal violet as described in Materials and Methods. The numbers on the dishes correspond to the following concentrations of 9-CRA, ATRA and MB. 1 = control; 2: MB (0.5 nM); 3 = 9-CRA (0.5 μM); 4. ATRA (0.5 μM); 5 = MB+CRA; 6. MB+ATRA; 7 = CRA+ATRA (0.5 μM); 8 = MB=(1 nM). Note that the combined treatment is more potent and that the growth of LNCaP-32 cells is more profoundly inhibited. doi:10.1371/journal.pone.0032846.g007

controlling PCA progression, epidemiological data have been controversial as both suppressive and stimulatory effects have been reported [24,79–81]. Androgens and retinoids are required for the maintenance of normal healthy prostate epithelium as in their absence glandular atrophy of the prostate ensues due to massive apoptosis of luminal epithelial cells [18,82]. Although retinoids

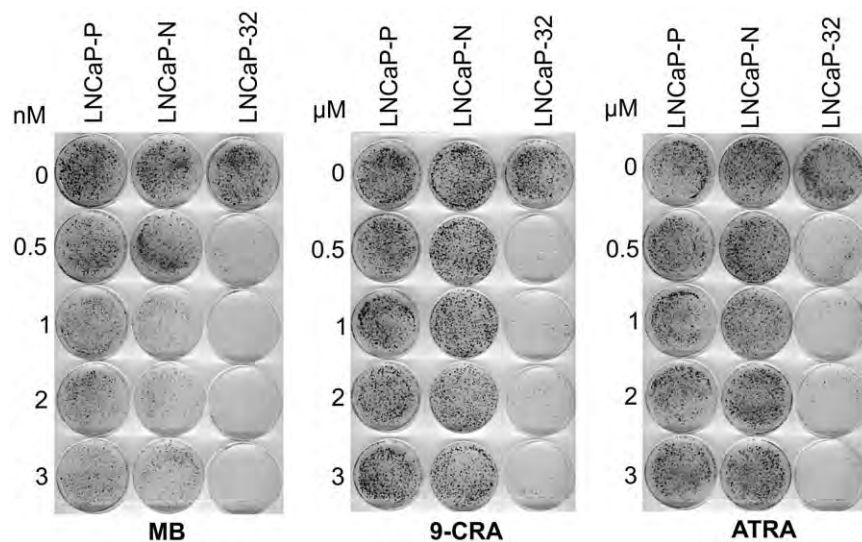


Figure 6. Connexin expression and junction formation accentuates the growth inhibitory effect of 9-CRA, ATRA and androgens in LNCaP cells. LNCaP-P, LNCaP-N and LNCaP-32 cells were seeded at a clonal density in 6 cm dishes in triplicate (2×10^3 cells per dish). After 24 h, cells were treated with the indicated concentrations of 9-CRA, ATRA and MB. Cells were grown until they formed visible colonies (21 d for LNCaP-P and LNCaP-N and 33 d for LNCaP-32). Medium was changed every 4 d. Colonies were fixed with formalin and stained with crystal violet as described in Materials and Methods. Note that the growth of LNCaP-32 cells is profoundly inhibited upon 9-CRA, ATRA and MB treatment as colonies are barely detectable. doi:10.1371/journal.pone.0032846.g006

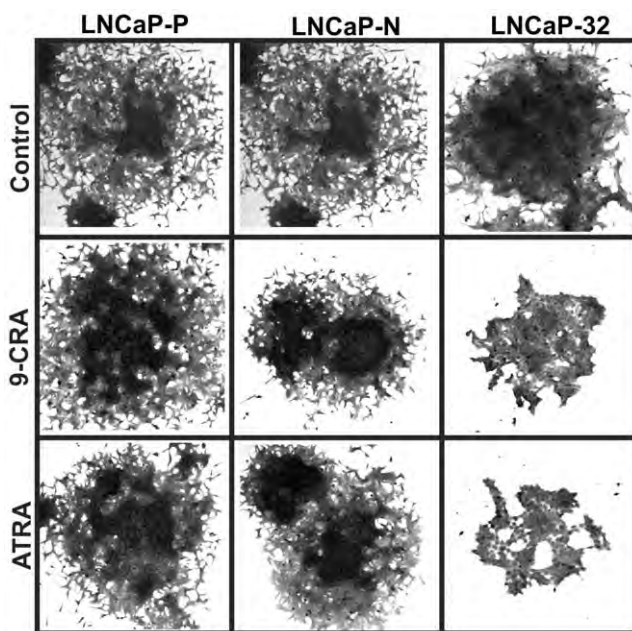


Figure 8. Retinoids affect the morphological phenotype of Cx32-expressing LNCaP cells. The morphological appearance of colonies of LNCaP-P, LNCaP-N and LNCaP-32 cells upon treatment with 9-CRA and ATRA is altered. Cx-null LNCaP-P and LNCaP-N cells form colonies of moderately packed cells with scattered edges whereas Cx32-expressing LNCaP-32 cells form colonies of compact cells with smooth edge. Note that upon treatment with 9-CRA and ATRA, LNCaP-P and LNCaP-N form colonies of more tightly packed cells with relatively smoother edges. Note also that these changes are profound in LNCaP-32 cells. For direct comparison of colony size and cell shape, all photographs were taken at the same magnification (40×). Colonies were fixed and photographed at day 21 (LNCaP-P and LNCaP-N) and day 28 d for LNCaP-32 cells.

doi:10.1371/journal.pone.0032846.g008

Table 3. Cx32 expression sensitizes LNCaP cells to growth inhibitory effect of 9-CRA, ATRA and MB.

Treatment	LNCaP-P	LNCaP-N	LNCaP-32
Experiment #			
1			
Control	8.2±1.8 (100±22)	7.5±1.4 (100±19)	6.8±1.8 (100±26)
MB	6.4±1.4 (78±22)	6.1±1.2 (81±20)	3.2±0.8 (47±25)
9-CRA	6.8±1.6 (83±23)	6.3±1.1 (84±17)	3.0±0.5 (44±17)
ATRA	6.2±1.3 (76±21)	5.9±1.3 (79±22)	2.9±0.6 (43±21)
Experiment #			
2			
Control	7.8±1.1 (100±14)	8.1±1.0 (100±12)	7.2±1.3 (100±18)
MB	6.3±1.0 (81±16)	6.5±1.2 (80±18)	3.3±0.6 (46±18)
9-CRA	6.5±0.9 (83±16)	6.7±1.5 (83±22)	3.1±0.4 (43±13)
ATRA	6.2±0.7 (79±11)	6.4±1.1 (79±17)	2.8±0.5 (39±18)

LNCaP-P, LNCaP-N and LNCaP-32 cells were seeded in 6-cm dishes in replicate (5×10^4 cells/dish) and treated with 9-CRA (1 μM), ATRA (1 μM), and MB (2.5 nM). Cells were grown for 8 days with a medium change at day 5. Cells were trypsinized and counted as described in Materials and Methods. The values represent Mean number of cells per dish $\times 10^5 \pm$ SE of the Mean. Values in the parentheses represent Means of % Growth \pm SE of the Mean.

doi:10.1371/journal.pone.0032846.t003

Table 4. Effect of 9-CRA, ATRA and MB on growth of Cx-null and Cx32-expressing LNCaP cells.

Treatment	LNCaP-P	LNCaP-N	LNCaP-32
Experiment # 1			
Control	8.0±1.3 (100±16)	8.5±1.2 (100±14)	7.8±1.3 (100±17)
MB (0.5 μM)	6.6±1.2 (83±18)	6.7±1.4 (81±21)	3.9±0.9 (50±23)
9-CRA	6.7±1.3 (84±19)	6.6±1.0 (84±15)	4.3±0.6 (55±14)
ATRA	6.5±1.5 (81±23)	6.1±1.2 (79±20)	4.1±0.4 (54±10)
MB+9-CRA	5.5±1.5 (69±27)	4.8±1.1 (56±21)	1.8±0.3 (23±17)
MB+ATRA	4.9±1.1 (61±22)	5.0±1.7 (59±21)	2.1±0.5 (27±24)
-CRA+ATRA	5.2±1.2 (65±23)	5.1±1.2 (64±21)	5.7±0.7 (73±12)
Experiment # 2			
Control	8.2±1.3 (100±16)	8.3±1.2 (100±14)	7.6±1.1 (100±14)
MB	6.1±1.0 (74±16)	6.8±1.0 (82±15)	3.1±0.4 (41±13)
9-CRA	6.0±0.9 (73±15)	6.4±1.3 (77±20)	3.5±0.3 (46±9)
ATRA	6.3±0.7 (77±11)	6.0±1.5 (72±25)	3.1±0.7 (41±23)
MB + 9-CRA	5.1±1.0 (62±20)	5.3±0.9 (64±17)	2.1±0.3 (28±14)
MB + ATRA	5.4±0.6 (66±12)	5.6±0.8 (67±14)	2.2±0.4 (29±18)
9-CRA + ATRA	4.9±0.8 (60±16)	4.9±0.6 (59±12)	4.7±0.5 (62±11)

LNCaP-P, LNCaP-N and LNCaP-32 cells were seeded in 6-cm dishes in replicate (5×10^4 cells/dish) and treated with 9-CRA (0.5 μM), ATRA (0.5 μM), and MB (1 nM) either alone or in combination. Cells were grown for 11 days with a medium change at day 4 and 7. Cell growth was determined as in Table 3. The values represent Mean number of cells per dish $\times 10^5 \pm$ SE of the Mean. Values in the parentheses represent Means of % Growth \pm SE of the Mean.

doi:10.1371/journal.pone.0032846.t004

have been known to be chemopreventive agents for decades and have been used as differentiating agents, their use in human clinical trials has been hampered due to pleiotropic and toxic effects [24,83,84]. Thus, the role of androgens and retinoids in suppressing and facilitating PCA progression as well as in maintaining the differentiated state of epithelial cells of normal prostate and prostate tumors has remained enigmatic [18,19,79,83,85]. In the light of the effects of androgens and 9-CRA and ATRA on junction formation and growth, and because of the potential interactions among AR and RXR receptor pathways, an investigation into their additive and/or synergistic effects on the assembly and disassembly of Cx32 into GJs might shed light on the mechanism by which retinoids and androgens affect growth, differentiation and apoptosis of normal and PCA cells.

Author Contributions

Conceived and designed the experiments: PPM SKB. Performed the experiments: LK PK KEJ. Analyzed the data: PPM PK KEJ. Contributed reagents/materials/analysis tools: SKB. Wrote the paper: PPM.

Reference

- Duester G (2008) Retinoic acid synthesis and signaling during early organogenesis. *Cell* 134: 921–931.
- Clagett-Dame M, DeLuca H (2002) The role of vitamin A in mammalian reproduction and embryonic development. *Ann Rev Nutr* 22: 347–381.
- Aranda A, Pascual A (2001) Nuclear hormone receptors and gene expression. *Physiol Rev* 81: 1269–1304.
- Pfahl M, Chytily F (1996) Regulation of metabolism by retinoic acid and its nuclear receptors. *Ann Rev Nutr* 16: 257–283.
- Ross S, McCaffery P, Drager U, De Luca L (2000) Retinoids in embryonal development. *Physiol Rev* 80: 1021–1054.
- Goodenough DA, Goliger JA, Paul DA (1996) Connexins, connexons, and intercellular communication. *Annual Review of Biochemistry* 65: 475–502.

7. Trosko J, Chang C-C (2001) Mechanism of up-regulated gap junctional intercellular communication during chemoprevention and chemotherapy of cancer. *Mutat Res* 480: 219–229.

8. Wei CJ, Xu X, Lo CW (2004) Connexins and cell signaling in development and disease. *Ann Rev Cell Dev Biol* 20: 811–838.

9. Beyer EC, Berthoud VM (2009) The Family of Connexin Genes. In: Harris A, Locke D, eds. *Connexins: A Guide* Springer. pp 3–26.

10. Laird DW (2006) Life cycle of connexins in health and disease. *Biochem J* 394: 527–543.

11. Laird DW (2010) The gap junction proteome and its relationship to disease. *Trends Cell Biol* 20: 92–101.

12. Naus CC, Laird DW (2010) Implications and challenges of connexin connections to cancer. *Nat Rev Cancer* 10: 435–441.

13. Habermann H, Chang WY, Birch L, Mehta P, Prins GS (2001) Developmental Exposure to Estrogens Alters Epithelial Cell Adhesion and Gap Junction Proteins in the Adult Rat Prostate. *Endocrinology* 142: 359–369.

14. Mehta PP, Perez-Stable C, Nadji M, Mian M, Asotra K, et al. (1999) Suppression of human prostate cancer cell growth by forced expression of connexin genes. *Dev Genetics* 24: 91–110.

15. Habermann H, Ray V, Prins G (2002) Alterations in gap junction protein expression in human benign prostatic hyperplasia and prostate cancer. *J Urol* 167: 655–660.

16. Govindarajan R, Song X-H, Guo R-J, Wheeck MJ, Johnson KR, et al. (2002) Impaired trafficking of connexins in androgen-independent human prostate cancer cell lines and its mitigation by α -catenin. *J Biol Chem* 277: 50087–50097.

17. Mitra S, Annamalai L, Chakraborty S, Johnson K, Song X, et al. (2006) Androgen-regulated Formation and Degradation of Gap Junctions in Androgen-responsive Human Prostate Cancer Cells. *Mol Biol Cell* 17: 5400–5416.

18. Marker P, Donjacour A, Dahiya R, Cunha G (2003) Hormonal, cellular, and molecular control of prostatic development. *Dev Biol* 253: 165–174.

19. Shen MM, Abate-Shen C (2010) Molecular genetics of prostate cancer: new prospects for old challenges. *Genes & Development* 24: 1967–2000.

20. Wilson J, Roth C, Warkany J (1953) An analysis of the syndrome of malformations induced by maternal vitamin A deficiency. Effects of restoration of vitamin A at various times during gestation. *Am J Anat* 92: 189–217.

21. Lohnes D, Kastner P, Dierich A, Mark M, LeMeur M, et al. (1993) Function of retinoic acid receptor gamma in the mouse. *Cell* 73: 643–658.

22. Huang J, Powell W, Khodavirdi A, Wu J, Makita T, et al. (2002) Prostatic intraepithelial neoplasia in mice with conditional disruption of the retinoid X receptor alpha allele in the prostate epithelium. *Cancer Res* 62: 4812–4819.

23. Altucci L, Gronemeyer H (2001) The promise of retinoids to fight against cancer. *Nat Rev Cancer* 1: 181–193.

24. Sporn MB (2002) Chemoprevention: an essential approach in preventing cancer. *Nat Rev Cancer* 2: 537–543.

25. Bertram J (1999) Carotenoids and Gene Regulation. *Nutr Rev* 57: 182–191.

26. Mehta P, Bertram J, Loewenstein W (1989) The actions of retinoids on cellular growth correlate with their actions on gap junctional communication. *J Cell Biol* 108: 1053–1065.

27. Mehta P, Loewenstein W (1991) Differential regulation of communication by retinoic acid in homologous and heterologous junctions between normal and transformed cells. *J Cell Biol* 113: 371–379.

28. Trosko J (2007) Gap Junctional Intercellular Communication as a Biological “Rosetta Stone” in Understanding, in a Systems Biological Manner, Stem Cell Behavior, Mechanisms of Epigenetic Toxicology, Chemoprevention and Chemotherapy. *J Membr Biol* 218: 93–100.

29. Kojima T, Murata M, Go M, Spray DC, Sawada N (2007) Connexins induce and maintain tight junctions in epithelial cells. *J Membr Biol* 217: 13–19.

30. Zhao X, Ly L, Peehl D, Feldman D (1999) Induction of androgen receptor by 1 α ,25-dihydroxyvitamin D₃ and 9-cis retinoic acid in LNCaP human prostate cancer cells. *Endocrinology* 140: 1205–1212.

31. Igawa T, Lin FF, Lee MS, Karan D, Batra SK, et al. (2002) Establishment and characterization of androgen-independent human prostate cancer LNCaP cell model. *Prostate* 50: 222–235.

32. Chakraborty S, Mitra S, Falk MM, Caplan S, Wheeck MJ, et al. (2010) E-cadherin differentially regulates the assembly of connexin43 and connexin32 into gap junctions in human squamous carcinoma cells. *J Biol Chem* 285: 10761–10776.

33. Govindarajan R, Chakraborty S, Falk MM, Johnson KR, Wheeck MJ, et al. (2010) Assembly of connexin43 is differentially regulated by E-cadherin and N-cadherin in rat liver epithelial cells. *Mol Biol Cell* 21: 4089–4107.

34. Mehta P, Bertram J, Loewenstein W (1986) Growth inhibition of transformed cells correlates with their junctional communication with normal cells. *Cell* 44: 187–196.

35. Van Slyke JK, Musil LS (2000) Analysis of connexin intracellular transport and assembly. *Methods* 20: 156–164.

36. Jongen WM, Fitzgerald DJ, Asamoto M, Piccoli C, Slaga TJ, et al. (1991) Regulation of connexin 43-mediated gap junctional intercellular communication by Ca²⁺ in mouse epidermal cells is controlled by E-cadherin. *J Cell Biol* 114: 545–555.

37. Meyer R, Laird D, Revel J-P, Johnson R (1992) Inhibition of gap junction and adherens junction assembly by connexin and A-CAM antibodies. *J Cell Biol* 119: 179–189.

38. Kojima T, Kokai Y, Chiba H, Yamamoto M, Mochizuki Y, et al. (2001) Cx32 but Not Cx26 Is Associated with Tight Junctions in Primary Cultures of Rat Hepatocytes. *Experimental Cell Research* 263: 193–201.

39. Kojima T, Spray DC, Kokai Y, Chiba H, Mochizuki Y, et al. (2002) Cx32 formation and/or Cx32-mediated intercellular communication induces expression and function of tight junctions in hepatocytic cell line. *Exp Cell Res* 276: 40–51.

40. Kempainen J, Wilson J (1996) Agonist and antagonist activities of hydroxyfluanamide and casodex relate to androgen receptor stabilization. *Urology* 48: 157–163.

41. Farla P, Hersmus R, Trapman J, Houtsmuller AB (2005) Antiandrogens prevent stable DNA-binding of the androgen receptor. *Journal of Cell Science* 118: 4187–4198.

42. Lasnitski I, Goodman D (1974) Inhibition of the effects of methylcholanthrene on mouse prostate in organ culture by vitamin A and its analogs. *Cancer Res* 34: 1564–1571.

43. Lasnitski I, Whitaker R, Withcombe J (1975) The effect steroid hormones on the growth pattern and RNA synthesis in human benign prostatic hyperplasia in organ culture. *Br J Cancer* 32: 168–178.

44. Manual M, Ghyselink NB, Chambon P (2006) Functions of the retinoid nuclear receptors: Lessons from the genetic and pharmacological dissections of the retinoic acid signaling pathway during mouse embryogenesis. *Ann Rev Pharm* 46: 451–480.

45. Vezina C, Allgeier SMT, Fritz W, Moore R, Strerath M, et al. (2008) Retinoic acid induces prostatic bud formation. *Dev Dyn* 237: 1321–1333.

46. Perissi V, Rosenfeld MG (2005) Controlling nuclear receptors: the circular logic of cofactor cycles. *Nat Rev Mol Cell Biol* 6: 542–554.

47. Bavamian S, Klee P, Allagnat F, Haefliger J-A, Meda P (2009) Connexins and secretion. In: Harris A, Locke D, eds. *Connexins: A Guide* Springer. pp 511–528.

48. Deryck R, Yancey S, Traub O, Willecke K, Revel J-P (1987) Major loss of the 28-KD protein of gap junction in proliferating hepatocytes. *J Cell Biol* 105: 1925–1934.

49. Habermann H, Ray V, Habermann W, Prins GS (2001) Alterations in gap junction protein expression in human benign prostatic hyperplasia and prostate cancer. *J Urol* 166: 2267–2272.

50. Kojima T, Sawada N, Oyamada M, Chiba H, Isomura H, et al. (1994) Rapid appearance of connexin 26-positive gap junctions in centrilobular hepatocytes without induction of mRNA and protein synthesis in isolated perfused liver of female rat. *J Cell Sci* 107(Pt 12): 3579–3590.

51. Kojima T, Mitaka T, Paul DL, Mori M, Mochizuki Y (1995) Reappearance and long-term maintenance of connexin32 in proliferated adult rat hepatocytes: use of serum-free L-15 medium supplemented with EGF and DMSO. *J Cell Sci* 108: 1347–1357.

52. Kokai Y, Murata M, Go M, Spray DC, Sawada N (2011) Connexins induce and maintain tight junctions in epithelial cells. *J Membr Biol* 217: 13–19.

53. Cunha G, Donjacour A, Cooke P, Mee S, Biggs R, et al. (1987) The endocrinology and developmental biology of the prostate. *Endocr Rev* 8: 338–362.

54. Lasnitski I (1976) Reversal of methylchoanthrene-induced changes in mouse prostates in vitro by retinoic acid and its analogues. *British Journal of Cancer* 34: 239–248.

55. Christov KT, Moon RC, Lantvit DD, Boone CW, Steele VE, et al. (2002) 9-cis-retinoic acid but not 4-hydroxyphenylretinamide inhibits prostate intraepithelial neoplasia in Noble rats. *Cancer Res* 62: 5178–5182.

56. Zhang X (2002) Vitamin A and apoptosis in prostate cancer. *Endocr Relat Cancer* 9: 87–102.

57. King TJ, Bertram JS (2005) Connexins as targets for cancer chemoprevention and chemotherapy. *Biochimica et Biophysica Acta (BBA) - Biomembranes* 1719: 146–160.

58. Trosko J (2006) Dietary modulation of the multistage, multimechanisms of human carcinogenesis: effects on initiated stem cells and cell-cell communication. *Nutr Cancer* 94: 102–110.

59. Trosko J (2006) From adult stem cells to cancer stem cells: Oct-4 Gene, cell-cell communication, and hormones during tumor promotion. *Ann NY Acad Sci* 1089: 36–58.

60. King TJ, Lampe PD (2004) Mice deficient for the gap junction protein Connexin32 exhibit increased radiation-induced tumorigenesis associated with elevated mitogen-activated protein kinase (p44/Erk1, p42/Erk2) activation. *Carcinogenesis* 25: 669–680.

61. King TJ, Lampe PD (2004) The Gap Junction Protein Connexin32 Is a Mouse Lung Tumor Suppressor. *Cancer Res* 64: 7191–7196.

62. Temme A, Buchmann A, Gabriel H-D, Nelles E, Schwarz M, et al. (1997) High incidence of spontaneous and chemically induced liver tumors in mice deficient for connexin 32. *Current Biology* 7: 713–716.

63. Dehm SM, Tindall DJ (2005) Regulation of androgen receptor signaling in prostate cancer. *Expert Review of Anticancer Therapy* 5: 63–74.

64. Iversen P (2002) Antiandrogen monotherapy: indications and results. *Urology* 60: 64–71.

65. Hernandez-Blazquez F, Joazeiro P, Omori Y, Yamasaki H (2001) Control of intracellular movement of connexins by E-cadherin in murine skin papilloma cells. *Exp Cell Res* 270: 235–247.

66. Blutt S, Allegretto EA, Pike JW, Weigel NL (1997) 1,25-dihydroxyvitamin D₃ and 9-cis-retinoic acid act synergistically to inhibit the growth of LNCaP

prostate cells and cause accumulation of cells in G₁. *Endocrinology* 138: 1491–1497.

67. Esquenet M, Swinnen JV, Heyns W, Verhoeven G (1996) Control of LNCaP proliferation and differentiation: actions and interactions of androgens, 1a, 25-dihydroxycholecalciferol, all-trans retinoic acid, 9-Cis Retinoic acid, and phenylacetate. *The Prostate* 28: 182–194.
68. Fong C-J, Sutkowski DM, Braun EJ, Bauer KD, Sherwood ER, et al. (1993) Effect of retinoid acid on the proliferation and secretory activity of androgen-responsive prostatic carcinoma cells. *The Journal of Urology* 149: 1190–1194.
69. Kokontis JM, Hay N, Liao S (1998) Progression of LNCaP prostate tumor cells during androgen deprivation: hormone-independent growth, repression of proliferation by androgen, and role for p27kip1 in androgen-induced cell cycle arrest. *Mol Endocrinol* 12: 941–953.
70. Murthy S, Marcelli M, Weigel N (2011) Stable expression of full length human androgen receptor in PC-3 prostate cancer cells enhances sensitivity to retinoic acid but not to 1a,25-Dihydroxyvitamin D3. *The Prostate* 56: 293–304.
71. Peehl D, Feldman D (2003) The role of vitamin D and retinoids in controlling prostate cancer progression. *Endocr Relat Cancer* 10: 131–140.
72. Schuurmans A, Bolt J, Veldscholte J, Mulder E (1991) Regulation of growth of LNCaP human prostate tumor cells by growth factors and steroid hormones. *J Steroid Biochem Molec Biol* 40: 193–197.
73. Umekita Y, Hiipakka RA, Kokontis JM, Liao S (1996) Human prostate tumor growth in athymic mice: Inhibition by androgens and stimulation by áfinasteride. *PNAS* 93: 11802–11807.
74. Goodenough DA, Paul DL (2009) Gap Junctions. *Cold Spring Harbor Perspectives Biology* 1: a002576.
75. Wang M, BERTHOUD VM, BEYER EC (2007) Connexin43 increases the sensitivity of prostate cancer cells to TNF{alpha}-induced apoptosis. *Journal of Cell Science* 120: 320–329.
76. Kardami E, Dang X, Iacobas DA, Nickel BE, Jeyaraman M, et al. (2007) The role of connexins in controlling cell growth and gene expression. *Progress in Biophysics and Molecular Biology* 94: 245–264.
77. McLachlan E, Shao Q, Wang HI, Langlois S, Laird DW (2006) Connexin act as tumor suppressors in three dimensional mammary cell organoids by regulating differentiation and angiogenesis. *Cancer Res* 66: 9886–9894.
78. Feldman D, Zhao X-Y, Krishnan AV (2000) Vitamin D and Prostate Cancer. *Endocrinology* 141: 5–9.
79. Altucci L, Gronemeyer H (2001) The promise of retinoids to fight against cancer. *Nat Rev Cancer* 1: 181–193.
80. Kolonel L, Hankin J, Yoshizawa C (1987) Vitamin A and prostate cancer in elderly men: enhancement of risk. *Cancer Res* 47: 2982–2985.
81. Reichman M, Hayes R, Ziegler R, Schatzkin A, Taylor P, et al. (1990) Serum vitamin A and subsequent development of prostate cancer in the first National Health and Nutrition Examination Survey Epidemiologic Follow-up Study. *Cancer Res* 50: 2311–2315.
82. Wilson JG, Roth CB, Warkany J (1953) An analysis of the syndrome of malformations induced by maternal vitamin A deficiency. Effects of restoration of vitamin A at various times during gestation. *Am J Anat* 92: 189–217.
83. Albinia A, Sporn MB (2007) The tumour microenvironment as a target for chemoprevention. *Nat Rev Cancer* 7.
84. Liby KT, Yore MM, Sporn MB (2007) Triterpenoids and retinoids as multifunctional agents for the prevention and treatment of cancer. *Nat Rev Cancer* 7: 357–369.
85. Sporn MB (2002) Chemoprevention: an essential approach in preventing cancer. *Nat Rev Cancer* 2: 537–543.

Phosphorylation on Ser-279 and Ser-282 of connexin43 regulates endocytosis and gap junction assembly in pancreatic cancer cells

Kristen E. Johnson, Shalini Mitra, Parul Katoch, Linda S. Kelsey, Keith R. Johnson, and Parmender P. Mehta

Department of Biochemistry and Molecular Biology and Department of Oral Biology, Eppley Institute for Research in Cancer and Allied Diseases, Eppley Cancer Center, University of Nebraska Medical Center, Omaha, NE 68198

ABSTRACT The molecular mechanisms regulating the assembly of connexins (Cx) into gap junctions are poorly understood. Using human pancreatic tumor cell lines BxPC3 and Capan-1, which express Cx26 and Cx43, we show that, upon arrival at the cell surface, the assembly of Cx43 is impaired. Connexin43 fails to assemble, because it is internalized by clathrin-mediated endocytosis. Assembly is restored upon expressing a sorting-motif mutant of Cx43, which does not interact with the AP2 complex, and by expressing mutants that cannot be phosphorylated on Ser-279 and Ser-282. The mutants restore assembly by preventing clathrin-mediated endocytosis of Cx43. Our results also document that the sorting-motif mutant is assembled into gap junctions in cells in which the expression of endogenous Cx43 has been knocked down. Remarkably, Cx43 mutants that cannot be phosphorylated on Ser-279 or Ser-282 are assembled into gap junctions only when connexons are composed of Cx43 forms that can be phosphorylated on these serines and forms in which phosphorylation on these serines is abolished. Based on the subcellular fate of Cx43 in single and contacting cells, our results document that the endocytic itinerary of Cx43 is altered upon cell-cell contact, which causes Cx43 to traffic by EEA1-negative endosomes en route to lysosomes. Our results further show that gap-junctional plaques formed of a sorting motif-deficient mutant of Cx43, which is unable to be internalized by the clathrin-mediated pathway, are predominantly endocytosed in the form of annular junctions. Thus the differential phosphorylation of Cx43 on Ser-279 and Ser-282 is fine-tuned to control Cx43's endocytosis and assembly into gap junctions.

Monitoring Editor

Asma Nusrat
Emory University

Received: Jul 25, 2012

Revised: Jan 17, 2013

Accepted: Jan 18, 2013

This article was published online ahead of print in MBoC in Press (<http://www.molbiolcell.org/cgi/doi/10.1091/mbo.12-07-0537>) on January 30, 2013.

Address correspondence to: Parmender P. Mehta (pmehta@unmc.edu).

Abbreviations used: AP, adaptor protein; Bx43KD, BxPC3 stably knocked-down cells; Bx43DKI, Bx43KD cells with knocked-in WT or mutant Cx43; CP43KD, Capan-1 stably knocked-down cells; CP43DKI, CP43KD cells with knocked-in WT or mutant Cx43; Cx, connexin; DAPI, 4',6-diamidino-2-phenylindole; GFP, green fluorescent protein; LY, Lucifer Yellow; MAP, mitogen-activated protein; mEGFP, Monomeric enhanced green fluorescent protein; PBS, phosphate-buffered saline; Rab5-DA, dominant-active Rab5; Rab5-DN, dominant-negative Rab5; Rab5-WT, wild-type Rab5; RT-PCR, reverse transcriptase polymerase chain reaction; shRNA, short hairpin RNA; TX100, Triton X-100; UTR, untranslated region; WT, wild type; YA/VD-Cx43, mutant Y286A/V289D.

© 2013 Johnson et al. This article is distributed by The American Society for Cell Biology under license from the author(s). Two months after publication it is available to the public under an Attribution–Noncommercial–Share Alike 3.0 Unported Creative Commons License (<http://creativecommons.org/licenses/by-nc-sa/3.0/>).

"ASCB®," "The American Society for Cell Biology®," and "Molecular Biology of the Cell®" are registered trademarks of The American Society of Cell Biology.

INTRODUCTION

Gap junctions, formed of proteins called connexins (Cx), are ensembles of several cell–cell channels that signal by permitting the direct exchange of small molecules between the cytoplasmic interiors of contiguous cells. Evidence is mounting that this form of signaling fulfills a homeostatic role through buffering of spatial gradients of nutrients and small molecules of <1500 Da (Goodenough and Paul, 2009). Connexins, which are designated according to molecular mass, are family of 21 related proteins, some of which are expressed in a tissue-specific manner, while others are expressed redundantly (Beyer and Berthoud, 2009). A cell–cell channel is formed when newly synthesized Cx oligomerize as a hexamer to form a connexon that, upon reaching the cell surface, docks with a connexon in an adjacent cell. A gap junction, often called a gap-junctional plaque, is formed when several such channels cluster.

The half-life of most Cxs has been determined to lie between 2 and 5 h both *in vivo* and *in vitro*, revealing gap-junctional plaques to be highly dynamic macromolecular complexes (Laird, 2006; Goodenough and Paul, 2009). Because a gap junction is a bicellular structure and is assembled by the collaborative effort of two cells, it is as yet not precisely known how the formation of a nascent gap-junctional plaque is initiated at the site of cell–cell contact, how the plaque assembles and grows, and how it is endocytosed and disassembled (Musil, 2009).

With regard to assembly, current evidence supports the notion that, once a plaque has been nucleated or a nascent gap junction formed, the plaque grows either when connexons, which have been delivered to the cell surface randomly, are recruited to its periphery by diffusion (Gaietta et al., 2002; Lauf et al., 2002; Thomas et al., 2005), or when connexons are directly delivered to the plaque itself (Shaw et al., 2007). Moreover, it is thought that docking of connexons occurs either in the plaque itself or in its vicinity. Furthermore, given the fact that an ensemble of cells has gap junctions of diverse sizes, it is also not known whether larger plaques arise from the coalescence of smaller plaques or by the continuous accretion of undocked or docked connexons to the plaque periphery. With regard to disassembly, recent studies have shown that gap junctions disassemble intricately, either through the endocytosis of the plaque in its entirety or through endocytosis of senescent plaque components from the center as double-membrane vesicles (Jordan et al., 2001; Gaietta et al., 2002; Piehl et al., 2007; Nickel et al., 2008; Falk et al., 2009). Recently gap junctions have also been found to be degraded by autophagy upon internalization (Hesketh et al., 2010; Lichtenstein et al., 2011; Bejarno et al., 2012; Fong et al., 2012).

Our previous studies with cadherin-null human squamous carcinoma cells showed that the assembly of Cx43, which is ubiquitously expressed (Laird, 2006), was facilitated by cell–cell adhesion mediated by cadherins although cadherins were not required to initiate the formation of nascent gap-junctional plaques. On the other hand, the assembly of Cx32, which is expressed in well-differentiated and polarized cells (Bosco et al., 2011), was induced only when cells acquired a partially polarized state (Chakraborty et al., 2010). Our subsequent studies with nontransformed rat epithelial cells showed that the assembly of Cx43 was differentially regulated by E-cadherin and N-cadherin at sites of cell–cell contact. When only E-cadherin was expressed, Cx43 was preponderantly assembled into large gap junctions, and when only N-cadherin was expressed, Cx43 was endocytosed prior to assembly into gap junctions (Govindarajan et al., 2010). These studies suggest that the assembly of Cxs into gap junctions upon arrival at the cell surface is subject to regulatory mechanisms at the site of cell–cell contact and may be dependent upon additional proteins that permit or impede assembly. The extent to which the assembly of a particular connexon into gap junctions upon arrival at the cell surface is determined by factors intrinsic to the connexon itself or by extrinsic factors, such as the direct or indirect interaction of a Cx with other cell surface-associated protein(s), has not yet been explored (Laird, 2010; Herve et al., 2012). Although many proteins have been shown to interact with Cxs either directly or indirectly, not much is known about the molecular nature of these interactions and how they impose local constraints to restrict or permit the assembly of a particular connexon upon arrival at the cell surface (Laird, 2010; Herve et al., 2012).

As a first step toward elucidating the molecular mechanisms by which the assembly of a particular connexon is regulated at the site of cell–cell contact, we chose a tumor cell line that expressed two or more Cxs and in which the assembly of one of the Cxs was efficient, while that of the other Cx was inefficient. Using human pancreatic

tumor cell line BxPC3, which expresses an exocrine pancreas-specific Cx, Cx26, as well as a ubiquitously expressed Cx, Cx43, we show that only the assembly of Cx43 into gap junctions is impaired, because it is selectively internalized prior to assembly. Moreover, we show that the defective assembly of Cx43 is caused by the endocytosis of connexons by the clathrin-mediated pathway. Furthermore, we provide evidence that defective assembly is restored by expressing a sorting-motif mutant of Cx43 that cannot be endocytosed by the clathrin-mediated pathway. In addition, we document that assembly of Cx43 can also be restored by preventing phosphorylation of Ser-279 or Ser-282, previously shown to be phosphorylated by mitogen-activated protein (MAP) kinase (Warn-Cramer et al., 1998). Finally, our results document that defective assembly can only be restored when connexons are composed of Cx43 forms that can be phosphorylated on Ser-279 and Ser-282 and Cx43 forms in which phosphorylation of these serines is abolished. Our results suggest that differential phosphorylation of Cx43 on these serines is fine-tuned to control endocytosis, plaque growth, and size.

RESULTS

Defective assembly of Cx43 in BxPC3 and Capan-1 cells

Cx32 and Cx26 are expressed in the acinar cells of the exocrine pancreas (Bavamian et al., 2009). We screened several human pancreatic cancer cell lines by semiquantitative reverse transcriptase PCR (RT-PCR) for the expression of Cxs (unpublished data) and chose two cell lines, BxPC3 and Capan-1, which expressed Cx43 and Cx26. As was reported earlier (Lahlou et al., 2005), upon immunocytochemical and Western blot analysis, we found that Cx43 was not assembled into gap junctions in either cell line and lay predominantly as discrete intracellular vesicular puncta dispersed throughout the cytoplasm (Figure 1A). On the other hand, Cx26 formed gap junctions in BxPC3 cells but remained intracellular in Capan-1 cells (Supplemental Figure S1, left panels). To substantiate the immunocytochemical data, we determined the extent of assembly of Cx43 into gap junctions biochemically by Western blot analysis of total and Triton X-100 (TX100)-soluble and TX100-insoluble fractions (VanSlyke and Musil, 2000) and upon *in situ* extraction with 1% TX100. The results showed that Cx43 remained predominantly detergent-soluble in both cell lines, as assessed by the disappearance of intracellular puncta (Figure 1B) and by the majority of Cx43 appearing in the detergent-soluble fraction (Figure 1C). For example, the mean number of Cx43 intracellular puncta in both cell lines after detergent extraction was reduced from 82 ± 13 ($n = 14$) and 104 ± 19 ($n = 17$) per cell to 11 ± 4 ($n = 13$) and 7 ± 3 ($n = 14$) per cell in BxPC3 and Capan-1 cells, respectively. Because Cx26 was assembled into gap junctions, whereas Cx43 was not, we next examined the assembly of Cx32 in BxPC3 and Capan-1 cells upon retroviral transduction. We found that Cx32 assembled into gap junctions in BxPC3 cells, but not in Capan-1 cells, as assessed immunocytochemically and biochemically with TX100-solubility assays (Figure S1). Altogether the results shown in Figures 1 and S1 suggest the following: 1) In BxPC3 cells, both Cx26 and Cx32 are efficiently assembled into gap junctions, but the assembly of Cx43 is selectively impaired. 2) In Capan-1 cells, the assembly of all three Cxs is impeded.

To examine whether the failure of Cx43 to assemble into gap junctions was due to impaired trafficking or to endocytosis prior to assembly into gap junctions, we used cell surface biotinylation, as well as markers for the secretory and the endocytic compartments, to assess its subcellular fate. Using biotinylation of E-cadherin as a positive control, we found that Cx43 was biotinylated significantly in both BxPC3 and Capan-1 cells (Figure 1D). However, immunocytochemical

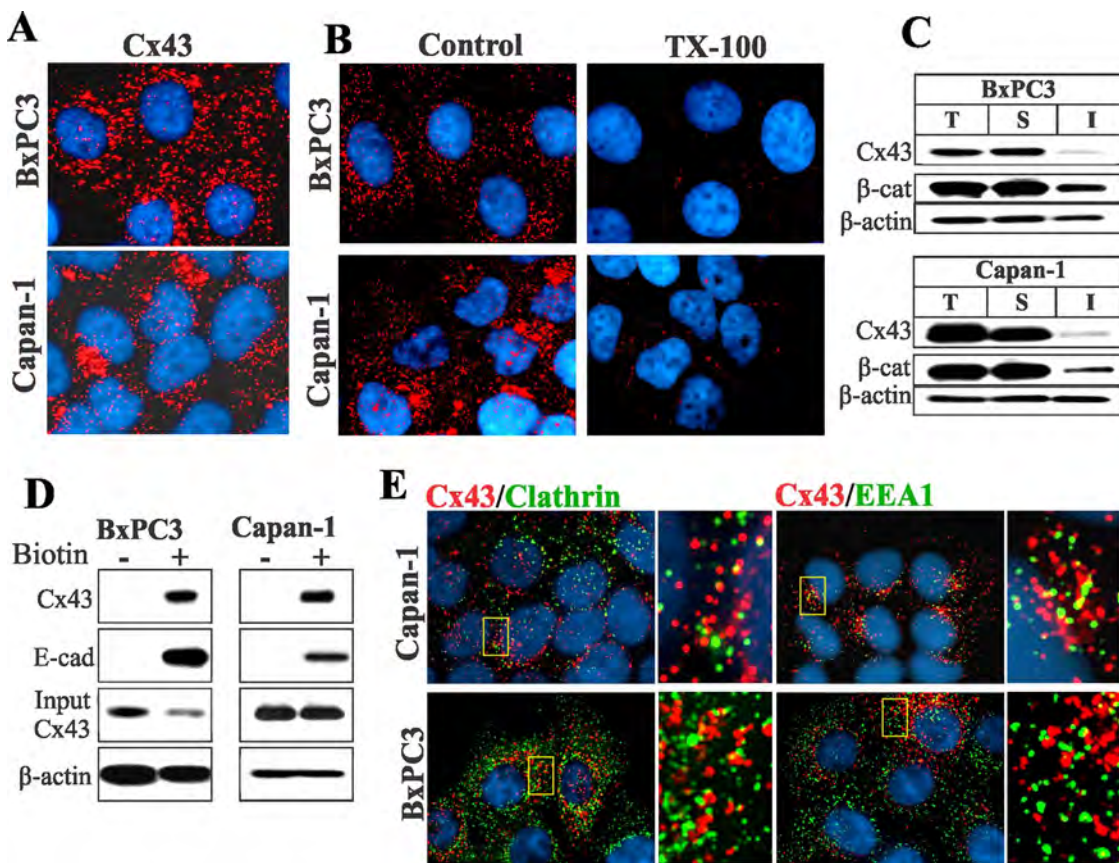


FIGURE 1: Cx43 fails to assemble into gap junctions in BxPC3 and Capan-1 cells. (A) Cells were immunostained for Cx43. Note that in both BxPC3 and Capan-1 cells, Cx43 (red) is seen as discrete intracellular puncta dispersed throughout the cytoplasm. (B) Loss of Cx43 intracellular puncta upon *in situ* extraction with 1% TX100 in BxPC3 and Capan-1 cells. Note loss of Cx43 intracellular puncta upon extraction with TX100. (C) Western blot analysis of Cx43 in total (T), TX100-soluble (S), and TX100-insoluble (I) fractions of cell lysates in BxPC3 and Capan-1 cells. Note that the majority of Cx43 is soluble in TX100 in both cell types. (D) Cx43 traffics to the cell surface in BxPC3 and Capan-1 cells. The cell surface proteins of BxPC3 and Capan-1 cells were biotinylated. Biotinylated proteins were pulled down by immobilized streptavidin and immunoblotted for Cx43. Biotinylation of E-cadherin (E-cad) was used as a positive control. For input, 10 µg total cell lysate was used. Note that Cx43 and E-cad were efficiently biotinylated in both cell lines. (E) Cells were immunostained for Cx43 (red), clathrin, and EEA1. Enlarged images of the boxed regions are shown on the right. Note that Cx43 does not colocalize discernibly with either marker.

analysis showed that Cx43 barely colocalized with clathrin (Roth, 2006), the early endocytic marker EEA1 (Mills et al., 1998), or caveolin 1 (Parton and Simons, 2007; Figures 1E and S2A). This conclusion was supported by quantitative analysis (Figure S2C). On the other hand, discernible colocalization was observed with GM130, a *cis*-Golgi-resident protein (Nakamura et al., 1995), and with caveolin 2 (Parton and Simons, 2007), which are markers for the secretory compartments (Figure S2A), as well as with the lysosomal marker Lamp1 (Rohrer et al., 1996; Hunziker and Geuze, 2011; Figure S2B). Taken together, these data suggest that intracellular accumulation of Cx43 in BxPC3 and Capan-1 cells is not caused by impaired trafficking to the cell surface, but by some mechanism that selectively interferes with its assembly into gap junctions, causing it to accumulate in intracellular vesicles, yet permitting the assembly of Cx32 and Cx26 into gap junctions.

Endocytosis of Cx43

Because Cx43 trafficked to the cell surface, yet failed to colocalize discernibly with endocytic markers, we used other approaches to examine whether it was endocytosed prior to assembly into gap

junctions. We first used hypertonic sucrose to inhibit the clathrin-mediated pathway (Heuser and Anderson, 1989) and filipin to inhibit the lipid-mediated pathway (Schnitzer et al., 1994). We found that exposure of cells to hypertonic conditions for 1–2 h caused the disappearance of Cx43 intracellular puncta and the concomitant increase in cell surface-associated Cx43, whereas filipin had no effect (unpublished data). These findings hinted that clathrin-mediated endocytosis was involved. Earlier studies had shown that the cytoplasmic tail of Cx43 harbored a consensus protein–protein interaction proline-rich motif and an overlapping putative tyrosine-based sorting motif (278-LSPMSPPGYKLV-289) that potentially targeted it for internalization via the clathrin-mediated pathway (Thomas et al., 2003). We therefore directly tested whether Cx43 interacted with the μ2 subunit of the clathrin adapter complex AP2 by using a yeast two-hybrid analysis (Figure 2A). The results showed that, while the cytoplasmic tail of wild-type (WT) Cx43 interacted with the μ2 subunit of AP2, Cx43 mutants (Y286A, V289D, and Y286A/V289D), in which either tyrosine or valine or both amino acids of the sorting motif had been mutated, did not. The mutant Y286A/V289D hereafter will be referred to as YA/VD-Cx43. All the

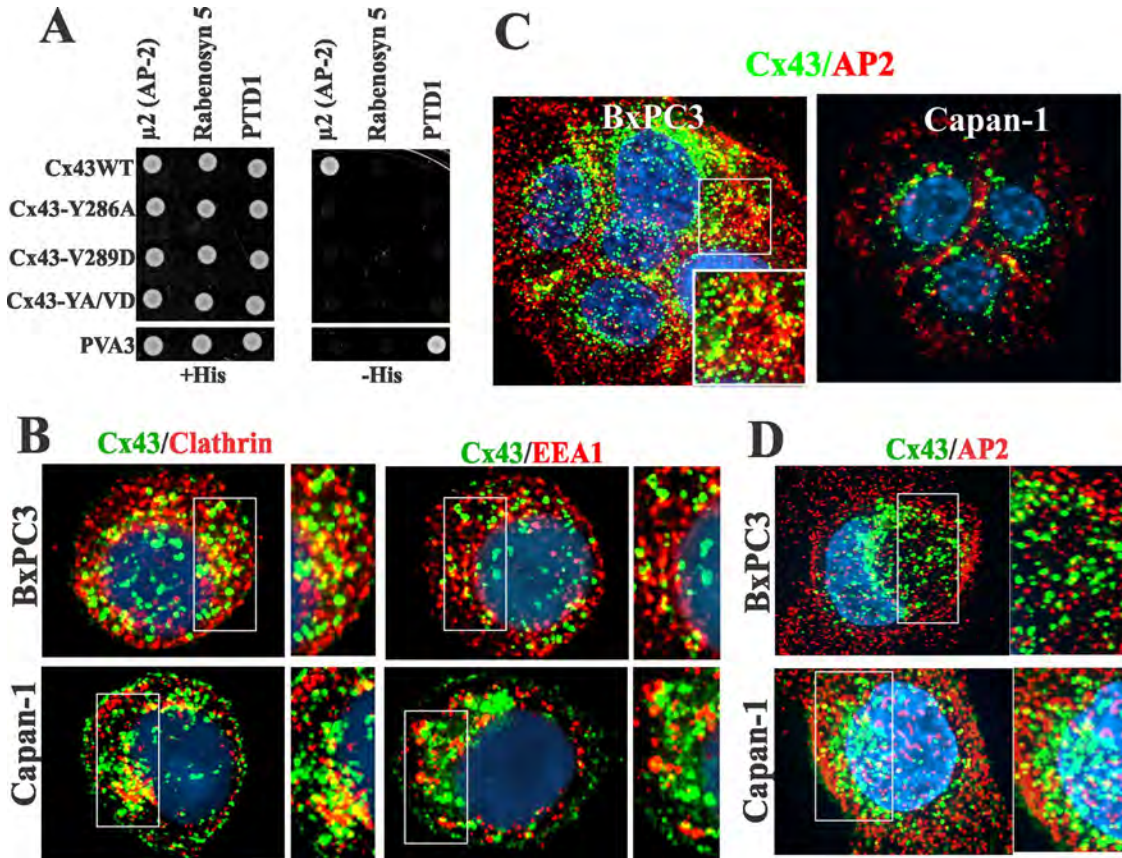


FIGURE 2: (A) In the yeast two-hybrid assay, Cx43 interacts with the μ 2 subunit of the AP2 complex in a sorting motif-dependent manner. Yeast were cotransformed with the indicated GAL4-binding domain and GAL4 transcription activation domain fusion constructs. Measured by growth on selective media (-His), only the wild-type (WT) tail of Cx43 interacted with the μ 2 subunit of the AP2 complex. PVA3 (p53) and PTD1 (large T-antigen) served as positive control, while rabinosyn-5 served as the negative control. (B) Cx43 (green) colocalizes with clathrin and EEA-1 in single cells. (C and D) Cx43 (green) colocalizes with the AP2 complex (red) in both single and contacting cells. (B–D) Outlined boxes are shown at higher power.

mutants and engineered constructs used are diagrammed in Figure 12 under *Materials and Methods* later in the paper.

Our previous studies showed that Cx43 colocalized extensively with clathrin and EEA1 in single cells but not in contacting cells (Govindarajan et al., 2010). Therefore we examined the subcellular fate of Cx43 in single BxPC3 and Capan-1 cells 24–36 h after seeding to determine whether it was endocytosed by the clathrin-mediated pathway. We rationalized that, due to the short half-life of Cx43, intracellular puncta in single cells would plausibly represent endocytosed connexons that had trafficked to the cell surface. We observed a marked colocalization of Cx43 with clathrin and EEA1 (Figure 2B), as well as with Lamp1 (Figure S3A), but no colocalization with caveolin 1 (Figure S3A). The data shown in Figure 2A prompted us to examine whether Cx43 would colocalize with the AP2 complex. The results showed that Cx43 colocalized discernibly with the AP2 complex both in contacting (Figure 2C) and single cells (Figure 2D). To determine whether AP2 complex interacts with WT-Cx43, we transiently expressed the monomeric enhanced green fluorescent protein (mEGFP)-tagged μ 2 subunit of the adaptor protein (AP2) complex (Ohno et al., 1995) in HEK293 cells, which express endogenous Cx43. The results showed that Cx43 could be immunoprecipitated from the total cell lysates with antibody to green fluorescent protein (GFP) green fluorescent protein (Figure S3B). We used HEK293 cells due to the low

transfection efficiencies of BxPC3 and Capan-1 cells. Altogether these data indicate that Cx43 interacts with the μ 2 subunit of AP2 complex either directly or indirectly.

To lend further support to the above data, and given the involvement of Rab5 in clathrin-mediated endocytosis (Bucci et al., 1992; Zerial and McBride, 2001), we also examined whether Rab5 was involved in the endocytosis of Cx43 (Figure S3). We transiently expressed wild-type Rab5 (Rab5-WT) and its dominant-active (Rab5-DA) and dominant-negative (Rab5-DN) mutants conjugated with EGFP in BxPC3 and Capan-1 cells. The results showed that expression of Rab5-DN profoundly reduced the number of EEA1-positive vesicles, suggesting that the generation of EEA1-positive vesicles was Rab5-dependent in both cell lines (unpublished data). In agreement with the effect of Rab5-DN on the generation of EEA1-positive vesicles, we found that the expression of Rab5-DN also drastically reduced the number of Cx43 intracellular puncta (Figure S3A). These results suggest that the generation of Cx43-positive intracellular vesicles depends on Rab5, which also regulates the productive endocytosis of Cx43. Altogether the above data demonstrate that Cx43 is endocytosed by the clathrin-mediated pathway in a Rab5-dependent manner in both cell types, but that Cx43 colocalizes with clathrin—and predominantly traffics via EEA1-positive endosomes—only in single cells, whereas in contacting cells, it traffics via EEA1-negative endosomes.

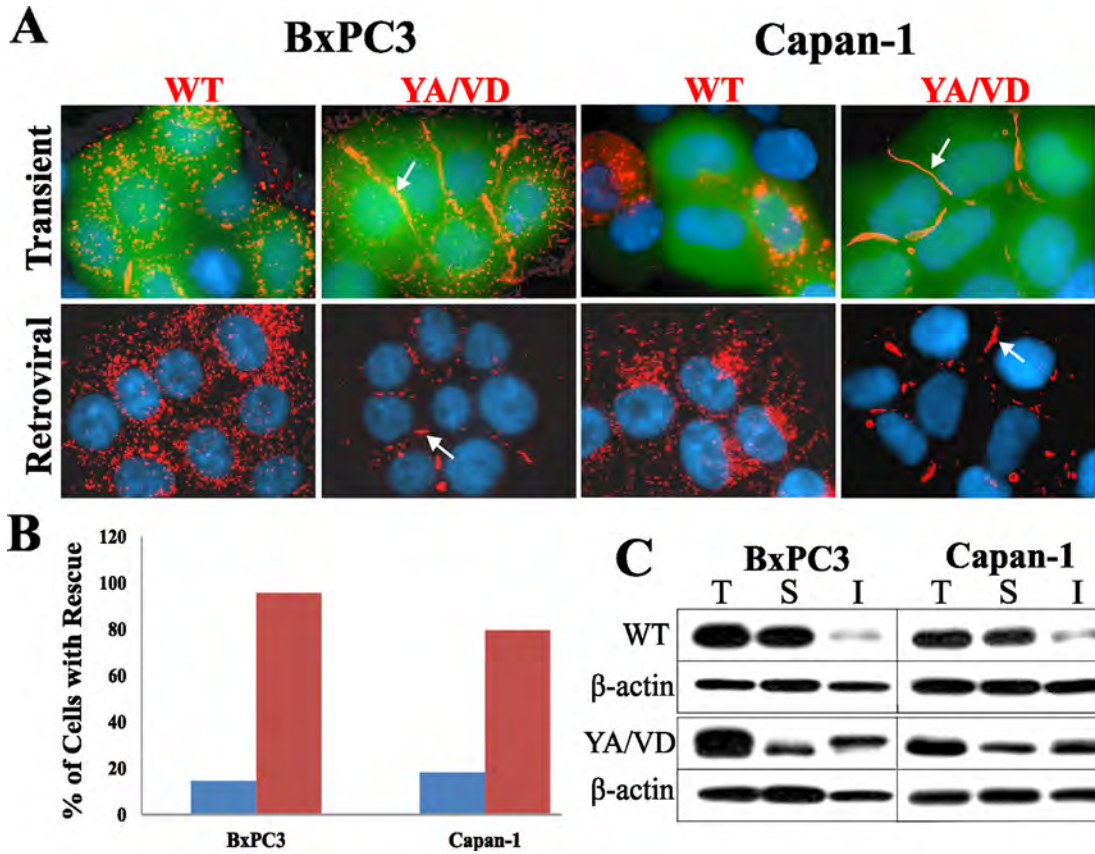


FIGURE 3: The sorting-motif mutant YA/VD-Cx43 restores gap junction assembly. (A) WT-Cx43 (WT) and YA/VD-Cx43 (YA/VD) were expressed in cells by transient transfection (top row) or by retroviral infection (bottom row). Cells were immunostained for Cx43. For transient expression, WT-Cx43 and YA/VD-Cx43 were cotransfected with EGFP to mark the transfected cells. Note the formation of gap junctions (arrows) in cells expressing YA/VD-Cx43. (B) The percentage of transfected cells that had gap junctions was determined by examining 20 cells from two experiments (blue bars: cells expressing WT-Cx43; red bars: cells expressing YA/VD-Cx43). Note the increase in gap junction number in cells transfected with YA/VD-Cx43. (C) Total (T), TX100-soluble (S), and TX100-insoluble (I) fractions were prepared from cells expressing retrovirally introduced WT-Cx43 or YA/VD-Cx43. Note the robust increases in the detergent-insoluble fractions in cells infected with YA/VD-Cx43.

Cells expressing YA/VD-Cx43 assemble gap junctions

Various Cx subtypes have been shown to oligomerize to form heteromeric connexons that are incorporated into gap-junctional plaques (Jiang and Goodenough, 1996; Valiunas et al., 2001; Churko et al., 2010). We hypothesized that the sorting-motif mutant YA/VD-Cx43, by forming heteromers with the endogenous Cx43, might affect junction assembly by inhibiting endocytosis. To pursue this hypothesis, we investigated whether expression of YA/VD-Cx43 would restore defective gap junction assembly in BxPC3 and Capan-1 cells. WT-Cx43 or YA/VD-Cx43 were transiently expressed in each cell type along with EGFP to mark transfected cells, and the formation of gap junctions was assessed immunocytochemically. The results showed that expressing YA/VD-Cx43 induced the formation of large gap-junctional plaques, while expressing WT-Cx43 did not (Figure 3A, top panels). To rule out that the restoration of junction assembly was an artifact of overexpression, we also expressed WT-Cx43 or YA/VD-Cx43 via recombinant retroviruses. The results showed that the retroviral expression of YA/VD-Cx43 restored gap junction assembly with a concomitant decrease in intracellular puncta, although not as robustly as upon transient expression (Figure 3A, bottom panels). Detergent-solubility assays showed the detergent-insoluble

fraction was substantially increased upon expressing YA/VD-Cx43 (Figure 3C), substantiating the data obtained from the immunocytochemical analysis.

To examine whether YA/VD-Cx43 restored assembly by incorporating into gap-junctional plaques that also contained the endogenous Cx43, we transiently expressed Myc-tagged YA/VD-Cx43 in BxPC3 and Capan-1 cells and examined whether all forms of Cx43 were incorporated into gap-junctional plaques. Within the sensitivity of the light microscope and based on the pattern of colocalization, the results showed that total Cx43 colocalized nearly completely with YA/VD-Cx43-Myc (Figure 4A). If endogenous Cx43 did not assemble with YA/VD-Cx43-Myc, some of the red signal would appear alone. To determine whether YA/VD-Cx43 formed heteromers with WT-Cx43, and to substantiate the immunocytochemical data, we transiently expressed both WT-Cx43EGFP and YA/VD-Cx43-Myc (or the reciprocally labeled protein) in HeLa cells. We examined whether the two proteins could be coimmunoprecipitated from the detergent-soluble fraction, since that fraction is likely to contain only connexons that are not incorporated into gap-junctional plaques (Van Slyke and Musil, 2000). We used HeLa cells for coimmunoprecipitation, because of the low transfection efficiencies of BxPC3 and Capan-1 cells. The results showed that

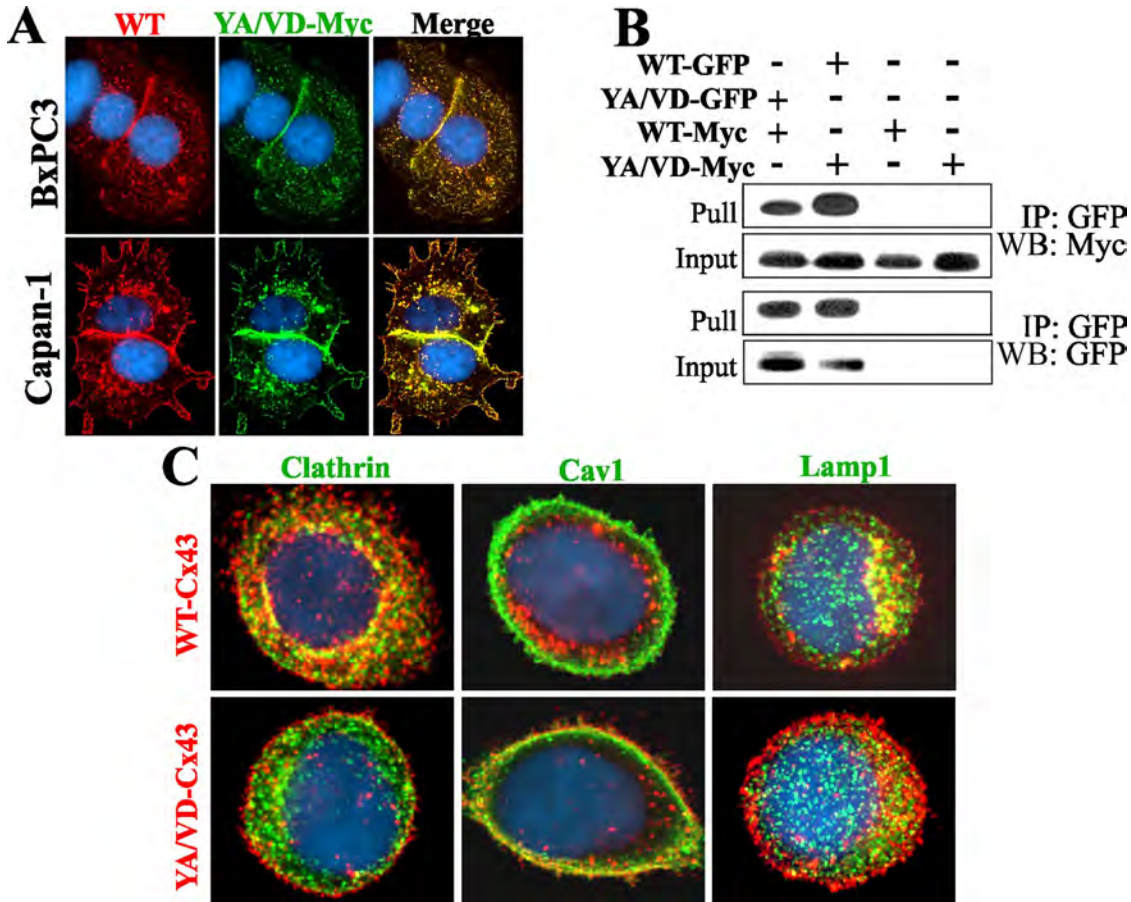


FIGURE 4: Sorting-motif mutant YA/VD-Cx43 restores defective gap junction assembly by incorporating into gap junctions and inhibiting clathrin-mediated endocytosis. (A) BxPC3 and Capan-1 cells expressing endogenous Cx43 were transiently transfected with YA/VD-Cx43-Myc (YA/VD-Myc) and immunostained for Myc and Cx43. Note the robust colocalization of YA/VD-Cx43-Myc with total Cx43 (WT) and the formation of gap junctions. (B) Coimmunoprecipitation of WT-Cx43 and YA/VD-Cx43. HeLa cells were transfected with YA/VD-Cx43EGFP (YA/VD-GFP), WT-Cx43-Myc (WT-Myc), WT-Cx43EGFP (WT-GFP), and YA/VD-Cx43-Myc (YA/VD-Myc) either alone or in the various combinations indicated. GFP-tagged proteins were pulled down with immobilized anti-GFP antibody. Note that YA/VD-Cx43-Myc coimmunoprecipitated with YA/VD-Cx43EGFP and WT-Cx43-Myc coimmunoprecipitated with YA/VD-Cx43EGFP. (C) Capan-1 cells, expressing endogenous Cx43 along with retrovirally introduced WT-Cx43 or YA/VD-Cx43, were seeded as single cells and immunostained for Cx43 (red) and either clathrin, Caveolin 1 (Cav1), or Lamp1 (green). Note that puncta composed of both endogenous Cx43 and retrovirally introduced WT-Cx43 colocalize extensively with clathrin and Lamp1 but not with Cav1. In contrast, puncta composed of both endogenous Cx43 and retrovirally introduced YA/VD-Cx43 fail to colocalize with clathrin, but colocalize discernibly with Cav1 at cell borders.

WT-Cx43 and YA/VD-Cx43 reciprocally coimmunoprecipitated with each other (Figure 4B).

To test whether the formation of heteromers between endogenous Cx43 and YA/VD-Cx43 restored gap junction assembly by inhibiting endocytosis of connexons, we examined the colocalization of Cx43 with clathrin in single Capan-1 cells expressing retrovirally introduced WT-Cx43 or YA/VD-Cx43 in addition to endogenous Cx43. The results showed that, in contrast with discernible colocalization of Cx43 with clathrin in single cells expressing retroviral WT-Cx43, no colocalization was observed in cells that expressed YA/VD-Cx43 (Figure 4C). We also found that, in contrast with WT-Cx43, heteromers of endogenous Cx43 and YA/VD-Cx43 colocalized discernibly with caveolin 1 (Figure 4C, bottom middle panel). Both WT-Cx43 and the heteromers of endogenous Cx43 and YA/VD-Cx43 were routed to lysosomes, as assessed by colocalization of Cx43 with Lamp1 in single cells expressing either WT-Cx43 or YA/VD-Cx43 (Figure 4C). Collectively the data shown in Figures 3 and

4 document that the expression of the YA/VD-Cx43 mutant restores gap junction assembly in BxPC3 and Capan-1 cells and that the restoration occurs through inhibition of clathrin-mediated endocytosis of connexons.

Phosphorylation of Ser-279 and Ser-282 of Cx43 and gap junction assembly

Phosphorylation of serine and tyrosine residues in or adjacent to sorting motifs modulates the endocytosis of many transmembrane proteins (Bonifacino and Traub, 2003; Moore et al., 2007; Traub, 2009). Thus we rationalized that the phosphorylation of Ser-279 and Ser-282 of Cx43, which lay near the sorting motif, might disrupt its assembly into gap junctions by inducing endocytosis. To test this notion, we created the following Cx43 mutants: 1) S279A and S279D, in which Ser-279 was substituted with alanine or its phosphomimetic, aspartic acid, respectively. 2) S282A and S282D, in which Ser-282 was substituted with alanine or aspartic acid,

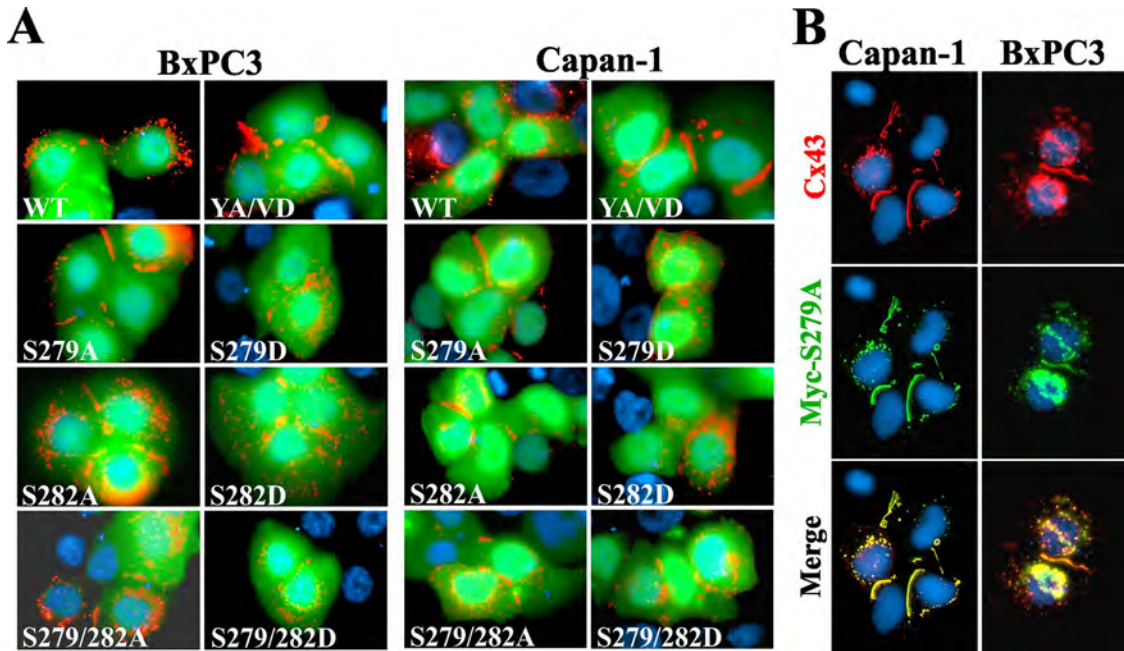


FIGURE 5: S279A and S282A mutants restore gap junction assembly. (A) BxPC3 and Capan-1 cells were transiently cotransfected with EGFP and the indicated Cx43 constructs. Cells were immunostained for Cx43 (red). Note that the S279A and S282A mutants restored gap junction assembly as robustly as the sorting-motif mutant YA/VD-Cx43, whereas S279D and S282D did not. (B) Capan-1 and BxPC3 cells were transiently transfected with Myc-tagged S279A and were immunostained for Cx43 (red) and Myc (green) after 24 h. Note the robust colocalization of total Cx43 with Myc.

respectively. 3) S279A/S282A and S279D/S282D, in which both Ser-279 and Ser-282 were substituted with alanine or aspartic acid, respectively. WT-Cx43 and the above mutants were transiently expressed in BxPC3 and Capan-1 cells along with EGFP to mark the transfected cells. The results showed that the expression of serine-to-alanine mutants (S279A and S282A) restored gap junction assembly, whereas expression of serine-to-aspartic acid mutants (S279D and S282D) had no discernible effect (Figure 5A). Moreover, mutants S279A and S282A restored gap junction assembly as robustly as YA/VD-Cx43 (Figure 5A). Furthermore, restoration with the double mutant S279A/S282A was not more robust than with the single mutants. To test whether mutants restored assembly by incorporating into gap-junctional plaques that also contained endogenous Cx43, we transiently expressed the Myc-tagged mutant S279A-Myc in BxPC3 and Capan-1 cells. The results showed that S279A-Myc colocalized extensively with total Cx43 both in the gap-junctional plaques and in intracellular vesicles (Figure 5B). Collectively these data suggest that phosphorylation on Ser-279 and/or Ser-282 of Cx43 impairs its assembly into gap junctions in BxPC3 and Capan-1 cells and preventing phosphorylation of these residues restores assembly.

Only the sorting-motif mutant assembles into gap junctions in cells with endogenous Cx43 knocked down

BxPC3 and Capan-1 cells express abundant endogenous Cx43 (Figure 1). To test whether those mutants that restored defective gap junction assembly upon transient expression would assemble into gap junctions by themselves, we stably knocked down endogenous Cx43 in both cell types with a short hairpin RNA (shRNA) targeting the 3' untranslated region (UTR). As assessed by Western blot analysis, the expression of endogenous Cx43 was nearly abolished in both cell lines upon knockdown (Figure S4A). Knockdown of Cx43 had no off-target effect on the expression level of seven

other randomly chosen cell junction and cytoskeletal proteins (Figure S4B). These stably knocked-down cells are hereafter referred to as Bx43KD (for BxPC3) and CP43KD (for Capan-1) cells.

We used recombinant retroviruses to knock in wild-type and mutant Cx43 in Bx43KD and CP43KD cells. Western blot analysis showed that the knocked-in WT-Cx43 and Cx43 mutants were expressed robustly (Figure 6A). However, unexpectedly, we observed that only YA/VD-Cx43 assembled into gap junctions, whereas the other mutants did not (Figure 6B). Hereafter, Bx43KD and CP43KD with knocked-in WT or mutant Cx43 will be referred to as Bx43KDKI and CP43KDKI cells, followed by the name of the constructs expressed. To substantiate the immunocytochemical data, we determined the assembly of knocked-in WT-Cx43, sorting-motif mutant YA/VD-Cx43, and mutants S279A and S279D biochemically by the TX100-solubility assay and upon *in situ* extraction with 1% TX100. We also performed functional analysis by scrape-loading and microinjection of gap junction-permeable fluorescent tracers. The results showed that only the YA/VD-Cx43 mutant assembled into detergent-insoluble, gap-junctional plaques, as assessed immunocytochemically (Figure 7A) and biochemically by the TX100-solubility assay (Figure 7B). Moreover, as assessed by scrape-loading and microinjection of gap junction-permeable fluorescent tracers Lucifer Yellow (LY), Alexa Fluor 560, and Alexa Fluor 594, only the YA/VD-Cx43 mutant formed functional cell-cell channels (Figure S4, C and D; see also Table 1). Finally, to further substantiate the above data, we retrovirally introduced the same mutants into the human prostate cancer cell line, LNCaP, which we have shown assembles Cxs into gap junctions efficiently (Mehta et al., 1999; Mitra et al., 2006; Kelsey et al., 2012). The results showed that, compared with WT-Cx43, mutant YA/VD-Cx43 formed large gap junctions, whereas mutants S279A and S279D assembled into small gap-junctional puncta, many of which appeared to be intracellular (Figure S5A). In sum, the data shown in Figures 6 and 7 suggest that the

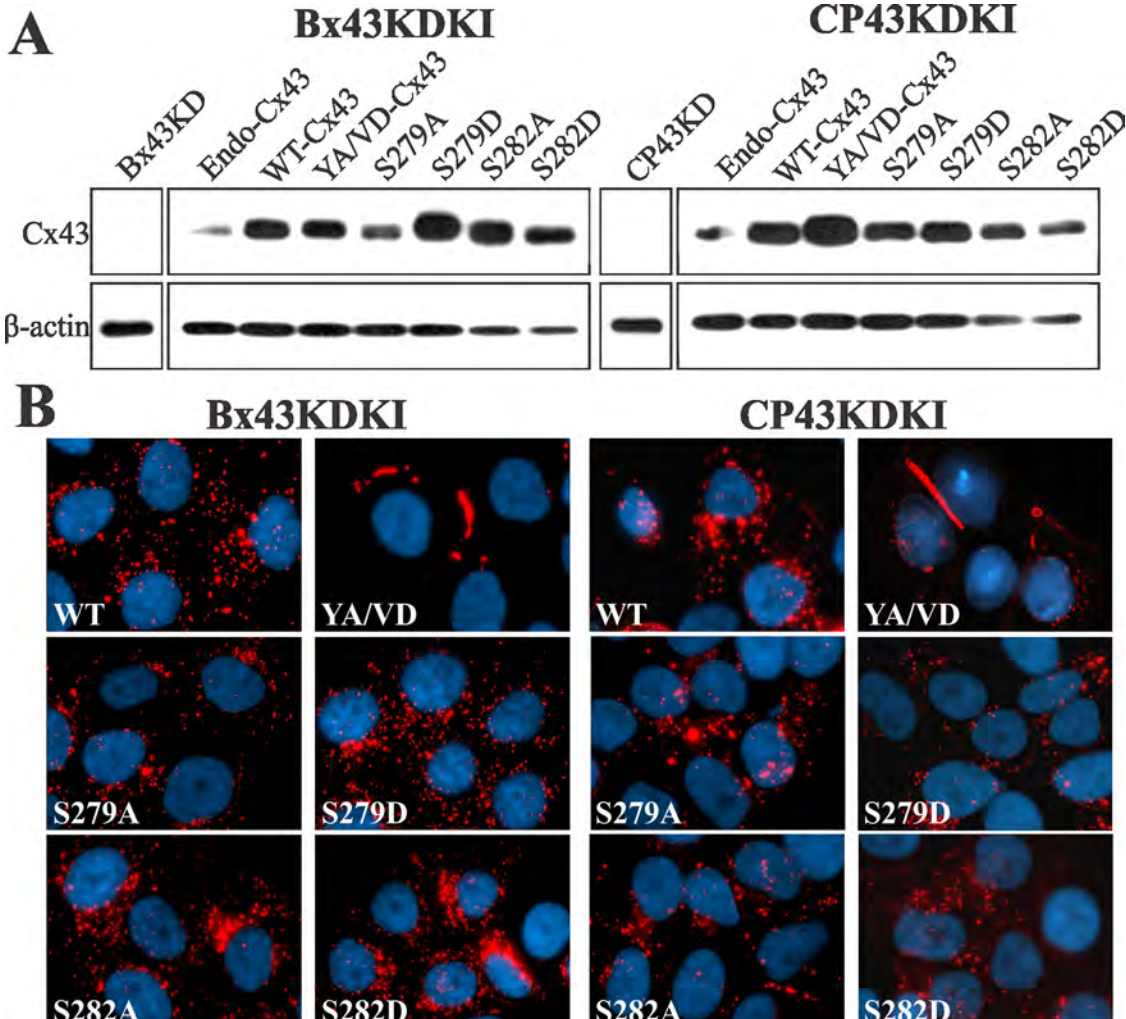


FIGURE 6: Assembly of sorting-motif and serine mutants of Cx43 into gap junctions in knockdown cells. (A) WT-Cx43 or the indicated mutants were knocked in to Bx43KD and CP43KD cells, and lysates were analyzed for Cx43 expression by Western blotting. Note that, compared with parental cells expressing endogenous Cx43 (Endo-Cx43), the knocked-in WT-Cx43 and Cx43 mutants are robustly expressed. No detectable expression is seen in CP43KD and Bx43KD cells. (B) Bx43KD and CP43KD cells expressing the knocked-in WT-Cx43 or Cx43-mutants were immunostained for Cx43. Note that only the sorting motif mutant YA/VD-Cx43 (YA/VD) assembles into gap junctions.

mutants S279A and S282A are unable to assemble into gap junctions in the absence of WT-Cx43.

Wild-type and mutant Cx43 are required for gap junction assembly

To determine directly whether both WT-Cx43 and the S279A mutant are required for junction assembly, we tested whether expression of WT-Cx43 would restore gap junction assembly in Bx43KDKI cells expressing knocked-in S279A. As controls, we also chose Bx43KDKI cells stably expressing either knocked-in WT-Cx43 or Cx43-S279D. WT-Cx43 was transiently expressed along with EGFP to mark the transfected cells (Figure 8A). The results showed the expression of WT-Cx43 restored junction assembly in Bx43KDKI cells expressing S279A but not in cells expressing S279D or WT-Cx43 (Figure 8A, compare middle panel with right and left panels). Similar data were obtained when WT-Cx43 was transiently transfected into CP43KDKI cells stably expressing S279A, S279D, or WT-Cx43 (unpublished data). To test whether WT-Cx43 was incorporated into gap-junctional plaques that also contained S279A,

we checked for colocalization. The results showed extensive colocalization of Myc-tagged WT-Cx43 with total Cx43. Notably, junction assembly was restored only in cells expressing S279A (Figure 8B, top row). Gap junctions were also assembled when Myc-tagged S279A was introduced into Bx43KDKI and CP43KDKI cells stably expressing S279D (unpublished data). Altogether the data shown in Figure 8, combined with those shown in Figures 5–7, suggest that S279A assembled into gap junctions only in the presence of WT-Cx43.

Trafficking, degradation, and subcellular fate of knocked-in WT-Cx43 and its mutants

In the next series of experiments, we examined whether the failure of knocked-in WT-Cx43 and mutants S279A, S279D, S282A, and S282D to assemble into gap junctions was due to impaired trafficking or differential degradation at the cell surface. Therefore we determined the trafficking and the kinetics of degradation of WT-Cx43 and the mutants by cell surface biotinylation. We found that WT-Cx43 and the various Cx43 mutants trafficked to the cell surface (Figure S5B).

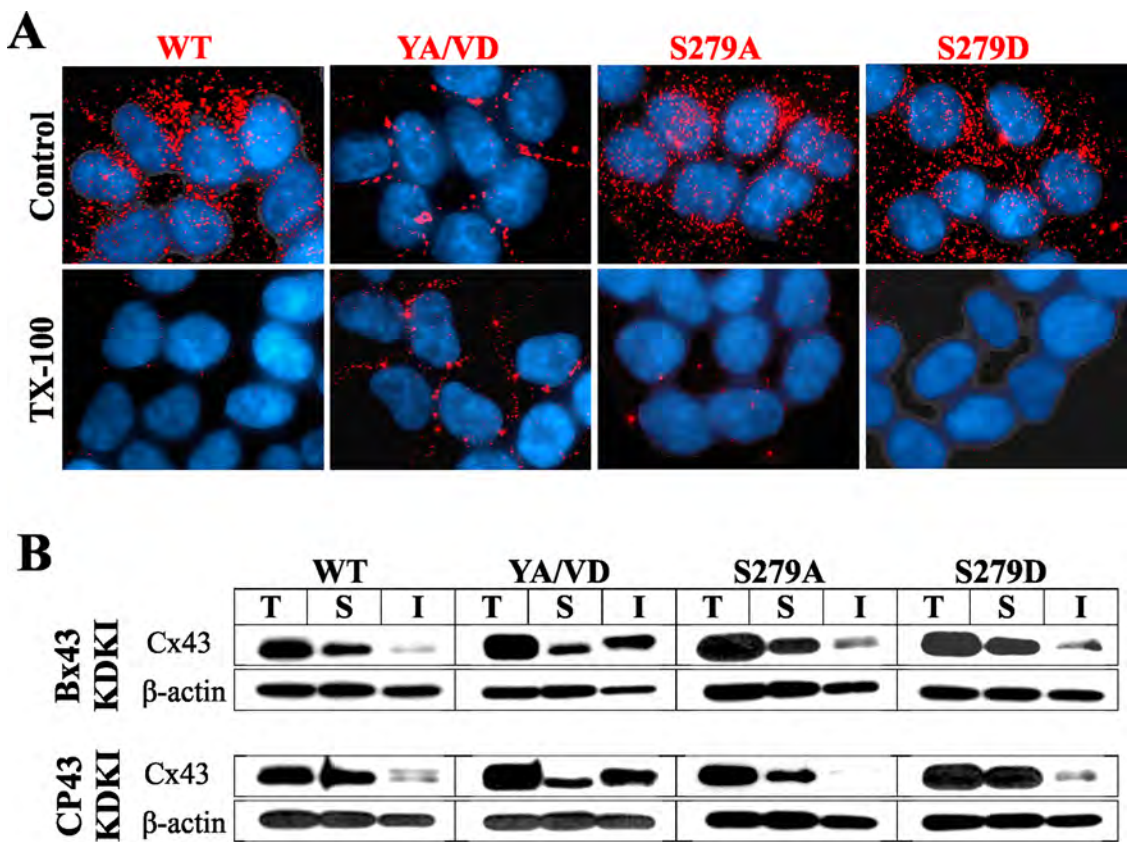


FIGURE 7: Detergent solubility of knocked-in WT-Cx43 and its sorting motif and serine mutants. (A) CP43KD cells expressing knocked-in WT-Cx43 and various mutants were extracted *in situ* with 1% TX100 and immunostained for Cx43. Note that only knocked-in YA/VD-Cx43 (YA/VD) assembles into detergent-resistant gap junction puncta. Note also that intracellular puncta of knocked-in WT-Cx43 (WT) and all other mutants are lost upon extraction with 1% TX100. (B) Western blot analysis of Cx43 in Total (T), TX100-soluble (S), and TX100-insoluble (I) fractions from CP43KD cells expressing knocked-in WT-Cx43 and the mutants. Note that only cells expressing knocked-in YA/VD-Cx43 have a discernible detergent-insoluble fraction. The blots were stripped and reprobed for β -actin to verify equal loading.

Cell type	Junctional tracer		
	LY	Alexa Fluor 488	Alexa Fluor 594
Capan-1 (parental)	0 (21)	0 (24)	15.4 \pm 3.3 (12)
CP43KD	0 (22)	0 (13)	0 (11)
CP43KDKI-WT-Cx43	0 (32)	0 (19)	0 (8)
CP43KDKI-S279A-Cx43	0 (24)	0 (14)	0 (10)
CP43KDKI-S279D-Cx43	0 (23)	0 (24)	0 (9)
CP43KDKI-YA/VD-Cx43	16 \pm 6 (33)	18 \pm 5 (21)	7 \pm 1 (40)

Cells were seeded in 6-cm dishes and grown to 70% confluence. Junctional transfer was measured after microinjecting the indicated fluorescent tracers. The numbers of fluorescent cell neighbors (mean \pm SE) were determined 1 min (LY), 3 min (Alexa Fluor 488), or 15 min (Alexa Fluor 594) after microinjection into the test cells. The total number of injection trials is shown in parentheses.

TABLE 1: Junctional transfer of various fluorescent tracers in parental Capan-1, CP43 knockdown (CP43KD) cells and in CP43KD cells expressing WT-Cx43 and various Cx43 mutants.

Moreover, the kinetics of degradation of all mutants, including YA/VD-Cx43, was not noticeably different from WT-Cx43 (Figure S5C). Because endogenously expressed Cx43 colocalized with clathrin in single parental BxPC3 and Capan-1 cells, we also examined the subcellular fate of knocked-in WT-Cx43, the sorting-motif mutant YA/VD-Cx43, and mutants S279A and S279D in CP43KDKI single cells. The results showed that, in single cells, the knocked-in WT-Cx43 and S279D colocalized discernibly with clathrin, whereas YA/VD-Cx43 and S279A barely colocalized (Figure S6A). Together the data shown in Figures S5 and S6 suggest that the efficient assembly of YA/VD-Cx43 and the inefficient assembly of WT-Cx43 and mutants S279A and S279D can be attributed neither to differential trafficking nor to differential degradation. These data further document that clathrin-mediated endocytosis appears to be the predominant pathway to internalize WT-Cx43 and mutant S279D connexons in single cells, whereas mutant YA/VD-Cx43 and S279A connexons are likely internalized by a non-clathrin-mediated pathway.

Internalization and degradation of mutant YA/VD-Cx43

Intracellular vesicular puncta in cells expressing knocked-in YA/VD-Cx43, the only mutant that formed gap junctions (Figure 6), were fewer, larger, and of diverse sizes that colocalized neither with caveolin 1 nor with clathrin (Figure S6B). We therefore investigated whether this mutant was internalized in the form of annular gap

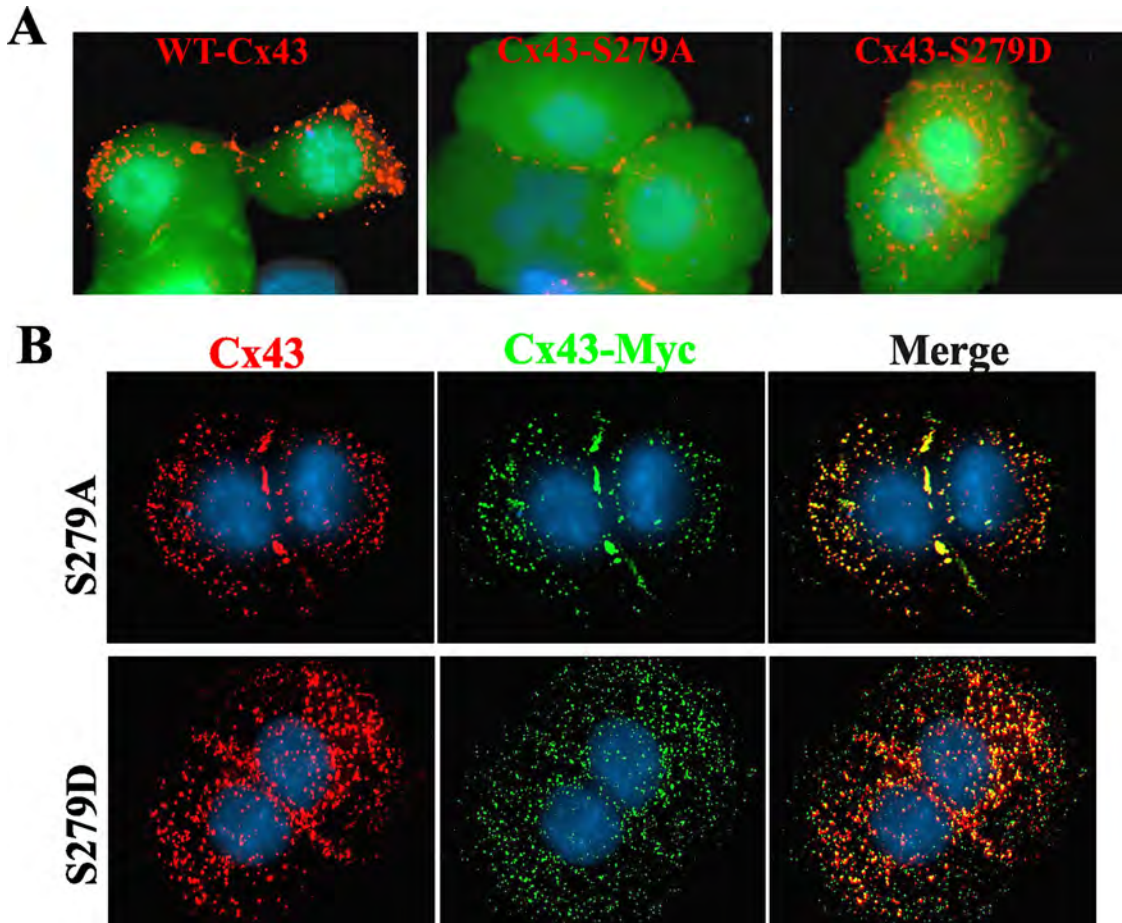


FIGURE 8: Mutant S279A assembles into gap junctions only in the presence of WT-Cx43. (A) Bx43KD cells stably expressing knocked-in WT-Cx43, S279A, and S279D were transfected with WT-Cx43 along with EGFP and immunostained for Cx43 (red). Note that only mutant S279A is assembled into gap junctions upon expression of WT-Cx43. (B) Bx43KD cells stably expressing knocked-in S279A-Cx43 (S279A) or S279D-Cx43 (S279D) were transiently transfected with Myc-tagged WT-Cx43 (Cx43-Myc) and immunostained for Cx43 (red) and Myc (green). Note that total Cx43 and Myc colocalize extensively, but only mutant S279A is assembled into gap junctions.

junctions. We examined whether these intracellular puncta were resistant to *in situ* extraction with 1% TX100. The results showed that the majority of intracellular puncta in YA/VD-Cx43-expressing cells was resistant to *in situ* extraction with TX100 (Figure 9A). To determine whether this mutant is targeted upon internalization for degradation by autophagy, we starved these cells for various times in the absence and presence of bafilomycin A1, which inhibits autophagy (Klionsky et al., 2008; Sarkar et al., 2009; Mizushima et al., 2010). We found that this mutant was degraded upon starvation (Figure 9B). Moreover, this mutant was predominantly internalized in the form of annular gap junctions upon starvation, and the degradation was prevented upon treatment with bafilomycin A1 (Figure 9, A and B). In contrast, degradation of knocked-in WT-Cx43 was minimally affected upon starvation and was not inhibited by bafilomycin A1 (unpublished data). These results suggest that the mutant YA/VD-Cx43 is predominantly internalized in the form of annular gap junctions, most likely by a clathrin-independent pathway, and is likely degraded by autophagy.

Cell–cell contact and the endocytic itinerary of Cx43

Because discernible colocalization of Cx43 with clathrin and EEA1 was observed only in single cells, and because Cx43 significantly

colocalized with AP2 and Lamp1 both in single and contacting cells, we rationalized that cell–cell contact might determine the endocytic route of Cx43. To test this notion, we first determined whether intracellular vesicles in contacting BxPC3 and Capan-1 cells were comprised of docked or undocked connexons or represented internalized minuscule annular gap junctions. To determine this, we first retrovirally expressed Cx43EGFP and Cx43mAPPLE in CP43KD and Bx43KD cells. We then cocultured Bx43KD cells expressing nearly equal levels of either Cx43EGFP or Cx43mAPPLE and, after allowing cells to aggregate as doublets in suspension, seeded them on glass coverslips (see Materials and Methods). We did the same for CP43KD cells infected with the constructs. The doublets of cells were examined 24 h after plating to quantify intracellular puncta that contained either Cx43EGFP or Cx43mAPPLE alone or both. As a control, the same experiment was done with cocultures of the human prostate cancer cell line LNCaP expressing retrovirally introduced Cx43EGFP or Cx43mAPPLE. The results showed that, in both CP43KD and Bx43KD cells, the intracellular vesicular puncta contained either Cx43EGFP or Cx43mAPPLE alone, but not both (Figure 10B). In contrast, LNCaP cells formed gap junctions and intracellular vesicles composed of both Cx43EGFP and Cx43mAPPLE (Figure 10C).

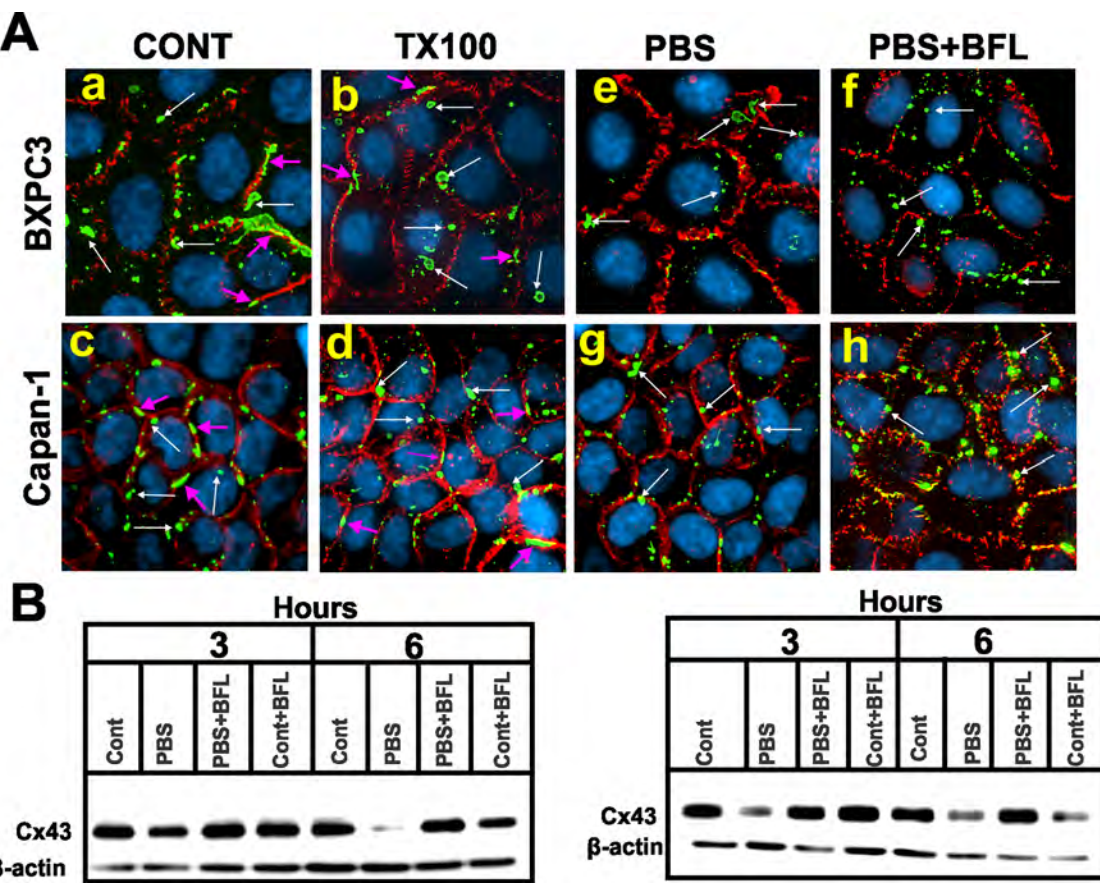


FIGURE 9: YA/VD-Cx43 is likely internalized in the form of annular gap junctions that are detergent resistant and degraded by autophagy. (A) Bx43KD and CP43KD cells expressing YA/VD-Cx43 were immunostained for Cx43 (green) and β-catenin (red). Cells were extracted in situ with 1% TX100 (b and d) or starved in PBS without (PBS e and g) or with baflomycin A1 (BFL PBS+BFL, f and h) for 3 h. (B) CP43KD (left) or Bx43KD (right) cells expressing YA/VD-Cx43 were starved in PBS with or without baflomycin A1 for the indicated times, and cell lysates were immunoblotted for Cx43. Note that the level of YA/VD-Cx43 decreases upon starvation, and the decrease is prevented by BFL. (A) Gap junctions at the areas of cell-cell contact are indicated by the pink arrows, whereas annular gap junctions are indicated by the white arrows. Note that both in normal medium and in PBS, the mutant YA/VD is internalized in the form of annular gap junctions and internalization is not prevented upon treatment with BFL.

To examine whether cell-cell contact alters the endocytic itinerary of Cx43, we cocultured CP43KD and Bx43KD cells with cells expressing knocked-in Cx43EGFP. The cocultures were immunostained for clathrin to examine whether clathrin colocalized with Cx43EGFP. We found that, in both CP43KD and Bx43KD cells expressing Cx43EGFP, no discernible colocalization of clathrin with Cx43 was observed in contacting cells (Figure 10A) but extensive colocalization was observed in single isolated cells (unpublished data). Taken together, the above results suggest that cell-to-cell contact alters the endocytic itinerary of Cx43 and that intracellular vesicular puncta in contacting BxPC3 and Capa-1 cells are made up of undocked connexons.

DISCUSSION

Molecular cues that govern the assembly of Cxs into gap junctions upon arrival at the surface are poorly understood. Through two different approaches, based on the subcellular fate of Cx43 in single and contacting cells and on the knock down and knock in of WT-Cx43 and its various mutants, we have uncovered some novel aspects of the molecular circuitry that orchestrates the assembly and the disassembly of gap junctions. First, our study shows that the

assembly of Cx43 is impaired in BxPC3 and Capa-1 cells because it is endocytosed by the clathrin-mediated pathway prior to its assembly into gap junctions. Second, our findings demonstrate that assembly is restored by expressing a sorting-motif mutant of Cx43 that cannot be endocytosed. Third, our results show that the phosphorylation on Ser-279 and Ser-282 disrupts gap junction assembly by inducing endocytosis of Cx43 by the clathrin-mediated pathway. Fourth, our study shows that Cx43 is assembled into gap junctions only when connexons are composed of forms that can be phosphorylated on Ser-279 and Ser-282 and forms in which phosphorylation on these serines is abolished. Finally, our results document that the endocytic itinerary of Cx43 is altered upon cell-cell contact: Cx43 traffics by EEA1-negative endosomes in contacting cells versus EEA1-positive endosomes in single cells. Our results imply that endocytosis of connexons seems to be the major control point that determines gap junction size and growth.

Endocytosis of Cx43 and gap junction assembly

The use of human pancreatic cancer cell lines Capa-1 and BxPC3, which coexpressed Cx43 and Cx26 endogenously and in which either both Cxs or only one of the two failed to assemble into gap

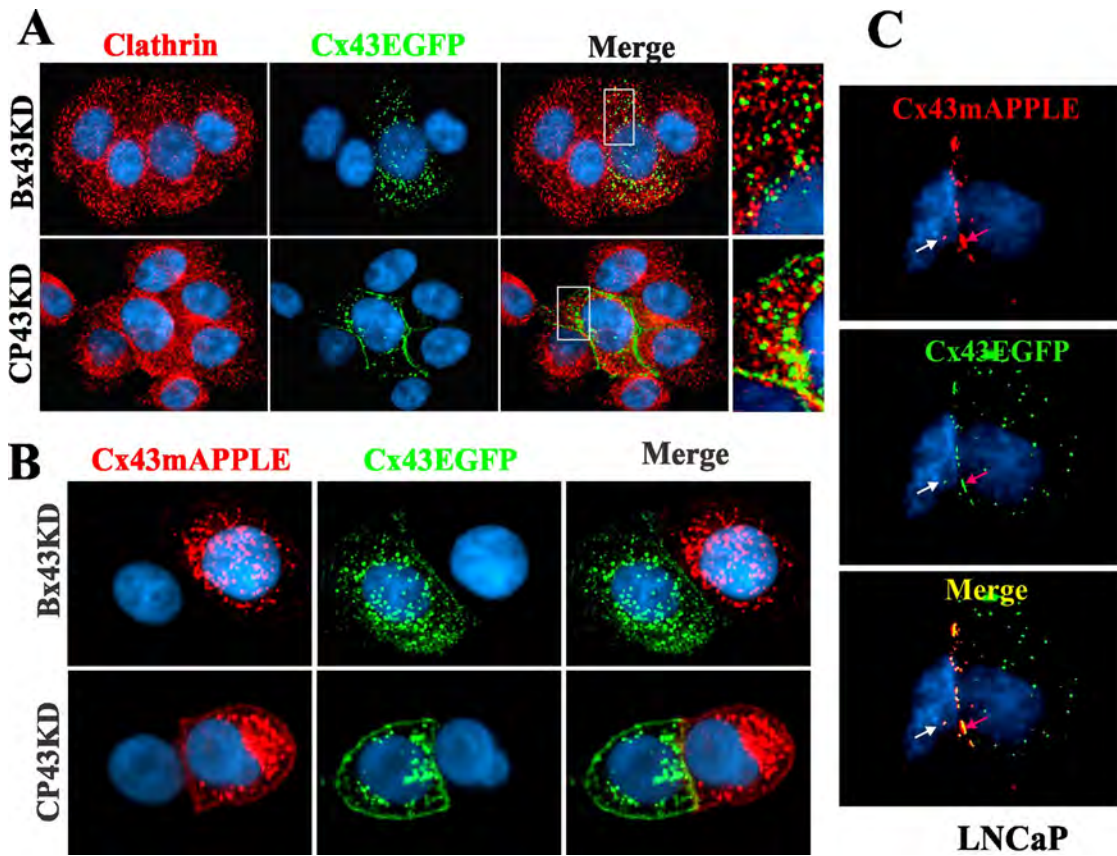


FIGURE 10: Cell–cell contact and the subcellular fate of Cx43. (A) Cell–cell contact alters the endocytic itinerary of Cx43. Bx43KD and CP43KD cells stably expressing knocked-in WT-Cx43EGFP were cocultured with Bx43KD and CP43KD cells, and the cultures were immunostained for clathrin (red). Note that Cx43EGFP does not discernibly colocalize with clathrin when the Cx43EGFP-expressing cells are in contact with Cx43KD cells. Occasional puncta that seem to colocalize with clathrin are likely to be undocked connexons that were endocytosed from the noncontacting cell surface. (B) Cx43 connexons fail to dock upon arrival at the cell surfaces of BxPC3 and Capan-1 cells. Bx43KD and CP43KD cells stably expressing knocked-in WT-Cx43EGFP or WT-Cx43mAPPLE were seeded on glass coverslips, as described in *Materials and Methods*. After 24 h, cells were fixed, stained for 4',6-diamidino-2-phenylindole (DAPI), and examined for colocalization of Cx43EGFP and Cx43mAPPLE. Note the absence of colocalization at the areas of cell–cell contact, as well as in the cytoplasm. (C) Cx43 is endocytosed as annular gap junctions in assembly-efficient LNCaP cells. LNCaP cells stably expressing Cx43EGFP or Cx43mAPPLE were cocultured for 24 h, fixed, stained for DAPI, and examined for the colocalization of Cx43EGFP and Cx43mAPPLE. Note that both gap junctions (red arrows) and intracellular vesicular puncta (white arrows) are composed of both Cx43EGFP and Cx43mAPPLE.

junctions, allowed us to address an important question: What are the intrinsic and extrinsic determinants that dictate the assembly of Cx43 into gap junctions in these cell lines, and what are their respective contributions? To explore the molecular basis of defective assembly of Cx43 in BxPC3 and Capan-1 cells, we searched for motifs in Cx43 itself that might govern its assembly into gap junctions. We first discovered that Cx43 trafficked to the cell surface in both cell types but was endocytosed prior to its assembly into gap junctions by the clathrin-mediated pathway in a Rab5-dependent manner via a tyrosine-based sorting motif in its cytoplasmic tail that likely mediated its interaction with the AP2 complex (Figures 1 and 2). Because both Cx26 and Cx32 assembled into gap junctions in BxPC3 cells, these results suggested that the defective assembly of Cx43 was not caused by spatial constraints imposed by extrinsic determinants, such as the expression of cell–cell adhesion molecules, which might have hindered the docking of connexons to form cell–cell channels and their subsequent clustering into gap junctions (Chakraborty *et al.*, 2010; Musil, 2009; Musil *et al.*, 1990; Wang and Mehta, 1995), but by the endocytosis of Cx43 itself.

Restoration of defective gap junction assembly

Our results showed that transient, as well as stable, expression of the sorting-motif mutant YA/VD-Cx43 restored defective gap junction assembly in BxPC3 and Capan-1 cells expressing endogenous Cx43. Moreover, assembly was also restored upon expressing mutants S279A, S282A, and S279/282A, which mimicked the nonphosphorylated state, but not upon expressing S279D, S282D, and S279/282D, which mimicked the phosphorylated state (Figure 5). Furthermore, restoration most likely occurred through the formation of heteromers with the endogenous Cx43 (Figures 4 and 5). These results raise intriguing issues with regard to the possible mechanisms that dictate the assembly of Cx43 into gap junctions in these cell types. The most likely explanation for these data are that phosphorylation of Ser-279 or Ser-282 regulates sorting motif-mediated endocytosis and that gap junction assembly is enhanced due to the inhibition of endocytosis of connexons composed of heteromers of Cx43 and either YA/VD-Cx43, S279A, or S282A, permitting them to be incorporated in the plaque. This interpretation is supported by the fact that both Ser-279 and Ser-282 lie close to the proline-rich

sorting motif of Cx43, and phosphorylation and dephosphorylation of serines near sorting motifs of many G-protein–coupled receptors have been shown to modulate their endocytosis by regulating their interaction with the AP2 complex (Pitcher et al., 1999; Bonifacino and Traub, 2003; Rapacciuolo et al., 2003; Chen et al., 2004; Kittler et al., 2005; Toshima et al., 2009; Traub, 2009; Moeller et al., 2010; Shukla et al., 2011). Moreover, Ser-279 and Ser-282 have previously been shown to be phosphorylated by MAP kinase (Warn-Cramer et al., 1996, 1998), which has been thought to mediate internalization of gap junctions in response to epidermal growth factor and tumor promoters (Kanemitsu and Lau, 1993; Ruch et al., 2001; Leithe and Rivedal, 2004a, 2004b; Leithe et al., 2009; Solan and Lampe, 2008, 2009). Furthermore, our results showing lack of discernible colocalization of clathrin and EEA1 with Cx43 in single cells that expressed heteromers of Cx43 and mutant YA/VD-Cx43 (Figure 4) but a robust colocalization in single cells that expressed only WT-Cx43 (Figures 2 and 4) lend further credence to the above notion. In contrast with their lack of colocalization with clathrin and EEA1, connexons composed of either Cx43 alone or of both Cx43 and YA/VD-Cx43, or S279A colocalized extensively with Lamp1, indicating that all were degraded in the lysosome (Figure S6). Moreover, it seems highly unlikely that the restored gap junctions were formed of cell–cell channels composed of homomeric connexons containing only Cx43, YA/VD-Cx43, or S279A, because channels formed of heteromeric connexons of different Cx subtypes have been demonstrated to readily assemble into functional gap junctions in diverse cell types (Jiang and Goodenough, 1996; Valiunas et al., 2001; Churko et al., 2010). Furthermore, in contacting cells that coexpressed endogenous Cx43 and YA/VD-Cx43 (Figure 4A) or mutant YA/VD-Cx43 alone (Figure S6B), only large vesicular Cx43 puncta of diverse sizes were observed; these did not colocalize with clathrin and caveolin 1 and may represent annular gap junctions.

Ser-279 and Ser-282 of Cx43 and gap junction assembly

A salient and the most striking result of our study is that gap junction assembly was induced only when connexons were composed of Cx43 forms that can be phosphorylated on Ser-279 and Ser-282 and forms in which phosphorylation was abolished (mutants S279A, S282A, and S279/282A). Gap junction assembly was impaired when connexons were predominantly composed of Cx43 forms that mimicked the phosphorylation on Ser-279 and Ser-282 and when connexons were composed of Cx43 forms in which phosphorylation on these residues was abolished (Figures 6–8). The most plausible interpretation of these data is that the phosphorylated Ser-279 and Ser-282 (either alone or together) in the Cx43 cytoplasmic tail, previously documented to be the substrates for MAP kinase (Warn-Cramer et al., 1996, 1998), regulate junction assembly not only by modulating endocytosis of connexons but also by influencing plaque growth by a mechanism(s) that remains to be defined. Several lines of evidence support this interpretation.

First, knock in of S279A, S282A, S279/282A, S279D, S282D, or S279/282D alone in Bx43KD and CP43KD cells did not induce gap junction assembly. Moreover, the assembly of S279A and S279D was also robustly attenuated in assembly-efficient LNCaP cells (Figure S5), which suggested that these mutants were able to assemble into small gap junction plaques, but the plaques either did not grow or failed to coalesce to form larger plaques. Second, transient expression of mutants S279A or S282A, but not mutants S279D or S282D, restored gap junction assembly in cells that expressed endogenous Cx43, and the effect was as robust as with YA/VD-Cx43 (Figure 5). Third, expression of Myc-tagged, WT-Cx43 induced gap junction assembly in Bx43KD cells stably expressing S279A but not

in cells expressing S279D (Figure 8). Moreover, S279A and S282A, like YA/VD-Cx43, also restored gap junction assembly through the formation of heteromers with the WT-Cx43 (Figures 5 and 8). Fourth, retroviral expression of only YA/VD-Cx43 resulted in the formation of gap junctions in Bx43KD and CP43KD cells and in assembly-efficient LNCaP cells (Figure S5). Although not demonstrated directly, YA/VD-Cx43 connexons are likely to contain Cx43 forms that are both phosphorylated and not phosphorylated on Ser-279/Ser-282. Moreover, cell surface biotinylation of YA/VD-Cx43, S279A, and S279D showed that they trafficked to the cell surface and were degraded with similar kinetics (Figure S5).

NEDD4 is a ubiquitin ligase that interacts with Cx43 via its tryptophan–tryptophan (WW) domains (Leykauf et al., 2006). NEDD4-dependent ubiquitylation of Cx43 could thus play a role in the failure of BxPC3 and Capan-1 to assemble Cx43-containing gap junctions. The WW2 domain of NEDD4 interacted with peptides containing the proline-rich tyrosine-based (PY) motif of Cx43 and was shown to have a slightly higher affinity for peptides with phosphoserines 279 and 282 than for their nonphosphorylated counterparts. However, the WW3 domain was speculated to be the dominant mediator of the binding of NEDD4 to Cx43, and full-length Cx43 with phosphoserines 279 and 282 did not interact with the WW3 domain. The phosphorylation of Ser-279 and Ser-282 by MAP kinase (Warn-Cramer et al., 1996, 1998) has been thought to mediate internalization of gap junctions in response to epidermal growth factor and tumor promoters (Kanemitsu and Lau, 1993; Leithe and Rivedal, 2004a, 2004b; Leithe et al., 2009; Solan and Lampe, 2008, 2009). However, we found that S279A and S282A failed to assemble in both Bx43KD and CP43KD (Figures 6 and 7). In addition, we found YA/VD-Cx43 assembled efficiently into gap junctions in the knockdown cells (Figures 6 and 7), in spite of the fact that Cx43-Y286A could still get ubiquitylated (Leykauf et al., 2006; Girao et al., 2009; Catarino et al., 2011). Thus the role that NEDD4 plays in the cells used in this study is unclear. Finally, the fact that gap junctions composed of mutant YA/VD-Cx43 in BxPC3 and Capan-1 cells appeared to be internalized in the form of annular junctions under both basal and starved conditions (Figure 9) suggests that clathrin-mediated endocytosis by AP2 cannot account for the internalization of this mutant. The pathway by which YA/VD-Cx43 and S279A and S282A are internalized and degraded remains to be explored in future studies.

Endocytic itinerary of Cx43 and cell–cell contact

A salient aspect of our results was that a major fraction of Cx43 appeared to reside in intracellular vesicles upon endocytosis. Despite this, discernible colocalization of Cx43 with clathrin and EEA1 was observed only in single cells—not in contacting cells (Figure 2). In contrast, in both single and contacting cells, Cx43 discernibly colocalized with AP2 and with Rab5, which is involved in clathrin-mediated endocytosis and acts upstream of EEA1 (Bucci et al., 1992; Zerial and McBride, 2001; Semerdjieva et al., 2008; Figures 2 and S3). These results were intriguing, given the fact that Cx43 trafficked to the cell surface in both cell types, and nearly all the Cx43 resided in intracellular vesicles that could be extracted in situ with 1% TX100 (Figures 1 and 7). Thus the intracellular vesicular puncta observed in these cells were not internalized annular gap junctions or aggregates of Cx43 that were detergent-resistant but represented vesicles that trafficked via EEA1-negative endosomes in contacting cells en route to the lysosomes. As Cx43 also did not discernibly colocalize with caveolin 1 (Figure S2), one plausible explanation for these data is that undocked connexons, upon clathrin-mediated endocytosis in single cells, traverse via EEA1-positive endosomes, whereas docked connexons and small minuscule annular gap junctions—which may

not have been resolved immunocytochemically—traverse via vesicles that are EEA1-negative. Although highly unlikely, sporadic colocalization of intracellular Cx43 with clathrin observed in contacting cells may represent clathrin-coated secretory vesicles (Bonifacino, 2004; Weisz and Rodriguez-Boulan, 2009; Gravotta et al., 2012).

When Bx43KD and CP43KD cells expressing either Cx43EGFP or Cx43mAPPLE were cocultured, we did not observe vesicles containing both Cx43EGFP and Cx43mAPPLE, suggesting that the vesicles arose predominantly from undocked connexons (Figure 10B). Moreover, in cocultures with knockdown cells, we saw no discernible colocalization of clathrin with Cx43 in contacting cells (Figure 10A), in contrast with robust colocalization seen in single cells. One interpretation of these results is that the endocytic itinerary of Cx43 is altered upon cell–cell contact, such that, after clathrin-mediated endocytosis, Cx43 traffics by EEA1-negative endosomes in contacting cells and by EEA1-positive endosomes in single cells. It is also possible that the spatiotemporal characteristics of clathrin coats of endocytic vesicles in contacting cells are different from those in single cells, such that they cannot be discerned in the captured static images of contacting cells. The existence of at least two modes of endocytic coat formation at the plasma membrane—classical clathrin-coated pits and clathrin-coated plaques with distinct spatiotemporal characteristics—has been described (Saffarian et al., 2009). It is worth considering that the connexons, unlike other well-studied transmembrane proteins, such as growth factor receptors and G-protein–coupled receptors (Moore et al., 2007; Shenoy and Lefkowitz, 2011), are hexamers of Cxs, which are known to interact with cytoplasmic proteins—that are also part of other junctional complexes—and are recruited to the site of cell–cell contact upon cell–cell adhesion (Laird, 2010; Herve et al., 2012). Thus, although there is no coherent theme for the roles of these proteins in junction assembly or disassembly, these attributes of connexons might impose unique spatial constraints on the endocytic machinery, causing Cxs to follow a noncanonical endocytic route in contacting cells but not in single cells (Boulant et al., 2011; McMahon and Boucrot, 2011; Sigismund et al., 2012).

Recent findings have shown that, upon internalization, cell surface–associated Cxs are degraded by autophagy and that inhibition of autophagy stabilizes the cell surface–associated pool of Cxs (Hesketh et al., 2010; Lichtenstein et al., 2011; Bejarno et al., 2012; Fong et al., 2012). Given the fact that the plasma membrane has now been shown to contribute to the formation of preautophagosomal structures (Ravikumar et al., 2010), it is tempting to speculate that cell–cell contact dictates the choice of the endocytic itinerary of Cx43, such that it traffics from noncontacting surfaces by EEA1-positive endosomes, whereas it is linked from contacting surfaces to vesicles destined to fuse with autophagosomes. Recent studies have identified the existence of a new class of early endosomes that bear the membrane adaptor proteins APPL1 and APPL2 (Miaczynska et al., 2004). These endosomes have been shown to be the precursors of EEA1-positive endosomes (Zoncu et al., 2009). Many transmembrane proteins have been demonstrated to interact with APPL1 and APPL2, which have been shown to act not only as effectors of Rab5 (Zhu et al., 2007) but also as dynamic scaffolds that modulate Rab5-associated signaling (Caruso-Neves et al., 2006; Mao et al., 2006; Varsano et al., 2006; Chial et al., 2008). Earlier studies had demonstrated or assumed that Cx43, after being endocytosed by the clathrin-mediated pathway, trafficked via EEA1-positive early endosomes to lysosomes for degradation (Leithe et al., 2006, 2009; Piehl et al., 2007; Gumpert et al., 2008; Nickel et al., 2008). Although it is as yet unknown how endocytic vesicles are directed to the autophagosomes, our results provide a plausible explanation for the distinct endocytic routes of Cx43 in

single versus contacting cells. The nature of the vesicles used for the trafficking of internalized Cx43 in contacting cells and how the endocytic fate of Cx43 is modulated by cell–cell contact remain to be investigated in these cell types at ultrastructural levels.

Conclusions

Although phosphorylation of the cytoplasmic tail of Cx43 on specific serines and tyrosines by protein kinases has been documented to regulate the function of cell–cell channels in both tissues and cell lines, evidence regarding its role in the assembly and disassembly of gap junctions has been correlative, and no coherent theme has yet emerged (Laird, 2005; Solan and Lampe, 2009). Our results demonstrate that phosphorylation on Ser-279 and Ser-282 not only disrupts gap junction assembly by triggering endocytosis of Cx43 prior to its assembly but also likely regulates plaque growth. Earlier pioneering studies of Musil and Goodenough demonstrated the existence of plaque-associated and detergent-resistant multiple phosphorylated forms of Cx43 and postulated these forms to be involved in the establishment and/or maintenance of gap-junctional plaques (Musil et al., 1990; Musil and Goodenough, 1991). Our results, showing that gap junction assembly is induced only when connexons are composed of Cx43 forms that can be phosphorylated and forms that cannot be phosphorylated on Ser-279 and Ser-282, provide direct evidence for this role. Our results, however, do not exclude the important role of phosphorylation and dephosphorylation of other serines in the cytoplasmic tail of Cx43, for example, Ser-365, Ser-364, and Ser-368, in determining gap junction assembly and disassembly (Solan et al., 2007; Solan and Lampe, 2008, 2009; TenBroek et al., 2001). Because Ser-279 and Ser-282 have also been found to be phosphorylated by multiple signaling pathways (Solan and Lampe, 2008), a question that remains to be answered is how the stoichiometry of heteromerization of the various phosphoforms of Cx43 and the differential phosphorylation and dephosphorylation of these sites is fine-tuned to control plaque growth and dynamics in BxPC3 and Capan-1 cells. It also remains to be determined whether this mechanism is used in normal cells *in vitro* and *in vivo* to regulate gap junction assembly. On the basis of our studies, we propose that endocytosis of connexons is the major control point that determines gap junction size and growth (as summarized in Figure 11).

MATERIALS AND METHODS

Cell culture

Several human pancreatic tumor cell lines were used initially to screen for the expression of Cx26, Cx32, Cx36, and Cx43 by RT-PCR (unpublished data). The cell lines were a gift from Surinder K. Batra (Department of Biochemistry and Molecular Biology, University of Nebraska Medical Center). For subsequent studies, two human pancreatic cancer cell lines, BxPC3 (CRL-1687) and Capan-1 (HTB-79), were purchased from the American Type Culture Collection (ATCC, Manassas, VA). The characterization of these cell lines has been described (Tan et al., 1986; Fanjul and Hollande, 1993). BxPC3 and Capan-1 cells were grown, respectively, in RPMI 1640 and DMEM (GIBCO, Grand Island, NY) containing 5% fetal bovine serum (FBS; Sigma-Aldrich, St. Louis, MO) in an atmosphere of 5% CO₂ at 37°C. Stock cultures were maintained weekly by seeding 5 × 10⁵ cells per 10-cm dish in 10 ml of complete culture medium with a medium change at day 3 or 4. New stocks were initiated every 3 mo from cells frozen in liquid nitrogen. The retroviral packaging cell lines EcoPack and PTi67 were grown as described previously (Mehta et al., 1999; Mitra et al., 2006). BxPC3 and Capan-1 cells were infected with various recombinant retroviruses, and pooled polyclonal cultures from ~2000 colonies were grown and maintained in complete medium

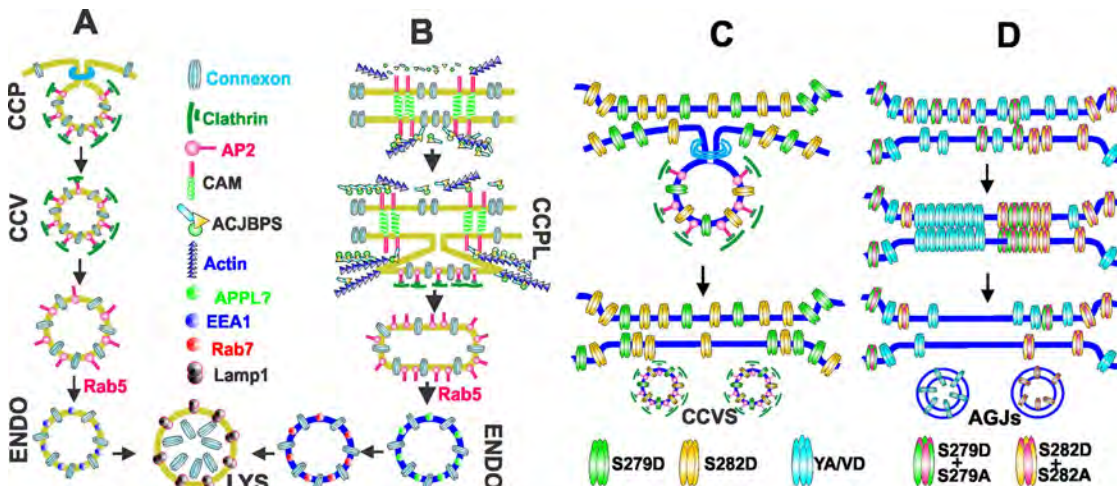


FIGURE 11: (A) In single cells, and from cell surfaces that are not in contact with other cells, connexons are endocytosed by clathrin-coated pits, which are directed toward the lysosomes for degradation by Rab5 via EEA1-positive endosomes. (B) Cell–cell contact is assumed to recruit various cell junction-associated proteins to the cell surface, where they establish a direct or an indirect link between the connexons and the actin cytoskeleton. From cell–cell contact areas, connexons are postulated to be endocytosed via clathrin-coated plaques, which are directed toward the lysosomes by Rab5 via noncanonical endosomes and intermediate vesicles yet to be characterized. (C) Phosphorylation of Cx43 on S279 and S282 induces connexon endocytosis via the clathrin-mediated pathway by enhancing Cx43's interaction with the AP2 complex, which is postulated to attenuate gap junction assembly. (D) Gap junction assembly is robustly induced when the interaction of the AP2 complex with the sorting motif is abolished through mutation or through dephosphorylation of Ser-279 and Ser-282 of some, but not all, connexin molecules in a connexon. It is postulated that the stoichiometry of phosphorylation and dephosphorylation of Ser-279 and Ser-282 of some connexin molecules in a connexon determines gap junction size, not only by regulating connexon endocytosis, but also by facilitating connexon–connexon docking to form cell–cell channels and their subsequent incorporation into gap-junctional plaques. Inhibition of clathrin-mediated endocytosis of connexons triggers internalization via the formation of annular gap junctions. ACJBPS = actin and cell junction binding proteins AGJs = annular gap junctions CAM = cell adhesion molecule CCP = clathrin-coated pit CCPL = clathrin-coated plaque CCV and CCVS = clathrin-coated vesicles ENDO = endosome, LYS = lysosome YA/VD = sorting motif mutant Cx43.

containing G418 (200 µg/ml), puromycin (0.5 µg/ml for BxPC3 and 1 µg/ml for Capan-1), or G418 plus puromycin (see Recombinant DNA constructs and retrovirus production and infection).

Antibodies and immunostaining

Rabbit polyclonal and mouse monoclonal antibodies against Cx43 and Cx32 and mouse anti-GM130, mouse anti-clathrin heavy chain, mouse anti-β-catenin, and rabbit anti-β-actin have been described previously (Mitra et al., 2006; Chakraborty et al., 2010; Govindarajan et al., 2010). A mouse monoclonal antibody against human Cx26 (13-8100) was purchased from Zymed Laboratories (San Francisco, CA). Mouse anti-caveolin 1 (610058), anti-caveolin 2 (610684), and anti-EEA1 (610457) were purchased from BD Transduction (San Jose, CA). We also used mouse monoclonal antibodies against Lamp1 (SC-20011; Santa Cruz Biotechnology, Santa Cruz, CA), c-Myc (MMS-150P; Covance, Princeton, NJ), and GFP (Roche Indianapolis, IN). A monoclonal antibody against human desmogliien-2 was a gift from James E. Wahl (Department of Oral Biology, University of Nebraska Medical Center).

For immunostaining, 5×10^5 BxPC3 and 4×10^5 Capan-1 cells were seeded on glass coverslips in six-well clusters and allowed to grow for 72 h, after which they were fixed with 2% paraformaldehyde and immunostained as described previously (Chakraborty et al., 2010; Govindarajan et al., 2010). Anti-rabbit and anti-mouse secondary antibodies, conjugated with Alexa Fluor 488 or Alexa Fluor 594 (Invitrogen), were used as appropriate. Immunostained cells were mounted on glass slides in SlowFade antifade (Invitrogen, Carlsbad, CA) medium. Images of immunostained cells were acquired with a

Leica DMRE microscope (Leica Microsystems, Wetzler, Germany) equipped with a Hamamatsu ORCA-ER2 CCD camera (Hamamatsu City, Japan) using a 63x oil objective (numerical aperture 1.35). Colocalization was measured in Z-stacked images taken 0.3 µm apart using the commercial image analysis program Velocity 6.0.1 (Improvision, Lexington, MA). Saturation of the detector, which would alter background adjustment, was prevented by minimizing exposure of each fluorescently tagged antibody during acquisition. A background-corrected Pearson's *r* was used to determine fluorescence colocalization as previously described (Barlow et al., 2010).

Detergent extraction and Western blot analysis

BxPC3 (3×10^6) and Capan-1 (2×10^6) cells were seeded in replicate 10-cm dishes with 10 ml of complete medium per dish. Cells were grown for 72 h. Cell lysis, detergent solubility assay with 1% Triton X-100 (TX100), and Western blot analysis were performed as described previously (Mitra et al., 2006; Chakraborty et al., 2010; Govindarajan et al., 2010). For the analysis of detergent-soluble and detergent-insoluble fractions by SDS-PAGE, normalization was based on equal cell number. For the detergent extraction of live cells *in situ*, BxPC3 and Capan-1 cells were seeded in six-well clusters containing glass coverslips at a density of 5×10^5 and 4×10^5 cells per well, respectively. After 72 h, cells were extracted *in situ* with 1% TX100 in isotonic medium (30 mM HEPES, pH 7.2, 140 mM NaCl, 1 mM CaCl₂, 1 mM MgCl₂) supplemented with protease inhibitor cocktail (Sigma-Aldrich) for 60 min at 4°C and then fixed and immunostained essentially as described previously (Govindarajan et al., 2002, 2010; Chakraborty et al., 2010).

Cell surface biotinylation assay

BxPC3 (5×10^5) and Capan-1 (4×10^5) cells were seeded in 6-cm dishes in replicate and grown to 70–80% confluence. The biotinylation reaction was performed at 4°C using freshly prepared EZ-Link Sulfo-NHS-SS Biotin reagent (Pierce, Rockford, IL) at 0.5 mg/ml in phosphate-buffered saline (PBS) supplemented with 1 mM CaCl₂ and 1 mM MgCl₂ (PBS-PLUS) for 1 h. The reaction was quenched with PBS-PLUS containing 20 mM glycine, and cells were lysed as described previously (Govindarajan *et al.*, 2002, 2010; Chakraborty *et al.*, 2010). The affinity precipitation of biotinylated proteins was performed with 200 µg of total protein using 100 µl of streptavidin-agarose beads (Pierce) on a rotator overnight at 4°C. The streptavidin-bound biotinylated proteins were eluted and resolved by SDS-PAGE followed by Western blotting as described previously (Govindarajan *et al.*, 2002, 2010; Chakraborty *et al.*, 2010). The kinetics of degradation of cell surface-associated Cx43 was determined as follows: after biotinylation, washing, and quenching of biotin, biotinylated proteins were chased at 37°C for various times before affinity precipitation with streptavidin. These methods have been described in our earlier studies (Govindarajan *et al.*, 2010). The protein concentration was determined using the BCA reagent (Pierce).

Recombinant DNA constructs and retrovirus production and infection

Wild-type rat Cx43 and its various mutants were cloned into pcDNA3.1 and the retroviral vector pLXSN using PCR cloning and standard recombinant DNA protocols. Mutants were generated by site-directed mutagenesis using a QuikChange kit (Stratagene, La Jolla, CA) according to the manufacturer's instructions. WT-Cx43 and its various mutants tagged in-frame with green (EGFP) fluorescent protein and with a Myc epitope were constructed using pEGFP-N1 and pMyc-CMV (Clontech, Mountain View, CA). All constructs were verified by DNA sequencing (ACGT, Wheeling, IL). These mutants are shown in Figure 12. For construction of an EGFP-tagged µ2 subunit of AP2 complex, a fragment of mouse µ2 corresponding to that in clone 3 µ2 (Ohno *et al.*, 1995) was tagged at the N-terminus with mEGFP (GFPµ2). Rat Cx43 tagged in-frame with mAPPLE was a gift from Matthias Falk (Department of Biological Sciences, Lehigh University). The source of the retroviral vector pSUPER.retro.puro and the construction of the retroviral vector LXSN-Cx32 have been described in our earlier studies (Mitra *et al.*, 2006; Chakraborty *et al.*, 2010). Rab5 and their constitutively active (pRab5Q67L) and dominant-negative (pRab5S34N) mutants tagged with EGFP were a gift from Steve Caplan (Department of Biochemistry and Molecular Biology, University of Nebraska Medical Center).

The retroviral vectors were used to produce recombinant retroviruses in EcoPack and PTi67 packaging cell lines as follows. EcoPack (Clontech) cells were seeded in duplicate at a density of 10^6 cells per 10-cm dish. The cells were transfected with 20 µg of retroviral vectors (plasmids) using Fugene for 6 h (Roche). The medium was replaced with 10 ml of fresh medium, and cells were incubated for additional 48 h, after which the medium containing the recombinant retrovirus was collected and filtered (0.45 µM; Millipore, Billerica, MA). For production of recombinant retrovirus for infection of target cells, amphotropic PTi67 cells were infected with the transiently produced recombinant retrovirus from EcoPack and selected in G418 (400 µg/ml), when infected with LXSN constructs, or puromycin (1 µg/ml), when infected with pSuper.retro.puro. The recombinant retrovirus produced from the pooled polyclonal cultures of PTi67 cells was assayed for the virus titer by colony-forming units as previously described (Mehta *et al.*, 1991). PTi67 cells producing the virus were frozen. BxPC3 and Capan-1 cells

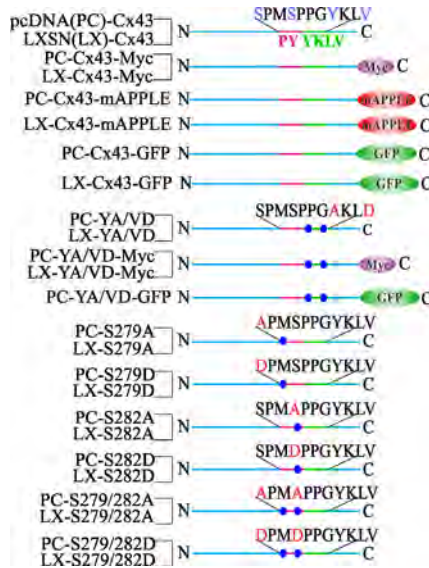


FIGURE 12: Diagram of the Cx43 constructs. Shown are the maps of wild-type and mutant Cx43 cloned into pcDNA (PC) and retroviral vector LXSN (LX), as indicated on the left. The constructs are tagged either with Myc or with red or green fluorescent proteins. The regions indicated are as follows: the proline rich region (PY) is pink, whereas the tyrosine-based sorting motif is green. The amino acid sequence of each indicated region is shown above each construct. Mutated residues are highlighted by red letters, and the relative position of each mutant is marked by blue circles. The amino and the carboxyl termini are indicated by N and C, respectively.

were multiply (two to four times) infected with various recombinant retroviruses produced from PTi67 cells and selected in either G418 (400 µg/ml) or puromycin (1 µg/ml for BxPC3 and 2 µg/ml for Capan-1) for 2–3 wk in complete medium. Pooled cultures from ~2000 colonies obtained from three to four dishes were expanded, frozen, and maintained in selection media containing G418 (200 µg/ml) and in G418 plus puromycin (1 µg/ml) for CP43KD and Bx43KD cells expressing the knocked-in constructs. Pooled polyclonal cultures were used within two to three passages for immunocytochemical and biochemical analyses.

Cell transfection

Twenty-four hours prior to transfection, Capan-1 (1.5×10^6) and BxPC3 (10^6) cells were seeded on glass coverslips in six-well clusters. Cells were transfected with various plasmids in duplicate using Fugene (Roche Diagnostics) according to the manufacturer's instructions. For transfection of single plasmids, 2 µg of plasmid DNA was used per well. For cotransfection of two plasmids, pEGFP (0.5 µg) and the plasmid DNA (1.5 µg), containing the gene whose expression was to be detected were mixed. Expression was analyzed 16–24 h posttransfection after cells were fixed and immunostained with the desired antibodies as previously described (Mitra *et al.*, 2006).

Yeast two-hybrid analysis

To test for the direct interaction of Cx43 with the µ2 subunit of AP-2 complex, we used yeast two-hybrid analysis (BD Biosciences/Clontech, Franklin Lakes, NJ). Briefly, the cytoplasmic tail of Cx43 (residues 240–382) was cloned into the EcoRI and BamHI sites of pGBT7 to give pGBT743-WT. Site-directed mutagenesis was then used to generate pGBT743-Y286A, pGBT743-V289D, and pGBT743-Y286A/V289D. pGADT7-T containing the µ2 subunit of

AP2 complex was a gift from Steve Caplan (Biochemistry and Molecular Biology, University of Nebraska Medical Center). These plasmids were used to transform *Saccharomyces cerevisiae* strain AH109 (BD Biosciences/Clontech) by the lithium acetate procedure, using the MATCHMAKER two-hybrid kit (BD Biosciences/Clontech) essentially as described (Naslavsky et al., 2006).

Immunoprecipitation

For the coimmunoprecipitation experiments shown in Figure 4, HeLa cells, grown to 50% confluence in 10-cm dishes, were transfected with 10 µg of pcDNACx43EGFP, pcDNACx43-Myc, pcDNA-Y286A/V289D-Cx43-Myc (YA/VD-Cx43-Myc), and pcDNA-YA/VD-Cx43-EGFP (YA/VD-Cx43EGFP) either alone or in combination. Twenty-four hours posttransfection, cells were harvested and lysed as described above in *Detergent extraction and Western blot analysis*. Following lysis and protein estimation, 1 mg of total protein was precleared with the Control Agarose Resin in the Pierce Co-IP Kit (Pierce) at 4°C for 1 h with gentle end-over-end mixing. The precleared lysate was then added to AminoLink Plus Coupling Resin, containing covalently bound monoclonal-GFP antibody (Roche) and incubated at 4°C for 16 h with gentle end-over-end mixing. After incubation, the GFP resin was washed three times in immunoprecipitation/wash buffer (Pierce) for 10 min with gentle shaking. Bound proteins were eluted from the GFP resin using the Co-IP kit elution buffer, containing primary amines (Pierce). For Western blot analysis, 5X reducing lane Marker Sample Buffer (Pierce) was added to the eluted samples to a final concentration of 1X. Pull down was assessed by Western blotting with monoclonal-Myc antibody.

Connexin43 knockdown

Accell small interfering RNAs (siRNAs) with target sequences to the 3' UTR of human Cx43 were purchased from Dharmacon/Thermo Scientific (Lafayette, CO). BxPC3 cells were seeded at a density of 8×10^4 cells per well in a 12-well cluster and, after 24 h, were transfected with the siRNAs using Oligofectamine according to the manufacturer's instructions (Invitrogen). Cells were incubated in the transfection medium mixture for 72 h, after which the medium was replaced with complete RPMI medium, and the cells were allowed to grow for an additional 24 h. Cells were harvested and lysed as described above, and knockdown was assessed by Western blot analysis.

The most potent Cx43 siRNA was selected and used to construct an shRNA. As a control, a scrambled sequence of the Cx43 siRNA was generated using siRNA Wizard software (InvivoGen, San Diego, CA). The shRNA oligos were purchased from Integrated DNA Technologies (Coralville, IA). The retroviral vector, pSUPER.retro.puro (OligoEngine, Seattle, WA), was used to produce shRNAs with the scrambled (Sh-Scr) Cx43 sequence (5'-GC-UAUAGGAUACGGAUAAU-3') and Cx43-targeting (Sh-Cx43) sequence (5'-GUAGUGGAUUCAAAGAACU-3') according to the manufacturer's instructions. The knockdown efficiency was assessed by transient transfection of these plasmids in BxPC3 and Capan-1 cells followed by Western blot and immunocytochemical analysis, as described above. After verification of knockdown, recombinant retroviruses containing Sh-Scr and Sh-Cx43 were produced in PTI67 cells, as described above. For stable knockdown, BxPC3 and Capan-1 cells were multiply infected with the recombinant retroviruses, and pooled polyclonal cultures were established as described in *Recombinant DNA Constructs and retrovirus production and infection*. Stable Cx43 knockdown BxPC3 and Capan-1 cells were designated as Bx43KD and CP43KD, respectively.

Single-cell and coculture experiments

For the single-cell experiments shown in Figures 2, S3, 4, and S6, BxPC3 and Capan-1 cells were seeded in six-well clusters at a density of $(2-5) \times 10^3$ cells per well in 2 ml of complete culture medium as previously described (Govindarajan et al., 2010). For the coculture experiments shown in Figure 10, Cx43EGFP or Cx43mAPPLE was introduced into Bx43KD and CP43KD cells using LXCx43EGFP and LXCx43mAPPLE, and pooled polyclonal cultures expressing each construct were established separately upon selection in G418, as described above. Bx43KD and CP43KD cells expressing either Cx43EGFP or Cx43mAPPLE were suspended in medium and then mixed together in a 1:1 ratio and allowed to aggregate in suspension for 4 h at 37°C in an atmosphere of 5% CO₂ to maximize the formation of doublets, triplets, and quadruplets. After 4 h, these cells were plated into six-well clusters at a density of 10^5 cells per well. After 20 h, cells were fixed and mounted on slides. For coculture experiments with the human prostate cancer cell line LNCaP, cells were infected with the retroviruses containing Cx43EGFP or Cx43mAPPLE, and cells expressing them were cocultured using the approach described above for BxPC3 and Capan-1 cells. To examine whether cell-cell contact determines Cx43 colocalization with clathrin, Bx43KD and CP43KD cells expressing Cx43EGFP were cocultured with Bx43KD and CP43KD cells at a ratio of 1:4, as described above, and colocalization of Cx43 with clathrin was determined upon immunostaining.

Quantitation of gap junction assembly/restoration

For quantifying gap junction assembly, pEGFP (0.5 µg) and the wild-type or mutant cDNAs (1.5 µg) were cotransfected into BxPC3, Capan-1, Bx43KD, and CP43KD cells as described above in *Cell transfection*. After 16–24 h, pairs of cells expressing equal levels of EGFP (as assessed visually) were counted for the formation of gap junctions, as exemplified by Figure 3. The percentage of cells with restored gap junctions was determined by counting 15–20 EGFP-expressing cells.

Communication assays

Gap-junctional communication was assayed by microinjecting fluorescent tracers LY (Lucifer Yellow; MW 443 Da lithium salt), Alexa Fluor 488 (MW 570 Da A-10436), or Alexa Fluor 594 (MW 760 Da A-10438), and by the scrape-loading assay as previously described (Govindarajan et al., 2002, 2010; Chakraborty et al., 2010; Kelsey et al., 2012). All Alexa dyes were purchased as hydrazide sodium salts from Molecular Probes (Carlsbad, CA), and stock solutions for microinjection were prepared in water at 10 mM. Eppendorf InjectMan and FemtoJet microinjection systems (models 5271 and 5242; Brinkmann Instrument, Westbury, NY) mounted on a Leica DMIRE2 microscope were used to microinject the fluorescent tracers. Junctional transfer of fluorescent tracers was quantitated by scoring the number of fluorescent cells (excluding the injected one) from the captured TIFF images either at 1 min (LY), 3 min (Alexa 488), or 15 min (Alexa 594) after microinjection into test cells as previously described (Mehta et al., 1986, 1999; Mitra et al., 2006; Chakraborty et al., 2010). Cells were scrape-loaded in 1 ml of medium containing rhodamine-conjugated fluorescent dextrans (10 kDa, 1 mg/ml, fixable) and LY (0.5%) essentially as previously described (Govindarajan et al., 2010).

ACKNOWLEDGMENTS

We thank Souvik Chakraborty for helpful discussion and suggestions. We thank Steve Caplan and Naava Naslavsky for help with the yeast two-hybrid analysis, as well as for helpful suggestions regarding endocytosis throughout the course of this study. We thank

Surinder Batra for providing us with the various pancreatic cancer cell lines for the initial screen, Maneesh Jain for RT-PCR analysis, and Matthias Falk for providing us with Cx43mAPPLE. This research was supported by National Institutes of Health grants CA113903, DOD PCRP PC-081198, and PC-111867 and Nebraska State grants LB506 (P.P.M.) and R0-1DE12308 (K.R.J.). We gratefully acknowledge support from the Nebraska Center for Cellular Signaling and Cancer Graduate Research Training Program of Eppley Institute in the form of fellowships to K.E.J.

REFERENCES

Barlow AL, MacLeod A, Noppen S, Sanderson J, Guérin CJ (2010). Colocalization analysis in fluorescence micrographs: verification of a more accurate calculation of Pearson's correlation coefficient. *Microsc Microanal* 16, 710–724.

Bavamian S, Klee P, Allagnat F, Haefliger JA, Meda P (2009). Connexins and secretion. In: *Connexins: A Guide*, ed. A. Harris and D. Locke, New York: Springer, 511–528.

Beijarno E, Girao H, Yuste A, Patel B, Marques C, Spray D, Pereira P, Cuervo A (2012). Autophagy modulates dynamics of connexons at the plasma membrane in an ubiquitin-dependent manner. *Mol Biol Cell* 23, 2156–2169.

Beyer EC, Berthoud VM (2009). The family of connexin genes. In: *Connexins: A Guide*, ed. A. Harris and D. Locke, New York: Springer, 3–26.

Bonifacino JS (2004). The mechanism of vesicle budding and fusion. *Cell* 116, 153–166.

Bonifacino JS, Traub LM (2003). Signals for sorting of transmembrane proteins to endosomes and lysosomes. *Annu Rev Biochem* 72, 395–447.

Bosco D, Haefliger JA, Meda P (2011). Connexins: key mediators of endocrine function. *Physiol Rev* 91, 1393–1445.

Boulant S, Kural C, Zeeh JC, Ubelmann F, Kirchhausen T (2011). Actin dynamics counteract membrane tension during clathrin-mediated endocytosis. *Nat Cell Biol* 13, 1124–1131.

Bucci C, Parton RG, Mather IH, Stunnenberg H, Simons K, Hoflack B, Zerial M (1992). The small GTPase rab5 functions as a regulatory factor in the early endocytic pathway. *Cell* 70, 715–728.

Caruso-Neves C, Pinheiro AA, Cai H, Souza-Menezes J, Guggino WB (2006). PKB and megalin determine the survival or death of renal proximal tubule cells. *Proc Natl Acad Sci USA* 103, 18810–18815.

Catarino S, Ramahlo J, Marques C, Pereira P, Girao H (2011). Ubiquitin-mediated internalization of connexin43 is independent of the canonical endocytic tyrosine-sorting signal. *Biochem J* 437, 255–269.

Chakraborty S, Mitra S, Falk MM, Caplan S, Wheelock MJ, Johnson KR, Mehta PP (2010). E-cadherin differentially regulates the assembly of connexin43 and connexin32 into gap junctions in human squamous carcinoma cells. *J Biol Chem* 285, 10761–10776.

Chen W, Ren XR, Nelson CD, Barak LS, Chen JK, Beachy PA, de Sauvage F, Lefkowitz RJ (2004). Activity-dependent internalization of Smoothened mediated by β-arrestin 2 and GRK2. *Science* 306, 2257–2260.

Chial HJ, Wu R, Ustach CV, McPhail LC, Mobley WC, Chen YQ (2008). Membrane targeting by APPL1 and APPL2: dynamic scaffolds that oligomerize and bind phosphoinositides. *Traffic* 9, 215–229.

Churko JM, Langlois S, Pan X, Shao Q, Laird DW (2010). The potency of the fs260 connexin43 mutant to impair keratinocyte differentiation is distinct from other disease-linked connexin43 mutants. *Biochem J* 429, 473–483.

Falk MM, Baker SM, Gumpert A, Segretain D, Buckheit RW (2009). Gap junction turnover is achieved by the internalization of small endocytic double-membrane vesicles. *Mol Biol Cell* 20, 3342–3352.

Fanjul M, Hollande E (1993). Morphogenesis of "duct-like" structures in three-dimensional cultures of human cancerous pancreatic duct cells (Capan-1). *In Vitro Cell Dev Biol* 29, 574–584.

Fong J, Kells R, Gumpert A, Marzillier J, Davidson M, Falk M (2012). Internalized gap junctions are degraded by autophagy. *Autophagy* 8, 738–755.

Gaietta GM, Deerinck TJ, Adams SR, Bouwer J, Tour O, Laird DW, Sosinsky GE, Tsien R, Ellisman MH (2002). Multicolor and electron microscopic imaging of connexin trafficking. *Science* 296, 503–507.

Girao H, Catarino S, Pereira P (2009). Eps15 interacts with ubiquitinated Cx43 and mediates its internalization. *Exp Cell Res* 315, 3587–3597.

Goodenough DA, Paul DL Gap junctions. *Cold Spring Harb Perspect Biol* 1, a002576.

Govindarajan R, Chakraborty S, Falk MM, Johnson KR, Wheelock MJ, Mehta PP (2010). Assembly of connexin43 is differentially regulated by E-cadherin and N-cadherin in rat liver epithelial cells. *Mol Biol Cell* 21, 4089–4107.

Govindarajan R, Song X-H, Guo R-J, Wheelock MJ, Johnson KR, Mehta PP (2002). Impaired trafficking of connexins in androgen-independent human prostate cancer cell lines and its mitigation by α-catenin. *J Biol Chem* 277, 50087–50097.

Gravotta D, Carvajal-Gonzalez J, Mattera R, Debordé S, Banfelder J, Bonifacino J, Rodriguez-Boulan E (2012). The clathrin adaptor AP-1A mediates basolateral polarity. *Developmental Cell* 22, 811–823.

Gumpert AM, Varco JS, Baker SM, Piehl M, Falk MM (2008). Double-membrane gap junction internalization requires the clathrin-mediated endocytic machinery. *FEBS Lett* 582, 2887–2892.

Herve JC, Derangeon ML, Sarrouilhe D, Giepmans BNG, Bourmeyster N (2012). Gap junctional channels are parts of multiprotein complexes. *Biochim Biophys Acta* 1818, 1844–1865.

Hesketh GG, Shah MH, Halperin VL, Cooke CA, Akar FG, Yen TE, Kass DA, Machamer CE, Van Eyk JE, Tomaselli GF (2010). Ultrastructure and regulation of lateralized connexin43 in the failing heart. *Circ Res* 106, 1153–1163.

Heuser JE, Anderson RG (1989). Hypertonic media inhibit receptor-mediated endocytosis by blocking clathrin-coated pit formation. *J Cell Biol* 108, 389–400.

Hunziker W, Geuze H (2011). Intracellular trafficking of lysosomal proteins. *EMBO J* 18, 379–389.

Jiang JX, Goodenough DA (1996). Heteromeric connexins in lens gap junction channels. *Proc Natl Acad Sci USA* 93, 1287–1291.

Jordan K, Chodock R, Hand A, Laird DW (2001). The origin of annular junctions: a mechanism of gap junction internalization. *J Cell Sci* 114, 763–773.

Kanemitsu M, Lau A (1993). Epidermal growth factor stimulates the disruption of gap junctional communication and connexin43 phosphorylation independent of 12-O-tetradecanoylphorbol 13-acetate-sensitive protein kinase C: the possible involvement of mitogen-activated protein kinase. *Mol Biol Cell* 4, 837–848.

Kelsey L, Katoch P, Johnson K, Batra SK, Mehta P (2012). Retinoids regulate the formation and degradation of gap junctions in androgen-responsive human prostate cancer cells. *PLoS One* 7, E32846.

Kittler JT et al. (2005). Phospho-dependent binding of the clathrin AP2 adaptor complex to GABA_A receptors regulates the efficacy of inhibitory synaptic transmission. *Proc Natl Acad Sci USA* 102, 14871–14876.

Klionsky DJ et al. (2008). Guidelines for the use and interpretation of assays for monitoring autophagy in higher eukaryotes. *Autophagy* 4, 151–175.

Lahhou H, Fanjul M, Pradayrol L, Susini C, Pyronnet Sp (2005). Restoration of functional gap junctions through internal ribosome entry site-dependent synthesis of endogenous connexins in density-inhibited cancer cells. *Mol Cell Biol* 25, 4034–4045.

Laird DW (2005). Connexin phosphorylation as a regulatory event linked to gap junction internalization and degradation. *Biochim Biophys Acta* 1711, 172–182.

Laird DW (2006). Life cycle of connexins in health and disease. *Biochem J* 394, 527–543.

Laird DW (2010). The gap junction proteome and its relationship to disease. *Trends Cell Biol* 20, 92–101.

Lauf U, Giepmans BNG, Lopez P, Braconnot S, Chen SC, Falk MM (2002). Dynamic trafficking and delivery of connexons to the plasma membrane and accretion to gap junctions in living cells. *Proc Natl Acad Sci USA* 99, 10446–10451.

Leithe E, Brech A, Rivedal E (2006). Endocytic processing of connexin43 gap junctions: a morphological study. *Biochem J* 393, 59–67.

Leithe E, Kjenseth A, Sirnes S, Stenmark H, Brech A, Rivedal E (2009). Ubiquitylation of the gap junction protein connexin-43 signals its trafficking from early endosomes to lysosomes in a process mediated by Hrs and Tsg101. *J Cell Sci* 122, 3883–3893.

Leithe E, Rivedal E (2004a). Epidermal growth factor regulates ubiquitination, internalization and proteasome-dependent degradation of connexin43. *J Cell Sci* 117, 1211–1220.

Leithe E, Rivedal E (2004b). Ubiquitination and down-regulation of gap junction protein connexin-43 in response to 12-O-tetradecanoylphorbol 13-acetate treatment. *J Biol Chem* 279, 50089–50096.

Leykauf K, Salek M, Bomke J, Frech M, Lehmann WD, Durst M, Alonso A (2006). Ubiquitin protein ligase Nedd4 binds to connexin43 by a phosphorylation-modulated process. *J. Cell Sci* 119, 3634–3642.

Lichtenstein A, Minogue PJ, Beyer EC, Berthoud VM (2011). Autophagy: a pathway that contributes to connexin degradation. *J Cell Sci* 124, 910–920.

Mao X et al. (2006). APPL1 binds to adiponectin receptors and mediates adiponectin signalling and function. *Nat Cell Biol* 8, 516–523.

McMahon HT, Boucrot E (2011). Molecular mechanism and physiological functions of clathrin-mediated endocytosis. *Nat Rev Mol Cell Biol* 12, 517–533.

Mehta P, Bertram J, Loewenstein W (1986). Growth inhibition of transformed cells correlates with their junctional communication with normal cells. *Cell* 44, 187–196.

Mehta P, Hotz-Wagenblatt A, Rose B, Shalloway D, Loewenstein WR (1991). Incorporation of the gene for a cell-to-cell channel protein into transformed cells leads to normalization of growth. *J Membr Biol* 124, 207–225.

Mehta PP, Perez-Stable C, Nadji M, Mian M, Asotra K, Roos B (1999). Suppression of human prostate cancer cell growth by forced expression of connexin genes. *Dev Genet* 24, 91–110.

Miaczynska M, Pelkmans L, Zerial M (2004). Not just a sink: endosomes in control of signal transduction. *Curr Opin Cell Biol* 16, 400–406.

Mills IG, Jones AT, Clague MJ (1998). Involvement of the endosomal autoantigen EEA1 in homotypic fusion of early endosomes. *Curr Biol* 8, 881–884.

Mitra S, Annamalai L, Chakraborty S, Johnson K, Song X, Batra SK, Mehta PP (2006). Androgen-regulated formation and degradation of gap junctions in androgen-responsive human prostate cancer cells. *Mol Biol Cell* 17, 5400–5416.

Mizushima N, Yoshimori T, Levine B (2010). Methods in mammalian autophagy research. *Cell* 140, 313–326.

Moeller HB, Praetorius J, Rutzler MR, Fenton RA (2010). Phosphorylation of aquaporin-2 regulates its endocytosis and protein-protein interactions. *Proc Natl Acad Sci USA* 107, 424–429.

Moore C, Milano S, Benovic JL (2007). Regulation of receptor trafficking by GRKs and arrestins. *Annu Rev Physiol* 69, 451–482.

Musil L, Cunningham BA, Edelman G, Goodenough D (1990). Differential phosphorylation of the gap junction protein connexin43 in junctional communication-competent and -deficient cell lines. *J Cell Biol* 111, 2077–2088.

Musil LS (2009). Biogenesis and degradation of gap junctions. In: *Connexins: A Guide*, ed. A. Harris and D. Locke, New York: Springer, 225–240.

Musil LS, Goodenough DA (1991). Biochemical analysis of connexin43 intracellular transport, phosphorylation, and assembly into gap junctional plaques. *J Cell Biol* 115, 1357–1374.

Nakamura N, Rabouille C, Watson R, Nilsson T, Hui N, Slusarewicz P, Kreis TE, Warren G (1995). Characterization of a cis-Golgi matrix protein, GM130. *J Cell Biol* 131, 1715–1726.

Naslavsky N, Rahajeng J, Sharma M, Jovi M, Caplan S (2006). Interactions between EHD proteins and Rab11-FIP2: a role for EHD3 in early endosomal transport. *Mol Biol Cell* 17, 163–177.

Nickel BM, DeFranco BH, Gay VL, Murray SA (2008). Clathrin and Cx43 gap junction plaque endoexocytosis. *Biochem Biophys Res Commun* 374, 679–682.

Ohno H, Stewart J, Fournier MC, Bosshart H, Rhee I, Miyatake S, Saito T, Gallusser A, Kirchhausen T, Bonifacino JS (1995). Interaction of tyrosine-based sorting signals with clathrin-associated proteins. *Science* 269, 1872–1875.

Parton RG, Simons K (2007). The multiple faces of caveolae. *Nat Rev Mol Cell Biol* 8, 185–194.

Piehl M, Lehmann C, Gumpert A, Denizot JP, Segretain D, Falk MM (2007). Internalization of large double-membrane intercellular vesicles by a clathrin-dependent endocytic process. *Mol Biol Cell* 18, 337–347.

Pitcher C, Höning S, Fingerhut A, Bowers K, Marsh M (1999). Cluster of differentiation antigen 4 (CD4) endocytosis and adaptor complex binding require activation of the cd4 endocytosis signal by serine phosphorylation. *Mol Biol Cell* 10, 677–691.

Rapacciuolo A, Suvarna S, Barki-Harrington L, Luttrell LM, Cong M, Lefkowitz RJ, Rockman HA (2003). Protein kinase A and G protein-coupled receptor kinase phosphorylation mediates β-1 adrenergic receptor endocytosis through different pathways. *J Biol Chem* 278, 35403–35411.

Ravikumar B, Moreau K, Jahreiss L, Puri C, Rubinsztein DC (2010). Plasma membrane contributes to the formation of pre-autophagosomal structures. *Nat Cell Biol* 12, 747–757.

Rohrer J, Schweizer A, Russell D, Kornfeld S (1996). The targeting of Lamp1 to lysosomes is dependent on the spacing of its cytoplasmic tail tyrosine sorting motif relative to the membrane. *J Cell Biol* 132, 565–576.

Roth MG (2006). Clathrin-mediated endocytosis before fluorescent proteins. *Nat Rev Mol Cell Biol* 7, 63–68.

Ruch RJ, Trosko J, Madhukar B (2001). Inhibition of connexin43 gap junctional intercellular communication by TPA requires ERK activation. *J Cell Biochem* 83, 163–169.

Saffarian S, Cocucci E, Kirchhausen T (2009). Distinct dynamics of endocytic clathrin-coated pits and coated plaques. *PLoS Biol* 7, e1000191.

Sarkar S, Korolchuk VI, Renna M, Winslow AR, Rubinsztein DC (2009). Methodological considerations for assessing autophagy modulators: a study with calcium phosphate precipitates. *Autophagy* 5, 307–313.

Schnitzer JE, Oh P, Pinney E, Allard J (1994). Filipin-sensitive caveole-mediated transport in endothelium: reduced transcytosis, scavenger endocytosis, capillary permeability of select macromolecules. *J Cell Biol* 127, 1217–1232.

Semerjiev S, Shortt B, Maxwell E, Singh S, Fonarev P, Hansen J, Schiavo G, Grant BD, Smythe E (2008). Coordinated regulation of AP2 uncoating from clathrin-coated vesicles by rab5 and hRME-6. *J Cell Biol* 183, 499–511.

Shaw RM, Fay AJ, Puthenveedu MA, von Zastrow M, Jan YN, Jan LY (2007). Microtubule plus-end-tracking proteins target gap junctions directly from the cell interior to adherens junctions. *Cell* 128, 547–560.

Shenoy SK, Lefkowitz RJ (2011). β-arrestin-mediated receptor trafficking and signal transduction. *Trends Pharmacol Sci* 32, 521–533.

Shukla AK, Xiao K, Lefkowitz RJ (2011). Emerging paradigms of β-arrestin-dependent seven transmembrane receptor signaling. *Trends Biochem Sci* 36, 457–469.

Sigmund S, Confalonieri S, Ciliberto A, Polo S, Scita G, Di Fiore PP (2012). Endocytosis and signaling: cell logistics shape the eukaryotic cell plan. *Physiol Rev* 92, 273–366.

Solan JL, Lampe PD (2008). Connexin43 in LA-25 cells with active V-Src is phosphorylated on Y247, Y265, S262, S279/282, and S368 via multiple signaling pathways. *Cell Commun Adhes* 15, 75–84.

Solan JL, Lampe PD (2009). Connexin43 phosphorylation: structural changes and biological effects. *Biochem J* 419, 261–272.

Solan JL, Marquez-Rosado L, Sorgen PL, Thornton PJ, Gafken PR, Lampe PD (2007). Phosphorylation at S365 is a gatekeeper event that changes the structure of Cx43 and prevents down-regulation by PKC. *J Cell Biol* 179, 1301–1309.

Tan M, Nowak N, Loor R, Ochi H, Sandberg A, Lopez C, Pkckern W, Cergian R, Douglass H, Chu T (1986). Characterization of a new primary human pancreatic tumor line. *Clin Invest* 4, 15–23.

TenBroek E, Lampe PD, Solan JL, Reynhout JK, Johnson R (2001). Ser364 of connexin43 and the upregulation of gap junction assembly by cAMP. *J Cell Biol* 155, 1307–1318.

Thomas M, Zosso N, Scerri I, Demaurex N, Chanson M, Staub O (2003). A tyrosine-based sorting signal is involved in connexin43 stability and gap junction turnover. *J Cell Sci* 116, 2213–2222.

Thomas T, Jordan K, Simek J, Shao Q, Jedeszko C, Walton P, Laird DW (2005). Mechanisms of Cx43 and Cx26 transport to the plasma membrane and gap junction regeneration. *J Cell Sci* 118, 4451–4462.

Toshima JY, Nakanishi Ji, Mizuno K, Toshima J, Drubin DG (2009). Requirements for recruitment of a G protein-coupled receptor to clathrin-coated pits in budding yeast. *Mol Biol Cell* 20, 5039–5050.

Traub LM (2009). Tickets to ride: selecting cargo for clathrin-regulated internalization. *Nat Rev Mol Cell Biol* 10, 583–596.

Valiunas V, Gemel J, Brink PR, Beyer EC (2001). Gap junction channels formed by coexpressed connexin40 and connexin43. *Am J Physiol Heart Circ Physiol* 281, H1675–H1689.

VanSlyke JK, Musil LS (2000). Analysis of connexin intracellular transport and assembly. *Methods* 20, 156–164.

Varsano T, Dong MQ, Niesman I, Gacula H, Lou X, Ma T, Testa JR, Yates JR, Farquhar MG (2006). GIPC is recruited by APPL to peripheral TrkA endosomes and regulates TrkA trafficking and signaling. *Mol Cell Biol* 26, 8942–8952.

Wang Y, Mehta PP (1995). Facilitation of gap junctional communication and gap junction formation by inhibition of glycosylation. *Eur J Cell Biol* 67, 285–296.

Warn-Cramer B, Cottrell GT, Burt JM, Lau AF (1998). Regulation of connexin-43 gap junctional intercellular communication by mitogen-activated protein kinase. *J Biol Chem* 273, 9188–9196.

Warn-Cramer B, Lampe P, Kurata W, Kanemitsu M, Loo L, Eckhart W, Lau A (1996). characterization of the mitogen-activated protein kinase phosphorylation sites on the connexin-43 gap junction protein. *J Biol Chem* 271, 3779–3786.

Weisz OA, Rodriguez-Boulan E (2009). Apical trafficking in epithelial cells: signals, clusters and motors. *J Cell Sci* 122, 4253–4266.

Zerial M, McBride H (2001). Rab proteins as membrane organizers. *Nat Rev Mol Cell Biol* 2, 107–117.

Zhu G et al. (2007). Structure of the APPL1 BAR-PH domain and characterization of its interaction with Rab5. *EMBO J* 26, 3484–3493.

Zoncu R, Perera RM, Balkin DM, Pirruccello M, Toomre D, De Camilli P (2009). A phosphoinositide switch controls the maturation and signaling properties of APPL endosomes. *Cell* 136, 1110–1121.

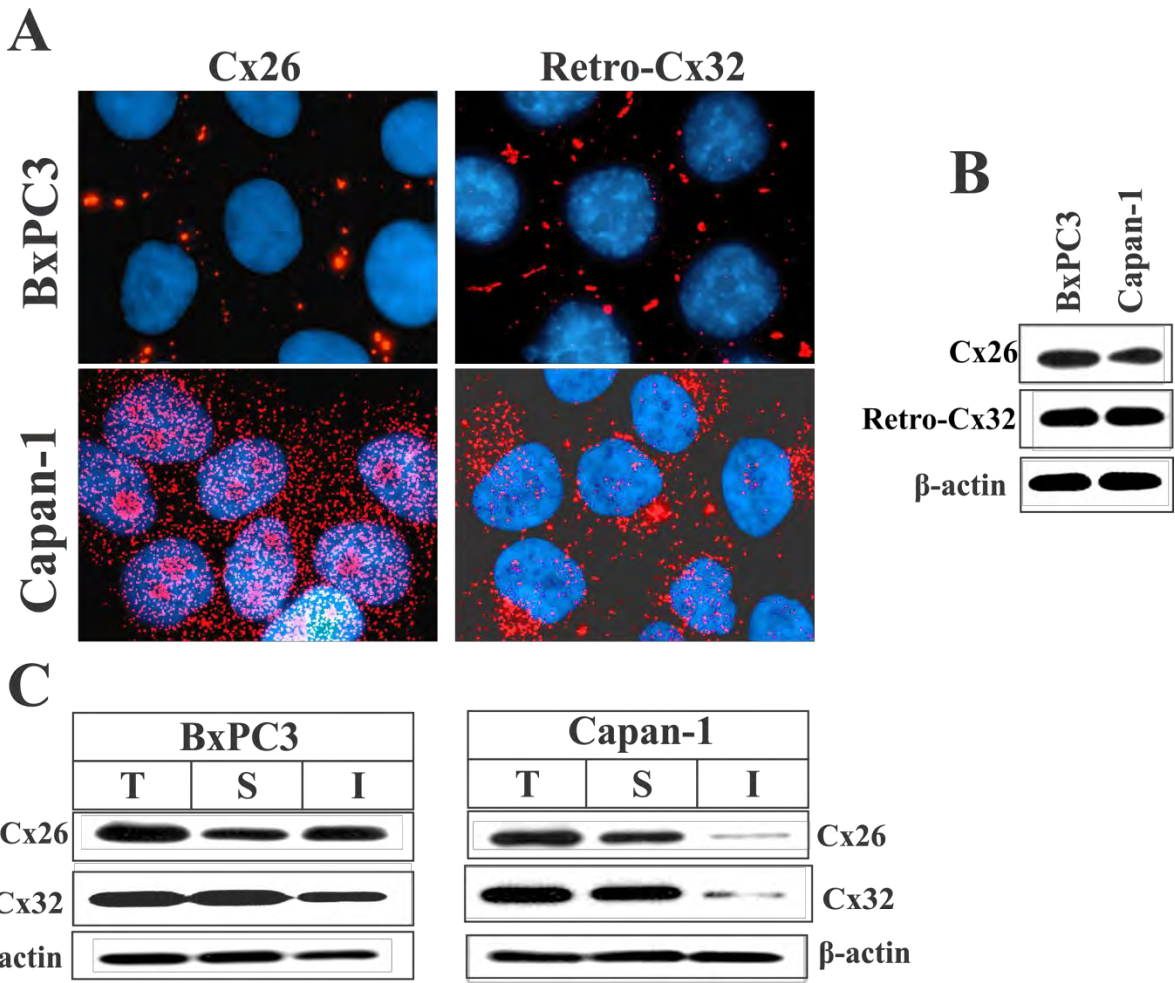


Figure S1. Cx26 and retrovirally expressed Cx32 are differentially assembled into gap junctions in BxPC3 and Capan-1 cells. A. Cells were immunostained for Cx26 and Cx32. Note that in BxPC3 both Cxs are assembled into gap junctions whereas in Capan-1 cells, they are not. B. Western blot analysis of lysates from BxPC3 and Capan-1 cells and of lysates from BxPC3 and Capan-1 cells retrovirally transduced with Cx32 (Retro-Cx32). Note that all Cxs are expressed abundantly in both cell types. C. Western blot analysis of Cx32 and Cx26 in Total (T), TX100-soluble (S), and TX100-insoluble (I) fractions of cell lysates in BxPC3 and Capan-1 cells. Note that a major fraction of both Cxs is TX100-insoluble in BxPC3 cells but the Cxs remain soluble in Capan-1 cells. The blots were also stripped and re-probed for β -actin.

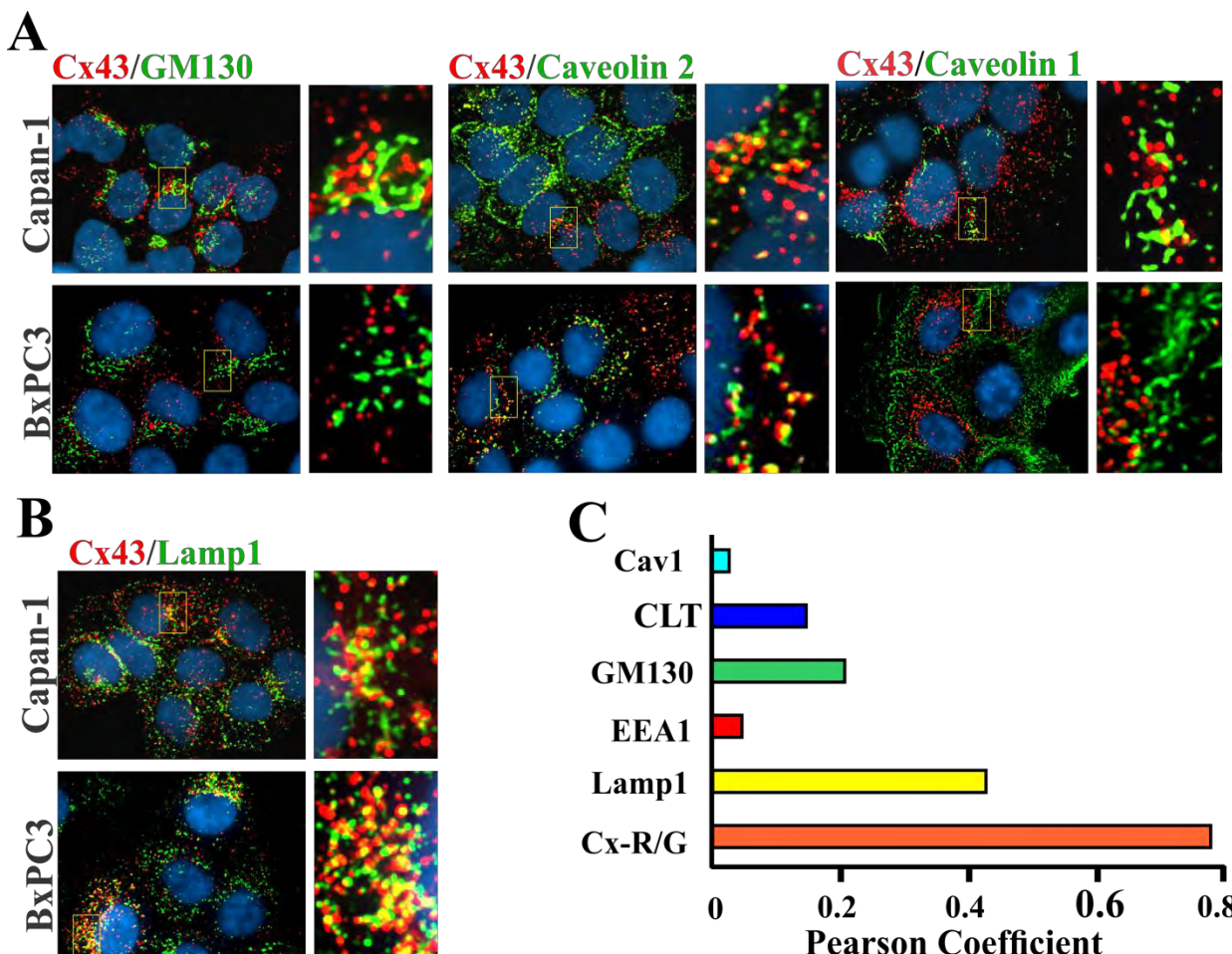


Figure S2. A. Colocalization of Cx43 with various markers. A. Colocalization of Cx43 with the secretory markers GM130 and caveolin2 and with the endocytic marker caveolin-1 (Cav1). BxPC3 and Capan-1 cells were immunostained for Cx43 (red) and various markers (green). B. Cx43 (red) extensively co-localizes with Lamp1 (green). For A and B, enlarged images of the boxed regions are shown on the right. C. Co-localization of Cx43 with various endocytic and secretory markers was quantitated by calculating the Pearson's coefficient (see Materials and Methods). The highest Pearson's coefficient (0.8) was obtained in cell images of cells immunostained with monoclonal and polyclonal antibodies targeting Cx26 using monoclonal and polyclonal antibodies followed by detection with Alexa-594 and Alexa-488-conjugated secondary antibodies (Cx-R/G). Note that significant co-localization with Cx43 is measured for only Lamp1 (0.4). The Pearson coefficients graphed are averaged from 10 separate images from 2 separate experiments. CLT=clathrin.

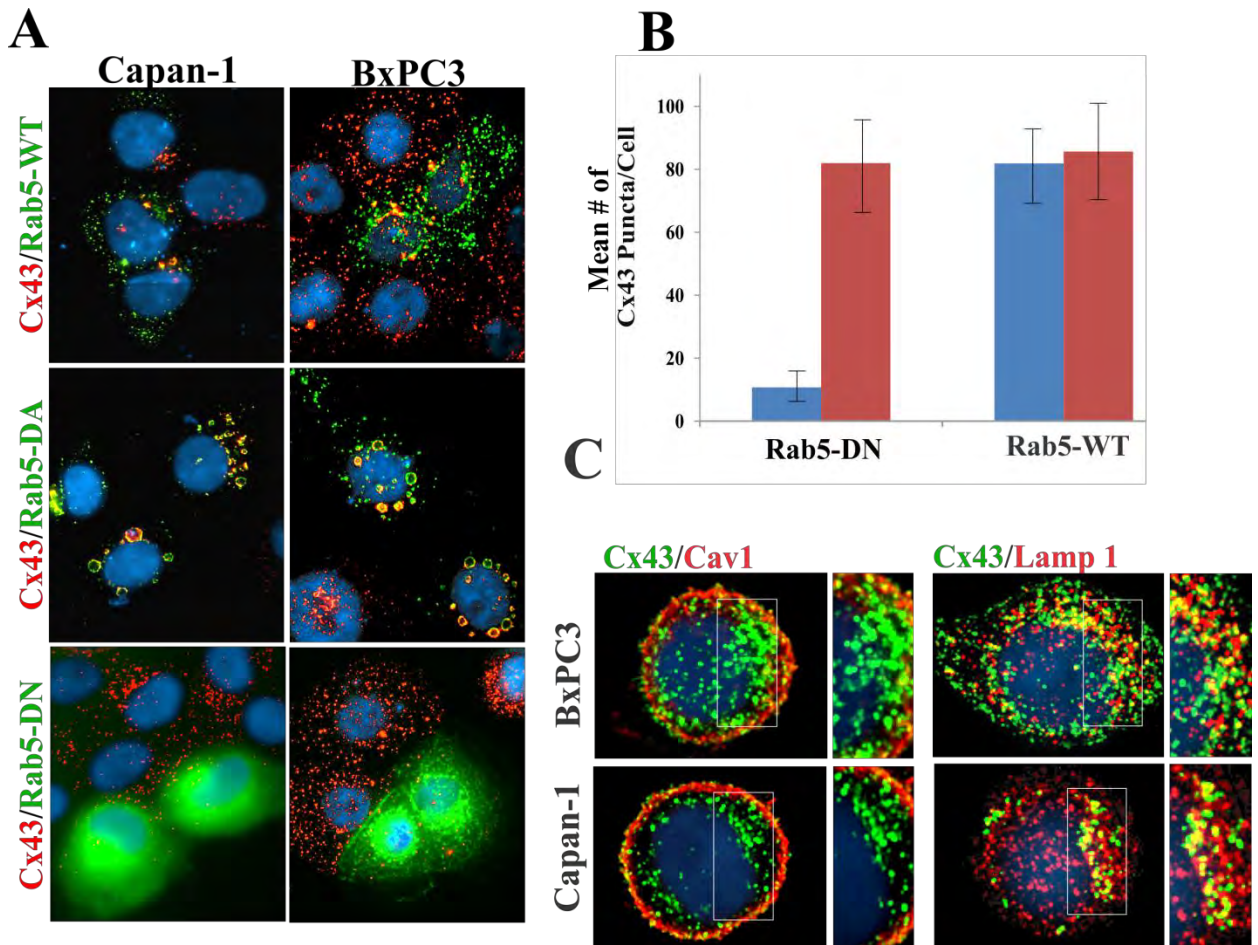


Figure S3. Cx43 is internalized by the clathrin-mediated pathway in Rab5 dependent manner. **A.** Cells were transfected with GFP-tagged Rab5-WT, dominant active Rab5 (Rab5-DA) or dominant negative Rab5 (Rab5-DN) and immunostained for Cx43. Note the disappearance of Cx43 puncta (red) in cells expressing Rab5-DN (green). **B.** Intracellular puncta were quantified in BxPC3 cells expressing Rab5-WT and Rab5-DN. Puncta from 15-20 cells were counted from two separate experiments. Blue and orange represent puncta from transfected and control cells, respectively. **C.** Cx43 co-localizes with Lamp1 but not with caveolin1 (Cav1) in single cells. Cells were immunostained for Cx43 (green) and either for Lamp1 or Cav1 (red). Note discernible co-localization of Cx43 with Lamp1 as shown in the enlarge image of the boxed region on the right.

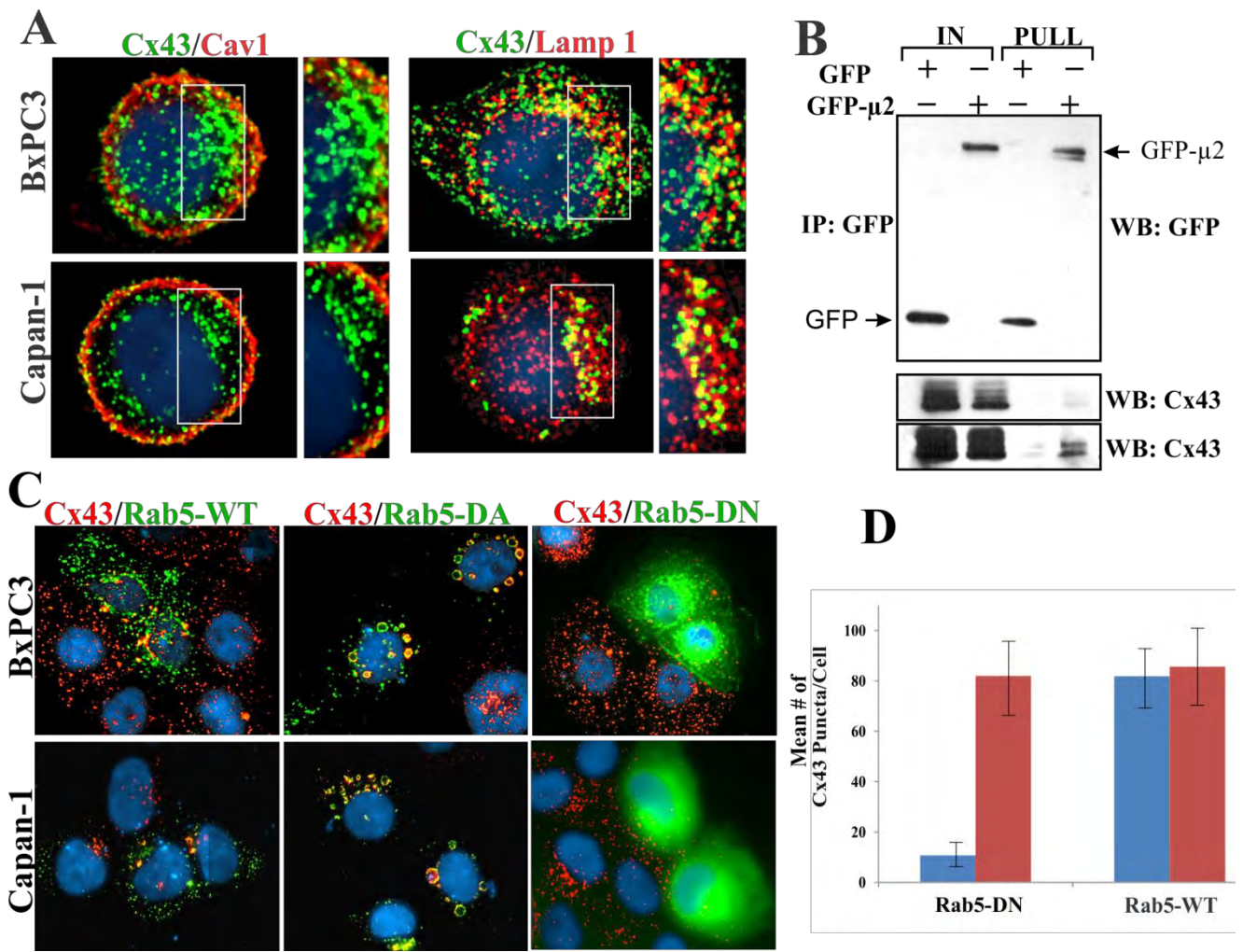


Figure S3. Cx43 is internalized by the clathrin-mediated pathway in Rab5 dependent manner. **A.** Cells were transfected with GFP-tagged Rab5-WT, dominant active Rab5 (Rab5-DA) or dominant negative Rab5 (Rab5-DN) and immunostained for Cx43. Note the disappearance of Cx43 puncta (red) in cells expressing Rab5-DN (green). **B.** Intracellular puncta were quantified in BxPC3 cells expressing Rab5-WT and Rab5-DN. Puncta from 15-20 cells were counted from two separate experiments. Blue and orange represent puncta from transfected and control cells, respectively. **C.** Cx43 co-localizes with Lamp1 but not with caveolin1 (Cav1) in single cells. Cells were immunostained for Cx43 (green) and either for Lamp1 or Cav1 (red). Note discernible co-localization of Cx43 with Lamp1 as shown in the enlarge image of the boxed region on the right.

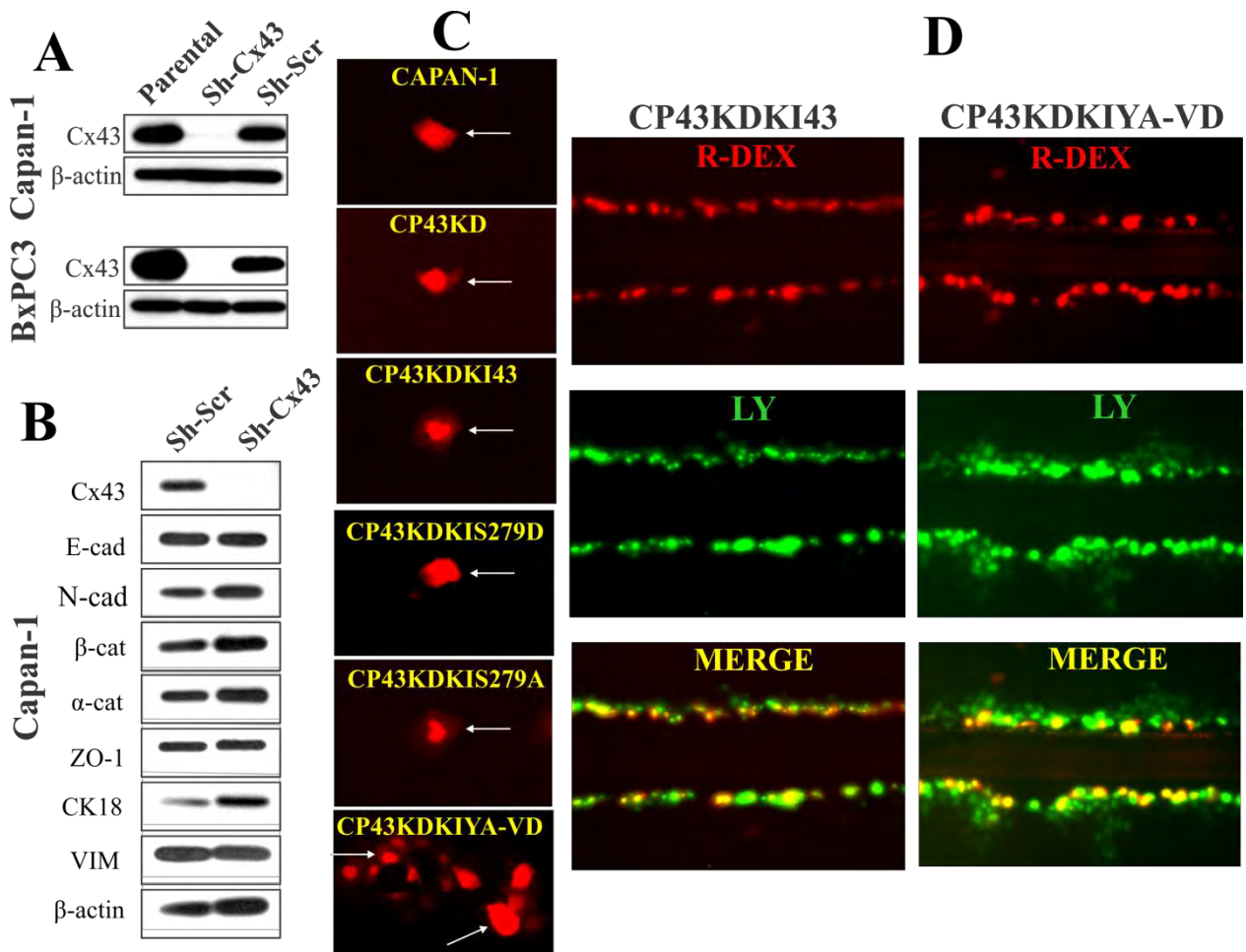


Figure S4. Knock-down of Cx43 in BxPC3 and Capan-1 cells with ShRNA.

AB. Lysates from Capan-1 and BxPC3 cells, expressing shRNA-Cx43 (Sh-Cx43) and ShRNA-Scr (Sh-Scr), were immunoblotted for Cx43. Note the robust knock down of Cx43. β-actin was used as a loading control. **B.** Cx43 knock-down has no off-target effects. The expression of seven junction- or cytoskeleton-associated proteins in Capan-1 expressing Sh-Cx43 and Sh-Scr was analyzed by Western blotting. The shRNA-Cx43 did not knock-down any of the indicated proteins except Cx43. **C & D.** Parental Capan-1 cells, knockdown cells and knockdown cells expressing one of the Cx43 mutants were microinjected with Alexa Fluor 594 (C) or scrape-loaded (D) with rhodamine-conjugated dextran (R-DEX) and Lucifer Yellow (LY). Note that only cells expressing the sorting-motif mutant YA-VD-Cx43 show cell-cell transfer of fluorescent tracers. The microinjected cells are indicated by the white arrows.

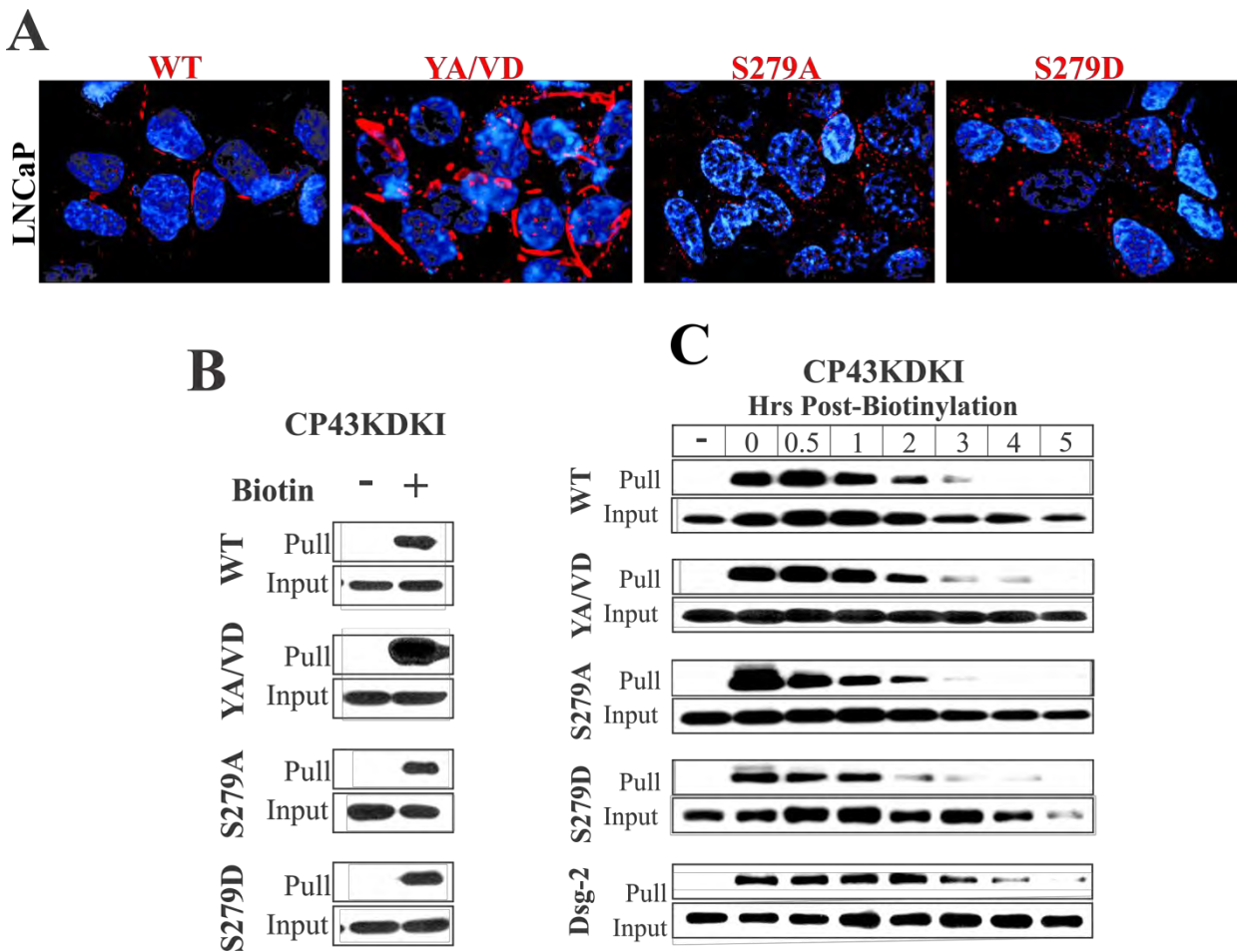


Figure S5. A. LNCaP cells stably expressing WT-Cx43 or the indicated mutants were immunostained for Cx43. Note that YA/VD-Cx43 forms large gap junctions whereas the mutants S279A and S279D form smaller gap junctions and contain many intracellular puncta. **B & C.** Trafficking and the kinetics of degradation of WT-Cx43 and the various mutants. CP43KD cells stably expressing knocked-in WT-Cx43 (WT), sorting-motif mutant YA/VD-Cx43 (YA/VD) or the indicated serine mutants were cell-surface biotinylated. Biotinylated proteins were pulled down by immobilized Streptavidin (Pull), and immunoblotted for Cx43 (**B**). Note that knocked-in WT-Cx43 and all the mutants are biotinylated. **C.** CP43KD cells expressing knocked-in WT-Cx43 or its mutants were biotinylated at 4°C and the kinetics of degradation were determined by incubating cells for various times at 37°C. Note that WT-Cx43 and the mutants are degraded with similar kinetics. Biotinylation of Desmoglien-2 (Dsg-2), a desmosome-associated protein, was used as a control. For the input, 10 µg of total protein was used and probed for Cx43.

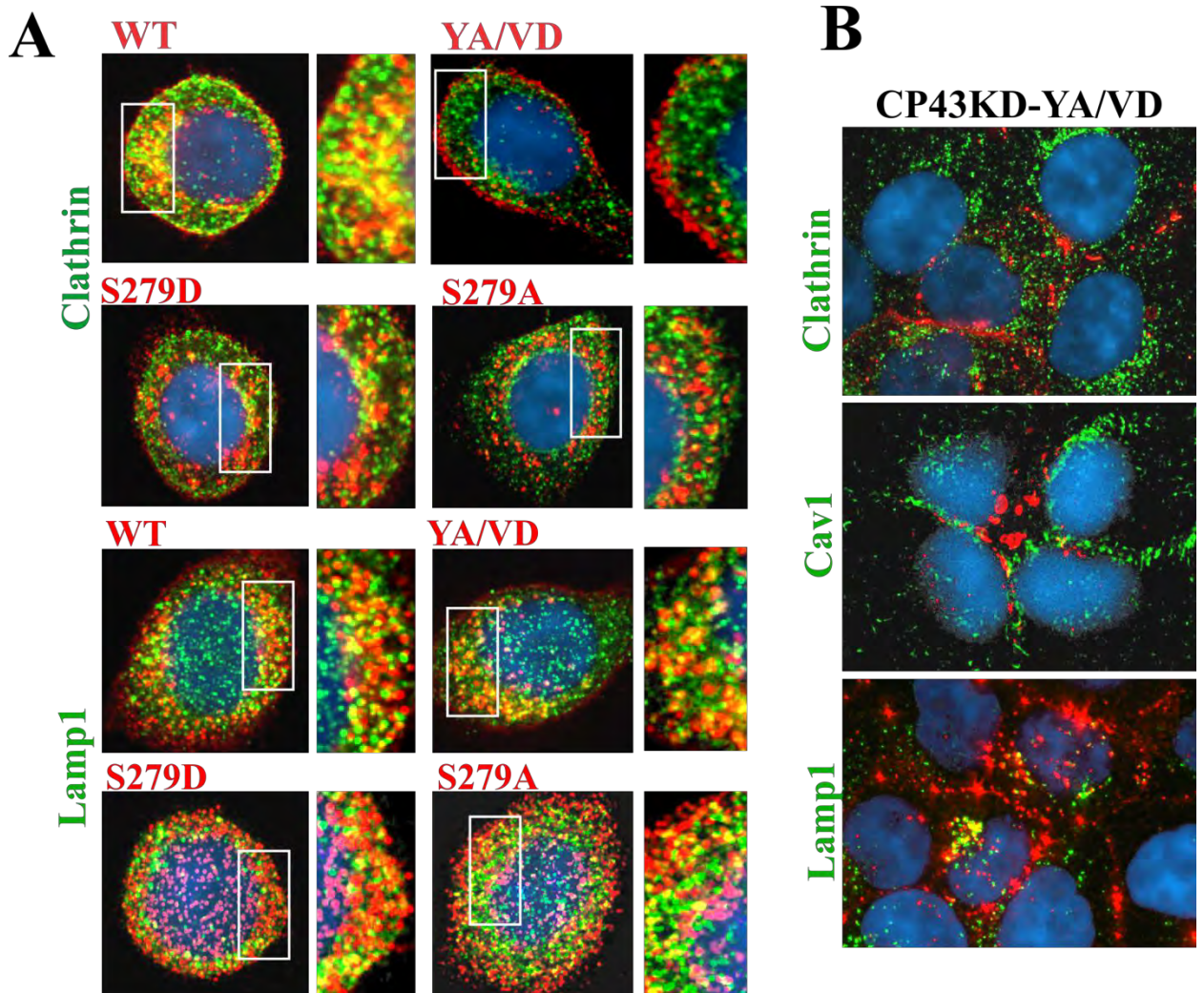


Figure S6. A. Subcellular fate of knocked-in WT-Cx43 and its mutants in CP43KD cells. A. CP43KD cells stably expressing knocked-in WT-Cx43 (WT), YA/VD-Cx43 (YA/VD), S279A or S279D were seeded at single cell density (see Materials and Methods) and immunostained for Cx43 (red), clathrin and Lamp1 (green). Note that WT-Cx43 and S279D co-localize robustly with clathrin whereas YA/VD-Cx43 and S279A do not discernibly co-localize. Note also that WT-Cx43 and all mutants co-localize extensively with Lamp1. B. Gap junctions composed of knocked-in sorting-motif mutant YA/VD-Cx43 (YA/VD) in CP43KD cells are internalized into larger vesicular puncta. CP43KD cells stably expressing YA/VD-Cx43 were immunostained for Cx43 (red), caveolin-1 (Cav1) and Lamp1 (green). Note relatively large and varied size of Cx43-containing intracellular puncta. Partial co-localization of intracellular Cx43 puncta with Lamp1 was observed. Note also the lack of co-localization of YA/VD-Cx43 with either Cav1 or clathrin.

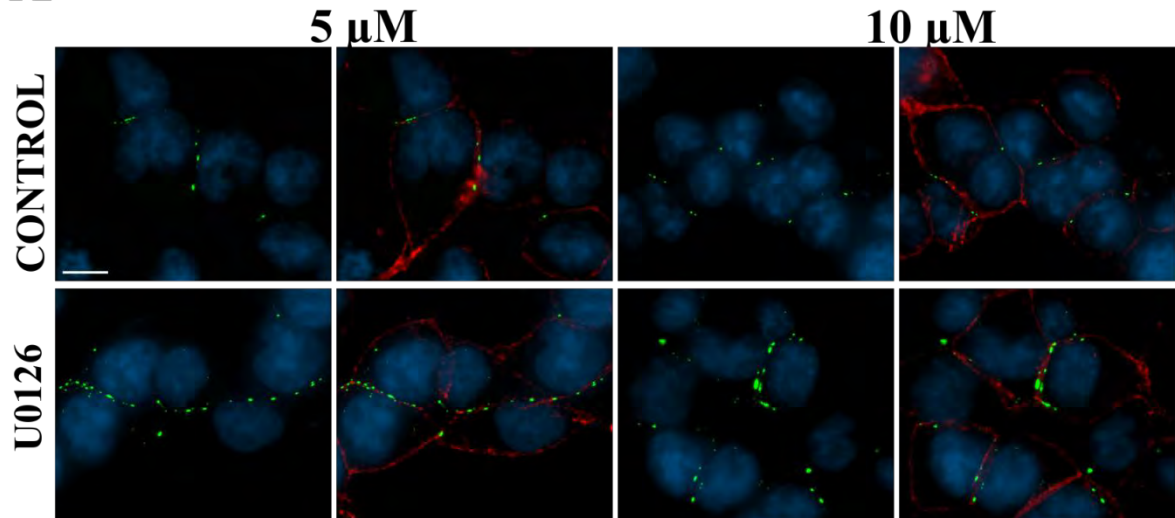
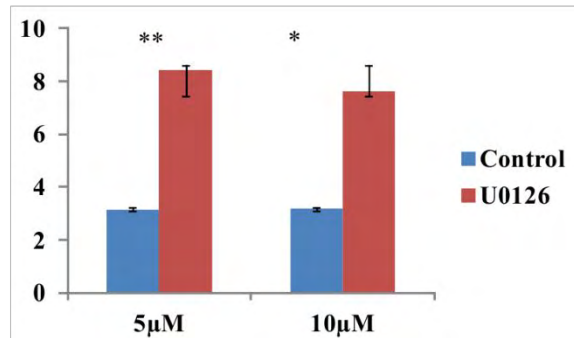
A**B****C**

Figure S7. Inhibition of MAP Kinase activity enhances gap junction assembly in LNCaP cells. **A.** Cx43-expressing LNCaP cells were treated with 5 or 10 μM U0126 for 30min. Cells were fixed and immunostained for Cx43 (green) and E-cadherin (red). Note that U0126 treatment increases the number as well as immunostaining intensity of Cx43-gap-junction puncta. **B.** Cells treated with 10 μM U0126 (TREAT) or 0.1 % DMSO (CNT) for the indicated time (in minutes) were lysed and probed with polyclonal antibody to phospho-ERK. Note inhibition of ERK activity. **C.** The average number of Cx43 gap junction puncta (green) from images of Control (blue bars) and U0126 treated (red bars) cells were counted from 3 random microscopic fields captured with a 63x oil objective. All cell-cell interfaces of approximately 20 μm or more were counted using the measure tool of Volocity. *=p<0.0001 as determined by the student's t-test.

Vitamin D3 Regulates the Formation and Degradation of Gap Junctions in Androgen-Responsive Human Prostate Cancer Cells
 --Manuscript Draft--

Manuscript Number:	PONE-D-13-49919
Article Type:	Research Article
Full Title:	Vitamin D3 Regulates the Formation and Degradation of Gap Junctions in Androgen-Responsive Human Prostate Cancer Cells
Short Title:	Vitamin D3 and gap junction assembly
Corresponding Author:	Parmender Paul Mehta University of Nebraska Medical Center Omaha, Nebraska UNITED STATES
Keywords:	Gap junctions, connexin, vitamin D3, prostate cancer
Abstract:	1 α -25(OH)2 vitamin D3, an active hormonal form of Vitamin D3, is a well-known chemopreventive and pro-differentiating agent. It has been shown to inhibit the growth of several prostate cancer cell lines. Gap junctions, formed of proteins called connexins, are ensembles of cell-cell channels, which permit the exchange of small growth regulatory molecules between adjoining cells. Cell-cell communication mediated by gap junctional channels is an important homeostatic control mechanism for regulating cell growth and differentiation. We have investigated the effect of 1 α -25(OH)2 vitamin D3 on the formation and degradation of gap junctions in an androgen-responsive prostate cancer cell line, LNCaP, which expresses retrovirally-introduced connexin32. This connexin is expressed by the luminal and well-differentiated cells of normal prostate and prostate tumors. Our results document that 1 α -25(OH)2 vitamin D3 enhances the expression of connexin32 and its subsequent assembly into gap junctions. Our results further show that 1 α -25(OH)2 vitamin D3 prevents androgen-regulated degradation of connexin32, post-translationally, independent of androgen receptor mediated signaling. Finally, our findings document that formation of gap junctions sensitizes connexin32-expressing LNCaP cells to the growth inhibitory effects of 1 α -25(OH)2 vitamin D3 and alters their morphology. These findings suggest that the growth-inhibitory effects of 1 α -25(OH)2 vitamin D3 in LNCaP cells may be related to its ability to modulate the assembly of connexin32 into gap junctions.
Order of Authors:	Linda Kelsey Parul Katoch Anuttoma Ray Shalini Mitra Souvik Chakraborty Parmender Paul Mehta
Suggested Reviewers:	James E Trosko, Ph.D Professor, University of Michigan East Lansing James.Trosko@hc.msu.edu Balakrishna Lokeshwar, PhD Professor, University of Miami blokeshw@med.miami.edu Matthias M Falk, Ph.D Professor, Lehigh University mmf4@lehigh.edu
Opposed Reviewers:	
Additional Information:	

Question	Response
<p>Competing Interest</p> <p>For yourself and on behalf of all the authors of this manuscript, please declare below any competing interests as described in the "PLoS Policy on Declaration and Evaluation of Competing Interests."</p> <p>You are responsible for recognizing and disclosing on behalf of all authors any competing interest that could be perceived to bias their work, acknowledging all financial support and any other relevant financial or competing interests.</p> <p>If no competing interests exist, enter: "The authors have declared that no competing interests exist."</p> <p>If you have competing interests to declare, please fill out the text box completing the following statement: "I have read the journal's policy and have the following conflicts"</p> <p>* typeset</p>	The authors have declared that no competing interests exist.
<p>Financial Disclosure</p> <p>Describe the sources of funding that have supported the work. Please include relevant grant numbers and the URL of any funder's website. Please also include this sentence: "The funders had no role in study design, data collection and analysis, decision to publish, or preparation of the manuscript." If this statement is not correct, you must describe the role of any sponsors or funders and amend the aforementioned sentence as needed.</p> <p>* typeset</p>	<p>This research was supported by NIH CA113903, DOD PCRP PC-081198 and PC-111867, Nebraska State Grant LB506 and R0-1DE12308.</p> <p>The funders had no role in study design, data collection and analysis, decision to publish, or preparation of the manuscript.</p>
<p>Ethics Statement</p> <p>All research involving human participants must have been approved by the authors' institutional review board or equivalent committee(s) and that board must be named by the authors in the manuscript. For research involving human participants, informed consent must have</p>	N/A

been obtained (or the reason for lack of consent explained, e.g. the data were analyzed anonymously) and all clinical investigation must have been conducted according to the principles expressed in the [Declaration of Helsinki](#). Authors should submit a statement from their ethics committee or institutional review board indicating the approval of the research. We also encourage authors to submit a sample of a patient consent form and may require submission of completed forms on particular occasions.

All animal work must have been conducted according to relevant national and international guidelines. In accordance with the recommendations of the Weatherall report, "[The use of non-human primates in research](#)" we specifically require authors to include details of animal welfare and steps taken to ameliorate suffering in all work involving non-human primates. The relevant guidelines followed and the committee that approved the study should be identified in the ethics statement.

Please enter your ethics statement below and place the same text at the beginning of the Methods section of your manuscript (with the subheading Ethics Statement). Enter "N/A" if you do not require an ethics statement.

November 26, 2013

Editors
PLoS One

Dear Editors:

We are submitting our manuscript entitled "Vitamin D₃ regulates the formation and degradation of gap junctions in androgen-responsive human prostate cancer cells". This manuscript reports two novel findings with regard to the formation and degradation of gap junctions composed of connexin32 in response to 1-25(OH)₂ Vitamin D₃ (1-25D) — an important hormone and a chemopreventive agent, which orchestrates prostate morphogenesis and oncogenesis in vivo and in vitro.

This manuscript is a sequel to our two earlier studies that dealt with the effect of androgens and retinoids on the formation and degradation of gap junctions in androgen-responsive human prostate cancer cells (Mol Biol Cell 17, 5400, 2006; Kelsey et al PLoS one 7, e32846, 2013). The findings reported in this manuscript point out hitherto undefined cross-talk between androgen-regulated and 1-25D-regulated signaling pathways with respect to assembly of connexin32 into gap junctions. Significantly, our findings show that formation of gap junctions augments the growth modulatory effect of 1-25D in androgen-responsive human prostate cancer cells.

We feel that the manuscript bodes very well with the general scope this journal. The findings reported in this manuscript have not been previously published anywhere. We will be more than happy to provide any additional information. With best wishes:

Sincerely,



Parmender P. Mehta, Ph.D
Professor
Department of Biochemistry and Molecular Biology
University of Nebraska Medical Center
Omaha, Nebraska, 68198

**Vitamin D₃ Regulates the Formation and Degradation of Gap Junctions in Androgen-Responsive
Human Prostate Cancer Cells**

Linda Kelsey, Parul Katoch, Anuttoma Ray, Shalini Mitra, Souvik Chakraborty, and Parmender P. Mehta

Department of Biochemistry and Molecular Biology, University of Nebraska Medical Center
Omaha, NE 68198, USA

Corresponding Author: Parmender P. Mehta, Ph.D.

Telephone: (402)-559-3826

Fax: (402)-559-6650

Email: pmehta@unmc.edu

Short Title: Vitamin D₃ and gap junction assembly

Keywords: Gap junctions, connexin, vitamin D3, prostate cancer

Abbreviations: Cx: connexin; GJ: gap junction; MB: mibolerone; 1-25D: 1 α -25(OH)₂ vitamin D₃, 9-CRA: 9-Cis Retinoic Acid; ATRA: All Trans Retinoic Acid ; PCA: Prostate Cancer; DHT: Di-hydrotestosterone; AR: androgen receptor; ERAD: Endoplasmic reticulum associated degradation

Abstract

1α -25(OH)₂ vitamin D₃, an active hormonal form of Vitamin D₃, is a well-known chemopreventive and pro-differentiating agent. It has been shown to inhibit the growth of several prostate cancer cell lines. Gap junctions, formed of proteins called connexins, are ensembles of cell-cell channels, which permit the exchange of small growth regulatory molecules between adjoining cells. Cell-cell communication mediated by gap junctional channels is an important homeostatic control mechanism for regulating cell growth and differentiation. We have investigated the effect of 1α -25(OH)₂ vitamin D₃ on the formation and degradation of gap junctions in an androgen-responsive prostate cancer cell line, LNCaP, which expresses retrovirally-introduced connexin32. This connexin is expressed by the luminal and well-differentiated cells of normal prostate and prostate tumors. Our results document that 1α -25(OH)₂ vitamin D₃ enhances the expression of connexin32 and its subsequent assembly into gap junctions. Our results further show that 1α -25(OH)₂ vitamin D₃ prevents androgen-regulated degradation of connexin32, post-translationally, independent of androgen receptor mediated signaling. Finally, our findings document that formation of gap junctions sensitizes connexin32-expressing LNCaP cells to the growth inhibitory effects of 1α -25(OH)₂ vitamin D₃ and alters their morphology. These findings suggest that the growth-inhibitory effects of 1α -25(OH)₂ vitamin D₃ in LNCaP cells may be related to its ability to modulate the assembly of connexin32 into gap junctions.

Introduction

The role of Vitamin D₃, and its active hormonal form 1 α -25(OH)₂ vitamin D₃ (1-25D), as an anti-neoplastic, pro-differentiating, and pro-apoptotic agent has been established in a wide variety of normal and malignant epithelial cells, including prostate cancer (PCA) [1–4]. The actions of 1-25D are mediated by binding to its receptor, VDR, one of the members of nuclear receptor superfamily, which is expressed in a wide variety of cells including prostate. The VDR heterodimerizes with the RXR receptor and binds to VDR response element to alter gene expression [1]. Based upon the observation that PCA mortality rates in the U.S are inversely proportional to the geographically incident ultraviolet radiation exposure from the sun, and that ultraviolet light is essential for vitamin D₃ synthesis in the skin, a role for this vitamin in decreasing the risk of developing PCA has been suggested [5,6]. Numerous *in vitro* studies show consistent growth inhibitory and differentiation-inducing effects of vitamin D₃ on prostate carcinoma cells, and animal studies show that it not only reduces the incidence of PCA by acting as a chemopreventive agent but also suppresses metastasis [7–10].

Gap junction (GJ)s are ensembles of cell-cell channels that signal non- canonically, by permitting the direct exchange of small molecules ($\leq 1500\text{Da}$) between the cytoplasmic interiors of contiguous cells [11]. The constituent proteins of GJs, called connexins (Cxs), are coded by 21 genes, which have been designated according to their molecular mass [12]. Cell-cell channels are bicellular structures formed by the collaborative effort of two cells. To form a GJ cell-cell channel, Cxs first oligomerize in the trans-Golgi network as a hexamer, called connexon, which docks with the connexon displayed on a contiguous cell [13,14]. Multiple lines of evidence now lend credence to the notion that cell-cell communication mediated by gap junctional channels is an important homeostatic control mechanism for regulating cell growth and differentiation and for curbing tumor promotion. For example, impaired Cx expression, or loss of GJ function, has been implicated in the pathogenesis of several types of cancers

and diseases [15–19]. Also, mutations in several Cx genes have been detected in genetic disorders characterized by aberrant cellular proliferation and differentiation [13,20].

Our previous studies showed that the expression of Cx32, which is expressed by the luminal cells of the prostate, coincided with the acquisition of the differentiated state of luminal cells [21,22]. Moreover, we documented that the progression of PCA from an androgen-dependent state to an invasive, androgen-independent state was characterized by the aberrant trafficking of Cx32 and/or impaired assembly into GJs [22–24]. Furthermore, our studies showed that forced expression of Cx32 into an indolent, androgen-responsive human PCA cell line, LNCaP, retarded cell growth *in vivo* and *in vitro* [22]. We have also shown that in LNCaP cells expressing Cx32, formation and degradation of GJs was regulated by androgens, which controlled the expression level of Cx32 posttranslationally by preventing its degradation by endoplasmic reticulum associated degradation (ERAD) [25]. Androgens are required to maintain the secretory (differentiation-related) function of luminal epithelial cells of normal prostate as depletion of androgens by surgical or chemical means triggers apoptosis or dedifferentiation of these cells [26–29]. Our recent studies have shown that retinoids, which also regulate the proliferation and differentiation of prostate epithelial cells [28,30], also enhance the assembly of Cx32 into GJs [31]. These studies lend credence to the notion that formation and degradation of GJs may be linked to the proliferation and differentiation of luminal prostate epithelial cells.

Like androgens and retinoids, vitamin D₃ is essential for the normal development of the prostate and has also been documented to modulate PCA progression [7,9]. Recent studies have shown that vitamin D suppressed prostatic epithelial neoplasia in Nkx3.1/PTEN transgenic mice [32]. Epidemiologic, cell culture, and clinical studies have implicated antitumor effects of 1-25D for PCA and it has been suggested to be a potent chemopreventive agent [3,4]. However, in contrast to colon cancer [1,33], the potential of effectiveness of 1-25D in the chemoprevention of PCA has remained

controversial despite numerous studies in transgenic mouse models of PCA and its use in clinical trials [1,2]. Earlier studies, including ours, have shown that the growth inhibitory and differentiation inducing effects of chemopreventive agents might be related to their ability to enhance gap junctional communication [34–38]. The luminal cells of normal prostate express Cx32 and form large GJs and progression of PCA is accompanied by loss of ability to form GJs [22,23]. Formation of GJs has been implicated in maintaining the polarized and differentiated state of epithelial cells [39]. These studies prompted us to examine the effect of 1-25D on the assembly of Cx32 into GJs in androgen-responsive human PCA cell line LNCaP. Because 1-25D has been shown to increase the expression of AR in LNCaP cells [40], we rationalized that it might modulate androgen-regulated formation and degradation of GJs and affect growth of androgen-responsive PCA cells that express Cx32. By using androgen-responsive LNCaP cells, which express retrovirally introduced Cx32 [25], we show that 1-25D enhances the assembly of Cx32 into GJs. Moreover, we further show that 1-25D prevents androgen-regulated degradation of GJs post-translationally, independent of AR-mediated signaling. Finally, our findings show that formation of GJs sensitizes LNCaP cells to growth inhibitory effects of 1-25D and alters their morphology.

Materials and Methods

Cell Culture

Androgen-responsive human PCA cell line, LNCaP, was a generous gift from Dr. Lin [41]. LNCaP-32 cells, one of the several clones of LNCaP cells expressing retrovirally transduced rat Cx32, and LNCaP-N cells, one of the several control clones selected in G418 after infection with the control retrovirus, have been described [25,31]. Parental LNCaP cells, hereafter referred to as LNCaP-P cells, were grown in RPMI containing 5% fetal bovine serum in an atmosphere of 5% CO₂/95% air whereas LNCaP-N and LNCaP-32 cells were maintained in RPMI containing 5 % fetal bovine serum containing

G418 at 200 µg/ml as described [25,31]. Steroid-depleted (charcoal-stripped) serum and phenol red free RPMI were obtained from HyClone Laboratories (Salt Lake City, UT).

Antibodies and Immunostaining

The sources of both monoclonal and polyclonal antibodies against Cx32 have been described previously [24,25,31,42,43]. Mouse anti-occludin (clone OC-3F10) was from Zymed laboratories Inc. (South San Francisco, CA). Rabbit antibodies against α- and β-catenin and mouse anti-β-actin (clone C-15) were from Sigma (St. Louis, MO). Monoclonal antibodies against E-cadherin (E-cad), α-catenin, β-catenin, generously provided by Drs. Johnson and Wheelock (Eppley Institute), have been described [25,42,43]. A rabbit polyclonal anti-AR receptor antibody was from Santa Cruz Biotech (sc-13062, San Diego, CA). Cells (1.5×10^5), seeded in six well clusters containing glass cover slips and allowed to grow to approximately 50 % confluence, were immunostained with various antibodies as described [24,25,31,42–44]. Secondary antibodies (rabbit or mouse), conjugated with Alexa 488 and Alexa 594, were used as appropriate. Images of immunostained cells were acquired with Leica DMRIE microscope (Leica Microsystems, Wetzler, Germany) equipped with Hamamatsu ORCA-ER2 CCD camera (Hamamatsu-City, Japan) and analyzed using image processing software (Volocity, Version 6.3; Improvision, Inc; Perkin Elmer) as described [42–44].

Stock Solutions

Stock solution of 1-25D (10 µM) was prepared in ethanol and stored in aliquots at -80°C protected from light. Synthetic androgen mibolerone (MB) and a natural androgen dihydro-testosterone (DHT) were purchased from BIOMOL (ENZO Life Sciences, Inc., Farmingdale, NY). Stock solutions of MB and DHT were prepared at 1 mM in ethanol and stored at -20 °C in small aliquots protected from light. They were appropriately diluted in the medium at the time of treatment. All experiments were performed in yellow light as described [36,37].

Androgen Depletion and Other Treatments

Cells were seeded in six well clusters with glass cover slips (1.5×10^5 cells per well) and in 6-cm (2 $\times 10^5$ cells per dish) and 10-cm dishes (3.5 $\times 10^5$ cells per dish) in 2, 4 and 10 ml complete medium, respectively. Cells were treated by replenishing with fresh medium containing various reagents at the desired concentration when they attained 50 % confluence. Controls were treated with ethanol such that the final concentration of the solvent did not exceed 0.1%. When cells were to be grown under androgen-depleted conditions, normal cell culture medium was replaced with androgen-depleted cell culture medium (phenol red-free RPMI containing 5 % charcoal-stripped serum). The controls received fresh medium containing normal serum.

Western Blot Analysis and Detergent Solubility of Connexin32

Cells (5×10^5) were seeded in 10 cm dishes in replicate in 10 ml of complete medium and grown to confluence in the presence and absence of various reagents. Cell lysis, detergent solubility assay with 1 % Triton X-100 (TX-100) and the expression level of Cx32 were analyzed by Western blot analysis as described [25,42,43]. Briefly, after lysis in buffer SSK (10 mM Tris, 1 mM EGTA, 1 mM PMSF, 10 mM NaF, 10 mM NEM, 10 mM Na₂VO₄, 10 mM iodoacetamide, 1% TX-100, pH 7.4), total, detergent-soluble and -insoluble extracts were separated by ultracentrifugation at 100,000 $\times g$ for 60 min (35,000 rpm in analytical Beckman ultracentrifuge; Model 17-65 using a SW50.1 rotor). The detergent-insoluble pellets were dissolved in buffer C (70 mM Tris/HCl, pH 6.8, 8 M urea, 10 mM NEM, 10 mM iodoacetamide, 2.5% SDS, and 0.1 M DTT). Following normalization based on cell number, the total and TX-100-soluble and -insoluble fractions were mixed with 4xSDS-loading buffer to a final concentration of 1x and incubated at room temperature for 1 h before SDS-PAGE analysis. Blots were developed with C-Digit (Li-COR, Lincoln, NE) using SuperSignal WestFemto Maximum Sensitivity Substrate (Thermo Scientific; Rockford, IL).

Communication Assays

Gap junctional communication was assayed by microinjecting Lucifer Yellow (MW 443 Da; Lithium salt), Alexa Fluor 488 (MW 570 Da; A-10436), and Alexa Fluor 594 (MW 760 Da; A-10438) using Eppendorf InjectMan and FemtoJet microinjection systems (models 5271 and 5242, Brinkmann Instrument, Inc. Westbury, NY) mounted on Leica DMIRE2 microscope. After capturing the images of microinjected cells with the aid of CCD camera (Retiga 2000R, FAST 1394) using QCapture (British Columbia, Canada), the permeability of various fluorescent tracers was quantitated by scoring the number of fluorescent cells at 1 min (Lucifer Yellow), 3 min (Alexa 488) and 15 min (Alexa 594) after microinjection into test cell as described [22,25,42,45].

Colony Formation and Cell Growth Assays

Cell growth was assessed either by colony forming assay or by counting the number of cells as described [22,45]. For colony forming assay, 1×10^3 cells were seeded in 6 cm dishes in triplicate in 3 ml culture medium. After 24 h, one ml medium containing 1-25D, MB or DHT was added to the dishes to give the desired final concentration. Cells were grown for 21 days, with a medium change every 4 days containing the appropriate concentration of the above reagents, when they formed visible colonies. Colonies in dishes were fixed with 3.7% buffered formaldehyde, stained with 0.025 % solution of crystal violet in PBS, and photographed. For measuring cell growth, 5×10^4 cells were seeded in 6 cm dishes in replicate and treated with 1-25D described above. Cells were allowed to grow for 10 days with a medium change at day 5. Cells were trypsinized and counted in a hemocytometer.

RESULTS

Vitamin D₃ Enhances Cx32 Expression Level

We used LNCaP-32 cells that express retrovirally transduced rat Cx32 described previously [25,31]. We previously showed that in LNCaP-32 cells androgens regulated the formation of GJs, post-

translationally, by controlling the expression level of Cx32 by inhibiting its ERAD-mediated degradation [25]. Our subsequent studies showed that androgen-regulated degradation of Cx32 was abrogated by all-trans retinoic acid (ATRA) and 9-Cis retinoic acid (9-CRA) [31]. We thus rationalized that 1-25D might act similar to ATRA and 9-CRA. Based on the earlier studies showing the effect of vitamin D on LNCaP cell growth [10,46–49], we treated LNCaP-32 cells with various concentrations of 1-25D to examine its effect on the expression level of Cx32. We found that 1-25D increased Cx32 expression level in a dose-dependent manner (Figure 1A). Significant enhancement was observed only at concentration above 1 nM. Concentrations higher than 10 nM were toxic to these cells as assessed by the colony formation assay (unpublished data). For subsequent studies we chose 10 nM 1-25D. Time course studies showed that the increase in Cx32 expression level occurred as early as 12 h post-treatment with 1-25D and reached a plateau at 72 h (Figure 1B). The effect of 1-25D on Cx32 expression level was as potent as of synthetic androgen, MB, and 9-CRA (Figure 1A,C). Moreover, combined treatment with 1-25D and MB was more effective in increasing Cx32 expression level (Figure 1C). Vitamin D₃ had previously been shown to affect the expression of level of E-cad, a constituent protein of adherens junctions, in colon cancer cells [33]. To determine if 1-25D also affected the expression level of adherens junction associated proteins, we measured the expression level of E-cad and its associated proteins α- and β-catenins as well as well tight junction associated proteins, ZO-1 and occludin, 72 h after treatment with 1-25D. The results showed that 1-25D had no significant effect on the expression level of E-cad and α- and β-catenins, however, the expression level of tight junction associated protein, occludin, was enhanced marginally but reproducibly (Figure 1D). As measured by semi-quantitative RT-PCR analysis, 1-25D neither induced the expression of endogenous Cx32 in LNCaP-P or LNCaP-N cells (data not shown) nor altered the expression level of retrovirally transcribed Cx32 mRNA in LNCaP-32 as documented previously [25].

Vitamin D₃ Enhances Gap Junction Assembly and Junctional Communication

We next examined the effect of 1-25D on the assembly of Cx32 into GJs. We found that,

concomitant with an increase in the expression level of Cx32, 1-25D also increased GJ assembly as assessed by immunocytochemical analysis (Figure 2A) and biochemically by Western blot analysis of total, Triton X (TX)100-soluble and –insoluble extracts at 48 h after treatment (Figure 2B). This biochemical method is based on the principle that Cxs, which are incorporated into GJs, become insoluble in TX100 whereas Cxs that are not incorporated into GJs remain soluble [50]. This assay has been reproducibly shown to measure the assembly of Cxs into GJs as documented by earlier studies [24,25,50]. Moreover, we found that enhancement of GJ assembly was accompanied by a 2-3 fold parallel increase in junctional communication as determined by the junctional transfer of three GJ permeable fluorescent tracers, Lucifer Yellow (MW 443), Alexa 488 (MW 570), and Alexa 594 (MW 760). For example, 1-25D increased junctional transfer of Alexa 594 (MW 760) 2-3 folds compared to controls (Table 1). The effect of 1-25D on junctional communication was as potent as of synthetic androgen, MB, and the natural androgen DHT (Table 1). To determine if 1-25D affected the assembly of other junctional complexes, we also examined the detergent-solubility of adherens and tight junction associated proteins. The rationale behind these studies was that E-cad has been shown to facilitate the assembly of Cxs into GJs [42,43,51], and Cx expression has been shown to facilitate the assembly of tight junctions and their constituent proteins [39]. We found that 1-25D had no significant effect on the solubility of E-cad and its associated proteins, α - and β -catenin, in TX-100 suggesting that their assembly was not further enhanced into adherence junctions. The assembly of tight junction associated proteins ZO-1 and occludin appear to be marginally enhanced (Figure 2B). Taken together, these data suggest that 1-25D, like androgens and retinoids, enhances the expression level of Cx32, and its subsequent assembly into GJs, without significantly altering the expression level of other cell junction associated proteins.

Vitamin D₃ Modulates Androgen-regulated Formation and Degradation of Gap Junctions

Earlier studies with LNCaP-32 cells had shown that androgen depletion caused degradation of Cx32 by ERAD, and that androgens enhanced GJ formation by re-routing the ERAD-targeted pool of

Cx32 to the cell surface, making it amenable for GJ assembly [25]. In subsequent studies, we showed that androgen-regulated formation and degradation of GJs was prevented by 9-CRA and ATRAs [31]. We rationalized that 1-25D might enhance GJ assembly by rescuing the ERAD-targeted pool of Cx32 like 9-CRA and ATRA. Therefore, we examined the expression level of Cx32 and its assembly into GJs upon androgen depletion in the presence and absence of 1-25D in LNCaP-32 cells. For these studies, we used androgen-depleted (charcoal-stripped) and phenol-red free cell culture medium to grow cells. As was observed in our earlier studies [25], we found that androgen-depletion decreased the expression level of Cx32 within 12 h, which not only was prevented upon addition of MB but also by 1-25D (Figure 3A). Moreover, combined treatment with MB and 1-25D appeared to be more effective in enhancing the expression level of Cx32 (Figure 3A, upper blot). We also found that androgen depletion decreased the expression level of AR, which was also prevented upon treatment with not only androgens but also with 1-25D (Figure 3A, bottom blot). To substantiate the above data, we further assessed the formation of GJs immunocytochemically (Figure 3B) and functionally by measuring the junctional transfer of Lucifer Yellow (MW 443 Da), Alexa 488 (MW 570 Da), and Alexa 594 (MW 760 Da) (Table 2). The results showed that androgen depletion reduced the number of GJs profoundly as assessed by lack of Cx32-specific immunostaining at cell-cell contact areas, while GJs were readily observed when androgen-depleted medium was supplemented with 1-25D and MB (Figure 3B). Functional assays showed that the junctional transfer of Lucifer Yellow, Alexa 488 and Alexa 594 decreased significantly upon androgen depletion, which was prevented upon replenishing androgen-depleted medium with MB and 1-25D (Table 2), thus substantiating the immunocytochemical data.

The immunocytochemical and junctional transfer data were further corroborated by the TX-100-solubility assay (Figure 3C). We also examined the effect of androgen-depletion on the detergent solubility of E-cad and β -catenin. The results showed that the depletion had no discernible effect as was observed in our earlier studies (Figure 3C). However, consistent with our earlier studies [25] , the androgen depletion increased the detergent-solubility of occludin but not ZO-1 (Figure 3C). We also

examined the effect of MB and 1-25D either alone or in combination on the formation of GJs in parental LNCaP-P and G418-resistant LNCaP-N cells and found that they had no effect (data not shown). Collectively, these data suggest that 1-25D prevents androgen-regulated degradation of Cx32 and enhances GJ formation in LNCaP-32 cells. Because combined treatment with androgens and 1-25D was neither significantly synergistic nor additive, it is likely that GJ formation was enhanced by rescuing the same pool of Cx32 that was targeted for ERAD upon androgen depletion. Moreover, as was observed in our earlier studies, the assembly and detergent-solubility of Cx32 and occludin into cell junctions, or vice versa, appears to be regulated coordinately [25].

1-25D Enhances Gap Junction Formation Independent of Androgen Receptor Function

Our data showed that 1-25D prevented the degradation of AR upon androgen depletion (Figure 3A, bottom blot). Also treatment of LNCaP cells with 1-25D had been shown to enhance AR expression level [40]. Thus, we considered the possibility that the effect of 1-25D on enhancement of GJ assembly depended on the function of AR alone — and not on the independent effect of 1-25D. To test this notion, we treated LNCaP-32 cells with the anti-androgen, Casodex (Bicalutamide), to block androgen action [52,53]. Casodex caused degradation of AR and abolished the effect of MB and DHT on Cx32 expression level (Figure 4A) as was observed in our earlier studies [25,31]. However, we found that Casodex had no effect on the enhancement of the expression level of Cx32 resulting from treatment with 1-25D in androgen-depleted medium (Figure 4A). To substantiate these data, we next examined the formation of GJs immunocytochemically in cells treated with Casodex in the presence and absence of MB and 1-25D. We found that GJs were not formed when cells were treated with Casodex in normal serum or in androgen-depleted medium containing MB as was observed in our earlier studies (Figure 4B) [25,31]. On the other hand, we found that GJs were abundantly formed when cells were treated with Casodex and 1-25D (Figure 4B). Altogether, these data suggest that the mechanism by which 1-25D prevents the degradation of Cx32 and enhances GJ formation upon androgen depletion is independent of AR.

Connexin32 Expression Alters the Growth Response of LNCaP Cells to 1-25D

Our earlier studies showed that Cx32 expression potentiated the growth inhibitory effect of 9-CRA and ATRA in LNCaP cells [31]. To test if 1-25D has similar effect on growth, we measured cell growth of LNCaP-32 cells at concentrations that were barely growth inhibitory to LNCaP-P cells. We determined cell growth by the colony forming assay as well as by counting the number of cells (Figure 5, Table 3; see Materials and Methods). As assessed visually by the size of the colonies, we found that the growth of LNCaP-32 cells was profoundly inhibited by 1-25D whereas the growth of LNCaP-P and LNCaP-N cells was not substantially affected (Figure 5A, B). These data were substantiated by measuring the growth of LNCaP-32 cells at two different concentrations (Table 3). For example, the growth of LNCaP-P and LNCaP-N cells was inhibited by only 20-25 % upon treatment with 1-25D (1nM and 2.5 nM) whereas the growth of LNCaP-32 cells was inhibited by 55-70 %. Moreover, we found that higher concentrations of 1-25D (5 and 10 nM) altered the morphology of LNCaP-32 cells profoundly such that LNCaP-32 cells treated with 1-25D appeared flatter and more epithelial-like whereas these changes were minimally observed in LNCaP-P and LNCaP-N cells (Figure 6).

DISCUSSION

The main findings of this study are as follows: 1. 1-25D enhances the expression level of Cx32 and its assembly into functional GJs in androgen-responsive LNCaP cells through inhibition of Cx32's degradation. 2. Formation of GJs sensitizes LNCaP cells to the growth inhibitory effect of 1-25D. We previously showed that 9-CRA and ATRA, the two well-known chemopreventive agents, also enhanced GJ assembly and sensitized these cells to their growth inhibitory effects [31]. Thus, it appears that GJ assembly is also the down-stream target of 1-25D in androgen-responsive LNCaP-32 cells, leading to suppression of growth. Several independent lines of inquiry prompted us to undertake these studies. First, growth inhibitory and chemopreventive effects of retinoids and vitamin D₃ had been previously documented to correlate with their ability to enhance the assembly of Cxs into GJs in other cancer cell

types [35–37,54]. Second, the differentiated and polarized state of epithelial cells of the prostate, as well as of several other exocrine glands and tissues, had generally been found to coincide with the expression of Cx32 and its assembly into GJs [22,23,55]. Third, numerous studies had shown that like androgens [28,29], retinoids [54,56–60], and 1-25D were essential for the growth and differentiation of the prostate [4,7,61]. Hence, we rationalized that its expression and assembly into GJs might as well as be regulated by 1-25D either alone or in conjunction with the androgens.

How might 1-25D enhance GJ assembly in LNCaP-32 cells? Nearly 50 % of newly synthesized Cx32 is degraded in the endoplasmic reticulum by ERAD [62]. We had previously shown that in LNCaP-32 cells, androgen depletion caused the degradation of nearly 70-80 % of Cx32 by ERAD, and degradation was prevented upon replenishment with the androgens, which allowed Cx32 to traffic to the cell surface and assemble into GJs [25]. These studies further showed that androgens neither induced the expression of Cx32 in Cx-null LNCaP-P cells nor increased the expression level of retrovirally driven Cx32 in LNCaP-32 cells [25,31]. Thus, in LNCaP-32 cells, androgens enhanced the expression level of Cx32 posttranslationally [25]. Although not tested directly, our data seem to suggest that 1-25D also enhances GJ assembly by preventing the androgen-regulated degradation of Cx32 by ERAD posttranslationally both under normal and androgen-depleted conditions. Like androgens, 1-25D neither induced the expression of the endogenous Cx32 in LNCaP-32 cells nor affected retroviral driven Cx32 mRNA transcripts. Our previous studies with LNCaP-32 cells showed that AR-mediated signaling was the sole determining factor in enhancing Cx32 expression level and preventing GJ degradation both under androgen-depleted or androgen-containing medium as Casodex, which inhibits AR-function [63], annulled the effect of androgens on Cx32 expression level and its subsequent assembly into GJs [25]. With regard to 1-25D effect, our data showed that it enhanced the expression level of AR under androgen-depleted conditions (Figure 4A). Therefore, it is possible that the effect of 1-25D in the absence of androgens may be indirectly caused by persistent and increased level of AR and its activation by the trace amounts of androgens present in the charcoal-stripped

medium. However, 1-25D also enhanced GJ assembly robustly in the presence Casodex in androgen-depleted medium, which robustly decreased AR level and inhibited AR function (Figure 4B). One plausible explanation for these findings is that 1-25D activates an AR-dependent mechanism under androgen-depleted conditions to rescue the ERAD-targeted pool of Cx32 yet triggers another signaling pathway to enhance GJ assembly when AR function is inhibited by Casodex both under normal and androgen-depleted conditions. Further studies are required to explore this possibility. Of note here are the findings that similar effects were also observed with 9-CRA and ATRA [31].

Cadherins have been shown to facilitate the assembly of Cxs into GJs. However, we failed to observe any significant effect on the expression and degradation of adherens junction associated proteins E-cad and α and β catenin both under normal and androgen-depleted conditions (Figures 2 and 3). Therefore, E-cad and its assembly into adherens junctions are not the likely targets of 1-25D in enhancing GJ assembly as was observed in human colon carcinoma cells [33]. The assembly of Cx32 into GJs has also been shown to affect TJ assembly [39,64]. Our previous studies had shown that androgen depletion increased the detergent-solubility of occludin, without significantly altering its expression level, and that the trafficking of occludin to the cell surface and its detergent-solubility was controlled by the assembly of Cx32 into GJs under androgen-depleted conditions [25]. Similar observations were also made in other cell lines [39,65,66]. In this regard, our data suggest that the assembly of Cx32 and occludin might as well be coordinately regulated by 1-25D, and that this may be one of the additional mechanisms by which 1-25D maintains the polarized state of prostate epithelial cells and acts as a differentiating and chemopreventive agent. Further studies are required to substantiate this notion.

1-25D has been shown to induce G0/G1 arrest, differentiation and apoptosis of tumor cells by modulating different signaling pathways to delay tumor progression in different cancer cell types; moreover, it has also been known to potentiate the cytotoxic effects of many chemotherapeutic agents

[1–3]. Several studies have shown that vitamin D inhibits the growth of PCA cell lines, including LNCaP, in both AR-dependent and –independent manner [10,46,47,67,68]. We found that the expression of Cx32 potentiated the growth inhibitory effect of 1-25D such that suppression of growth was observed at doses which had no discernible effect on the growth of Cx-null LNCaP cells (Figure 5, Table 3). For example, doses of 1-25D — that were barely growth inhibitory to LNCaP-P and LNCaP-N cells — robustly inhibited the growth of LNCaP-32 cells (see Table 3). Earlier studies had shown that LNCaP cells were sensitized to undergo apoptosis by tumor necrosis factor α , TRAIL, and anti-Fas antibodies when Cx43 was expressed via adenoviruses to which Cx-null LNCaP cells were resistant [69]. Moreover, expression of Cx32 not only inhibits the growth of cells but also induces differentiation in breast cancer cell lines as well as in LNCaP cells [22,70,71].

What might be the possible explanation for the growth suppressive effects of 1-25D with regard to the assembly of Cx32 into GJs? The signaling pathways that are activated or suppressed upon formation and degradation of GJs to impact cell growth and differentiation are not well-understood [16,17,72–76]. Elegant studies in Cx32 knockout mice revealed increased activation of mitogen-activated protein kinases and decreased level of tumor suppressor p27Kip1 [77–79]. While it is well-known that 1-25D suppresses the growth of several human PCA cell lines, the effect appear not to depend on the expression level of vitamin D receptor. For example, only LNCaP cells were found to be exquisitely sensitive to the growth inhibitory effect of 1-25D whereas other PCA cell lines, such as PC-3, DU-145 and ALVA-31, were barely sensitive despite the fact that all cell types expressed nearly similar levels of vitamin D receptor [47,68,80,81]. Also, in LNCaP cells the growth suppression by 1-25D was mediated via increased expression of cyclin-dependent kinase inhibitors p21waf1/cip1 and p27kip1 as well as through hyper-phosphorylation of retinoblastoma protein, resulting in G0/G1 arrest [47]. Given the fact that Cx expression also has an impact on cell cycle [76,82], it is possible that transmission of growth regulatory signals through channels composed of Cx32 activates signaling pathways that increase the expression of gene-regulatory proteins involved in the control of cell cycle

progression as proposed [18,76]. Given the multiple effects of 1-25D on different tumor cell types, it is at present difficult to envisage how its chemopreventive, pro-differentiating and growth-inhibitory effects are related to its ability to regulate formation and degradation of GJs [16–18,74,76,83]. More elaborate studies are underway to explore the molecular basis of the augmentation of growth suppressive effect of 1-25D in LNCaP cells upon formation of GJs.

Several pre-clinical and clinical trials have suggested that a decrease in vitamin D₃ levels contributes to the development and possibly to the progression of human PCA [1,2,84,85]. Connexin32 is expressed by the luminal epithelial cells of normal prostate and is aberrantly assembled in the epithelial cells of prostate tumors [22,23]. Because GJs have been implicated in maintaining the polarized and differentiated state of epithelial cells [39], we propose that the chemopreventive effects 1-25D in PCA may result from its ability to enhance formation of GJs. Our results show that GJ assembly is the down-stream target of signaling initiated by 1-25D and that formation of GJs sensitizes PCA cells to its growth modulatory influence. Because loss of cell junctions is a hallmark of PCA progression [29] and might occur as early as prostatic intraepithelial neoplasia [86,87], understanding basic cell and molecular biological mechanisms by which 1-25D might govern the formation of GJs will provide new insights with regard to signaling pathways utilized to maintain the polarized and the differentiated state of epithelial cells in prostate tumors. This should open innovative avenues for designing new therapeutic approaches to delay the onset of malignancy as loss of polarization is the earliest changes that may initiate PCA progression [86].

Reference List

1. Fleet JC, Desmet M, Johnson R, Li Y (2012) Vitamin D and cancer: a review of molecular mechanisms. *Biochemical Journal* 441: 61-76.
2. Deeb KK, Trump DL, Johnson CS (2007) Vitamin D signalling pathways in cancer: potential for anticancer therapeutics. *Nat Rev Cancer* 7: 684-700.

3. Swami S, Krishnan AV, Feldman D (2011) Vitamin D metabolism and action in the prostate: Implications for health and disease. *Molecular and Cellular Endocrinology* 347: 61-69.
4. Krishnan AV, Feldman D (2010) Molecular pathways mediating the anti-inflammatory effects of calcitriol: implications for prostate cancer chemoprevention and treatment. *Endocr Relat Cancer* 17: R19-R38.
5. Schwartz GG, Hulka BS (1990) Is vitam D deficiency a risk factor for prostate cancer? *Anticancer Res* 10: 1307-1311.
6. Schwartz GG, Hill CC, Oeler TA, Becich MJ, Bahnsen RR (1995) 1,25-Dihydroxy-16-ene-23-yne-vitaminD3 and prostate cancer proliferation *in vivo*. *Urology* 46: 365-369.
7. Konety BR, Schwartz GG, Acierno JS, Becich MJ, Getzenberg (1996) The role of vitamin D in normal prostate growth and differentiation. *Cell Growth Diff* 7: 1563-1570.
8. Lokeshwar BL (1999) Inhibition of prostate cancer metastasis *in vivo*: a comparison of 1,25-dihydroxy vitamin D (calcitriol) and EB1089. *Cancer Epidemiol Biomark Prev* 8: 241.
9. Peehl D, Feldman D (2003) The role of vitamin D and retinoids in controlling prostate cancer progression. *Endocr Relat Cancer* 10: 131-140.
10. Yang ES, Maiorino CA, Roos BA, Knight SR, Burnstein KL (2002) Vitamin D-mediated growth inhibition of an androgen-ablated LNCaP cell line model of human prostate cancer. *Mol Cell Endocrinol* 186: 69-79.
11. Goodenough DA, Paul DL (2009) Gap Junctions. *Cold Spring Harbor Perspectives Biology* 1: a002576.
12. Beyer EC, Berthoud VM (2009) The Family of Connexin Genes. In: Harris A, Locke D, editors. *Connexins: A Guide*. Springer. pp. 3-26.
13. Laird DW (2006) Life cycle of connexins in health and disease. *Biochem J* 394: 527-543.
14. Thevenin AF, Kowal TJ, Fong JT, Kells RM, Fisher CG, Falk MM (2013) Proteins and Mechanisms Regulating Gap-Junction Assembly, Internalization, and Degradation. *Physiology* 28: 93-116.
15. Crespin S, Defamie N, Cronier L, Mesnil M (2009) Connexins and carcinogenesis. In: Harris A, Locke D, editors. *Connexinss: A Guide*. pp. 529-542.
16. Naus CC, Laird DW (2010) Implications and challenges of connexin connections to cancer. *Nat Rev Cancer* 10: 435-441.
17. Trosko J (2006) From adult stem cells to cancer stem cells: Oct-4 Gene, cell-cell communication, and hormones during tumor promotion. *Ann NY Acad Sci* 1089: 36-58.
18. Trosko J (2007) Gap Junctional Intercellular Communication as a Biological "Rosetta Stone" in Understanding, in a Systems Biological Manner, Stem Cell Behavior, Mechanisms of Epigenetic Toxicology, Chemoprevention and Chemotherapy. *J Memb Biol* 218: 93-100.
19. Wei CJ, Xu X, Lo CW (2004) Connexins and cell signaling in development and disease. *Ann*

Rev Cell Dev Biol 20: 811-838.

20. Xu J, Nicholson BJ (2013) The role of connexins in ear and skin physiology-Functional insights from disease-associated mutations. *Biochimica et Biophysica Acta (BBA) - Biomembranes* 1828: 167-178.
21. Habermann H, Chang WY, Birch L, Mehta P, Prins GS (2001) Developmental Exposure to Estrogens Alters Epithelial Cell Adhesion and Gap Junction Proteins in the Adult Rat Prostate. *Endocrinology* 142: 359-369.
22. Mehta PP, Perez-Stable C, Nadji M, Mian M, Asotra K, Roos B (1999) Suppression of human prostate cancer cell growth by forced expression of connexin genes. *Dev Genetics* 24: 91-110.
23. Habermann H, Ray V, Prins G (2002) Alterations in gap junction protein expression in human benign prostatic hyperplasia and prostate cancer. *J Urol* 167: 655-660.
24. Govindarajan R, Song X-H, Guo R-J, Wheelock MJ, Johnson KR, Mehta PP (2002) Impaired trafficking of connexins in androgen-independent human prostate cancer cell lines and its mitigation by α -catenin. *J Biol Chem* 277: 50087-50097.
25. Mitra S, Annamalai L, Chakraborty S, Johnson K, Song X, Batra SK, Mehta PP (2006) Androgen-regulated Formation and Degradation of Gap Junctions in Androgen-responsive Human Prostate Cancer Cells. *Mol Biol Cell* 17: 5400-5416.
26. Abate-Shen C, Shen M (2000) Molecular genetics of prostate cancer. *Genes Dev* 14: 2410-2434.
27. Cunha G, Donjacour A, Cooke P, Mee S, Bigsby R, Higgins S, Sugimura Y (1987) The endocrinology and developmental biology of the prostate. *Endocr Rev* 8: 338-362.
28. Marker P, Donjacour A, Dahiya R, Cunha G (2003) Hormonal, cellular, and molecular control of prostatic development. *Dev Biol* 253: 165-174.
29. Shen MM, Abate-Shen C (2010) Molecular genetics of prostate cancer: new prospects for old challenges. *Genes & Development* 24: 1967-2000.
30. Aboseif S, Dahiya R, Narayan P, Cunha G (1997) Effect of retinoic acid on prostate development. *Prostate* 31: 161-167.
31. Kelsey L, Katoch P, Johnson K, Batra SK, Mehta P (2012) Retinoids regulate the formation and degradation of gap junctions in androgen-responsive human prostate cancer cells. *PLoS ONE* 7: E32846.
32. Banach-Petrosky W, Ouyang X, Gao H, Nader K, Ji Y, Suh N, DiPaola RS, Abate-Shen C (2006) Vitamin D Inhibits the Formation of Prostatic Intraepithelial Neoplasia in Nkx3.1; Pten Mutant Mice. *Clinical Cancer Research* 12: 5895-5901.
33. Palmer HG, Gonzalez-Sancho JM, Espada J, Berciano MT, Puig I, Baulida J, Quintanilla M, Cano A, De Herreros AG, Lafarga M, Munoz A (2001) Vitamin D(3) promotes the differentiation of colon carcinoma cells by the induction of E-cadherin and the inhibition

of beta-catenin signaling. *J Cell Biol* 154: 369-387.

34. Bertram J (1999) Carotenoids and Gene Regulation. *Nutr Rev* 57: 182-191.
35. King TJ, Bertram JS (2005) Connexins as targets for cancer chemoprevention and chemotherapy. *Biochimica et Biophysica Acta (BBA) - Biomembranes* 1719: 146-160.
36. Mehta P, Loewenstein W (1991) Differential regulation of communication by retinoic acid in homologous and heterologous junctions between normal and transformed cells. *J Cell Biol* 113: 371-379.
37. Mehta P, Bertram J, Loewenstein W (1989) The actions of retinoids on cellular growth correlate with their actions on gap junctional communication. *J Cell Biol* 108: 1053-1065.
38. Trosko J, Chang C-C (2001) Mechanism of up-regulated gap junctional intercellular communication during chemoprevention and chemotherapy of cancer. *Mutat Res* 480: 219-229.
39. Kojima T, Murata M, Go M, Spray DC, Sawada N (2007) Connexins induce and maintain tight junctions in epithelial cells. *J Membr Biol* 217: 13-19.
40. Zhao X, Ly L, Peehl D, Feldman D (1999) Induction of androgen receptor by 1alpha,25-dihydroxyvitamin D3 and 9-cis retinoic acid in LNCaP human prostate cancer cells. *Endocrinology* 140: 1205-1212.
41. Igawa T, Lin FF, Lee MS, Karan D, Batra SK, Lin MF (2002) Establishment and characterization of androgen-independent human prostate cancer LNCaP cell model. *Prostate* 50: 222-235.
42. Chakraborty S, Mitra S, Falk MM, Caplan S, Wheelock MJ, Johnson KR, Mehta PP (2010) E-cadherin differentially regulates the assembly of connexin43 and connexin32 into gap junctions in human squamous carcinoma cells. *J Biol Chem* 285: 10761-10776.
43. Govindarajan R, Chakraborty S, Falk MM, Johnson KR, Wheelock MJ, Mehta PP (2010) Assembly of connexin43 is differentially regulated by E-cadherin and N-cadherin in rat liver epithelial cells. *Mol Biol Cell* 21: 4089-4107.
44. Johnson KE, Mitra S, Katoch P, Kelsey LS, Johnson KR, Mehta PP (2013) Phosphorylation on Ser-279 and Ser-282 of connexin43 regulates endocytosis and gap junction assembly in pancreatic cancer cells. *Mol Biol Cell* 24: 715-733.
45. Mehta P, Bertram J, Loewenstein W (1986) Growth inhibition of transformed cells correlates with their junctional communication with normal cells. *Cell* 44: 187-196.
46. Yang ES, Burnstein KL (2003) Vitamin D Inhibits G1 to S Progression in LNCaP Prostate Cancer Cells through p27Kip1 Stabilization and Cdk2 Mislocalization to the Cytoplasm. *J Biol Chem* 278: 46862-46868.
47. Zhuang S-H, Burnstein KL (1998) Antiproliferative effect of 1 α ,25-dihydroxyvitamin D3 in human prostate cancer cell line LNCaP involves reduction of cyclin-dependent kinase 2 activity and persistent G1 accumulation. *Endocrinology* 139: 1197-1207.

48. Lokeshwar B (1999) Inhibition of prostate cancer metastasis *in vivo*: a comparison of 1,25-dihydroxy vitamin D (calcitrol) and EB1089. *Cancer Epidemiol Biomark Prev* 8: 241.
49. Zhao X, Peehl D, Navone N, Feldman D (2000) 1alpha,25-dihydroxyvitamin D3 inhibits prostate cancer cell growth by androgen-dependent and androgen-independent mechanisms. *Endocrinology* 141: 2548-2556.
50. VanSlyke JK, Musil LS (2000) Analysis of connexin intracellular transport and assembly. *Methods* 20: 156-164.
51. Musil L, Cunningham BA, Edelman G, Goodenough D (1990) Differential phosphorylation of the gap junction protein connexin43 in junctional communication-competent and -deficient cell lines. *J Cell Biol* 111: 2077-2088.
52. Kemppainen J, Wilson J (1996) Agonist and antagonist activities of hydroxyfluamide and casodex relate to androgen receptor stabilization. *Urology* 48: 157-163.
53. Farla P, Hersmus R, Trapman J, Houtsmuller AB (2005) Antiandrogens prevent stable DNA-binding of the androgen receptor. *Journal of Cell Science* 118: 4187-4198.
54. Trosko J (2006) Dietary modulation of the multistage, multimechanisms of human carcinogenesis: effects on initiated stem cells and cell-cell communication. *Nutr Cancer* 94: 102-110.
55. Bosco D, Haefliger JA, Meda P (2011) Connexins: Key Mediators of Endocrine Function. *Physiol Rev* 91: 1393-1445.
56. Vezina C, Allgeier SMT, Fritz W, Moore R, Strerath M, Bushman W, Peterson R (2008) Retinoic acid induces prostatic bud formation. *Dev Dyn* 237: 1321-1333.
57. Lasnitzki I (1976) Reversal of methylchoantherene-induced changes in mouse prostates *in vitro* by retinoic acid and its analogues. *British Journal of Cancer* 34: 239-248.
58. Lasnitzki I, Goodman D (1974) Inhibition of the effects of methylcholanthrene on mouse prostate in organ culture by vitamin A and its analogs. *Cancer Res* 34: 1564-1571.
59. Christov KT, Moon RC, Lantvit DD, Boone CW, Steele VE, Lubet RA, Kelloff GJ, Pezzuto JM (2002) 9-cis-retinoic acid but not 4-(hydroxyphenyl)retinamide inhibits prostate intraepithelial neoplasia in Noble rats. *Cancer Res* 62: 5178-5182.
60. Manual M, Ghyselink NB, Chambon P (2006) Functions of the retinoid nuclear receptors: Lessons from the genetic and pharmacological dissections of the retinoic acid signaling pathway during mouse embryogenesis. *Ann Rev Pharm Tox* 46: 451-480.
61. Swami S, Krishnan AV, Wang JY, Jensen K, Horst R, Albertelli MA, Feldman D (2012) Dietary Vitamin D3 and 1,25-Dihydroxyvitamin D3 (Calcitriol) Exhibit Equivalent Anticancer Activity in Mouse Xenograft Models of Breast and Prostate Cancer. *Endocrinology* 153: 2576-2587.
62. VanSlyke JK, Deschenes SM, Musil LS (2001) Intracellular transport, assembly, and degradation of wild-type and disease-linked mutant gap junction proteins. *Mol Biol Cell*

11: 1933-1946.

63. Iversen P (2002) Antiandrogen monotherapy: indications and results. *Urology* 60: 64-71.
64. Kokai Y, Murata M, Go M, Spray DC, Sawada N (2011) Connexins induce and maintain tight junctions in epithelial cells. *J Membr Biol* 217: 13-19.
65. Kojima T, Kokai Y, Chiba H, Yamamoto M, Mochizuki Y, Sawada N (2001) Cx32 but Not Cx26 Is Associated with Tight Junctions in Primary Cultures of Rat Hepatocytes. *Experimental Cell Research* 263: 193-201.
66. Kojima T, Spray DC, Kokai Y, Chiba H, Mochizuki Y, Sawada N (2002) Cx32 formation and/or Cx32-mediated intercellular communication induces expression and function of tight junctions in hepatocytic cell line. *Exp Cell Res* 276: 40-51.
67. Shen R, Sumitomo M, Dai J, Harris A, Kaminetzky D, Gao M, Burnstein KL, Nanus DM (2000) Androgen-Induced Growth Inhibition of Androgen Receptor Expressing Androgen-Independent Prostate Cancer Cells Is Mediated by Increased Levels of Neutral Endopeptidase. *Endocrinology* 141: 1699.
68. Zhuang S-H, Schwartz GG, Cameron D, Burnstein KL (1997) Vitamin D receptor content and transcriptional activity do not fully predict antiproliferative effects of vitamin D in human prostate cancer cell lines. *Mol Cell Endo* 83-90.
69. Wang M, BERTHOUD VM, BEYER EC (2007) Connexin43 increases the sensitivity of prostate cancer cells to TNF $\{\alpha\}$ -induced apoptosis. *Journal of Cell Science* 120: 320-329.
70. Hirschi KK, Xu C, Tsukamoto T, Sager R (1996) Gap junction genes Cx26 and Cx43 individually suppress the cancer phenotype of human mammary carcinoma cells and restore differentiation potential. *Cell Growth Diff* 7: 861-870.
71. Mao AJ, Bechberger J, Lidington D, Galipeau J, Laird DW, Naus CCG (2000) Neuronal Differentiation and Growth Control of Neuro-2a Cells After Retroviral Gene Delivery of Connexin43. *The Journal of Biological Chemistry* 275: 34407-34414.
72. Langlois Sp, Cowan KN, Shao Q, Cowan BJ, Laird DW (2010) The Tumor-Suppressive Function of Connexin43 in Keratinocytes Is Mediated in Part via Interaction with Caveolin-1. *Cancer Research* 70: 4222-4232.
73. Langlois S, Maher AC, Manias JL, Shao Q, Kidder GM, Laird DW (2007) Connexin Levels Regulate Keratinocyte Differentiation in the Epidermis. *J Biol Chem* 282: 30171-30180.
74. McLachlan E, Shao Q, Wang HI, Langlois S, Laird DW (2006) Connexins act as tumor suppressors in three dimensional mammary cell organoids by regulating differentiation and angiogenesis. *Cancer Res* 66: 9886-9894.
75. Plante I, Stewart MKG, Barr K, Allan AL, Laird DW (2010) Cx43 suppresses mammary tumor metastasis to the lung in a Cx43 mutant mouse model of human disease. *Oncogene* 30: 1681-1692.
76. Kardami E, Dang X, Iacobas DA, Nickel BE, Jeyaraman M, Srisakuldee W, Makazan J, Tanguy

S, Spray DC (2007) The role of connexins in controlling cell growth and gene expression. *Progress in Biophysics and Molecular Biology* 94: 245-264.

77. King TJ, Lampe PD (2005) Altered tumor biology and tumorigenesis in irradiated and chemical carcinogen-treated single and combined connexin32/p27Kip1-deficient mice. *Communication and Cell Adhesion* 293-305.

78. King TJ, Lampe PD (2004) Mice deficient for the gap junction protein Connexin32 exhibit increased radiation-induced tumorigenesis associated with elevated mitogen-activated protein kinase (p44/Erk1, p42/Erk2) activation. *Carcinogenesis* 25: 669-680.

79. King TJ, Gurley KE, Prunty J, Shin JL, Kemp CJ, Lampe PD (2005) Deficiency in the gap junction protein connexin32 alters p27Kip1 tumor suppression and MAPK activation in a tissue-specific manner. *Oncogene* 24: 1718-1726.

80. Blutt S, Allegretto EA, Pike JW, Weigel NL (1997) 1,25-dihydroxyvitamin D₃ and 9-cis-retinoic acid act synergistically to inhibit the growth of LNCaP prostate cells and cause accumulation of cells in G₁. *Endocrinology* 138: 1491-1497.

81. Skowronski RJ, Peehl DM, Feldman D (1993) Vitamin D and prostate cancer: 1,25 Dihydroxyvitamin D₃ receptors and actions in human prostate cancer cell lines. *Endocrinology* 132: 1952-1960.

82. Chen S-C, Pelletier DB, Ao P, Boynton AL (1995) Connexin43 reverses the phenotype of transformed cells and alters their expression of cyclin/cyclin-dependent kinases. *Cell Growth Diff* 6: 681-690.

83. Laird DW (2010) The gap junction proteome and its relationship to disease. *Trends Cell Biol* 20: 92-101.

84. Schwartz G, Hulka BS (1990) Is vitamin D deficiency a risk factor for prostate cancer? *Anticancer Res* 10: 1307-1311.

85. Ahn J, Peters U, Albanes D, Purdue MP, Abnet CC, Chatterjee N, Horst RL, Hollis BW, Huang WY, Shikany JM, Hayes RB, For the Prostate LCaOCSTPT (2008) Serum Vitamin D Concentration and Prostate Cancer Risk: A Nested Case-Control Study. *Journal of the National Cancer Institute* 100: 796-804.

86. Bostwick DG, Qian J (2004) High-grade prostatic intraepithelial neoplasia. *Mod Pathol* 17: 360-379.

87. Bostwick DG (1992) Prostatic intraepithelial neoplasia (PIN): current concepts. *J Cell Biochem* 16H: 10-19.

Tables and Figure Legends

Table 1. Effect of 1,25D and androgen on the junctional transfer of fluorescent tracers in LNCaP-32 cells.

Junctional Tracer	Expt #	Junctional Transfer ^a			
		NS	NS+1-25D ^b	NS+DHT ^b	NS+MB ^b
Lucifer Yellow	1	11.3±2.1(17)	27.4±3.1(19)	25.6±5.1(21)c	34.7±5.7(22)
	2	13.1±3.1(19)	29.7±5.3(18)	29.1±7.3(27)	38.1±8.3(20)
Alexa-488	1	14.1±5.3(17)	26.7±4.9(27)	26.9.±6.9(23)	31.2±7.1(24)
	2	11.3 ±3.9 (22)	21.3±4.2(24)	23.5±5.1(28)	27.3±8.2(29)
Alexa-594	1	6.2± 2.1 (20)	19.3±3.3(22)	15.4±3.8(27)	13.7± 2.3(23)
	2	7.7± 2.7(27)	16.5 ±4.5(29)	17.7 ±5.4(19)	14.9±4.1 (26)

LNCaP-32 cells, seeded in 6 cm dishes in replicate, were grown to 65-70 % confluence. Junctional transfer was measured after microinjecting fluorescent tracers (see Materials and Methods).

a: The number of fluorescent cell neighbors (mean ± SE) 1 min (Lucifer Yellow), 3 min (Alexa-488) and 15 min (Alexa-594) after microinjection into test cell. The total number of injection trials is shown in parentheses.

b: Cells were treated for 48 h with 1-25D, DHT (10 nM) and MB (2.5 nM).

Table 2. Effect of 1-25D and androgens on junctional transfer of fluorescent tracers in LNCaP-32 cells under androgen-depleted conditions.

Treatment	Exp #	Junctional Tracer		
		LY	Alexa488	Alexa-594
NS	1	13.3±3.7(31)	23.7±4.3(29)	17.7±3.9(27)
	2	12.2±2.5(32)	29.1±6.4(23)	15.3±5.4(21)
Strip	1	1.9±0.6(25)	2.9±0.3(26)	1.1± 0.3(21)
	2	2.5±0.9(28)	2.3±0.7.(22)	0(17)
Strip+MB	1	27.3±.4.5(37)	27±3.9(28)	16.1±2.9(27)
	2	31.7±5.4(26)	34.1±6.7(24)	17.1±3.9(29)
Strip+1-25D	1	29.7±4.9(20)	33.7±7.6(22)	14.7±4.1(23)
	2	30.1±6.1(26)	30.2±5.5(29)	15.1±5.3 (22)
Strip+DHT	1	19.2±2.9(26)	27.2±6.3(27)	18.1±5.1(33)
	2	23.1±4.3(20)	29.8±6.1(23)	15.6±5.3(26)

LNCaP-32 cells were seeded as described in the legend to Table 1. Cells were switched to charcoal-stripped, androgen-depleted medium (Strip) for 48 h in the presence and absence of 1-25D and synthetic (MB) and the natural (DHT) androgens. Junctional transfer was quantified as described in Table 1 legend and in Materials and Methods.

Table 3. Cx32 expression sensitizes LNCaP cells to growth inhibitory effect of 1-25D.

Treatment	LNCaP-P	LNCaP-N	LNCaP-32
Experiment # 1			
Control	7.9 ± 1.5 (100 ± 19)	7.1 ± 1.1 (100 ± 15)	6.5 ± 1.6 (100 ± 25)
MB (2.5 nM)	6.1 ± 1.4 (77 ± 23)	6.2 ± 1.2 (87 ± 19)	3.7 ± 0.8 (57 ± 22)
1-25D (1 nM)	6.8 ± 1.3 (86 ± 19)	6.8 ± 1.1 (96 ± 16)	2.9 ± 0.3 (45 ± 10)
1-25D (2.5 nM)	5.9 ± 0.9 (75 ± 15)	6.3 ± 1.0 (89 ± 16)	1.9 ± 0.4 (29 ± 21)
Experiment # 2			
Control	7.7 ± 1.8 (100 ± 23)	7.1 ± 1.7 (100 ± 24)	6.7 ± 1.5 (100 ± 22)
MB (2.5 nM)	6.7 ± 1.1 (87 ± 16)	6.3 ± 1.2 (89 ± 19)	3.8 ± 0.6 (57 ± 16)
1-25D (1 nM)	6.2 ± 0.6 (81 ± 10)	6.6 ± 1.3 (93 ± 20)	2.8 ± 0.8 (42 ± 29)
1-25D (2.5 nM)	6.6 ± 0.9 (86 ± 14)	6.2 ± 1.5 (87 ± 24)	2.2 ± 0.7 (33 ± 32)

LNCaP-P, LNCaP-N and LNCaP-32 cells were seeded in 6-cm dishes in replicate (5×10^4 cells/dish) and treated with 1-25D (1 nM or 2.5 nM) and MB (2.5 nM). Cells were grown for 10 days with a medium change at day 2 and 5. Cells were trypsinized and counted as described in Materials and Methods. The values represent Mean number of cells per dish $\times 10^5 \pm$ SE of the Mean. Values in the parentheses represent Means of % Growth \pm SE of the Mean.

Figure legends

Figure 1. 1-25D increases Cx32 expression level. Cx32-expressing LNCaP-32 cells were treated with the 1-25D, 9-CRA, DHT and MB as indicated. **A.** Dose-dependent enhancement of Cx32 expression level upon 1-25D treatment for 48 h. Note that significant enhancement is observed only at concentrations above 1 nM. **B.** Kinetics of enhancement of Cx32 expression level upon treatment with 1-25D (10 nM) for the indicated times. Note that enhancement is observed as early as 12 h. **C.** Combined treatment with 1-25D with MB or 9-CRA is more effective in increasing Cx32 expression level than treatment with the single agent alone. **D.** Effect of 1-25D on adherens and tight junction associated proteins. Expression of adherens junction proteins E-cadherin (E-cad), α -catenin (α -cat), β -catenin (β -cat), and tight junction associated protein occludin (Occl) was analyzed by Western blot analysis of total cell lysate (10 μ g). Note that only the expression of occludin appears to change noticeably.

Figure 2. 1-25D enhances the assembly of Cx32 into gap junctions. LNCaP-32 cells, grown either in six well clusters or 10-cm dishes, were treated with 1-25D (10 nM), MB (5 nM) and 1-25D plus MB for 48 h. **A.** Assembly of Cx32 (green) into GJs was assessed immunocytochemically. E-cad is shown in red. Note that GJ formation was enhanced upon treatment with 1-25D and MB. **B.** TX100 solubility assay was used to measure the assembly of Cx32 into GJs, of occludin (Occl) and ZO-1 into tight junctions, and of adherens junction proteins, E-cadherin (E-cad) and α -catenin (α -cat). Note that both the total level and the detergent-insoluble fraction of Cx32 increased significantly. Note the absence of significant effect on adherens junction associated proteins, E-cad, and tight junction associated protein, occludin (Occl). In (A), the nuclei (blue) are stained with DAPI.

Figure 3. 1-25D blocks androgen-regulated degradation of Cx32 and gap junctions. LNCaP-32 cells, seeded in six well clusters or 10 cm dishes, were switched to charcoal-stripped (androgen-depleted) medium (ST). GJ assembly and the expression level of Cx32 were determined by Western blot

analysis (**A**), immunocytochemically (**B**), and biochemically by TX-100 solubility assay (**C**) in the presence and absence of 1-25D (5 and 10 nM) and MB (2.5 nM). TX-100 soluble and insoluble fractions as well as immunocytochemical assay were performed between 12-24 h post-stripping as described in Materials and Methods. Note that GJs are degraded upon androgen depletion and degradation is blocked upon 1-25D treatment. Note also that the TX-100 soluble fraction of E-cad (E-cad), β -catenin (β -cat) and ZO-1 is not significantly affected. Note also that TX-100 insoluble fraction of occludin (Occl) is decreased whereas the soluble fraction has increased. In (B), the nuclei (blue) were stained with DAPI.

Figure 4. Effect of 1-25D and MB on the expression level of Cx32, AR and the formation of gap junctions in the presence and the absence of Casodex. LNCaP-32 cells, seeded on glass cover slips, were grown to 70 % confluence. Cells were then grown for additional 24 h in normal medium (NS), androgen-depleted medium alone (ST), normal serum supplemented with Casodex (10 μ M; NS+CDX), androgen-depleted medium supplemented with MB (ST+MB), MB and Casodex (ST+MB+CDX), 1-25D (ST+1-25D), 1-25D and Casodex (ST+1-25D+CDX) and in normal serum with 1-25D (NS+1-25D). Expression level Cx32 and AR were analyzed by Western blotting (**A**) and immunocytochemically (**B**) as described in Materials and methods. Note that GJs (green) are not degraded in cells treated with 1-25D both in the presence and absence of Casodex whereas they are degraded in normal serum and androgen-depleted but MB supplemented medium containing Casodex. In **B**, E-cad is shown in red and the nuclei (blue) are stained with DAPI.

Figure 5. Connexin32 expression and junction formation augments the growth inhibitory effect of 1-25D. LNCaP-P, LNCAP-N and LNCaP-32 cells were seeded at clonal density (2×10^3) and treated with 1-25D (1 nM) after 24h. Cells were grown for 21 days with a medium change every 4 days

when they formed colonies. Colonies were fixed and stained with crystal violet. **A.** Representative dishes showing colonies. **B.** Morphology of the individual colonies at higher magnification. Note the robust decrease in colony size in 1-25D-treated dishes.

Figure 6. 1-25D alters the morphological phenotype of Cx32-expressing LNCaP cells. LNCaP-P, LNCaP-N and LNCaP-32 cells were seeded at a density of 2-3 x10⁴ per 6-cm dish and treated with the indicated concentrations of 1-25D after 24 hrs. After 5 days, cells were fixed and stained with crystal violet. Note robust morphological changes in LNCaP-32 cells treated with 1-25D.

Acknowledgment

This research was supported by NIH CA113903, DOD PCRP PC-081198 and PC-111867, Nebraska State Grant LB506 (PPM) and R0-1DE12308 (Keith R. Johnson). We thank Dr. Keith R. Johnson for helpful discussion and for various cadherin and catenin antibodies. We gratefully acknowledge support from the Nebraska Center for Cellular Signaling in the form of partial salary support to Linda Kelsey.

Figure 1

[Click here to download high resolution image](#)

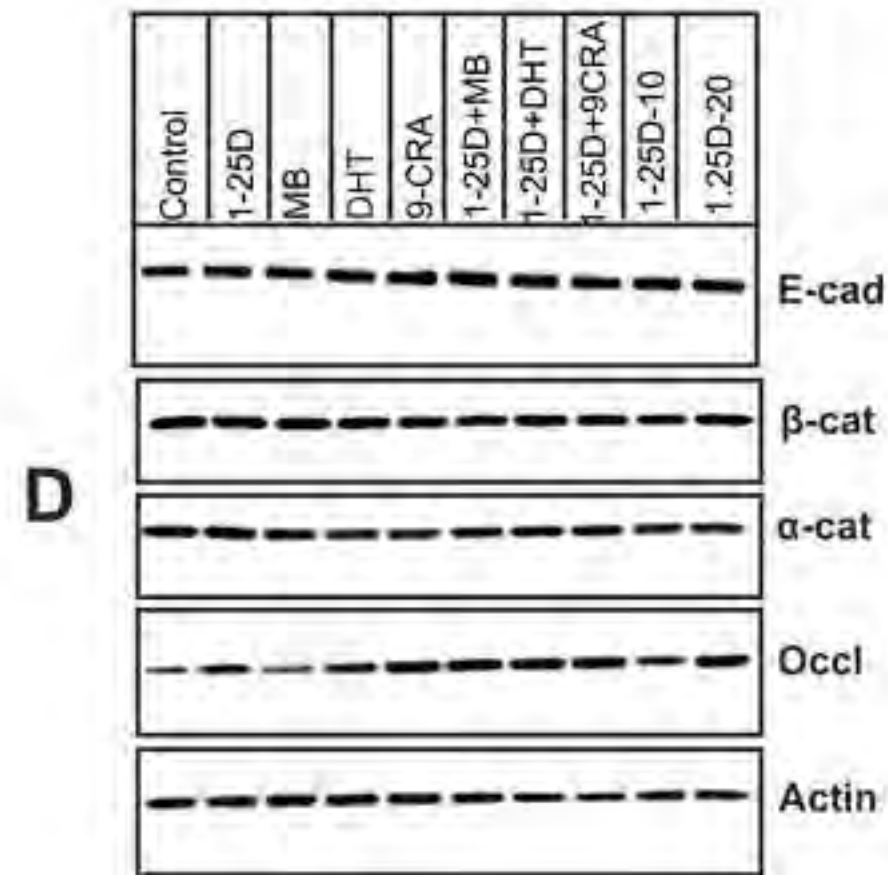
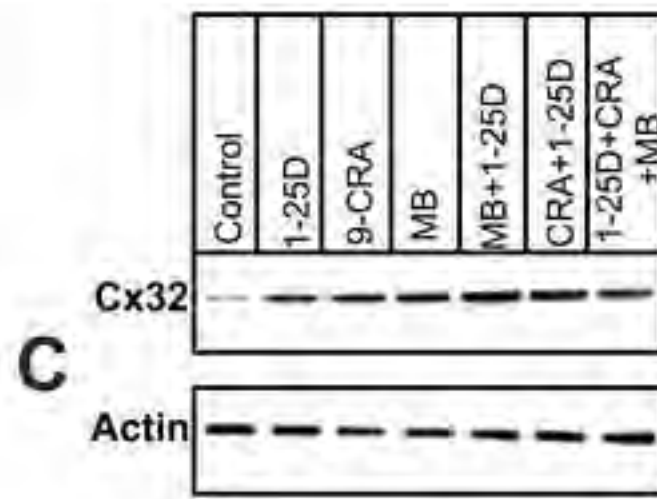
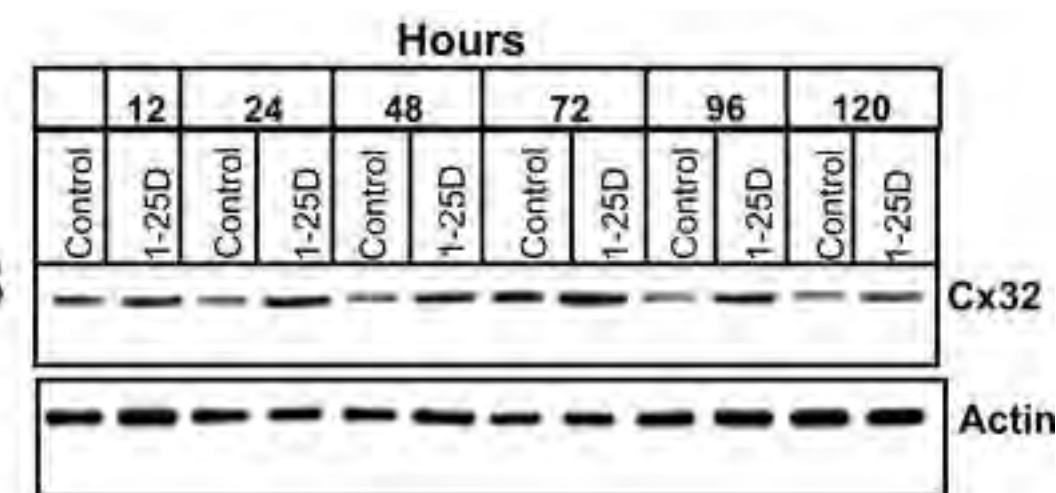
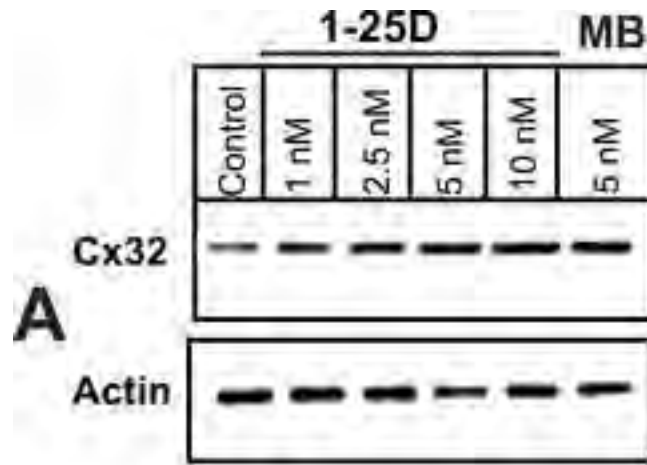


Figure 2

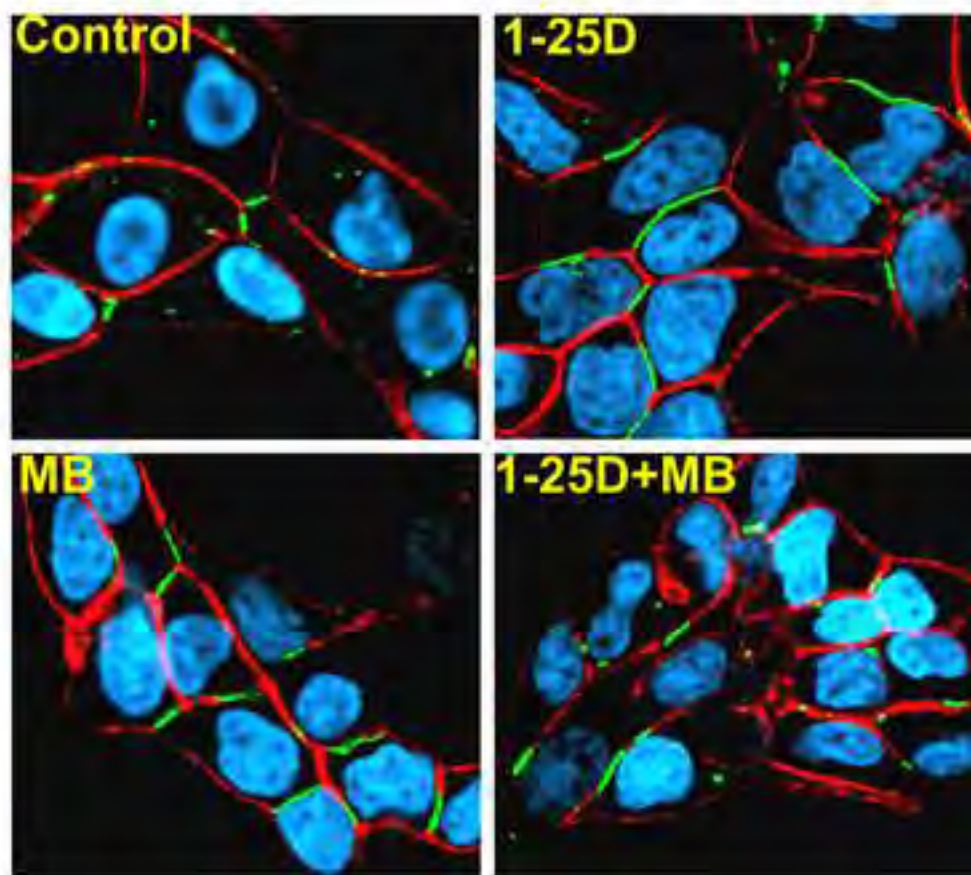
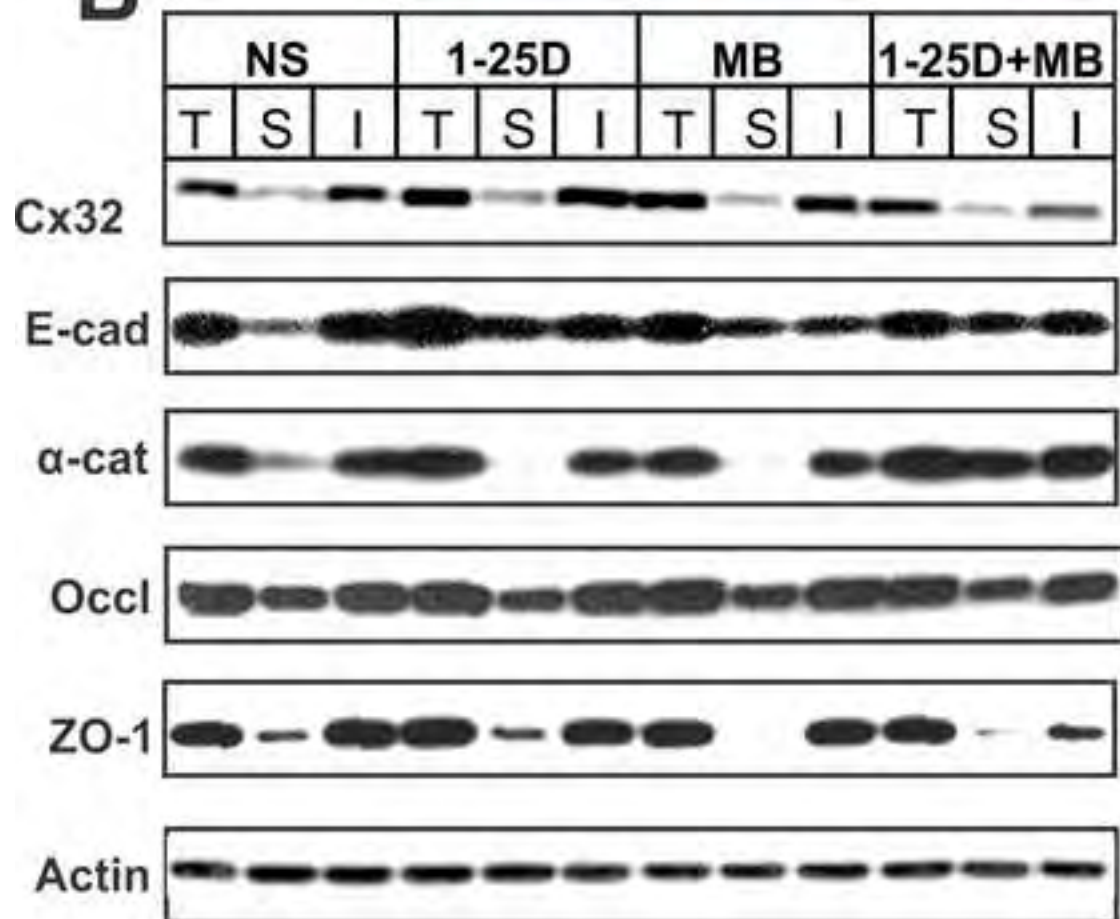
[Click here to download high resolution image](#)**A****B**

Figure 3

[Click here to download high resolution image](#)

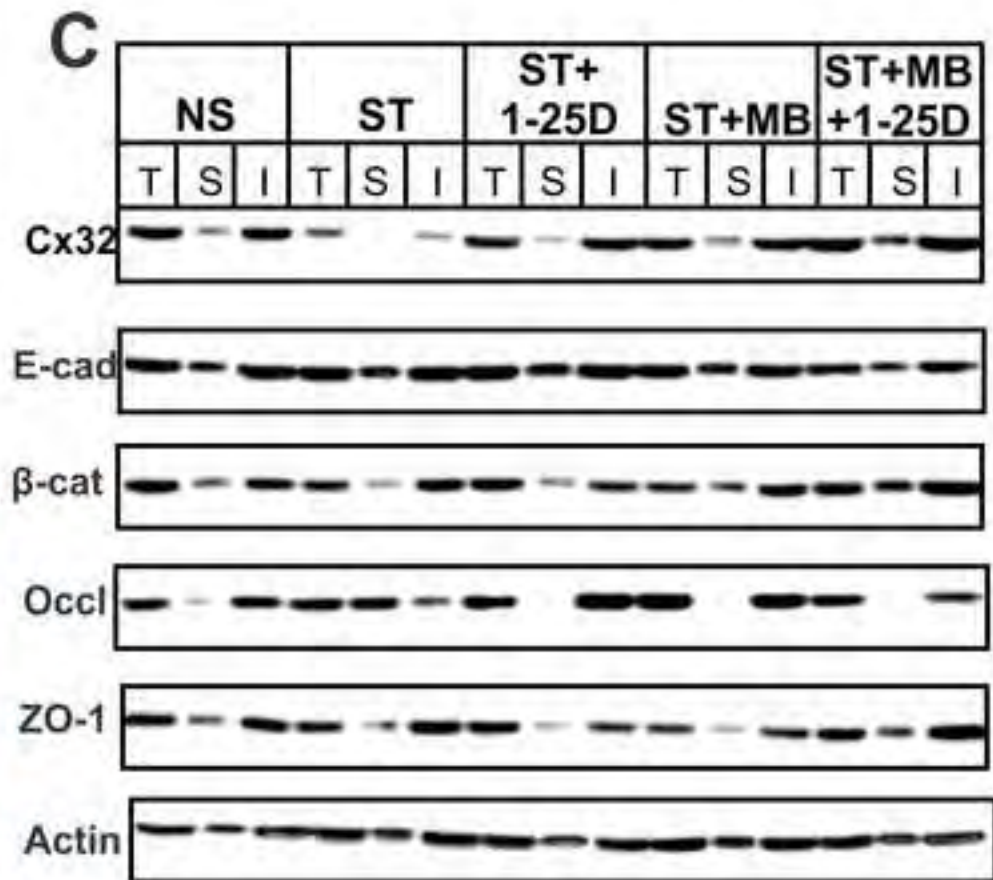
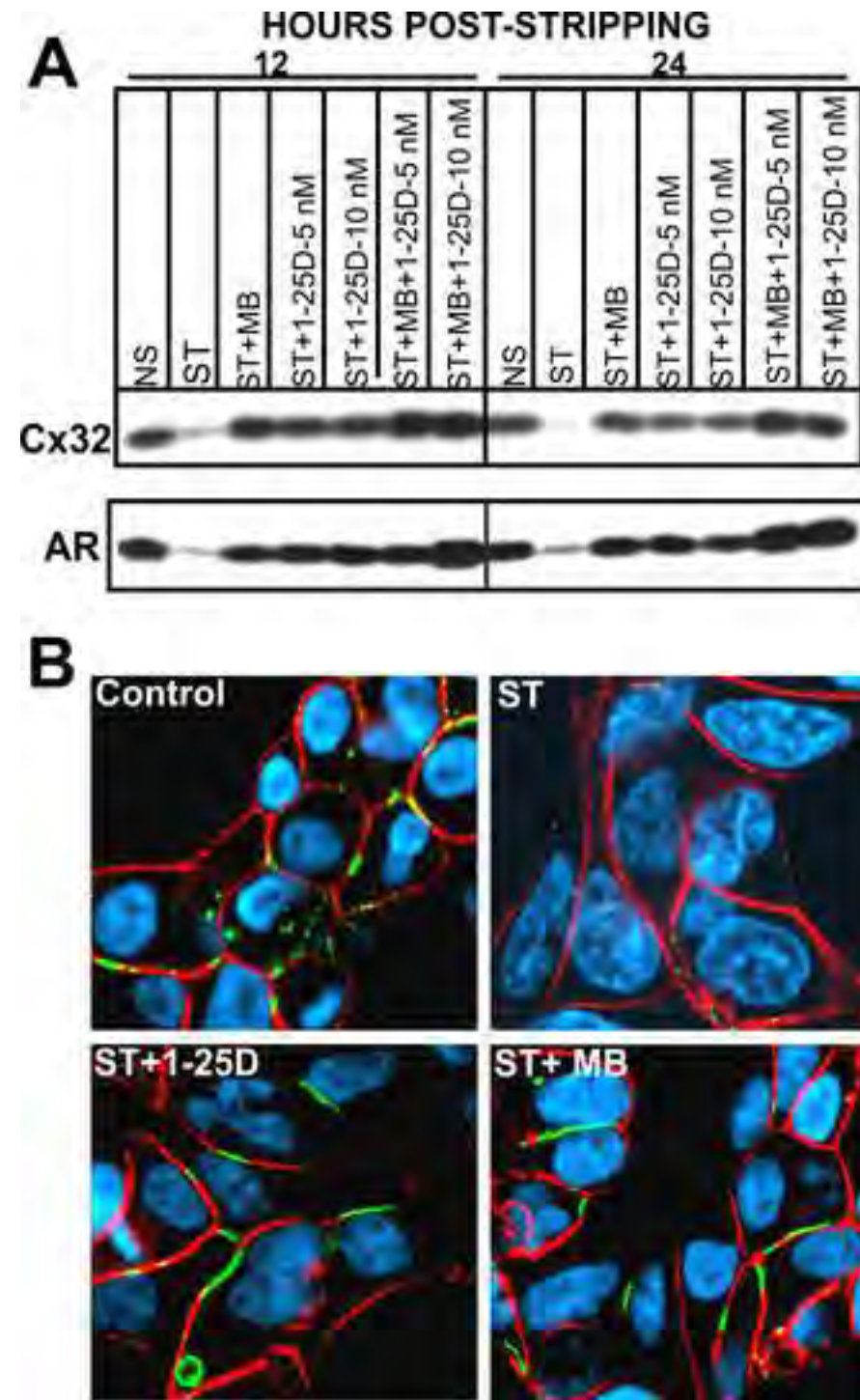


Figure 4

[Click here to download high resolution image](#)

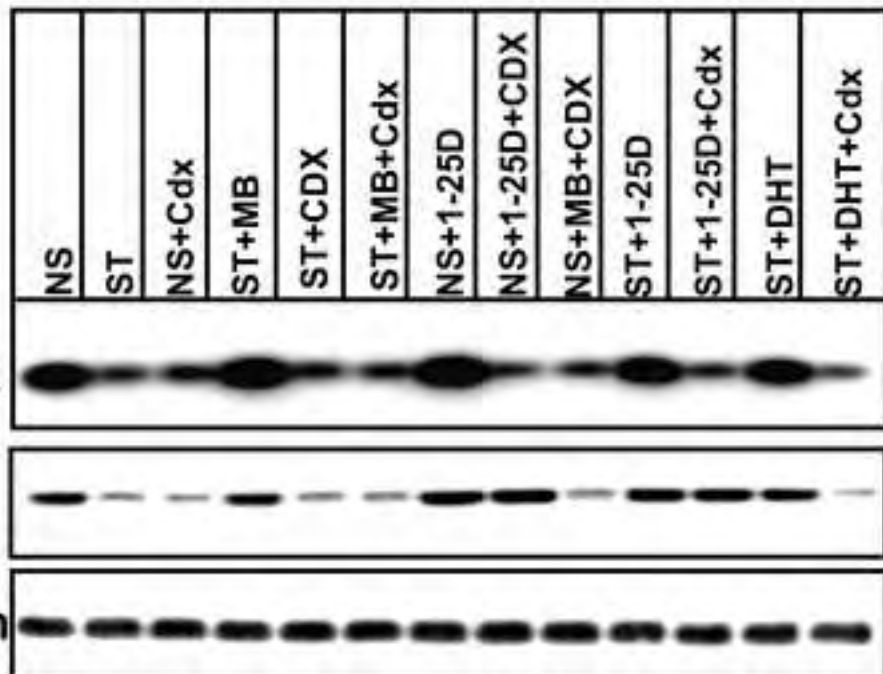
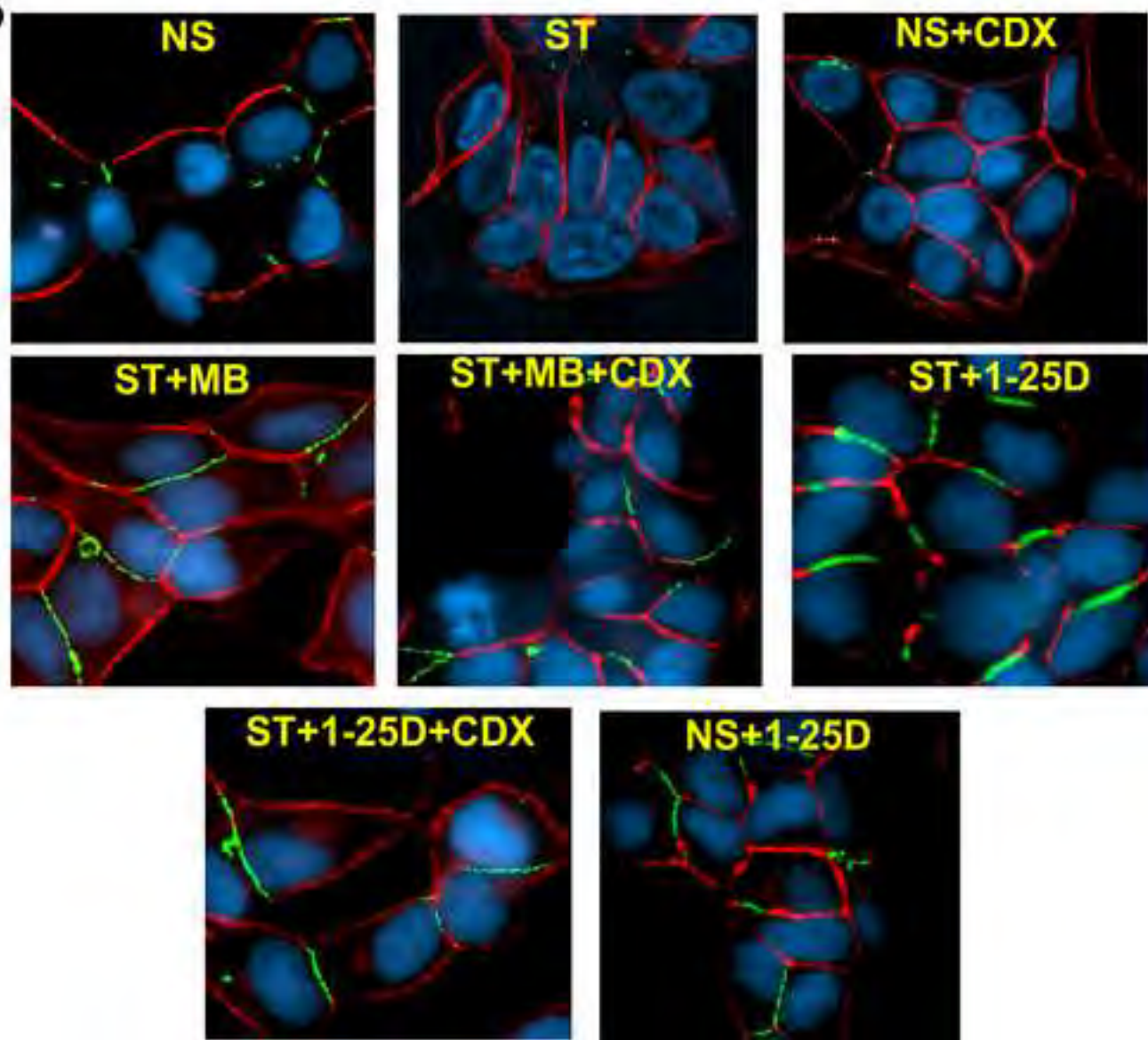
A**B**

Figure 5

[Click here to download high resolution image](#)

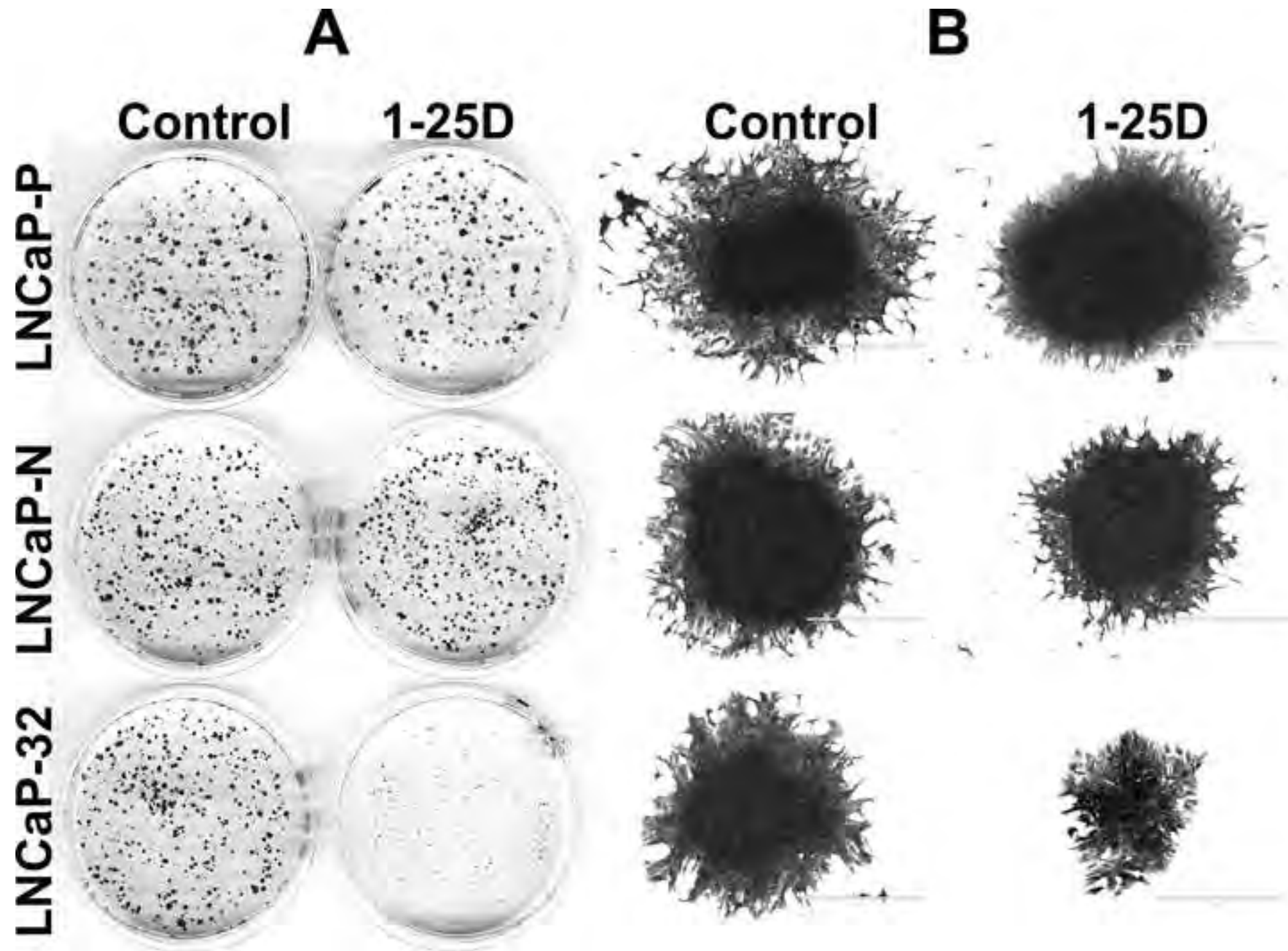


Figure 6

[Click here to download high resolution image](#)

